universität wien

DISSERTATION

Titel der Dissertation

Stress Response in *Candida glabrata*

angestrebter akademischer Grad

Doktor der Naturwissenschaften (Dr. rer.nat.)

Verfasserin / Verfasser:	Mag. Andreas ROETZER
Matrikel-Nummer:	9702886
Dissertationsgebiet (lt. Studienblatt):	Genetik - Mikrobiologie
Betreuerin / Betreuer:	Univ.-Prof. Dr. Christoph Schüller

Wien, am 25. September, 2008

Aus den Kürzesten Geschichten (V)

Der Papagei

Einer sprach plötzlich nur noch nach, was er hörte. Wie geht es dir? fragte ein Freund. Wie geht es dir? antwortete er. Der Freund wurde seiner überdrüssig. Auf der Straße sprach man ihn an: Wie komme ich zum Bahnhof? Wie komme ich zum Bahnhof? erwiderte er. Man schüttelte den Kopf über ihn. Noch ein Bier, sagte der Kellner. Noch ein Bier, lallte er. Die Gastronomen wußten sich seiner zu bedienen. Sein Verhalten wurde erörtert. Eine, die ihn gekannt hatte, war bei vielen Erörterungen dabeigesessen. Als sie einander zufällig begegneten, sagte sie: Du bist ein Trottel. Du plapperst nur nach, was dir andere vorsagen. Grinsend schwieg er.

(Clemens Berger, Der gehängte Mönch, Erzählungen. edition lex liszt 12)

Table of Contents

1. Introduction:

Yeasts belong to the large and diverse fungal kingdom. This ubiquitous microorganism appears in various shapes and at different environments. Fungi in general are heterotrophic organisms, which possess a chitinous cell wall and sterol-containing cell membranes. Several species are pathogens of humans or other animals. Single celled yeasts belong to the division Ascomycota, the largest taxonomic group within this kingdom. Within this division we find the class Saccharomycotina consisting of the most prominent genera *Saccharomyces* and *Candida*.

The species *Saccharomyces cerevisiae* is one of the most studied model organisms in molecular and cell biology. It is also known as baker´s (or brewer´s) yeast due to its common use in baking and brewing. The majority of the species among the genus *Candida* belong to the group of opportunistic human fungal pathogens. The most prevalent members are *Candida albicans* and *Candida glabrata* [1]. One exception of this taxonomy is the encapsulated yeast *Cryptococcus neoformans*, which belongs to the division Basidiomycota. In general, *Candida* species live as commensals of the skin and the gastrointestinal and genitourinary tracts in mammalian hosts. As part of the human flora, they can enter the bloodstream occasionally and cause infections (candidemia or candidiasis). This can be life-threatening for severely immunocompromised persons, such as cancer, transplant or AIDS patients. Therefore, candidiasis is referred as opportunistic disease.

In the following I will concentrate partly on *C. glabrata* including its successful adaptation to environmental changes inside and outside the host. How do *C. glabrata* cells adapt to changing environments? Which specific responses are crucial for prolonged survival? As part of its pathogenic lifestyle, *C. glabrata* has to get along with drugs and a hostile environment. Cells have to counteract defence mechanisms of the immune system. In general, fungal cells get phagocytosed, when they start to disseminate throughout the entire mammalian host. I tried to find out more about how *C. glabrata* cells react to changing environments, such as internalization by phagocytic cells.

From a phylogenetic point of view, *C. glabrata* is closely related to *Saccharomyces spp*. Its particular positioning among the clade of yeasts will be discussed first.

Candida glabrata – a *S. cerevisiae*-like pathogen?

Among the phylogenetic clade of *Candida* species, *Candida glabrata* has a unique position, closely related to *S. cerevisiae* and distinct from other *Candida* species (Figure 1) [2, 3]. During evolution, a whole-genome duplication (WGD) occurred prior to the divergence of *S. cerevisiae* and *C. glabrata* [4, 5] from other Ascomycetes yeasts. The genome of *C. glabrata* has been sequenced five years ago [4]. It consists of 12.3Mb and 13 chromosomes and has a G+C content of 38.8%, which is close to that of *Saccharomyces cerevisiae* (38.3%). About 5000 putative open reading frames were predicted. The genomes of *S. cerevisiae* and *C. glabrata* display a high degree of synteny. Moreover, the overwhelming majority of *S. cerevisiae* genes have obvious *C. glabrata* orthologues [4].

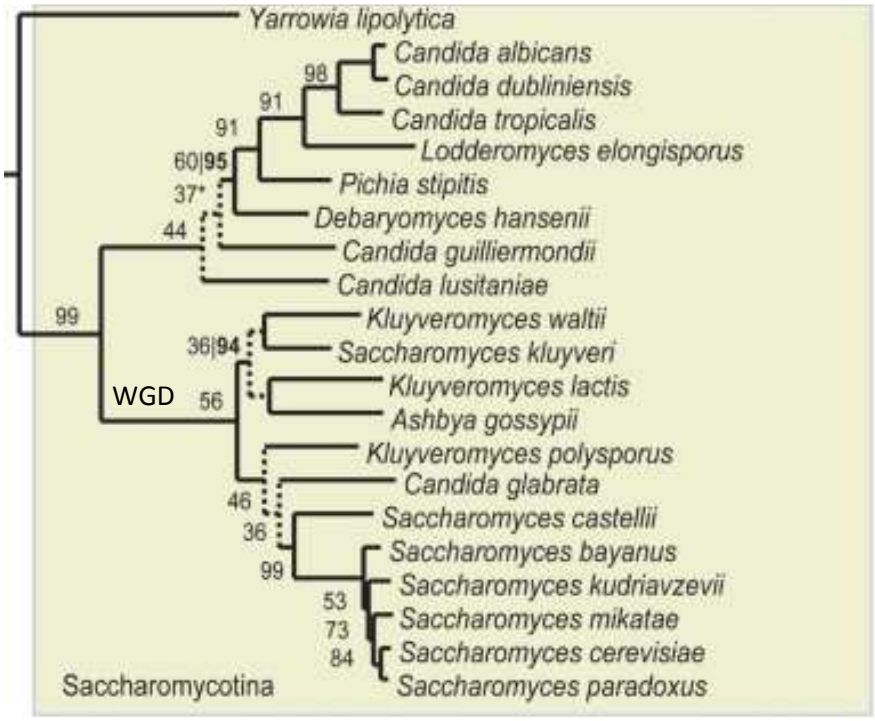

Figure 1. Phylogenetic tree representing the evolutionary relationships among the class Saccharomycotina considered in the study of Marcet-Houben *et al*. This tree resulted from the Maximum Likelihood phylogenetic analysis of the concatenated alignment of 69 widespread proteins. "Numbers on the nodes indicate two different types of support values. The first number indicates the percentage of trees in the phylome that support the specific arrangement of the three or four groups of species defined by its daughter nodes. A second number (in bold) indicates the bootstrap support when this is lower than 100. Branches with dashed lines indicate evolutionary relationships that are supported by less than 50% of the trees in the phylome" (adapted from Marcet-Houben *et al*, 2009).

Compared to S. cerevisiae, *C. glabrata* has lost many metabolism-associated genes again (*e.g*. for galactose or sucrose assimilation), probably because of its close relation to the mammalian host [6]. In addition, *C. glabrata* is an auxotroph for three vitamins: thiamine, niacin and pyridoxine [7, 8]. So far all clinical isolates of *C. glabrata* were haploid, but nevertheless this yeast owns components of a mating machinery similar to *S. cerevisiae* [9]. Moreover, mating type switching occurs during infection in clinical isolates, demonstrating a striking variation of phenotypes from different anatomical sites in patients [10]. Interestingly, an uneven mating type distribution was found in isolates from clinical samples: 80% of the strains are MATa [11]. The genome encodes for three mating type loci (*MTL1*, *MTL2* and *MTL3*) and in addition, encodes the HO endonuclease, which initiates mating type switching in *S. cerevisiae* [12, 13]. Although *C. glabrata* is classified as asexual yeast, its mating type machinery per se seems to be intact [9] and much more similar to *S. cerevisiae* than to *C. albicans*.

Similar to *C. albicans*, *C. glabrata* can undergo phenotypic switching [14, 15] an adaptation required for successful establishing in the human host. In *C. albicans*, white cells are ovoid, budding yeast cells that form white, domed colonies, while opaque cells are large and elongated and form gray, flat colonies; these cells have different infectious properties and different transcriptional profiles [16]. Phenotypic switching of the white to the opaque form significantly increases mating [17]. Additionally, the ability of *C. albicans* to switch from cells that make white colonies to cells that make opaque colonies correlates with survival in different host tissues [18, 19]. Although white cells are more suited for bloodstream infections, opaque cells are better at colonizing skin surfaces in mice [20]. *C. glabrata* switches spontaneously, reversibly and at high frequency among four phenotypes distinguishable by graded colony coloration on agar containing 1mM $CuSO_{(4)}$: white (Wh), light brown (LB), dark brown (DB) and very dark brown (vDB) [10, 14]. These phenotypes in turn can switch to the irregular wrinkle (IWr) phenotype [14], which displays a highly wrinkled colony morphology. Interestingly, DB has an advantage over other switch phenotypes in colonizing two major target organs in a mouse model, the spleen and liver [10, 21]. For *C. albicans*, the formation of hyphae is one important contribution to virulence [22, 23]. In contrast, *C. glabrata* does not undergo similar morphological switches inside the host. Similar to *S. cerevisiae*, it has been shown that *C. glabrata* can form pseudohyphae in response to nitrogen starvation [24]. Additionally, components of the mitogen-activated protein (MAP) kinase pathway, which induces pseudohyphae in *S. cerevisiae*, were also found in *C. glabrata*. Ste12, a conserved transcriptional regulator, is essential for nitrogen starvation-induced formation of pseudohyphae. Furthermore, the *ste12*Δ mutant shows attenuated virulence in a mouse model [25]. However, pseudohyphal forms of *C. glabrata* have

never been found in clinical specimens [2]. The formation of hyphae by *C. albicans* is also essential for escaping engulfment by cytotoxic cells like macrophages. *C. glabrata* pseudohyphae seem to be dispensable or even absent during infection of the human body. Therefore, *C. glabrata* seems to have developed other strategies than *C. albicans* to successfully colonize its niche inside the mammalian host.

Despite the fact that *C. glabrata* and *S. cerevisiae* share many similarities, it is more likely that the discrepancies characterize the pathogenicity of *C. glabrata*. For example, the *EPA* (Epithelial Adhesins) gene family, encoding GPI-anchored cell wall proteins, which mediate adherence to epithelial or cells surfaces, is not present in *S. cerevisiae* [2]. *EPA* gene products are involved in adherence and biofilm formation but affects virulence of *C. glabrata* [26-29]. *C. glabrata* is able to adhere to mammalian cells, an interaction that depends on the CgEpa1 lectin. *CgEPA1* is a member of a larger family of highly related genes encoded in subtelomeric clusters [30]. Due to their subtelomeric localization, *EPA* genes are subject to transcriptional silencing. In *S. cerevisiae*, silencing of subtelomeric genes is dependent on several trans-acting factors, such as Sir2, Sir3 and Sir4 [31, 32]. It has been shown recently, that *C. glabrata* cells with mutations in these silencing factors are hyperadherent to cultured epithelial cells [27, 28]. In addition, hyperadherent *C. glabrata sir3*Δ mutants displayed better colonization efficiency in kidneys of mice [27]. Interestingly, lack of nicotinic acid triggers *EPA* gene expression. Since *C. glabrata* is an auxothroph for this vitamin, cells are dependent on extracellular sources. In the absence of nicotinic acid, derepression of *EPA* genes occurs, resulting in better adherence [28].

Taken together, although *EPA* genes are absent in *S. cerevisiae*, *C. glabrata* shares more similarities with *S. cerevisiae* than with *C. albicans*. Nevertheless, adaptation to mammalian hosts led to *C. glabrata*-specific, yet mostly unknown, mechanisms to sustain survival in this niche.

Environmental stress response mechanisms in fungi.

Investigation of the response of C. glabrata and other pathogens to environmental conditions might provide additional information about the specific host-pathogen interactions. In the following, I will give an overview of the state-of-the-art knowledge about important stress responses of non-pathogenic and pathogenic yeasts. Ascomycota occupy diverse niches in nature. The majority of these niches does not stay constant, but changes quickly and continuously. Adaptation of gene expression through transcriptional regulation is a key mechanism in fungal response to fluctuating environmental conditions. Environmental stress causes activation of a

variety of signaling mechanisms each responding to a particular situation, such as oxidative stress or nutrimental starvation and in parallel induces a stereotypic general response. In *S. cerevisiae,* this response was first described and is referred to as general stress response or environmental stress response (ESR) [33, 34]. Stress responses might be divided into acute stress response, repair and starvation responses. Acute stress is for example exposure to high temperature. Repair processes are also constantly required as for example reactive oxygen species (ROS) are generated continuously in metabolizing cells. Finally, starvation response has also a component of the contribution of internal stores and the adaptation of metabolism. For example, glucose is the favored carbon source of yeasts and its shortage induces a broad spectrum of activators and genes. In case of continuous starvation, one important strategy is to recycle internal resources by autophagy [35]. Its importance for non-pathogenic and pathogenic microbes will be discussed below.

Furthermore, pathogenic fungi have to cope with antifungal drugs in hospitals. The selective pressure favors the occurrence of drug resistant strains, which are able to spread to other hosts *e.g*. in a clinical environment. Cells can develop resistance due to changes in the cell wall composition, which lead to impaired drug uptake. In addition, mutations in drug targets, such as lanosterol 14α-demethylase (Erg11), or their changing expression pattern can abolish susceptibility [36]. Furthermore, it is known that ATP-binding cassette (ABC) transporters also play a crucial role in the development of multidrug resistance (MDR) [37, 38]. MDR is mainly based on the overexpression of membrane transporters, which efflux chemically different compounds out of the cell. Finally, pathogenic yeasts encounter serious threats in the host such as patrolling phagocytic cells. Engulfment by these causes a rapid and dramatic change of their close environment, requiring a rapid adaptation to sustain dissemination. In the following part, the most prevalent aspects of stress responses, which can affect survival and dissemination of potentially pathogenic yeasts, are discussed. This includes the general stress response, responses to oxidative stress and carbon starvation, inducible autophagy and the response to application of antifungal drugs.

I. General Environmental Stress Response:

In *S. cerevisiae*, the ESR was originally described as a set of ~900 genes. One third gets induced, whereas about 600 genes are repressed upon induction of various types of stress, such as osmotic stress, heat shock, oxidative stress, nutrient starvation or extreme pH [33, 34]. Magnitude and kinetics of the ESR are dependent on the

severity of applied stresses. Comparable ESR patterns have been characterized in *Schizosaccharomyces pombe* and to a certain extent in *C. albicans* [39, 40]. For *S. cerevisiae, C. albicans and S. pombe* one major mechanism for controlling general stress responses are p38-type SAP kinases (stress-activated mitogen-activated protein kinases). The SAPKs, Hog1 (*S. cerevisiae,* see Figure 2), Sty1 (*S. pombe*) and CaHog1 (*C. albicans*) are all activated by hyperosmolarity, oxidative stress and to a varying degree by heavy metals. Notably, the HOG pathway of *C. glabrata* functions in a very similar manner to *S. cerevisiae*, in being activated by osmotic stress and additionally by weak acids [41].

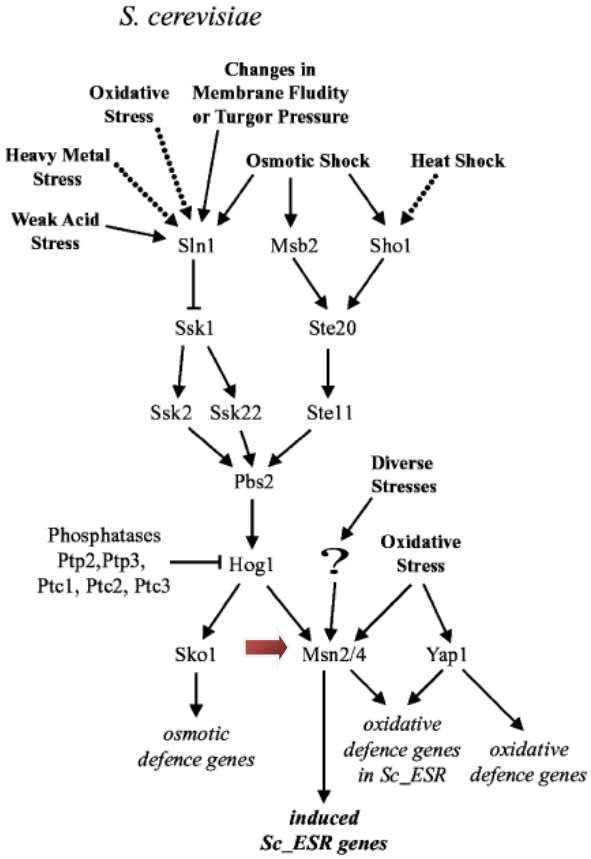

Figure 2. The Hog1–Msn2/4 pathways in *S. cerevisiae*. (adapted from Gasch AP, 2007).

In *S. cerevisiae* a second general stress mediating mechanism based on the transcription factor Msn2 and its paralogue Msn4 exists (Figure 2) [34, 42]. These are activated by a variety of stress conditions and changing nutrient supply situations such as glucose exhaustion [33, 34, 43]. Together, these factors affect almost 90% of the genes induced in the ESR. They also have a role in both chronological and replicative ageing [44, 45]. During high nutrient supply Msn2 is hyperphosphorylated and

inactivated by the PKA and TOR (target of rapamycin) pathways [43, 46, 47]. Activation of Msn2 and Msn4 causes their rapid accumulation in the nucleus and recruitment to chromatin. Msn2 has separate functional domains for nuclear import (NLS), nuclear export (NES) and DNA binding. The C_2H_2 Zn finger DNA binding domain at the C-terminus recognizes the stress response element (STRE). Stress signaling requires a region in the N-terminal part of Msn2 which includes its NES and a short stretch of high similarity to Msn4 designated homology domain 1 (HD1) [43, 46-48].

The *C. glabrata* orthologues CgMsn2 and CgMsn4 contain this conserved motif referred to as HD1, also present in Msn2 orthologues from fungi closely related to *S. cerevisiae* [49]. Transcript profiles of *C. glabrata msn2*Δ*msn4*Δ mutants show that they regulate part of the CgESR and are described in [Results]. In contrast, Msn2-like factors do not appear to play a role in regulating stress response in *C. albicans* and *S. pombe.* The *C. albicans* Msn2-like transcription factor designated CaMsn4 is not involved in the environmental stress response [50]. In addition, the Hog1 Map kinase orthologues play a more general role in stress response in *C. albicans* and *S. pombe.* These differences point to distinct strategies for regulating the stress response in fungi. Interestingly, in both *S. cerevisiae* and *S. pombe*, the ESR is suggested to be involved in cross-protection. Cross protection is defined as acquired resistance to a severe dose of the same or a different stress following the exposure to a non-lethal dose of a particular stress type [51-54]. Nevertheless, recent findings indicate that the primary function of adapted gene expression is to provide protection against impending stress rather than a protective role against the original stimulus [55]. Stress resistance is not acquired by plain activation of the ESR, but seems to be determined by condition specific responses, since cross-stress protection includes different regulatory pathways and therefore varies between different stresses. Msn2 and Msn4 play distinct roles in response to different stresses, which might be due to a different phosphorylation status in response to a particular condition [56].

II. Oxidative stress response:

Oxidative stress is of outstanding interest for fungi. All organisms, growing in an aerobic environment, have to deal with reactive oxygen species (ROS). In general, those species are occasionally produced during metabolic processes. In the special case of phagocytosis ROS is produced actively through macrophages and neutrophils. ROS, such as hydrogen peroxide (H_2O_2) or superoxide and hydroxyl radicals ($O_2^{\bullet-}$, $OH^{\bullet}$) can harm the cell by reacting with cellular structures, including proteins and DNA.

One essential pathway to generate ATP used by aerobic living organisms is the electron transport chain located in the mitochondrial membranes. Normally, molecular oxygen is reduced to produce water. However, occasionally, oxygen is incompletely reduced, resulting in superoxide radicals. Another metabolic process producing ROS is the β-oxidation of lipids. In contrast to higher eukaryotes that also have mitochondrial participation, fatty acid β-oxidation in yeast is restricted to peroxisomes [57, 58]. β-oxidation products are exported out of the peroxisome to mitochondria for full oxidation to CO_2 and H_2O. During the first step of decomposing fatty acids, $FADH_2$ is produced, which in turn gets reoxidized to FAD producing H_2O_2, which is decomposed by catalase.

In the phagolysosome of phagocytic cells, the NADPH oxidase complex consists of plasma membrane-associated enzymes [59]. It catalyzes the production of superoxide (O_2^-), serving as initial source for the production of several ROS to mediate oxidative destruction of engulfed microorganisms.

Cells counteract oxidative stress, using various, often redundant antioxidant systems (Figure 3) [60, 61]. Most important cellular redox balance and efficient removal of ROS are two small proteins: glutaredoxins (GRX) and thioredoxins (TRX) [62, 63]. Both act as antioxidants, but are reduced differently.

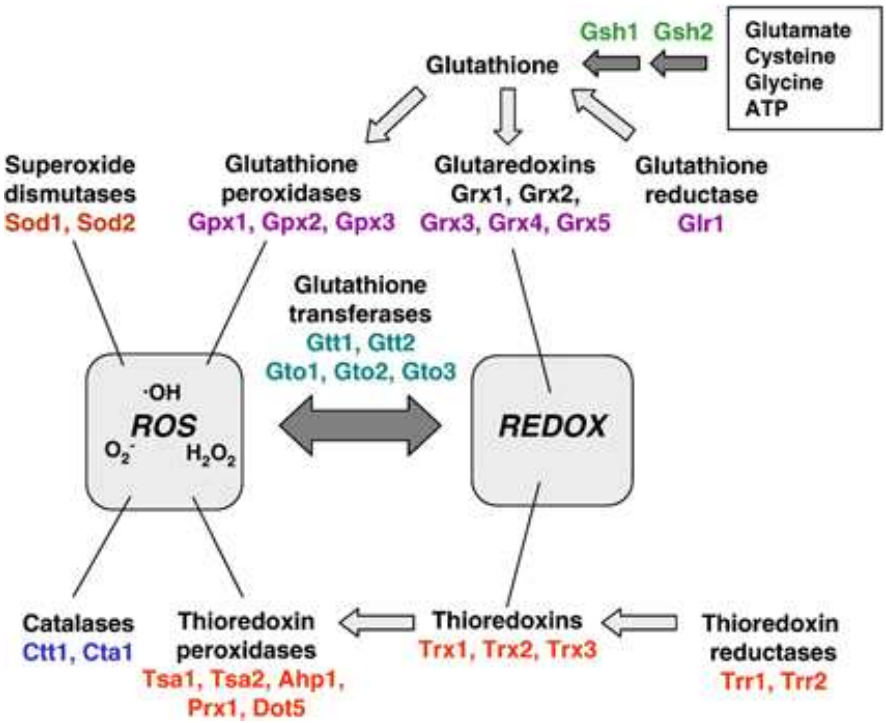

Figure 3. Enzymatic systems involved in ROS detoxification and in control of the redox state in *S. cerevisiae*, including their interrelationships (taken from Herrero *et al*, 2008).

The ubiquitous enzymes thioredoxins are kept in the reduced state by thioredoxin reductases (TRR) [64, 65]. Thioredoxins also act as electron donors to peroxidases (TSA, Thiol Specific Antioxidant) [66, 67]. Related glutaredoxins share many of the functions of thioredoxins, but are reduced by glutathione (GSH), a tripeptide, which acts a cofactor. Glutathione is predominantly kept in its reduced form, by activity of the glutathione reductase (GLR), the primary enzyme that controls the redox state of GSH, which is directly regulated by ROS [68]. GSH acts also as cofactor for glutathione peroxidases (GPX), which therefore reduce lipid hydroperoxides to alcohols and further reduce free H_2O_2 to water [62]. Glutathione tranferases (GST) conjugate GSH to a variety of exogenous and endogenous compounds, including products of oxidative stress [69, 70]. GSH-conjugated molecules are then excreted or transported into vacuoles, resulting in detoxification. Omega-class GSTs, a specific group of glutathione transferases (*GTO* genes, Glutathione Transferase Omega-like) have a different active site, but show similar oxidoreductase activities [69, 71]. Those ubiquitous transferases appear to be involved in various redox reactions. .The *S. cerevisiae* Gto1 is important for biosynthesis of sulfur amino acids [72]. In addition, cells can induce superoxide dismutases (SOD), which convert superoxides to H_2O_2 and oxygen. Further, the catalase, an enzyme present in nearly all living organisms, can decompose H_2O_2 to water and oxygen. In case of DNA, reactive oxygen species can lead to oxidation or hydrolysis (*e.g*. deamination, the conversion of C to U) of bases. If one of the two strands is defect, the other strand can act as template for repair [73]. Damaged or misfolded proteins as a consequence of ROS are rapidly degraded by the proteasome [74]. In conclusion, several enzymes cooperate for the destruction of ROS, supporting the overall importance of constant defence and repair.

Genes coding for ROS defence factors are often under control of specific transcription factors and are induced by oxidative stress. As part of the ESR, genes involved in oxidative stress response have been found to be activated by Msn2/4 in *S. cerevisiae* in response to diverse stresses [34]. Additionally, these genes are under control of other transcription factors in yeast. For *S. cerevisiae, C. albicans and S. pombe* the most prominent factor is a bZIP DNA-binding protein of the AP-1 family [75]. Yap1, Cap1 and Pap1 are known to induce a similar regulon upon oxidative stress induction [76-78]. Skn7 is a second factor involved in oxidative stress response in *S. cerevisiae* and to a lesser extent in *C. albicans* [79, 80]. Skn7 encodes a transcription factor, which is also implicated in the regulation of cell wall biosynthesis and the cell cycle [81, 82]. In *S. cerevisiae,* Skn7 and Yap1 control the vast majority of oxidative stress-inducible genes [83, 84].

What is the contribution of oxidative stress response to virulence and pathogen defense? Within the phagosome of phagocytic cells, engulfed yeasts seem to experience mild oxidative stress [85]. The exact role of transcription regulators is still unclear. Cap1 dependent genes are up-regulated in *C. albicans* in a mouse model [85]. In *C. glabrata skn7*Δ and *yap1*Δ mutants are less resistant to oxidative stress [86]. In contrast to *C. glabrata*, the sole catalase of *C. albicans* CaCtt1 has an impact on virulence in mice [87]. Other oxidative stress genes have been found to affect virulence in *C. albicans* and *C. neoformans* [88-91]. The exact impact of Skn7 and Yap1 remains to be elucidated and their role in *C. glabrata* is described in [Results].

III. Carbon starvation response:

The nutritional environment determines cellular behavior in various ways. Growth and proliferation are strictly dependent on available carbon sources. For microorganisms, extracellular compounds serve as both nutrients and signals. These signals must be transduced into a cellular response by key regulators, many of which are protein kinases (Figure 4) [92, 93]. Beside mannose and fructose, glucose is the preferred carbon source of *S. cerevisiae*; its presence represses numerous genes involved in alternative carbon catabolism [94]. *S. cerevisiae* is the best investigated yeast regarding glucose signaling. Several partially overlapping systems are known to participate in glucose signaling in yeast, such as Snf1, Ras/PKA, Gpr1/Gpa2, or Snf3/Rgt2, which controls the expression of glucose carriers [95, 96]. Several genes, such as the *HXT* family, encode different glucose transporters with varying affinities for the substrates [97, 98]. Snf3 and Rgt2 proteins are glucose carrier homologues but are unable to carry out active glucose transport; instead, Snf3 and Rgt2 mediate regulation of active glucose carriers by low and high glucose concentrations (see below) [99, 100].

Snf1, the yeast homolog of mammalian AMP-activated protein kinase, is a central component of glucose repression. The Snf1p kinase complex belongs to a highly conserved family of serine/threonine protein kinases, and homologues to each of the subunits (Snf1, Snf4, Sip1, Sip2, and Gal83) have been found in all eukaryotes, including plants and mammals [101-105]. Snf1 influences gene expression upon glucose depletion through activation of the transcriptional activators Cat8 and Adr1 and inactivation of the Mig1-containing repressor complex [106, 107]. Growth of cells in the presence of alternative carbon sources, such as glycerol or ethanol, activates Snf1 through phosphorylation by one of three upstream kinases [108-110]. In the presence

of glucose, the Reg1/Glc7 protein phosphatase 1 complex dephosphorylates and inactivates Snf1 [111]. Comparisons of transcriptional changes following glucose shortage revealed that up to 500 genes are regulated either directly or indirectly by Snf1 [112]. Upon activation, Snf1 also phosphorylates Sip4, a transcriptional activator involved in the positive regulation of gluconeogenesis, to allow expression of glucose-repressed genes [113].

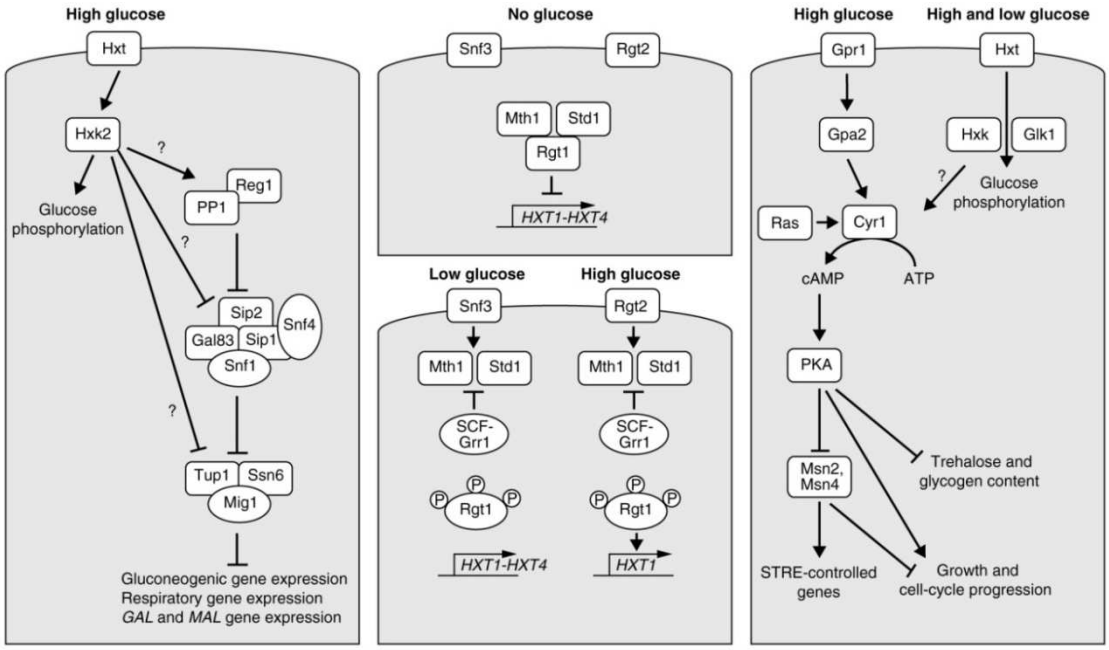

Figure 4. A simplified overview about three well-characterized glucose-sensing pathways: the Snf1 repression pathway, the Rag2/Snf3 glucose carrier pathway and the cAMP/PKA pathway (including Gpr1/Gpa2) represent the most prominent glucose responses (adapted from Geladé *et al*, 2003).

Further, in the absence of glucose, transcription factor Rgt1 acts in a complex with the two glucose-specific regulators Std1 and Mth1 as a transcriptional repressor of the *HXT1-HXT4* genes [99]. When glucose is present, the transcription factor Rgt1 is inactivated through the ubiquitin-ligase complex SCF-Grr1 which initiates degradation of the regulator proteins Mth1 and Std1 [114, 115]. This results in a rapid dissociation of Rgt1 from the *HXT* promoters. Snf3 triggers the induction of *HXT1-HXT4* in response to low glucose concentrations. High glucose concentrations enhance *HXT1* expression through Rgt2 in a process that converts Rgt1 into a transcriptional activator.

The Ras/PKA pathway plays the central role in responding to changes in glucose concentration. Glucose addition to cells increases the level of GTP-bound Ras, which in turn elevates intracellular cAMP and subsequently activates PKA [116]. Gpr1, a membrane G protein coupled receptor, and Gpa2, the alpha subunit of this G protein,

comprise a nutrient sensing pathway that works in parallel with Ras to activate PKA [117, 118]. High glucose concentrations activate cAMP synthesis by the adenylate cyclase Cyr1 through the Gpr1/Gpa2 G-protein-coupled receptor system in a glucose-phosphorylation-dependent manner. Nevertheless, it seems to play only a minor role in the transcriptional response to glucose [95]. Notably, the same pathway is present in *C. albicans* [119].

In yeast, the main downstream target for cAMP is the cAMP-dependent protein kinase A (PKA). PKA negatively regulates the general stress transcription factor Msn2 in *S. cerevisiae*. During high nutrient supply Msn2 is phosphorylated and inactivated by PKA. PKA phosphorylation sites in its NLS are phosphorylated PKA when glucose is available and rapidly dephosphorylated and activated by glucose starvation [46, 120]. This contributes to rapid nuclear import of the transcription factor. Additionally, the TOR pathway is involved in nutritional control in *S. cerevisiae* as well as in *S. pombe* [121, 122]. Further, starvation of amino acids, glucose and purines leads to the activation of Gcn2, a protein kinase that phosphorylates the translation initiation factor eIF2, which in turn leads to a general decrease of initiation of protein synthesis [123]. Unlike *S. cerevisiae* or *C. albicans*, *C. glabrata* does not ferment or assimilate other sugar such as sucrose, maltose or galactose [6, 124-127]. Trehalose, a glucose dimer, is the only sugar other than glucose that is assimilated by a majority of *C. glabrata* strains. Notably, disruption of the homologue *CgSNF1* in *C. glabrata* resulted in the loss of the ability to utilize trehalose [6]. Further, in *C. glabrata*, the localization of the orthologue CgMig1 is glucose dependent, which is described in [Results].

Carbon utilization is essential for proliferation of all living cells. Although different yeasts have specific carbon source preferences, transduction signals and subsequent carbon uptake systems are highly conserved [6, 127-129].

IV. Autophagic processes in response to continuous starvation:

A very important mechanism for overcoming starvation conditions is autophagy [130]. Autophagy is a process whereby almost all constituents of the cell get continuously recycled to help organisms to sustain crucial cellular functions and to overcome periods of nutrient starvation. Two types of cargo selection by autophagy are known: selective and non-selective autophagy (Figure 5). During the non-selective process bulk cytosol and other cytoplasmic components are randomly sequestered into autophagosomes. This process can also selectively eliminate specific proteins, protein complexes and organelles, and is under control of the TOR pathway, which is necessary for sensing and transducing nutrient availability [131-133]. When nutrients

are limiting, haploid yeast cells exit the mitotic cell cycle and enter a stationary phase, which is characterized by changes in transcription pattern and reduced protein synthesis [134]. *S. cerevisiae* and other yeasts harbor two homologous *TOR* genes, *TOR1* and *TOR2,* each encoding a serine/threonine kinase [135]. These kinases are involved in mediating translation, ribosome biogenesis, transport of nutrients and autophagy in response to nutrient availability.

However, the best characterized type of selective autophagy is the cytoplasm-to-vacuole targeting (Cvt) pathway, which is only found in *S. cerevisiae*; two hydrolases are directly transported from the cytoplasm into the vacuole where they are enzymatically processed into their mature form [136]. In *S. cerevisiae*, most of the organelles and macromolecular complexes are degraded by macro-autophagy, which involves the formation of double-membrane autophagosomes sequestering the structures that have to be degraded [137]. Autophagosomes fuse with the lysosome/vacuole, delivering the cargo. Additionally, a related process called micro-autophagy exists, in which the vacuole limiting membrane directly engulfs cytosolic material [138].

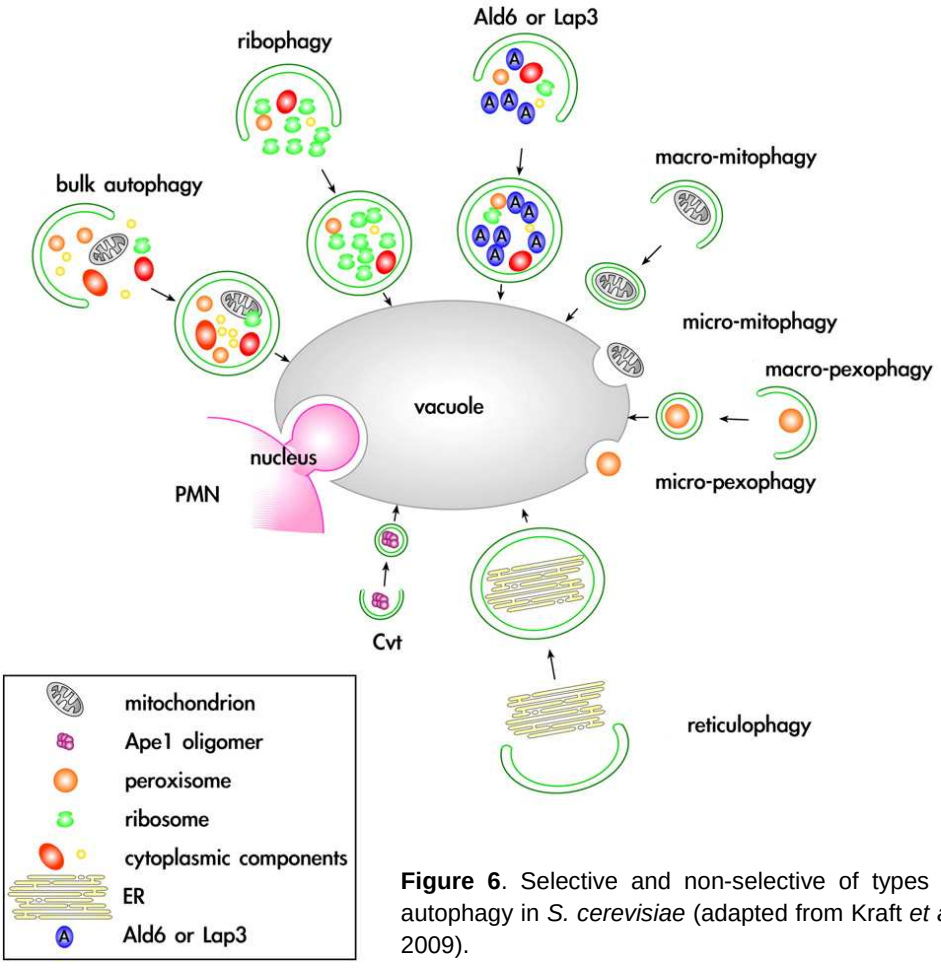

Figure 6. Selective and non-selective of types of autophagy in *S. cerevisiae* (adapted from Kraft *et al*, 2009).

There exist several subtypes of autophagy. Selective mitophagy, pexophagy, reticulophagy and ribophagy are important for a fast adaptation to regularly changing surroundings [139-144]. Furthermore, in *S. cerevisiae*, a process called piecemeal micro-autophagy of the nucleus (PMN) leads to the pinching off and degradation of non-essential portions of the nucleus into the vacuole in response to starvation conditions [145, 146]. More than 30 autophagy-related (Atg) proteins involved in autophagy have been identified in yeast [147]. On the other hand, certain subtypes of autophagy require factors, which are not involved in other autophagic processes. For example, Atg11 is involved in the Cvt pathway and pexophagy but is not required for non-selective autophagy in *S. cerevisiae* [148]. Interestingly, ubiquitin is involved selective cargo recognition as a signaling molecule [149]. The cargo destined for degradation is marked with ubiquitin, which is then recognized by an adaptor component to mediate the inclusion of the cargo into an autophagosome.

Autophagy could also be an issue for pathogenic yeasts as described in [Results]. Cells engulfed in macrophages are isolated from the environment and thus have to resort to endogenous resources. Notably, the encapsulated yeast *C. neoformans* requires autophagy during infection [150]. *ATG8* deficient strains displayed a significantly attenuated virulence in a mouse model. In addition, in *C. neoformans*, autophagy related genes are up-regulated upon during infection [151]. In contrast, *C. albicans* cells lacking *ATG9* were unable to induce autophagy, but showed no diminished survival rate [152]. Cells were able to kill macrophages through hyphae formation and escaped apparent depletion of nutrients.

Autophagy is an essential process to overcome common situations of nutrient deprivation. Importance of autophagy for phagocytosed fungal cells depends on morphological properties and strategies to escape from the phagosome [153].

V. Antifungal Drug Response:

Available antifungal agents can be divided into groups according to their modes of action. Antifungals work by exploiting differences between mammalian and fungal cells. Most of them impair membrane integrity (polyenes), ergosterol biosynthesis (azoles) or inhibit macromolecule synthesis (flucytosine). Resistance to flucytosine is common and usually arises from the loss or mutation of cytosine permeases (involved in its uptake), or other relevant enzymes [154]. Toxic compounds in the environment require an immediate cellular adaptation. In *S. cerevisiae* it has been shown that this rapid adaptation also includes induction of the general stress response [34].

Continuous application of antifungal drugs favored the development of multidrug resistance (MDR) pathways, which confer resistance to a broad spectrum of unrelated chemicals. In general, MDR is based on the overexpression of membrane transporters, which export chemically different compounds by either gene amplification or change of transcription [38]. In *S. cerevisiae*, MDR is referred to as pleiotropic drug response (PDR) [155]. At least 10 transcription factors are regulating about 70 genes [156]. Among those, Pdr1 is involved in induction of the largest set of genes (about 50). Pdr1 and its functional homologue Pdr3 can confer resistance to a broad variety of unrelated drugs through inducing expression of several ATP-binding cassette transporters, such as Pdr5 and Pdr15 [157-159]. Pdr1 seems to be active under normal growth conditions, since one of its target genes, the ABC transporter Pdr5, is highly expressed [160]. In *C. albicans*, two functional homologues of Pdr5, Cdr1 and Cdr2 (for Candida drug resistance), have been identified, which were involved in drug resistance [161, 162]. However, the regulation seems to work differently in *C. albicans*, since the responsible transcription factor, Tac1, induces only five genes [163]. In *C. glabrata* however, the exact mechanisms involved in drug resistance are not completely understood. It has been shown that increased expression of *CgCDR1* confers resistance to azole treatment in AIDS patients [164]. Deletion of *CgCDR1* in *C. glabrata* led to an increased susceptibility against azole derivatives. Further, a second, CgCdr2, and a third ABC transporter, CgSnq2, contribute to elevated azole resistance [165, 166]. Accordingly, the disruption of *CgPDR1* ceased *CgSNQ2* expression and decreased azole resistance. Beside the beneficial effect for elder or immunocompromised persons of applying antifungal drugs, the functional immune system of mammalian hosts is able to counteract fungal infections via innate and adapted immunity. This will be discussed below. However, multidrug resistance pathways induced by various applied chemicals seems to be conserved among opportunistic pathogenic yeasts.

How does the immune system of the human host counteract *Candida* infections?

Immunocompetence is essential to withstand infections of opportunistic fungal pathogens. *C. albicans* and *C. glabrata* infections induce a similar but not identical immune system response [167]. The presence of hyphae in tissues of *C. albicans*-infected mice causes a significant inflammatory response, characterized by an early neutrophilic infiltrate, followed by a mononuclear cell infiltrate composed mainly of macrophages. In contrast, the cell infiltrate into tissues of *C. glabrata*-infected mice was composed primarily of macrophages [167, 168]. Further, a dose dependent rapid induction of anti-inflammatory cytokines in response to *C. albicans* was found [169].

Similarly, a fast induction of cytokines, including TNF-α, IL-12 and IFN-γ, and lack of induction of IL-10 does occur upon systemic *C. glabrata* infection. TNF-α seems to play a key role in innate resistance to systemic *C. albicans* and *C. glabrata* infections, as neutralization of endogenous TNF-α activity alone results in significant increase in growth in infected tissues [167, 170-172]. TNF-α facilitates phagocytic cell activation, which results in altered cell functional responses including increased both adherence and phagocytosis [173]. Interestingly, IL-10 impairs development of a protective immune response to *C. albicans*, due to downregulation of phagocytic cell effector mechanisms [174, 175].

Helper T lymphocytes, which are activated through antigen presenting cells, secrete cytokines to mobilize macrophages and to initiate proliferation and differentiation of T and B lymphocytes. T helper cells can be divided into T_h1 and T_h2 cells. They differ in cytokine secretion and subsequent activation of phagocytic cells. The T_h1 differentiation pathway is a response to engulfed or intracellular microbes. IFNγ is produced and macrophages become activated. T_h2 differentiation is linked to allergens or helminthes. Antibodies stimulated by T_h2 cytokines do not promote phagocytosis. Concerning *Candida* infections, it is thought that there is a dynamic balance of T_h1 and T_h2 responses [176]. For example, IL-12 production is required for the development of T_h1-cell responses that are maintained in the presence of physiological levels of IL-4 and IL-10 [177, 178]. Accordingly, a regulated balance of directive cytokines, such as IL-4, IL-10, and IL-12, rather than the relative absence of opposing cytokines, appears to be required for development and maintenance of $_T$h1 reactivity in mice. Taken together, T_h1 response conferring a phagocyte-dependent immunity is critical for opposing infectivity of the commensals and clearing the yeast from infected tissue [176, 179, 180].

Interestingly, in contrast to the observations described above, B cell knockout mice are resistant to mucosal and systemic candidiasis of endogenous origin but are susceptible to experimental systemic candidiasis [181]. Further, in liver transplant patients, their serum antibody to CgHsp90 was associated with survival from disseminated disease with *C. albicans* [182]. Further, liposome-based mannan vaccines protect against experimental infection in mice, demonstrating an induced antibody-mediated immunity for protection against systemic candidiasis [183, 184].

The more we find out about the situation in the bloodstream and in tissues during ongoing dissemination, the more exactly we can determine the important roles of cell-mediated and humoral immunity. However, cell-mediated immunity is based on the activation of phagocytic cells. Upon internalization, engulfed cells have to adapt to

a new microenvironment. Investigating the strategies of microbes to sustain phagocytosis is essential to reveal their routes for dissemination.

In vivo situation during phagocytosis.

Phagocytosis is a specific form of endocytosis involving the vesicular internalization of microbes. Engulfment of foreign intruders is carried out by professional phagocytic cells, such as neutrophils, macrophages, dendritic cells and mast cells. The phagocytic cell sends out membrane projections (pseudopodia) that make contact with extracellular particles. Multiple Receptor ligand interactions occur between the phagocytic cell and the microbe that will be ingested. This results in the formation of an intracellular vesicle. This so-called phagosome is a prison-like, hostile environment. After internalization of pathogenic cells, these organelles undergo a maturation process, resulting in an acidic phagolysosome with pH 4.5-5.5 equipped with mature hydrolytic enzymes [185, 186]. Inhibition of phagolysosomal acidification and associated lysosomal fusion reduced germ tube formation of *C. albicans* [187].

In addition, the NADPH oxidase complex mediates oxidative destruction of internalized microorganisms through catalysing ROS [59]. It was found that engulfed *Candida* cells are exposed to ROS when they come into contact with phagocytic cells in the bloodstream, but that oxidative killing is no longer a significant threat once an infection has been established in the kidney of mice. Investigation of the oxidative stress response of these cells indicated a mild stress situation [85]. Quantification of fluorescence levels of induced reporter proteins suggested that they were exposed to an oxidative stress that is equivalent to about 0.4mM H_2O_2 for early and late infection time points. The involvement of oxidative stress as defence strategy is not restricted to fungal infections. Invading bacteria, such as *Staphylococcus aureus*, or the malaria parasites *Plasmodium sp*., also face ROS stress upon engulfment [188, 189].

Besides being exposed to oxidative stress, cells engulfed in macrophages are sealed from the environment and thus have to rely on endogenous resources or those acquired from the phagocytic cell. *C. albicans* engulfed within macrophages induces genes involved in non-fermentative carbon metabolism [190, 191]. In detail, ingestion of *C. albicans* cells by macrophages enforced two reprogramming events: the early and the late response. Early response is based on the reconfiguration of carbon metabolism: cells shift from glycolysis, the metabolic pathway to convert glucose, to gluconeogenesis, the generation of glucose from non-carbohydrate carbon substrates

[192, 193]. Transcript profiles also showed a clear induction of genes required to convert fatty acids to glucose. Further, this shift is accompanied by a massive downregulation of genes involved in translation. The late response is a resumption of glycolysis and restoration of the translation machinery, and is induced as *C. albicans* escapes through formation of hyphae [191]. Moreover, the glyoxylate cycle, required to channel fatty acid derived carbon into catabolism, is a virulence determinant for *C. albicans* [194]. Similar to engulfed *S. cerevisiae* cells, phagocytosis also up-regulates the most important enzymes of the glyoxylate cycle, isocitrate lyase (*ICL1*) and malate synthase (*MLS1*) in *C. albicans*. *C. albicans* mutants lacking *ICL1* are markedly less virulent in mice than the wild type.

In addition, other nutrient restrictions might be crucial as well. Phagocytes use iron-binding proteins to reduce iron availability. It has recently been shown, that lactoferrin restrains infection of the filamentous fungal pathogen *Aspergillus fumigatus* [195]. Lactoferrin is a multifunctional protein, which can be found mainly at mucosal areas as part of the innate defence. Its antimicrobial activity is based on scavenging free iron and its specific interaction with microbial components, thereby interrupting the attachment to cell membranes of the host [196, 197]. Human lactoferrin is also able to kill *C. albicans* in a dose- and time-dependent manner [198].

However, in case of *C. glabrata*, the *in vivo* situation is still unclear. *C. glabrata* experiences mild oxidative stress and in parallel sustained carbon starvation stress inducing autophagy, as described in [Results]. Obviously, when the immune system is compromised, the opportunistic pathogen *C. glabrata* has the ability to counteract engulfment and propagate dissemination.

Besides overcoming the oxidative burst and nutrient shortage, cells might actively try to sabotage maturation of the phagosome. Bacteria have developed effective strategies to survive engulfment. For example, it is known that intracellular *Mycobacterium* species can inhibit phagosomal maturation, including inhibition of acidification of the phagosome and inhibition of phagosome-lysosome fusion [199, 200]. Infantile mice are more susceptible to bacterial infection due to lack of acidification of the lysosomes of macrophages [201]. Strikingly, pretreatment with IFN-γ could rescue acidification. There is evidence that there exists a direct link between cytokine effects on the host cell and phagosome maturation in the macrophage [202]. If this is crucial to repress bacterial infection, this might be important for infections by yeasts as well.

Taken together, fungal cells have to overcome a multiple stress situation during prolonged engulfment. The strategy for escaping from phagocytic cells is still unclear for *C. glabrata*.

References

1. Pfaller, M.A. and D.J. Diekema, Twelve years of fluconazole in clinical practice: global trends in species distribution and fluconazole susceptibility of bloodstream isolates of *Candida*. Clin Microbiol Infect, 2004. **10 Suppl 1**: p. 11-23.
2. Kaur, R., *et al*., A yeast by any other name: *Candida glabrata* and its interaction with the host. Curr Opin Microbiol, 2005. **8**(4): p. 378-84.
3. Marcet-Houben, M. and T. Gabaldon, The tree versus the forest: the fungal tree of life and the topological diversity within the yeast phylome. PLoS ONE, 2009. **4**(2): p. e4357.
4. Dujon, B., *et al.*, Genome evolution in yeasts. Nature, 2004. **430**(6995): p. 35-44.
5. Kellis, M., B.W. Birren, and E.S. Lander, Proof and evolutionary analysis of ancient genome duplication in the yeast *Saccharomyces cerevisiae*. Nature, 2004. **428**(6983): p. 617-24.
6. Petter, R. and K.J. Kwon-Chung, Disruption of the *SNF1* gene abolishes trehalose utilization in the pathogenic yeast *Candida glabrata*. Infect Immun, 1996. **64**(12): p. 5269-73.
7. Ma, B., *et al*., Assimilation of NAD(+) precursors in *Candida glabrata*. Mol Microbiol, 2007. **66**(1): p. 14-25.
8. Li, Y., *et al*., Efficient pyruvate production by a multi-vitamin auxotroph of *Torulopsis glabrata*: key role and optimization of vitamin levels. Appl Microbiol Biotechnol, 2001. **55**(6): p. 680-5.
9. Wong, S., *et al.*, Evidence from comparative genomics for a complete sexual cycle in the 'asexual' pathogenic yeast *Candida glabrata*. Genome Biol, 2003. **4**(2): p. R10.
10. Brockert, P.J., *et al*., Phenotypic switching and mating type switching of *Candida glabrata* at sites of colonization. Infect Immun, 2003. **71**(12): p. 7109-18.
11. Brisse, S., *et al*., Uneven distribution of mating types among genotypes of *Candida glabrata* isolates from clinical samples. Eukaryot Cell, 2009. **8**(3): p. 287-95.
12. Srikantha, T., S.A. Lachke, and D.R. Soll, Three mating type-like loci in *Candida glabrata*. Eukaryot Cell, 2003. **2**(2): p. 328-40.
13. Butler, G., *et al*., Evolution of the MAT locus and its Ho endonuclease in yeast species. Proc Natl Acad Sci U S A, 2004. **101**(6): p. 1632-7.
14. Lachke, S.A., *et al*., Phenotypic switching and filamentation in *Candida glabrata*. Microbiology, 2002. **148**(Pt 9): p. 2661-74.
15. Hull, C.M. and J. Heitman, Fungal mating: *Candida albicans* flips a switch to get in the mood. Curr Biol, 2002. **12**(22): p. R782-4.
16. Soll, D.R., Gene regulation during high-frequency switching in *Candida albicans*. Microbiology, 1997. **143 (Pt 2)**: p. 279-88.
17. Miller, M.G. and A.D. Johnson, White-opaque switching in *Candida albicans* is controlled by mating-type locus homeodomain proteins and allows efficient mating. Cell, 2002. **110**(3): p. 293-302.
18. Kvaal, C., *et al.*, Misexpression of the opaque-phase-specific gene *PEP1* (*SAP1*) in the white phase of *Candida albicans* confers increased virulence in a mouse model of cutaneous infection. Infect Immun, 1999. **67**(12): p. 6652-62.
19. Kvaal, C.A., T. Srikantha, and D.R. Soll, Misexpression of the white-phase-specific gene *WH11* in the opaque phase of *Candida albicans* affects switching and virulence. Infect Immun, 1997. **65**(11): p. 4468-75.
20. Lachke, S.A., *et al.*, Skin facilitates *Candida albicans* mating. Infect Immun, 2003. **71**(9): p. 4970-6.
21. Srikantha, T., *et al*., Dark brown is the more virulent of the switch phenotypes of *Candida glabrata*. Microbiology, 2008. **154**(Pt 11): p. 3309-18.

22. Sudbery, P., N. Gow, and J. Berman, The distinct morphogenic states of *Candida albicans*. Trends Microbiol, 2004. **12**(7): p. 317-24.
23. Kumamoto, C.A. and M.D. Vinces, Contributions of hyphae and hypha-co-regulated genes to *Candida albicans* virulence. Cell Microbiol, 2005. **7**(11): p. 1546-54.
24. Csank, C. and K. Haynes, Candida glabrata displays pseudohyphal growth. FEMS Microbiol Lett, 2000. **189**(1): p. 115-20.
25. Calcagno, A.M., *et al.*, *Candida glabrata STE12* is required for wild-type levels of virulence and nitrogen starvation induced filamentation. Mol Microbiol, 2003. **50**(4): p. 1309-18.
26. Kapteyn, J.C., H. Van Den Ende, and F.M. Klis, The contribution of cell wall proteins to the organization of the yeast cell wall. Biochim Biophys Acta, 1999. **1426**(2): p. 373-83.
27. Castano, I., *et al.*, Telomere length control and transcriptional regulation of subtelomeric adhesins in *Candida glabrata*. Mol Microbiol, 2005. **55**(4): p. 1246-58.
28. Domergue, R., *et al*., Nicotinic acid limitation regulates silencing of Candida adhesins during UTI. Science, 2005. **308**(5723): p. 866-70.
29. Iraqui, I., et al., The Yak1p kinase controls expression of adhesins and biofilm formation in *Candida glabrata* in a Sir4p-dependent pathway. Mol Microbiol, 2005. **55**(4): p. 1259-71.
30. De Las Penas, A., *et al.*, Virulence-related surface glycoproteins in the yeast pathogen *Candida glabrata* are encoded in subtelomeric clusters and subject to *RAP1*- and *SIR*-dependent transcriptional silencing. Genes Dev, 2003. **17**(18): p. 2245-58.
31. Grunstein, M., Molecular model for telomeric heterochromatin in yeast. Curr Opin Cell Biol, 1997. **9**(3): p. 383-7.
32. Pryde, F.E. and E.J. Louis, Limitations of silencing at native yeast telomeres. EMBO J, 1999. **18**(9): p. 2538-50.
33. Causton, H.C., *et al*., Remodeling of yeast genome expression in response to environmental changes. Mol Biol Cell, 2001. **12**(2): p. 323-37.
34. Gasch, A.P., *et al.*, Genomic expression programs in the response of yeast cells to environmental changes. Mol Biol Cell, 2000. **11**(12): p. 4241-57.
35. Mizushima, N., Autophagy: process and function. Genes Dev, 2007. **21**(22): p. 2861-73.
36. Lupetti, A., *et al*., Molecular basis of resistance to azole antifungals. Trends Mol Med, 2002. **8**(2): p. 76-81.
37. Vanden Bossche, H., *et al*., Antifungal drug resistance in pathogenic fungi. Med Mycol, 1998. **36 Suppl 1**: p. 119-28.
38. Wolfger, H., Y.M. Mamnun, and K. Kuchler, Fungal ABC proteins: pleiotropic drug resistance, stress response and cellular detoxification. Res Microbiol, 2001. **152**(3-4): p. 375-89.
39. Gasch, A.P., Comparative genomics of the environmental stress response in ascomycete fungi. Yeast, 2007. **24**(11): p. 961-76.
40. Enjalbert, B., *et al.*, Role of the Hog1 stress-activated protein kinase in the global transcriptional response to stress in the fungal pathogen *Candida albicans*. Mol Biol Cell, 2006. **17**(2): p. 1018-32.
41. Gregori, C., *et al.*, The high-osmolarity glycerol response pathway in the human fungal pathogen *Candida glabrata* strain ATCC 2001 lacks a signaling branch that operates in baker's yeast. Eukaryot Cell, 2007. **6**(9): p. 1635-45.
42. Martinez-Pastor, M.T., *et al*., The *Saccharomyces cerevisiae* zinc finger proteins Msn2p and Msn4p are required for transcriptional induction through the stress response element (STRE). EMBO J, 1996. **15**(9): p. 2227-35.
43. Boy-Marcotte, E., *et al*., Msn2p and Msn4p control a large number of genes induced at the diauxic transition which are repressed by cyclic AMP in *Saccharomyces cerevisiae*. J Bacteriol, 1998. **180**(5): p. 1044-52.
44. Fabrizio, P., *et al.*, Regulation of longevity and stress resistance by Sch9 in yeast. Science, 2001. **292**(5515): p. 288-90.

45. Powers, R.W., 3rd, *et al.*, Extension of chronological life span in yeast by decreased TOR pathway signaling. Genes Dev, 2006. **20**(2): p. 174-84.
46. Gorner, W., *et al.*, Nuclear localization of the C2H2 zinc finger protein Msn2p is regulated by stress and protein kinase A activity. Genes Dev, 1998. **12**(4): p. 586-97.
47. Gorner, W., *et al*., Acute glucose starvation activates the nuclear localization signal of a stress-specific yeast transcription factor. EMBO J, 2002. **21**(1-2): p. 135-44.
48. Durchschlag, E., *et al*., Nuclear localization destabilizes the stress-regulated transcription factor Msn2. J Biol Chem, 2004. **279**(53): p. 55425-32.
49. Roetzer, A., *et al.*, *Candida glabrata* environmental stress response involves *Saccharomyces cerevisiae* Msn2/4 orthologous transcription factors. Mol Microbiol, 2008. **69**(3): p. 603-20.
50. Nicholls, S., *et al*., Msn2- and Msn4-like transcription factors play no obvious roles in the stress responses of the fungal pathogen *Candida albicans*. Eukaryot Cell, 2004. **3**(5): p. 1111-23.
51. Moradas-Ferreira, P. and V. Costa, Adaptive response of the yeast Saccharomyces cerevisiae to reactive oxygen species: defences, damage and death. Redox Rep, 2000. **5**(5): p. 277-85.
52. Lewis, J.G., R.P. Learmonth, and K. Watson, Induction of heat, freezing and salt tolerance by heat and salt shock in *Saccharomyces cerevisiae*. Microbiology, 1995. **141 (Pt 3)**: p. 687-94.
53. Lee, J., I.W. Dawes, and J.H. Roe, Adaptive response of *Schizosaccharomyces pombe* to hydrogen peroxide and menadione. Microbiology, 1995. **141 (Pt 12)**: p. 3127-32.
54. Ribeiro, M.J., *et al.*, Trehalose synthesis is important for the acquisition of thermotolerance in *Schizosaccharomyces pombe*. Mol Microbiol, 1997. **25**(3): p. 571-81.
55. Berry, D.B. and A.P. Gasch, Stress-activated genomic expression changes serve a preparative role for impending stress in yeast. Mol Biol Cell, 2008. **19**(11): p. 4580-7.
56. Garreau, H., *et al*., Hyperphosphorylation of Msn2p and Msn4p in response to heat shock and the diauxic shift is inhibited by cAMP in *Saccharomyces cerevisiae*. Microbiology, 2000. **146 (Pt 9)**: p. 2113-20.
57. Hiltunen, J.K., *et al.*, The biochemistry of peroxisomal beta-oxidation in the yeast *Saccharomyces cerevisiae*. FEMS Microbiol Rev, 2003. **27**(1): p. 35-64.
58. van Roermund, C.W., et al., Fatty acid metabolism in *Saccharomyces cerevisiae*. Cell Mol Life Sci, 2003. **60**(9): p. 1838-51.
59. Babior, B.M., NADPH oxidase: an update. Blood, 1999. **93**(5): p. 1464-76.
60. Miller, R.A. and B.E. Britigan, Role of oxidants in microbial pathophysiology. Clin Microbiol Rev, 1997. **10**(1): p. 1-18.
61. Herrero, E., *et al*., Redox control and oxidative stress in yeast cells. Biochim Biophys Acta, 2008. **1780**(11): p. 1217-35.
62. Herrero, E., *et al*., Glutaredoxins in fungi. Photosynth Res, 2006. **89**(2-3): p. 127-40.
63. Carmel-Harel, O. and G. Storz, Roles of the glutathione- and thioredoxin-dependent reduction systems in the *Escherichia coli* and saccharomyces cerevisiae responses to oxidative stress. Annu Rev Microbiol, 2000. **54**: p. 439-61.
64. Trotter, E.W. and C.M. Grant, Thioredoxins are required for protection against a reductive stress in the yeast *Saccharomyces cerevisiae*. Mol Microbiol, 2002. **46**(3): p. 869-78.
65. Ross, S.J., *et al.*, Thioredoxin peroxidase is required for the transcriptional response to oxidative stress in budding yeast. Mol Biol Cell, 2000. **11**(8): p. 2631-42.
66. Trotter, E.W., *et al*., The yeast Tsa1 peroxiredoxin is a ribosome-associated antioxidant. Biochem J, 2008. **412**(1): p. 73-80.
67. Munhoz, D.C. and L.E. Netto, Cytosolic thioredoxin peroxidase I and II are important defenses of yeast against organic hydroperoxide insult: catalases and peroxiredoxins

cooperate in the decomposition of H_2O_2 by yeast. J Biol Chem, 2004. **279**(34): p. 35219-27.
68. Grant, C.M., *et al*., Yeast glutathione reductase is required for protection against oxidative stress and is a target gene for yAP-1 transcriptional regulation. Mol Microbiol, 1996. **21**(1): p. 171-9.
69. Hayes, J.D., J.U. Flanagan, and I.R. Jowsey, Glutathione transferases. Annu Rev Pharmacol Toxicol, 2005. **45**: p. 51-88.
70. Sheehan, D., *et al*., Structure, function and evolution of glutathione transferases: implications for classification of non-mammalian members of an ancient enzyme superfamily. Biochem J, 2001. **360**(Pt 1): p. 1-16.
71. Whitbread, A.K., *et al*., Characterization of the omega class of glutathione transferases. Methods Enzymol, 2005. **401**: p. 78-99.
72. Barreto, L., *et al*., A peroxisomal glutathione transferase of *Saccharomyces cerevisiae* is functionally related to sulfur amino acid metabolism. Eukaryot Cell, 2006. **5**(10): p. 1748-59.
73. Slupphaug, G., B. Kavli, and H.E. Krokan, The interacting pathways for prevention and repair of oxidative DNA damage. Mutat Res, 2003. **531**(1-2): p. 231-51.
74. Poppek, D. and T. Grune, Proteasomal defense of oxidative protein modifications. Antioxid Redox Signal, 2006. **8**(1-2): p. 173-84.
75. Moye-Rowley, W.S., K.D. Harshman, and C.S. Parker, Yeast *YAP1* encodes a novel form of the jun family of transcriptional activator proteins. Genes Dev, 1989. **3**(3): p. 283-92.
76. Schnell, N., B. Krems, and K.D. Entian, The *PAR1* (*YAP1*/*SNQ3*) gene of *Saccharomyces cerevisiae*, a c-jun homologue, is involved in oxygen metabolism. Curr Genet, 1992. **21**(4-5): p. 269-73.
77. Zhang, X., *et al*., Analysis of the oxidative stress regulation of the *Candida albicans* transcription factor, Cap1p. Mol Microbiol, 2000. **36**(3): p. 618-29.
78. Quinn, J., *et al*., Distinct regulatory proteins control the graded transcriptional response to increasing H(2)O(2) levels in fission yeast *Schizosaccharomyces pombe*. Mol Biol Cell, 2002. **13**(3): p. 805-16.
79. Krems, B., C. Charizanis, and K.D. Entian, The response regulator-like protein Pos9/Skn7 of *Saccharomyces cerevisiae* is involved in oxidative stress resistance. Curr Genet, 1996. **29**(4): p. 327-34.
80. Singh, P., *et al*., *SKN7* of *Candida albicans*: mutant construction and phenotype analysis. Infect Immun, 2004. **72**(4): p. 2390-4.
81. Brown, J.L., S. North, and H. Bussey, *SKN7*, a yeast multicopy suppressor of a mutation affecting cell wall beta-glucan assembly, encodes a product with domains homologous to prokaryotic two-component regulators and to heat shock transcription factors. J Bacteriol, 1993. **175**(21): p. 6908-15.
82. Morgan, B.A., *et al*., A yeast transcription factor bypassing the requirement for *SBF* and *DSC1*/*MBF* in budding yeast has homology to bacterial signal transduction proteins. EMBO J, 1995. **14**(22): p. 5679-89.
83. Lee, J., *et al*., Yap1 and Skn7 control two specialized oxidative stress response regulons in yeast. J Biol Chem, 1999. **274**(23): p. 16040-6.
84. Morgan, B.A., *et al*., The Skn7 response regulator controls gene expression in the oxidative stress response of the budding yeast *Saccharomyces cerevisiae*. EMBO J, 1997. **16**(5): p. 1035-44.
85. Enjalbert, B., *et al*., Niche-specific activation of the oxidative stress response by the pathogenic fungus *Candida albicans*. Infect Immun, 2007. **75**(5): p. 2143-51.
86. Cuellar-Cruz, M., *et al*., High resistance to oxidative stress in the fungal pathogen *Candida glabrata* is mediated by a single catalase, Cta1p, and is controlled by the transcription factors Yap1p, Skn7p, Msn2p, and Msn4p. Eukaryot Cell, 2008. **7**(5): p. 814-25.

87. Nakagawa, Y., T. Kanbe, and I. Mizuguchi, Disruption of the human pathogenic yeast *Candida albicans* catalase gene decreases survival in mouse-model infection and elevates susceptibility to higher temperature and to detergents. Microbiol Immunol, 2003. **47**(6): p. 395-403.
88. Chaves, G.M., *et al*., *Candida albicans GRX2*, encoding a putative glutaredoxin, is required for virulence in a murine model. Genet Mol Res, 2007. **6**(4): p. 1051-63.
89. Hwang, C.S., *et al*., Copper- and zinc-containing superoxide dismutase (Cu/Zn*SOD*) is required for the protection of *Candida albicans* against oxidative stresses and the expression of its full virulence. Microbiology, 2002. **148**(Pt 11): p. 3705-13.
90. Johnson, C.H., *et al*., Redundancy, phylogeny and differential expression of *Histoplasma capsulatum* catalases. Microbiology, 2002. **148**(Pt 4): p. 1129-42.
91. Cox, G.M., *et al.*, Superoxide dismutase influences the virulence of Cryptococcus neoformans by affecting growth within macrophages. Infect Immun, 2003. **71**(1): p. 173-80.
92. Wilson, W.A. and P.J. Roach, Nutrient-regulated protein kinases in budding yeast. Cell, 2002. **111**(2): p. 155-8.
93. Gelade, R., *et al*., Multi-level response of the yeast genome to glucose. Genome Biol, 2003. **4**(11): p. 233.
94. Carlson, M., Glucose repression in yeast. Curr Opin Microbiol, 1999. **2**(2): p. 202-7.
95. Wang, Y., *et al*., Ras and Gpa2 mediate one branch of a redundant glucose signaling pathway in yeast. PLoS Biol, 2004. **2**(5): p. E128.
96. Santangelo, G.M., Glucose signaling in *Saccharomyces cerevisiae*. Microbiol Mol Biol Rev, 2006. **70**(1): p. 253-82.
97. Ozcan, S. and M. Johnston, Function and regulation of yeast hexose transporters. Microbiol Mol Biol Rev, 1999. **63**(3): p. 554-69.
98. Greatrix, B.W. and H.J. van Vuuren, Expression of the *HXT13*, *HXT15* and *HXT17* genes in *Saccharomyces cerevisiae* and stabilization of the HXT1 gene transcript by sugar-induced osmotic stress. Curr Genet, 2006. **49**(4): p. 205-17.
99. Ozcan, S., *et al*., Two glucose transporters in *Saccharomyces cerevisiae* are glucose sensors that generate a signal for induction of gene expression. Proc Natl Acad Sci U S A, 1996. **93**(22): p. 12428-32.
100. Ozcan, S., J. Dover, and M. Johnston, Glucose sensing and signaling by two glucose receptors in the yeast *Saccharomyces cerevisiae*. EMBO J, 1998. **17**(9): p. 2566-73.
101. Stapleton, D., *et al*., Mammalian 5'-AMP-activated protein kinase non-catalytic subunits are homologs of proteins that interact with yeast Snf1 protein kinase. J Biol Chem, 1994. **269**(47): p. 29343-6.
102. Erickson, J.R. and M. Johnston, Genetic and molecular characterization of *GAL83*: its interaction and similarities with other genes involved in glucose repression in *Saccharomyces cerevisiae*. Genetics, 1993. **135**(3): p. 655-64.
103. Bouly, J.P., *et al*., *Arabidopsis thaliana* proteins related to the yeast *SIP* and *SNF4* interact with AKINalpha1, an *SNF1*-like protein kinase. Plant J, 1999. **18**(5): p. 541-50.
104. Goffrini, P., *et al*., *FOG1* and *FOG2* genes, required for the transcriptional activation of glucose-repressible genes of *Kluyveromyces lactis*, are homologous to *GAL83* and *SNF1* of *Saccharomyces cerevisiae*. Curr Genet, 1996. **29**(4): p. 316-26.
105. Jiang, R. and M. Carlson, The Snf1 protein kinase and its activating subunit, Snf4, interact with distinct domains of the Sip1/Sip2/Gal83 component in the kinase complex. Mol Cell Biol, 1997. **17**(4): p. 2099-106.
106. Young, E.T., *et al*., Multiple pathways are co-regulated by the protein kinase Snf1 and the transcription factors Adr1 and Cat8. J Biol Chem, 2003. **278**(28): p. 26146-58.
107. Treitel, M.A., S. Kuchin, and M. Carlson, Snf1 protein kinase regulates phosphorylation of the Mig1 repressor in *Saccharomyces cerevisiae*. Mol Cell Biol, 1998. **18**(11): p. 6273-80.

108. Nath, N., R.R. McCartney, and M.C. Schmidt, Yeast Pak1 kinase associates with and activates Snf1. Mol Cell Biol, 2003. **23**(11): p. 3909-17.
109. Hong, S.P., *et al.*, Activation of yeast Snf1 and mammalian AMP-activated protein kinase by upstream kinases. Proc Natl Acad Sci U S A, 2003. **100**(15): p. 8839-43.
110. Wilson, W.A., S.A. Hawley, and D.G. Hardie, Glucose repression/derepression in budding yeast: *SNF1* protein kinase is activated by phosphorylation under derepressing conditions, and this correlates with a high AMP:ATP ratio. Curr Biol, 1996. **6**(11): p. 1426-34.
111. Sanz, P., *et al.*, Regulatory interactions between the Reg1-Glc7 protein phosphatase and the Snf1 protein kinase. Mol Cell Biol, 2000. **20**(4): p. 1321-8.
112. Tachibana, C., *et al*., Combined global localization analysis and transcriptome data identify genes that are directly coregulated by Adr1 and Cat8. Mol Cell Biol, 2005. **25**(6): p. 2138-46.
113. Vincent, O. and M. Carlson, Sip4, a Snf1 kinase-dependent transcriptional activator, binds to the carbon source-responsive element of gluconeogenic genes. EMBO J, 1998. **17**(23): p. 7002-8.
114. Schmidt, M.C., *et al*., Std1 and Mth1 proteins interact with the glucose sensors to control glucose-regulated gene expression in *Saccharomyces cerevisiae*. Mol Cell Biol, 1999. **19**(7): p. 4561-71.
115. Li, F.N. and M. Johnston, Grr1 of *Saccharomyces cerevisiae* is connected to the ubiquitin proteolysis machinery through Skp1: coupling glucose sensing to gene expression and the cell cycle. EMBO J, 1997. **16**(18): p. 5629-38.
116. Rolland, F., *et al.*, The role of hexose transport and phosphorylation in cAMP signalling in the yeast *Saccharomyces cerevisiae*. FEMS Yeast Res, 2001. **1**(1): p. 33-45.
117. Rolland, F., *et al.*, Glucose-induced cAMP signalling in yeast requires both a G-protein coupled receptor system for extracellular glucose detection and a separable hexose kinase-dependent sensing process. Mol Microbiol, 2000. **38**(2): p. 348-58.
118. Kubler, E., *et al*., Gpa2p, a G-protein alpha-subunit, regulates growth and pseudohyphal development in *Saccharomyces cerevisiae* via a cAMP-dependent mechanism. J Biol Chem, 1997. **272**(33): p. 20321-3.
119. Maidan, M.M., *et al.*, The G protein-coupled receptor Gpr1 and the Galpha protein Gpa2 act through the cAMP-protein kinase A pathway to induce morphogenesis in *Candida albicans*. Mol Biol Cell, 2005. **16**(4): p. 1971-86.
120. De Wever, V., *et al*., A dual role for PP1 in shaping the Msn2-dependent transcriptional response to glucose starvation. EMBO J, 2005. **24**(23): p. 4115-23.
121. Rohde, J.R., *et al*., Nutritional control via Tor signaling in *Saccharomyces cerevisiae*. Curr Opin Microbiol, 2008. **11**(2): p. 153-60.
122. Weisman, R. and M. Choder, The fission yeast *TOR* homolog, tor1+, is required for the response to starvation and other stresses via a conserved serine. J Biol Chem, 2001. **276**(10): p. 7027-32.
123. Hinnebusch, A.G. and K. Natarajan. Gcn4p, a master regulator of gene expression, is controlled at multiple levels by diverse signals of starvation and stress. Eukaryot Cell 2002 Feb [cited 1 1]; 2002/11/29:[22-32].
124. McCourtie, J. and L.J. Douglas, Relationship between cell surface composition, adherence, and virulence of *Candida albicans*. Infect Immun, 1984. **45**(1): p. 6-12.
125. Batista, A.S., L.C. Miletti, and B.U. Stambuk, Sucrose fermentation by *Saccharomyces cerevisiae* lacking hexose transport. J Mol Microbiol Biotechnol, 2004. **8**(1): p. 26-33.
126. Bhat, P.J. and T.V. Murthy, Transcriptional control of the *GAL/MEL* regulon of yeast *Saccharomyces cerevisiae*: mechanism of galactose-mediated signal transduction. Mol Microbiol, 2001. **40**(5): p. 1059-66.
127. Brown, V., J. Sabina, and M. Johnston, Specialized sugar sensing in diverse fungi. Curr Biol, 2009. **19**(5): p. 436-41.

128. Rubio-Texeira, M., A comparative analysis of the *GAL* genetic switch between not-so-distant cousins: *Saccharomyces cerevisia*e versus *Kluyveromyces lactis*. FEMS Yeast Res, 2005. **5**(12): p. 1115-28.
129. Kusch, H., *et al*., A proteomic view of *Candida albicans* yeast cell metabolism in exponential and stationary growth phases. Int J Med Microbiol, 2008. **298**(3-4): p. 291-318.
130. Kraft, C., F. Reggiori, and M. Peter, Selective types of autophagy in yeast. Biochim Biophys Acta, 2009.
131. Kamada, Y., T. Sekito, and Y. Ohsumi, Autophagy in yeast: a TOR-mediated response to nutrient starvation. Curr Top Microbiol Immunol, 2004. **279**: p. 73-84.
132. Dubouloz, F., *et al*., The TOR and EGO protein complexes orchestrate microautophagy in yeast. Mol Cell, 2005. **19**(1): p. 15-26.
133. Hardwick, J.S., *et al*., Rapamycin-modulated transcription defines the subset of nutrient-sensitive signaling pathways directly controlled by the Tor proteins. Proc Natl Acad Sci U S A, 1999. **96**(26): p. 14866-70.
134. Werner-Washburne, M., *et al*., Stationary phase in the yeast *Saccharomyces cerevisiae.* Microbiol Rev, 1993. **57**(2): p. 383-401.
135. Barbet, N.C., *et al*., TOR controls translation initiation and early G1 progression in yeast. Mol Biol Cell, 1996. **7**(1): p. 25-42.
136. Shintani, T., *et al*., Mechanism of cargo selection in the cytoplasm to vacuole targeting pathway. Dev Cell, 2002. **3**(6): p. 825-37.
137. Huang, W.P. and D.J. Klionsky, Autophagy in yeast: a review of the molecular machinery. Cell Struct Funct, 2002. **27**(6): p. 409-20.
138. Kunz, J.B., H. Schwarz, and A. Mayer, Determination of four sequential stages during microautophagy in vitro. J Biol Chem, 2004. **279**(11): p. 9987-96.
139. Kim, I., S. Rodriguez-Enriquez, and J.J. Lemasters, Selective degradation of mitochondria by mitophagy. Arch Biochem Biophys, 2007. **462**(2): p. 245-53.
140. Hamasaki, M., *et al.*, Starvation triggers the delivery of the endoplasmic reticulum to the vacuole via autophagy in yeast. Traffic, 2005. **6**(1): p. 56-65.
141. Bernales, S., S. Schuck, and P. Walter, ER-phagy: selective autophagy of the endoplasmic reticulum. Autophagy, 2007. **3**(3): p. 285-7.
142. Kraft, C., *et al*., Mature ribosomes are selectively degraded upon starvation by an autophagy pathway requiring the Ubp3p/Bre5p ubiquitin protease. Nat Cell Biol, 2008. **10**(5): p. 602-10.
143. Iwata, J., *et al*., Excess peroxisomes are degraded by autophagic machinery in mammals. J Biol Chem, 2006. **281**(7): p. 4035-41.
144. Dunn, W.A., Jr., *et al*., Pexophagy: the selective autophagy of peroxisomes. Autophagy, 2005. **1**(2): p. 75-83.
145. Roberts, P., *et al*., Piecemeal microautophagy of nucleus in *Saccharomyces cerevisiae*. Mol Biol Cell, 2003. **14**(1): p. 129-41.
146. Krick, R., *et al*., Piecemeal microautophagy of the nucleus requires the core macroautophagy genes. Mol Biol Cell, 2008. **19**(10): p. 4492-505.
147. Xie, Z. and D.J. Klionsky, Autophagosome formation: core machinery and adaptations. Nat Cell Biol, 2007. **9**(10): p. 1102-9.
148. Kim, J., *et al*., Cvt9/Gsa9 functions in sequestering selective cytosolic cargo destined for the vacuole. J Cell Biol, 2001. **153**(2): p. 381-96.
149. Kim, P.K., *et al.*, Ubiquitin signals autophagic degradation of cytosolic proteins and peroxisomes. Proc Natl Acad Sci U S A, 2008. **105**(52): p. 20567-74.
150. Hu, G., *et al*., PI3K signaling of autophagy is required for starvation tolerance and virulenceof *Cryptococcus neoformans*. J Clin Invest, 2008. **118**(3): p. 1186-97.
151. Fan, W., *et al*., *Cryptococcus neoformans* gene expression during murine macrophage infection. Eukaryot Cell, 2005. **4**(8): p. 1420-33.

152. Palmer, G.E., M.N. Kelly, and J.E. Sturtevant, Autophagy in the pathogen *Candida albicans*. Microbiology, 2007. **153**(Pt 1): p. 51-8.
153. Palmer, G.E., D.S. Askew, and P.R. Williamson, The diverse roles of autophagy in medically important fungi. Autophagy, 2008. **4**(8): p. 982-8.
154. Vanden Bossche, H., P. Marichal, and F.C. Odds, Molecular mechanisms of drug resistance in fungi. Trends Microbiol, 1994. **2**(10): p. 393-400.
155. Fardeau, V., *et al*., The central role of *PDR1* in the foundation of yeast drug resistance. J Biol Chem, 2007. **282**(7): p. 5063-74.
156. Moye-Rowley, W.S., Transcriptional control of multidrug resistance in the yeast *Saccharomyces*. Prog Nucleic Acid Res Mol Biol, 2003. **73**: p. 251-79.
157. Balzi, E., *et al*., The multidrug resistance gene *PDR1* from *Saccharomyces cerevisiae*. J Biol Chem, 1987. **262**(35): p. 16871-9.
158. Delaveau, T., *et al*., *PDR3,* a new yeast regulatory gene, is homologous to *PDR1* and controls the multidrug resistance phenomenon. Mol Gen Genet, 1994. **244**(5): p. 501-11.
159. Schüller, C., *et al*., Membrane-active compounds activate the transcription factors Pdr1 and Pdr3 connecting pleiotropic drug resistance and membrane lipid homeostasis in *Saccharomyces cerevisiae*. Mol Biol Cell, 2007. **18**(12): p. 4932-44.
160. Mamnun, Y.M., C. Schüller, and K. Kuchler, Expression regulation of the yeast *PDR5* ATP-binding cassette (ABC) transporter suggests a role in cellular detoxification during the exponential growth phase. FEBS Lett, 2004. **559**(1-3): p. 111-7.
161. Prasad, R., S.K. Murthy, and V. Gupta, Multiple drug resistance in *Candida albicans*. Acta Biochim Pol, 1995. **42**(4): p. 497-504.
162. Sanglard, D., *et al*., Cloning of *Candida albicans* genes conferring resistance to azole antifungal agents: characterization of *CDR2*, a new multidrug ABC transporter gene. Microbiology, 1997. **143 (Pt 2)**: p. 405-16.
163. Coste, A.T., *et al.*, *TAC1,* transcriptional activator of *CDR* genes, is a new transcription factor involved in the regulation of *Candida albicans* ABC transporters *CDR1* and *CDR2.* Eukaryot Cell, 2004. **3**(6): p. 1639-52.
164. Sanglard, D., *et al*., The ATP binding cassette transporter gene *CgCDR1* from *Candida glabrata* is involved in the resistance of clinical isolates to azole antifungal agents. Antimicrob Agents Chemother, 1999. **43**(11): p. 2753-65.
165. Sanglard, D., F. Ischer, and J. Bille, Role of ATP-binding-cassette transporter genes in high-frequency acquisition of resistance to azole antifungals in *Candida glabrata*. Antimicrob Agents Chemother, 2001. **45**(4): p. 1174-83.
166. Torelli, R., *et al*., The ATP-binding cassette transporter-encoding gene *CgSNQ2* is contributing to the *CgPDR1*-dependent azole resistance of *Candida glabrata*. Mol Microbiol, 2008. **68**(1): p. 186-201.
167. Brieland, J., *et al*., Comparison of pathogenesis and host immune responses to *Candida glabrata* and *Candida albicans* in systemically infected immunocompetent mice. Infect Immun, 2001. **69**(8): p. 5046-55.
168. Soll, D.R., High-frequency switching in *Candida albicans*. Clin Microbiol Rev, 1992. **5**(2): p. 183-203.
169. Mencacci, A., *et al*., CD4+ T-helper-cell responses in mice with low-level *Candida albicans* infection. Infect Immun, 1996. **64**(12): p. 4907-14.
170. Louie, A., et al., Tumor necrosis factor alpha has a protective role in a murine model of systemic candidiasis. Infect Immun, 1994. **62**(7): p. 2761-72.
171. Marquis, G., *et al*., Histochemical and immunochemical study of the fate of *Candida albicans* inside human neutrophil phagolysosomes. J Leukoc Biol, 1991. **50**(6): p. 587-99.
172. Mencacci, A., *et al.*, Defective co-stimulation and impaired Th1 development in tumor necrosis factor/lymphotoxin-alpha double-deficient mice infected with *Candida albicans*. Int Immunol, 1998. **10**(1): p. 37-48.

173. Hachicha, M., *et al.*, Regulation of chemokine gene expression in human peripheral blood neutrophils phagocytosing microbial pathogens. J Immunol, 1998. **160**(1): p. 449-54.
174. Roilides, E., *et al.*, Suppressive effects of interleukin-10 on human mononuclear phagocyte function against *Candida albicans* and *Staphylococcus aureus*. J Infect Dis, 1998. **178**(6): p. 1734-42.
175. Romani, L., *et al*., Neutralization of IL-10 up-regulates nitric oxide production and protects susceptible mice from challenge with *Candida albicans.* J Immunol, 1994. **152**(7): p. 3514-21.
176. Romani, L., Innate and adaptive immunity in *Candida albicans* infections and saprophytism. J Leukoc Biol, 2000. **68**(2): p. 175-9.
177. Mencacci, A., et al., IL-10 is required for development of protective Th1 responses in IL-12-deficient mice upon *Candida albicans* infection. J Immunol, 1998. **161**(11): p. 6228-37.
178. Mencacci, A., *et al.*, Endogenous interleukin 4 is required for development of protective CD4+ T helper type 1 cell responses to *Candida albicans*. J Exp Med, 1998. **187**(3): p. 307-17.
179. Romani, L., Immunity to *Candida albicans*: Th1, Th2 cells and beyond. Curr Opin Microbiol, 1999. **2**(4): p. 363-7.
180. Clemons, K.V., *et al.*, Pathogenesis I: interactions of host cells and fungi. Med Mycol, 2000. **38 Suppl 1**: p. 99-111.
181. Wagner, R.D., *et al*., B cell knockout mice are resistant to mucosal and systemic candidiasis of endogenous origin but susceptible to experimental systemic candidiasis. J Infect Dis, 1996. **174**(3): p. 589-97.
182. Matthews, R.C., J.P. Burnie, and S. Tabaqchali, Isolation of immunodominant antigens from sera of patients with systemic candidiasis and characterization of serological response to *Candida albicans*. J Clin Microbiol, 1987. **25**(2): p. 230-7.
183. Han, Y., R.P. Morrison, and J.E. Cutler, A vaccine and monoclonal antibodies that enhance mouse resistance to *Candida albicans* vaginal infection. Infect Immun, 1998. **66**(12): p. 5771-6.
184. Han, Y., M.A. Ulrich, and J.E. Cutler, *Candida albicans* mannan extract-protein conjugates induce a protective immune response against experimental candidiasis. J Infect Dis, 1999. **179**(6): p. 1477-84.
185. Geisow, M.J., P. D'Arcy Hart, and M.R. Young, Temporal changes of lysosome and phagosome pH during phagolysosome formation in macrophages: studies by fluorescence spectroscopy. J Cell Biol, 1981. **89**(3): p. 645-52.
186. Levitz, S.M., *et al*., *Cryptococcus neoformans* resides in an acidic phagolysosome of human macrophages. Infect Immun, 1999. **67**(2): p. 885-90.
187. Kaposzta, R., *et al*., Rapid recruitment of late endosomes and lysosomes in mouse macrophages ingesting *Candida albicans*. J Cell Sci, 1999. **112 (Pt 19)**: p. 3237-48.
188. Becker, K., *et al*., Oxidative stress in malaria parasite-infected erythrocytes: host-parasite interactions. Int J Parasitol, 2004. **34**(2): p. 163-89.
189. Voyich, J.M., *et al.*, Insights into mechanisms used by *Staphylococcus aureus* to avoid destruction by human neutrophils. J Immunol, 2005. **175**(6): p. 3907-19.
190. Prigneau, O., *et al.*, Genes involved in beta-oxidation, energy metabolism and glyoxylate cycle are induced by *Candida albicans* during macrophage infection. Yeast, 2003. **20**(8): p. 723-30.
191. Lorenz, M.C., J.A. Bender, and G.R. Fink, Transcriptional response of *Candida albicans* upon internalization by macrophages. Eukaryot Cell, 2004. **3**(5): p. 1076-87.
192. Flores, C.L., *et al*., Carbohydrate and energy-yielding metabolism in non-conventional yeasts. FEMS Microbiol Rev, 2000. **24**(4): p. 507-29.
193. Barelle, C.J., *et al*., Niche-specific regulation of central metabolic pathways in a fungal pathogen. Cell Microbiol, 2006. **8**(6): p. 961-71.

194. Lorenz, M.C. and G.R. Fink, The glyoxylate cycle is required for fungal virulence. Nature, 2001. **412**(6842): p. 83-6.
195. Zarember, K.A., *et al.*, Human polymorphonuclear leukocytes inhibit *Aspergillus fumigatus* conidial growth by lactoferrin-mediated iron depletion. J Immunol, 2007. **178**(10): p. 6367-73.
196. Ward, P.P., E. Paz, and O.M. Conneely, Multifunctional roles of lactoferrin: a critical overview. Cell Mol Life Sci, 2005. **62**(22): p. 2540-8.
197. Weinberg, E.D., Human lactoferrin: a novel therapeutic with broad spectrum potential. J Pharm Pharmacol, 2001. **53**(10): p. 1303-10.
198. Soukka, T., J. Tenovuo, and M. Lenander-Lumikari, Fungicidal effect of human lactoferrin against *Candida albicans*. FEMS Microbiol Lett, 1992. **69**(3): p. 223-8.
199. Chua, J., *et al.*, A tale of two lipids: Mycobacterium tuberculosis phagosome maturation arrest. Curr Opin Microbiol, 2004. **7**(1): p. 71-7.
200. Gomes, M.S., *et al.*, Survival of *Mycobacterium avium* and *Mycobacterium tuberculosis* in acidified vacuoles of murine macrophages. Infect Immun, 1999. **67**(7): p. 3199-206.
201. Saito, F., *et al.*, Inefficient phagosome maturation in infant macrophages. Biochem Biophys Res Commun, 2008. **375**(1): p. 113-8.
202. Via, L.E., *et al.*, Effects of cytokines on mycobacterial phagosome maturation. J Cell Sci, 1998. **111 (Pt 7)**: p. 897-905.

Aim of this work:

Although *Candida glabrata* shares the same genus name with *Candida albicans*, it is much closer related to *Saccharomyces cerevisiae*. Therefore it was the aim to find out more about striking similarities and discrepancies between *C. glabrata* and *S. cerevisiae*. Despite their close relatedness, only *C. glabrata* evolved into a commensal/pathogen.

The following study can be divided in three parts:

1) Characterization of the environmental stress response (ESR) in *C. glabrata*.

S. cerevisiae, *S. pombe* and *C. albicans* have a qualitatively similar ESR. It was the aim to define the genome wide environmental stress response expression profile of *C. glabrata*. Therefore cells were exposed to different stress such as heat stress, glucose starvation, osmotic and oxidative stress. Further, in *S. cerevisiae*, Msn2 and Msn4 are important transcription factors of the ESR. Comparing several putative Msn2-like sequences, a related group of fungi among the class Saccharomycotina possessing Msn2 orthologues was identified. In *C. glabrata*, orthologues for Msn2 and Msn4 were found. Their role in the ESR and their contribution to virulence was investigated.

2) Analysis of the in vivo situation upon engulfment through primary mouse macrophages.

To erase microbes, phagocytic cells try to catch and engulf them. Captured intruders have evolved different strategies to resist engulfment. For example, *C. albicans* is able to escape phagocytosis through hyphae formation. To investigate the response of *C. glabrata* to engulfment, fluorescent reporter proteins were employed. Microscopy revealed a transient acute oxidative stress and lasting glucose starvation inside the phagosome of macrophages. During prolonged phagocytosis, a decline of peroxisome numbers due to pexophagy was observed. CgAtg11 and CgAtg17 were found to be crucial factors to mediate this response. Both selective and non-selective autophagic processes were shown to contribute to survival.

3) Investigation of the role of the two oxidative stress response transcription factors CgSkn7 and CgYap1 in *C. glabrata* in vitro and in vivo.

In *S. cerevisiae*, two transcription factors, Skn7 and Yap1, are responsible for rapid transcription upon oxidative stress. In *C. glabrata,* the orthologous transcription factors CgSkn7 and CgYap1 induce the majority of crucial genes of the oxidative stress regulon. Their contribution to virulence was investigated in an ex vivo model.

Additionally, analysis of the binding capacities of CgSkn7 and CgYap1 revealed a strict dependence on each other to induce expression of set of target genes. Finally, during glucose starvation, numerous genes of the oxidative stress regulon get induced, which may mimic the in vivo situation upon engulfment by phagocytes.

2. Results:

2.1. *Candida glabrata* environmental stress response involves *Saccharomyces cerevisiae* Msn2/4 orthologues transcription factors

2.2. Autophagy supports *Candida glabrata* survival during phagocytosis

2.3. CgSkn7 and CgYap1 mediate key responses to oxidative stress in *Candida glabrata*

2.4. Major results obtained

Molecular Microbiology (2008) 69(3), 603–620 ■
doi:10.1111/j.1365-2958.2008.06301.x
First published online 16 June 2008

Candida glabrata environmental stress response involves *Saccharomyces cerevisiae* Msn2/4 orthologous transcription factors

Andreas Roetzer,[1] Christa Gregori,[2] Ann Marie Jennings,[3] Jessica Quintin,[4] Dominique Ferrandon,[4] Geraldine Butler,[3] Karl Kuchler,[2] Gustav Ammerer[1] and Christoph Schüller[1]*

[1]*University of Vienna, Max F. Perutz Laboratories, Department of Biochemistry, A-1030 Vienna, Austria.*
[2]*Medical University Vienna, Max F. Perutz Laboratories, CD Laboratory for Infection Biology, A-1030 Vienna, Austria.*
[3]*School of Biomolecular and Biomedical Science, Conway Institute, University College Dublin, Belfield, Dublin 4, Ireland.*
[4]*FranceEquipe Fondation Recherche Médicale, UPR 9022 du CNRS, IBMC, 15, rue R. Descartes F67084 Strasbourg Cedex France.*

Summary

We determined the genome-wide environmental stress response (ESR) expression profile of *Candida glabrata*, a human pathogen related to *Saccharomyces cerevisiae*. Despite different habitats, *C. glabrata*, *S. cerevisiae*, *Schizosaccharomyces pombe* and *Candida albicans* have a qualitatively similar ESR. We investigate the function of the *C. glabrata* syntenic orthologues to the ESR transcription factor Msn2. The *C. glabrata* orthologues CgMsn2 and CgMsn4 contain a motif previously referred to as HD1 (homology domain 1) also present in Msn2 orthologues from fungi closely related to *S. cerevisiae*. We show that regions including this motif confer stress-regulated intracellular localization when expressed in *S. cerevisiae*. Site-directed mutagenesis confirms that nuclear export of CgMsn2 in *C. glabrata* requires an intact HD1. Transcript profiles of CgMsn2/4 mutants and CgMsn2 overexpression strains show that they regulate a part of the CgESR. CgMsn2 complements a *S. cerevisiae msn2* null mutant and in stressed *C. glabrata* cells, rapidly translocates from the cytosol to the nucleus. CgMsn2 is required for full resistance against severe osmotic stress and rapid and full induction of trehalose synthesis genes (*TPS1*, *TPS2*). Constitutive activation of CgMsn2 is detrimental for *C. glabrata.* These results establish an Msn2-regulated general stress response in *C. glabrata*.

Accepted 12 May, 2008. *For correspondence. E-mail christoph.schueller@univie.ac.at; Tel. (+43) 1 4277 52815; Fax (+43) 1 4277 9528.

Introduction

Adaptation of gene expression through regulation of transcription is a key mechanism in fungal response to fluctuating environmental conditions. Environmental stress causes activation of a variety of signalling mechanisms each responding to the particular situation, such as heat shock or osmotic stress, and in parallel evokes a stereotypic general response. In *Saccharomyces cerevisiae*, this response was first described and is referred to as general stress response or environmental stress response (ESR) (Gasch *et al.*, 2000; Causton *et al.*, 2001). Comparable ESR patterns have been characterized in *Schizosaccharomyces pombe* and to a certain extent in *Candida albicans* (Smith *et al.*, 2004; Enjalbert *et al.*, 2006; Gasch, 2007). *Candida glabrata* is more closely related to *S. cerevisiae* than *C. albicans* and *S. pombe* (Fitzpatrick *et al.*, 2006), and is the second most common fungal pathogen isolated from humans (Kaur *et al.*, 2005; Pfaller and Diekema, 2007). Infection rates are relatively low but have been constant during the last decade (Sandven *et al.*, 2006). The ESR of *C. glabrata* is currently relatively unexplored.

For *S. cerevisiae*, *C. albicans* and *S. pombe*, one major mechanism for controlling general stress responses are p38-type SAP kinases (stress-activated mitogen-activated protein kinases). The SAPKs, Hog1, Sty1 and CaHog1 are all activated by hyperosmolarity and oxidative stress, and to a varying degree by other stress agents, such as cadmium (Chen *et al.*, 2003; Smith *et al.*, 2004; Enjalbert *et al.*, 2006). The HOG (high osmolarity glycerol) pathway of *C. glabrata* functions in a similar manner to *S. cerevisiae* (Gregori *et al.*, 2007).

Fig. 1. Comparison of genome-wide expression levels in response to environmental changes in *C. glabrata* and *S. cerevisiae*.
A. Hierarchical clustering. Transcript profiles were determined by hybridization to genome-wide *C. glabrata* microarrays. The sets represent average inductions of replicate profiles of *C. glabrata* wild-type strain (4166 ORFs) after treatment with 0.4 mM H_2O_2, upon glucose starvation, heat shock by incubation at 42°C and hyperosmolarity stress treatment with 0.5 M NaCl (left panel). All treatments were done at 30°C for 20 min. The developed profile was compared with corresponding *S. cerevisiae* expression data (Gasch *et al.*, 2000) (right panel). Major clusters are labelled corresponding to induced and to repressed genes (labelled as 1 and 2), in both *C. glabrata* and *S. cerevisiae*.
B. Genes involved in four different stress responses were clustered after specific selection (heat stress > 11-fold, osmotic stress > sixfold, oxidative stress > sixfold and glucose starvation > 10-fold). Identified clusters in both *C. glabrata* and *S. cerevisiae* are indicated. Gene names correspond to *C. glabrata* systematic ORF designations and their corresponding *S. cerevisiae* orthologues.
C. The overlap between the CgESR and ScESR patterns is depicted as Venn diagram. CgESR was defined as described in Fig. 2A, with genes induced or repressed at least in one tested condition; ScESR data are from Gasch *et al.* (2000).

In *S. cerevisiae*, a second general stress-mediating mechanism based on the transcription factor Msn2 and its paralogue Msn4 exists (Martinez-Pastor *et al.*, 1996; Estruch, 2000; Gasch *et al.*, 2000; Causton *et al.*, 2001; Hohmann, 2002). They are activated by a variety of stress conditions and changing nutrient supply situations, such as the exhaustion of the preferred carbon source glucose (Choo and Klug, 1994; Martinez-Pastor *et al.*, 1996; DeRisi *et al.*, 1997; Boy-Marcotte *et al.*, 1998; Gasch *et al.*, 2000; Rep *et al.*, 2000; Causton *et al.*, 2001; Hasan *et al.*, 2002; Cameroni *et al.*, 2004; Schüller *et al.*, 2004; Teixeira *et al.*, 2006). They also have a role in both chronological and replicative ageing (Fabrizio *et al.*, 2001; 2004; Powers *et al.*, 2006). During high-nutrient supply, Msn2 is inactivated by the PKA (protein kinase A) and TOR (target of rapamycin) pathways (Boy-Marcotte *et al.*, 1998; Görner *et al.*, 1998; Garreau *et al.*, 2000; Görner *et al.*, 2002). Activation of Msn2 and Msn4 causes their rapid accumulation in the nucleus and recruitment to chromatin. Msn2 has separate functional domains for nuclear import (nuclear localization signal, NLS), nuclear export (nuclear export signal, NES) and DNA binding. The C_2H_2 Zn finger DNA binding domain at the C-terminus recognizes the stress response element (STRE). The NLS is found adjacent to the DNA binding domain; it is phosphorylated and inactivated by PKA when glucose is available and rapidly dephosphorylated and activated by glucose starvation (Görner *et al.*, 2002; De Wever *et al.*, 2005). Stress signalling requires a region in the N-terminal part of Msn2 which includes its NES and a short stretch of high similarity to Msn4 designated homology domain 1 (HD1) (Görner *et al.*, 1998; Görner *et al.*, 2002; Durchschlag *et al.*, 2004; Boy-Marcotte *et al.*, 2006). A variety of stress conditions lead to inhibition of nuclear export of Msn2 by an unknown mechanism. The NES and its surrounding region might therefore represent a crucial determinant for the identification of stress-regulated Msn2 orthologues.

Msn2-like factors do not appear to play a role in regulating the stress response in *C. albicans* and *S. pombe.* The *C. albicans* Msn2 orthologue transcription factor designated CaMsn4 (orf 19.4752) is not involved in the ESR (Nicholls *et al.*, 2004). In addition, the Hog1 Map kinase plays a more general role in stress response in *C. albicans* and *S. pombe.* These differences point to distinct strategies for regulating the stress response in different fungi.

Here we investigate ESR transcription patterns of *C. glabrata* and provide evidence that it uses an *S. cerevisiae*-like Msn2-directed stress response. We identify *C. glabrata* Msn2 and Msn4 orthologues based on a motif present in the Msn2/4 NES (HD1) and also in putative Msn2 orthologues of *Ashbya gossypii* and *Kluyveromyces lactis*. Furthermore, we find that *C. glabrata* and *S. cerevisiae* share many common Msn2 target genes. CgMsn2 is required for resistance against severe osmotic stress. In addition, comparison of ESR transcript patterns identifies core similarities and differences between the *S. cerevisiae*, *C. albicans*, *S. pombe* and *C. glabrata* stress responses.

Results

The ESR pattern of C. glabrata *is orthologous to* S. cerevisiae

The global immediate transcriptional response of *C. glabrata* to a set of environmental conditions was determined via microarray analysis. Conditions chosen were acute carbon starvation by removal of glucose from the medium, mild osmotic stress (0.5 M NaCl), heat stress (42°C) and mild oxidative stress (0.4 mM hydrogen peroxide). The treatment times were 20 min at 30°C to avoid indirect transcriptional responses. Transcript profiles were determined by hybridization to genome-wide *C. glabrata* microarrays. Expression data were filtered and averaged. From the 5063 genes spotted in duplicate, 4166 gave useful data under at least one tested condition. The entire data set was analysed for co-regulated genes by hierarchical clustering (Eisen *et al.*, 1998).

Similar to the common stress response identified in *S. cerevisiae*, *C. glabrata* has a set of induced and repressed genes common to several stress conditions (Fig. 1A). To compare the *C. glabrata* expression pattern with *S. cerevisiae* data, we used a similarity-based annotation of orthologous genes (Feldmann, 2000) (http://cbi.labri.fr/Genolevures/). Expression data for *S. cerevisiae* exposed to comparable conditions, such as glucose starvation, 0.32 mM H_2O_2, heat stress (37°C) and 1 M Sorbitol osmotic stress, were extracted from published ESR data

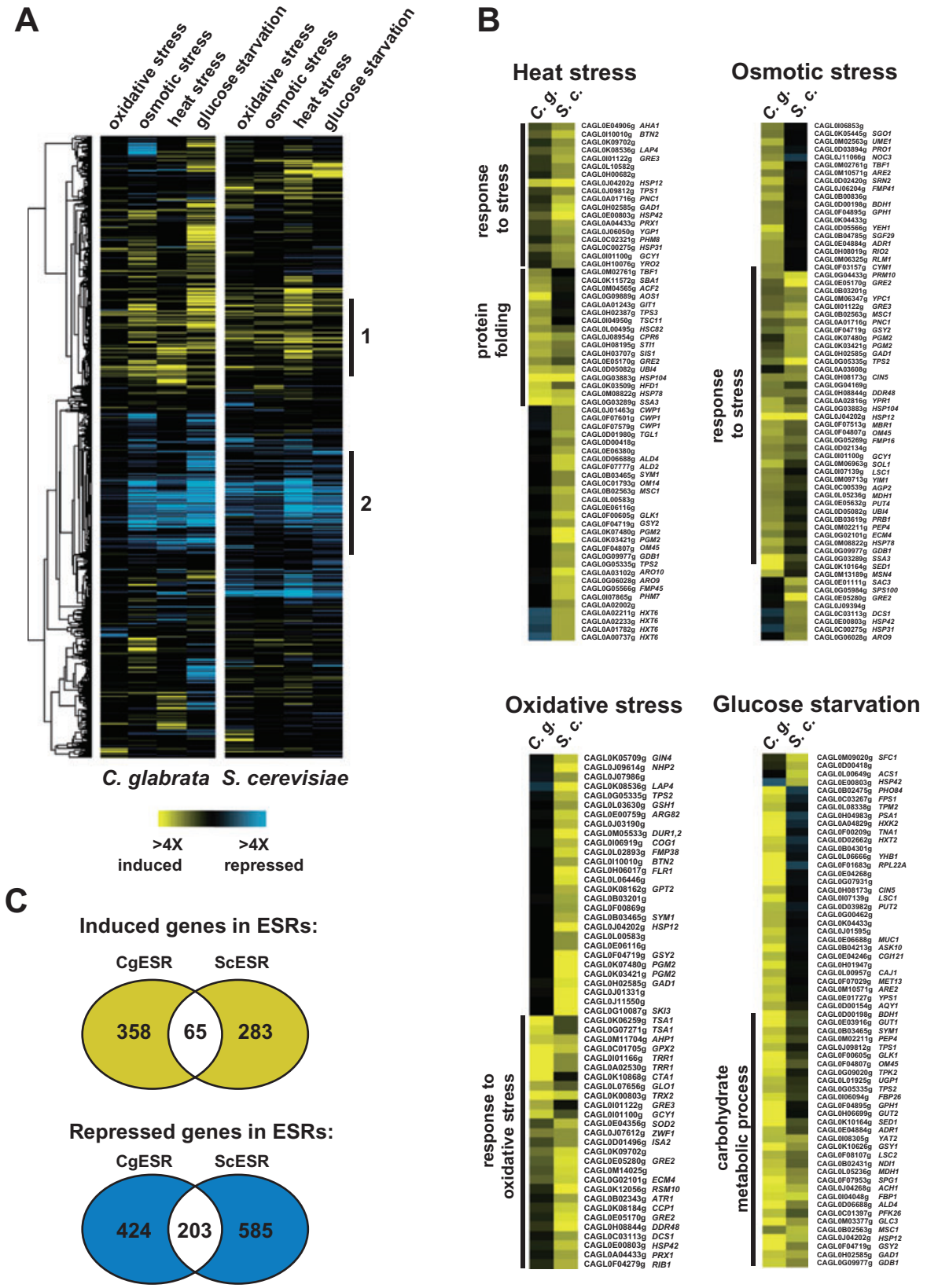

(Gasch *et al*., 2000). *C. glabrata* has a optimal growth temperature of 37°C and was therefore heat-stressed at 42°C. Available evidence suggests that NaCl and Sorbitol are comparable in the concentrations used (Hirasawa *et al*., 2006). Analysis of both ESR data sets highlights clusters corresponding to induced and repressed genes for all environmental conditions (Fig. 1A). This indicates a conserved transcriptional response between *C. glabrata* and *S. cerevisiae*. More detailed comparison of individual stress conditions shows induction of expression of orthologous genes (Fig. 1B). For example, heat stress induces expression of conserved HSP genes in both organisms (*HSP12*, *HSP42*, *HSP78*, *HSP31*, *HSP104*), whereas oxidative stress affects a smaller set of genes in *C. glabrata*. The hydrogen peroxide concentration chosen (0.4 mM) is stressful for *S. cerevisiae* laboratory strains. Furthermore, 0.4 mM H_2O_2 *in vitro* corresponds to the *in vivo* oxidative burden in phagocytic cells as judged by the similar transcriptional response of *C. albicans* (Enjalbert *et al*., 2007). However, *C. glabrata* strains are much more resistant to oxidative stress *in vitro* and have a less pronounced response to this concentration. Nevertheless, we find a characteristic pattern of induced genes with functions in oxidative stress response. These include core oxidative stress response genes, such as *TRR1*, *TRX1*, *CTA1*, *SOD1* and *GPX1*.

Glucose starvation and osmotic stress each induce a set of genes orthologous to *S. cerevisiae*. These include *GPH1*, *TPS1*, *TPS2*, *UGP1*, *GSY1* and *GLK1* for glucose starvation and *GRE3*, *PGM2*, *HSP12*, *DDR48* or *SSA3* during osmotic stress. The elevated expression of *TPS1*, *TPS2* and also *TPS3* is perhaps important, as trehalose has a protective role against environmental stresses (Petter and Kwon-Chung, 1996). Taken together, these patterns suggested that the ESR is conserved between *S. cerevisiae* and *C. glabrata*. The overlap between the two ESR patterns is depicted as a Venn diagram of conserved induced and repressed genes (Fig. 1C). The vast majority of repressed genes in both *S. cerevisiae* and *C. glabrata* are involved in ribosome biogenesis. Interestingly and in contrast to *S. cerevisiae*, expression of *C. glabrata* genes involved in sterol biosynthesis (*ERG1*, *ERG2*, *ERG3*, *ERG11*, *ERG13* and *ERG25*) was repressed under all conditions tested. *ERG3* and *ERG11* deletions confer azole resistance (Geber *et al*., 1995).

Some differences between both ESRs are notable. The detailed data are available as supplementary files. *TBF1*, encoding a Telobox-containing general regulatory factor (Bilaud *et al*., 1996), is highly upregulated in *C. glabrata*, whereas it is mainly downregulated in *S. cerevisiae* throughout the conditions compared. *PHO84*, a high-affinity inorganic phosphate transporter and low-affinity manganese transporter (Bun-Ya *et al*., 1991), is downregulated during all stress responses in *S. cerevisiae*, but upregulated in *C. glabrata* during oxidative stress and glucose starvation. The integral membrane protein *VPH2*, required for vacuolar H^+-ATPase function (Jackson and Stevens, 1997), is highly induced in all tested conditions in *C. glabrata*, whereas it is slightly induced only by oxidative stress in *S. cerevisiae.*

Part of the ESR is also conserved between *C. glabrata*, *S. pombe*, *C. albicans* and *S. cerevisiae.* To compare expression patterns of the four fungi, we used reported orthologous genes between *S. pombe*, *C. albicans* and *S. cerevisiae* (Enjalbert *et al*., 2006). We extended this list by adding the corresponding *C. glabrata* genes with gene similarity data reported by the Genolevures consortium. Data used to generate these figures are available as supplementary files. Comparison of the specific expression profiles revealed a striking overlap between orthologous genes of the individual species for osmotic stress-induced genes (Fig. S2A) and oxidative stress-induced genes (Fig. S2B).

Orthologues of general stress transcription factors Msn2 and Msn4 in C. glabrata

To explore the regulation of the *C. glabrata* ESR (referred hereafter as CgESR), we compared transcription patterns with the *S. cerevisiae* ESR (ScESR). We defined the CgESR by selecting genes from the *C. glabrata* data set which are induced or repressed more than fourfold in at least one condition. This selection resulted in a set of 760 CgESR genes. Of these, 268 genes overlap with the 868 ScESR genes (Gasch *et al*., 2000) (Fig. S3A and S3B). Many of the shared stress-induced genes are induced in *S. cerevisiae* upon overexpression of the general stress transcription factor Msn2 (Chua *et al*., 2006) (Fig. 2A column *MSN2 OE*). Furthermore, Msn2 binding sites (STRE; WAGGGG) are present in many CgESR genes. This suggested that the evolutionary conservation of the ESR is not limited to the set of regulated genes, but also extends to the transcriptional control of those genes.

To identify orthologues of *S. cerevisiae* Msn2 (ScMsn2) in *C. glabrata*, we searched for predicted open reading frames (ORF) comprising C_2H_2 Zn-cluster DNA binding domains in available fungal genomes. One further recognizable feature of ScMsn2 is its central region, which confers regulated nuclear export. This is conserved in the paralogue Msn4, and was previously described as HD1 (Görner *et al*., 1998). We detected putative Msn2 (CAGL0F05995g) and Msn4 (CAGL0M13189g) orthologues with HD1 domains at synthenic positions in the *C. glabrata* genome (Fig. 2B). *K. lactis* and *A. gossypii* contain a single orthologue of both genes that also contain an HD1 domain, which we have designated Msn2. The HD1 domain is not present in the single Msn2/4 orthologue in *C. albicans* and related species, nor

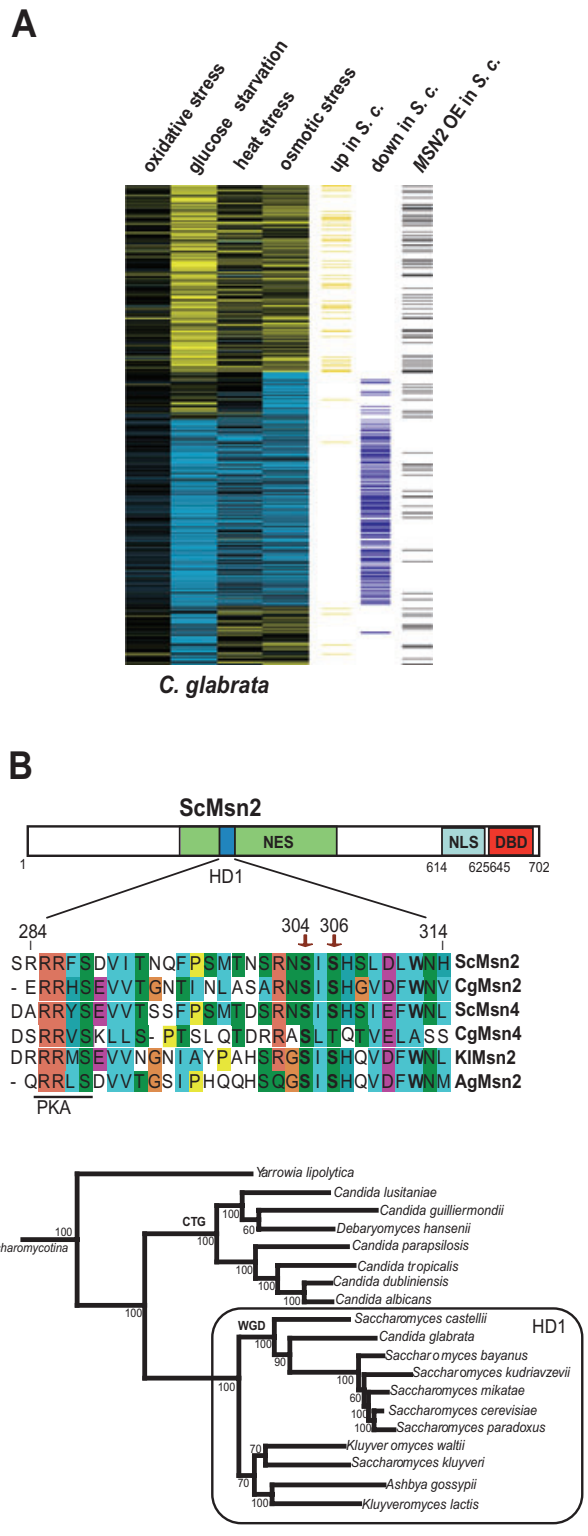

Fig. 2. CgESR is similar to ScESR and includes many Msn2-regulated genes.
A. The CgESR shown here includes 760 genes selected by being induced or repressed significantly (fourfold) in one of the tested conditions. Columns 5 (up in S.c.) and 6 (down in S.c.) show the corresponding ScESR genes from *S. cerevisiae*. Column 7 (MSN2 OE in S.c.) displays induction of the orthologous *S. cerevisiae* genes by *MSN2* overexpression (Chua *et al.*, 2006).
B. Alignment of Msn2 orthologous sequences including the HD1. The shared core motif corresponds to positions 284–314 of ScMsn2. The HD1 signature was detected only in close relatives of *S. cerevisiae*, circled in the phylogeny (taken from Fitzpatrick *et al.*, 2006). The sequences used in the alignment are: *S. cerevisiae* (YMR037C, ScMsn2; YKL062W, ScMsn4), *A. gossypii* (ABR089C, AgMsn2), *C. glabrata* (CAGL0F05995g, CgMsn2; CAGL0M13189g, CgMsn4) and *K. lactis* (KLLA0F26961g, KlMsn2).

in similar proteins from *Yarrowia lipolytic*, nor *S. pombe* (Fig. 2B).

Stress-regulated nuclear export of both ScMsn2 and ScMsn4 requires an extended region, including the HD1. To pinpoint the HD1 region of the ScMsn2/4 orthologues as a functional component of the NES, we tested if these regions are sufficient to confer stress-regulated intracellular localization. We expressed parts containing the HD1 but not the NLS and the C-terminal Zn-finger DNA binding domains of the *K. lactis*, *A. gossypii* and *C. glabrata* Msn2 orthologues as GFP fusions in *S. cerevisiae* (Fig. 3A). Sequences were amplified from genomic DNA and fused to an N-terminal nuclear localization signal (SV40NLS) to support constitutive nuclear import. Expression of the fusion genes was driven by the Sc*ADH1* promoter. Cells were grown to early exponential phase, exposed to osmotic stress (0.5 M NaCl) or weak acid stress (10 mM sorbic acid), and the intracellular distribution of the GFP fusion proteins was recorded by fluorescence microscopy. The GFP fusion proteins of the internal regions of Msn2 and Msn4 from *S. cerevisiae* and *C. glabrata*, and Msn2 from *K. lactis* and *A. gossypii*, accumulated rapidly in the nucleus under stress conditions (Fig. 3A). We also analysed the localization of orf19.4752 (CaMsn4), the *C. albicans* orthologue of both ScMsn2 and ScMsn4 (Nicholls *et al.*, 2004). CaMsn4 has a similar Zn-finger DNA binding region to the *S. cerevisiae* and *C. glabrata* proteins, but lacks a significant similarity to HD1. The GFP fusion protein comprising the CaMsn4 N-terminal 517 amino acids was constitutively enriched in the nucleus in unstressed cells and stress-induced nuclear accumulation was not detectable. As presented below, point mutations in the conserved residues of the HD1 in CgMsn2 also abolish the NES function (Fig. 4C). These data suggest that regulated nuclear export requires the HD1 domain.

To verify if CgMsn2 functions as a stress-responsive transcription factor, we tested whether CgMsn2 can replace and complement the function of ScMsn2 in *S. cerevisiae*. We expressed full-length *CgMSN2* in a *S. cerevisiae* strain lacking *ScMSN2* and *ScMSN4*. The entire *CgMSN2* reading frame was fused to CFP and its expression driven by the constitutive *ADH1* promoter. In unstressed cells, CgMsn2–CFP was distributed mainly in the cytoplasm, similar to the analogous ScMsn2–GFP protein. Several environmental stress conditions induced

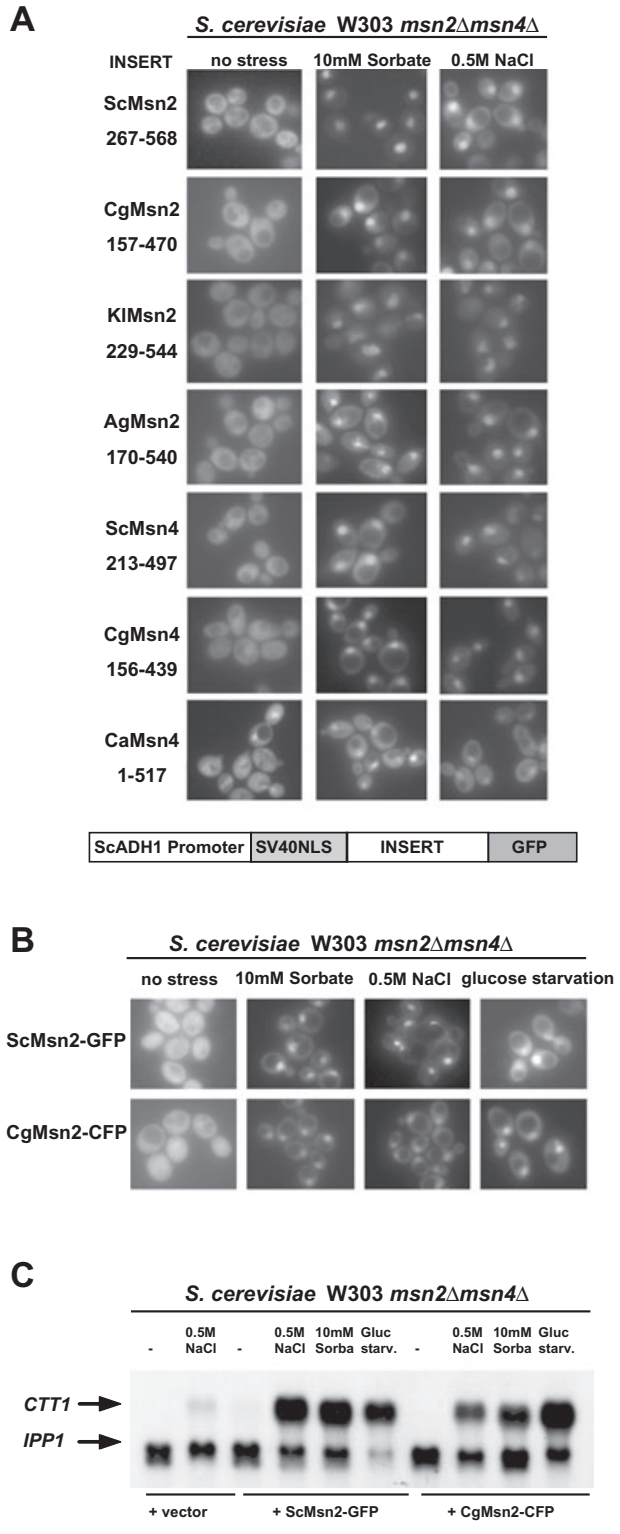

Fig. 3. Regulated localization control is functionally conserved in Msn2-like factors.
A. Indicated regions of Msn2 and Msn4 orthologues were fused to GFP and a SV40-NLS. GFP fusion plasmids were expressed in *S. cerevisiae* strain W303-1A *msn2Δ msn4Δ*. Localization of GFP fusions was determined by fluorescence microscopy in unstressed cells and 10 min after exposure to weak acid stress (10 mM sorbic acid) and osmotic stress (0.5 M NaCl).
B. *S. cerevisiae* W303-1A *msn2Δ msn4Δ* strains containing plasmids expressing either CgMsn2–CFP or ScMsn2–GFP driven by the Sc*ADH1* promoter (pAMG, pACgMC) were grown to exponential phase and exposed to conditions as indicated. Localization was recorded after 10 min by fluorescence microscopy of living cells.
C. mRNA levels of the Msn2-regulated gene *CTT1* and the control *IPP1* were visualized on Northern blots after 20 min stress treatment.

rapid nuclear concentration of CgMsn2 in *S. cerevisiae* (Fig. 3B). Next we investigated whether CgMsn2 can complement ScMsn2 and confer stress-regulated gene activation in *S. cerevisiae*. CgMsn2–CFP was expressed in a *S. cerevisiae* strain lacking both *MSN2* and *MSN4* genes (W303 *msn2Δ msn4Δ*) exposed to osmotic, weak acid and glucose starvation stress. mRNA levels of a target gene of ScMsn2, the *CTT1* gene coding for catalase T, were analysed by Northern hybridization. As shown in Fig. 3C, CgMsn2 supported the stress induction of *CTT1* transcripts in a very similar manner to ScMsn2.

CgMsn2 is regulated by stress in C. glabrata

These results suggested that CgMsn2 might be the functional orthologue of ScMsn2. To examine the regulation of CgMsn2 in *C. glabrata*, we first analysed its intracellular localization under stress conditions. CgMsn2 was expressed as CgMsn2–CFP fusion driven by the *CgADH1* promoter (Fig. 4A). Live microscopy of CgMsn2–CFP localization revealed a rapid and reversible nuclear accumulation regulated by environmental stress conditions, such as acute glucose starvation, osmotic stress, heat shock, oxidative stress and ethanol stress (Fig. 4A). CgMsn2 activity as a transcriptional activator is not changed by the presence of the C-terminal CFP fusion. In contrast, CgMsn2–CFP failed to accumulate in the nucleus during weak organic acid stress (10 mM sorbic acid, 30 mM propionic acid). Interestingly, CgMsn2–CFP expressed in *S. cerevisiae* accumulates in the nucleus during weak acid stress. This difference in the response of CgMsn2 during weak acid stress could be either a consequence of the higher resistance of *C. glabrata* to weak acids compared with *S. cerevisiae*, which is not the case (Gregori *et al.*, 2007), or the absence of a mechanism signalling weak acid stress to CgMsn2 *C. glabrata*.

CgMsn2 accumulates in the nucleus within 4 min following acute carbon source starvation, and subsequent addition of glucose (2%) results in rapid nuclear export (Fig. 4B). The kinetics are very similar to those observed in *S. cerevisiae* (data not shown). To demonstrate that the integrity of the HD1 region is important for NES function, we constructed a mutant derivative by replacing two conserved serine residues S230 and S232 with alanine. The

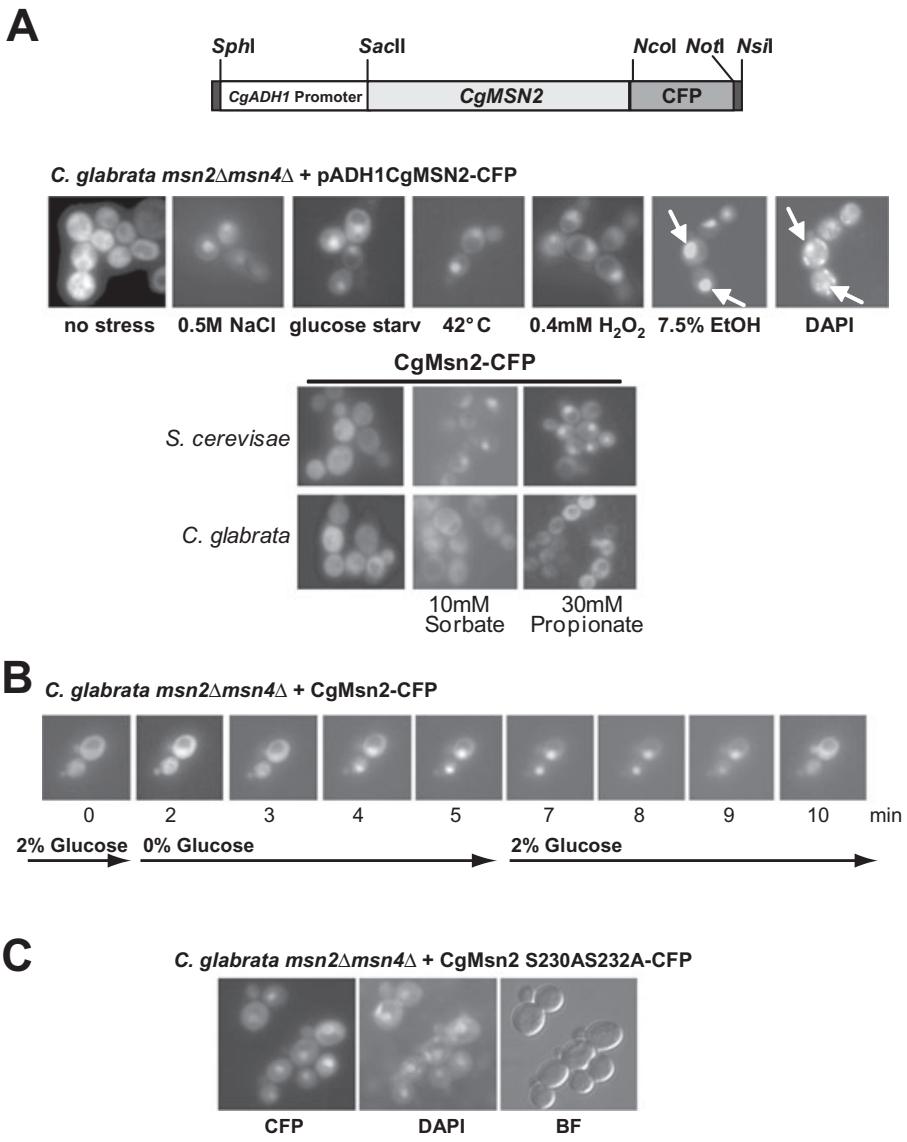

Fig. 4. *C. glabrata* CgMsn2 nuclear localization is stress-regulated.
A. The CgADH1-*CgMsn2–CFP* construct is illustrated schematically and the positions of used restrictions sites are indicated. Localization of CgMsn2–CFP in the *C. glabrata* strain *Cg msn2Δmsn4Δ* was determined by fluorescence microscopy. CFP fluorescence was recorded in exponentially growing cells approximately 10 min after exposure to the indicated stress conditions. Nuclei were stained by addition of 2 μg ml^{-1} 4,6 diamidino-2-phenylindol (DAPI) dye to the cultures 10 min prior to microscopy. In living cells, nucleic acids, such as the mitochondrial DNA, are also stained by DAPI, resulting in background staining. CgMsn2 localization during weak acid stress. CgMsn2–CFP accumulates in *S. cerevisiae* in the nucleus during weak acid stress (10 mM sorbic acid, 30 mM propionic acid). CgMsn2–CFP does not accumulate in the nucleus in *C. glabrata*. Arrows indicate stained nuclear DNA.
B. Nucleocytoplasmic shuttling of CgMsn2–CFP during glucose starvation and re-feeding. Localization of CgMsn2–CFP was visualized by fluorescence microscopy of *C. glabrata* cells fixed to a coverslip with Concanavalin A and localization of the CFP fusion was visualized by fluorescence microscopy.
C. Localization of CgMsn2 S230AS232A–CFP in unstressed cells. *Cg msn2Δmsn4Δ* cells expressing CgMsn2 S230AS232A–CFP were grown in rich media to early logarithmic phase and localization of the CFP fusion protein was determined by fluorescence microscopy.
D. Viability of Cg *msn2Δmsn4Δ* mutant cells expressing Msn2 variants. Cultures of *Cg msn2Δmsn4Δ* transformed with the empty vector as a control, or with a plasmid expressing *CgMSN2* under the control of the native promoter, were incubated in selective media containing 2 M NaCl for 2 and 20 h. Cell suspensions were spotted in 10-fold dilutions on YPD plates and incubated at 37°C over night. Cultures of *Cg msn2Δmsn4Δ* transformed with the empty vector, or with plasmids expressing *CgMSN2* under the control of the native or *CgADH1* promoter, or expressing *CgMSN2 S230AS232A–CFP*, were grown in selective media at 30°C for 10 days. Cells were then spotted in 10-fold dilutions on YPD and SC-Trp plates incubated at 37°C over night and growth recorded.
E. High expression of CgMsn2 S230AS232A confers cold sensitivity. Replica-plated patches of *Cg msn2Δmsn4Δ* transformed with the above vectors were grown on selective plates overnight at 37°C, plates were kept at 4°C and room temperature as a control for 14 days. Plates were replica-plated to fresh and incubated at 37°C over night and growth recorded. Viability was also tested by colony-forming assay showing a threefold reduced colony-forming ability (0.38 of wild type; SD = 0.12; $P = 0.05$).

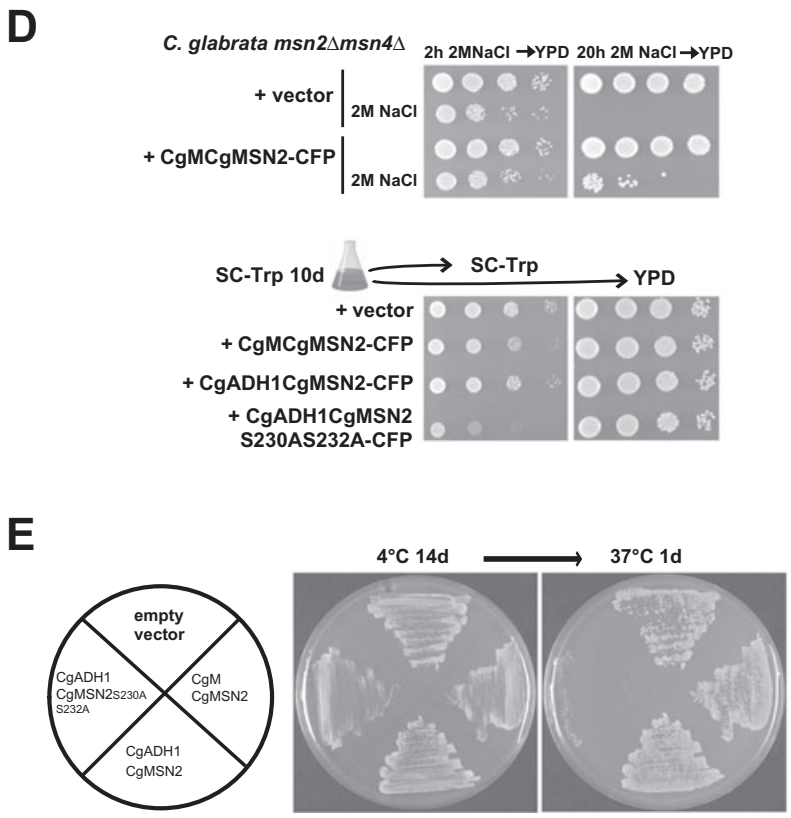

Fig. 4. *cont.*

corresponding positions in the ScMsn2 ORF are indicated by arrows in Fig. 2B. As predicted, we find the CgMsn2 S230AS232A-CFP mutant constitutively enriched in the nucleus in unstressed cells, presumably as a result of impaired nuclear export and the basal activity of its nuclear localization signal (Fig. 4C).

We further tested the role of *CgMSN2* for *C. glabrata* survival under extreme osmotic stress. We generated a strain (*Cg msn2Δmsn4Δ*) lacking both CgMsn2 and CgMsn4 by homologous gene replacement with the *CgHIS3* and *ScURA3* genes respectively. The correct integrations were confirmed by Southern blot (Fig. S1). The *Cg msn2Δmsn4Δ* strain has no obvious growth phenotype under laboratory conditions, similar to *S. cerevisiae msn2Δmsn4Δ* double mutants. Cultures of *Cg msn2Δmsn4Δ* cells transformed with the empty vector as a control, or with a plasmid expressing *CgMsn2–CFP* under the control of the native *CgMSN2* promoter, were grown to early exponential phase and exposed to a severe hyperosmotic stress (2 M NaCl). Viability was assayed after 2 and 20 h incubation by plating of cells in 10-fold serial dilutions. This assay shows that after 2 h of incubation with 2 M NaCl, viability was similar of both strains. However, after 20 h of exposure to 2 M NaCl, cells lacking Msn2 lost viability while the viability of those expressing *CgMSN2* was significantly improved.

Expression of stress genes is tightly regulated and de-regulation has often adverse consequences. We therefore tested if high activity of CgMsn2 compromises long-term viability of *C. glabrata*. *Cg msn2Δmsn4Δ* cells transformed with plasmids expressing *CgMSN2–CFP or CgMSN2 S230AS232A–CFP* driven by the *ADH1* promoter were grown for 10 days at 30°C in selective media. Viability was then assayed by spotting 10-fold dilutions. Cells expressing the constitutive nuclear mutant were significantly underrepresented compared with wild type and vector control (about two- to threefold, Fig. 4D, middle panel). The equal cell number on YPD suggests that the *CgMSN2 S230AS232A–CFP* plasmid, but not the other plasmids, was counter-selected in the culture. Cells carrying the mutant plasmid were also cold-sensitive (Fig. 4E).

Taken together, these data demonstrate that nuclear transport of CgMsn2 is highly regulated and requires the integrity of the HD1 region. CgMsn2 is beneficial under extreme stress conditions and its constitutive expression seems to be detrimental.

The CgMsn2 regulon is related to the ScMsn2 regulon

ScMsn2 has about 100–150 target genes depending on the conditions (Gasch *et al.*, 2000; Schüller *et al.*, 2004).

To define the targets of CgMsn2, we compared the expression profiles of *C. glabrata* wild type and *Cg msn2Δmsn4Δ* mutant strains during osmotic stress and acute glucose starvation. We also compared in parallel the mRNA profiles of cells carrying plasmids with the CgMsn2 gene under its own or the *CgADH1* promoter (construct pCgADH1CgMsn2–CFP). Many stress genes influenced by the absence of Msn2 are also induced by the overexpression of *CgMSN2* (Fig. 5A, right panels, supplementary data). Furthermore, we find that *C. glabrata* and *S. cerevisiae* share a set of 21 Msn2 targets that are also part of the 65 induced genes shared between the ScESR and CgESR (Fig. 5B). All the genes found in this core set possess at least one STRE site in their promoters. STRE-like sequences were detected among the CgMsn2-regulated genes by an unbiased heuristic search using AlignAce in the upstream regions of the selected CgMsn2-regulated genes (Hughes *et al*., 2000) and are depicted in the form sequence logo (Fig. 5A, lower panel). The most salient gene functions are connected to stress response (*HSP42*, *HSP12*, *SML1*, *DDR48*), glycogen and trehalose metabolism (*TPS1*, *NTH1*, *TPS2*, *YGP1*) or DNA repair (*SML1*, ribonucleotide reductase) based on GO-terms analysis (*P*-values < 0.005). Detailed data are available as supplementary files. However, genes regulated only in *C. glabrata* by CgMsn2 include the glyoxylate cycle enzyme *MDH3* (cytoplasmic malate dehydrogenase), the glycolytic enzyme *FBP26* (fructose-2,6-bisphosphatase) and *PHM8* involved in phosphate metabolism, suggesting that there is different wiring of some metabolic pathways between the two species. In addition, there are changes in expression of signalling components, such as the casein kinase *YCK1* involved in cell morphogenesis, which are specific to *C. glabrata.* Together, these data show that CgMsn2 has a broad set of target genes and that many of them are conserved between *S. cerevisiae* and *C. glabrata*. A smaller set of CgMsn2 and ScMsn2 target genes are conserved stress genes also in *S. pombe* and *C. albicans* (Fig. S2C). *C. glabrata* is a nicotinamide adenine dinucleotide (NAD+) auxotroph and its growth is dependent on exogenous supply of NAD+ precursors. A main part of the NAD+ metabolism is the Preiss-Handler pathway, where the nicotinamidase Pnc1 ultimately converts precursors to NAD+ (Ma *et al*., 2007). *PNC1* is upregulated in *S. cerevisiae* and *C. glabrata* during oxidative and osmotic stress (Fig. S2C).

CgMsn2 is required for rapid induction of osmotic stress-induced transcription of trehalose synthesis genes in C. glabrata

To confirm the function of CgMsn2 as a stress-regulated transcription factor, we measured the expression of

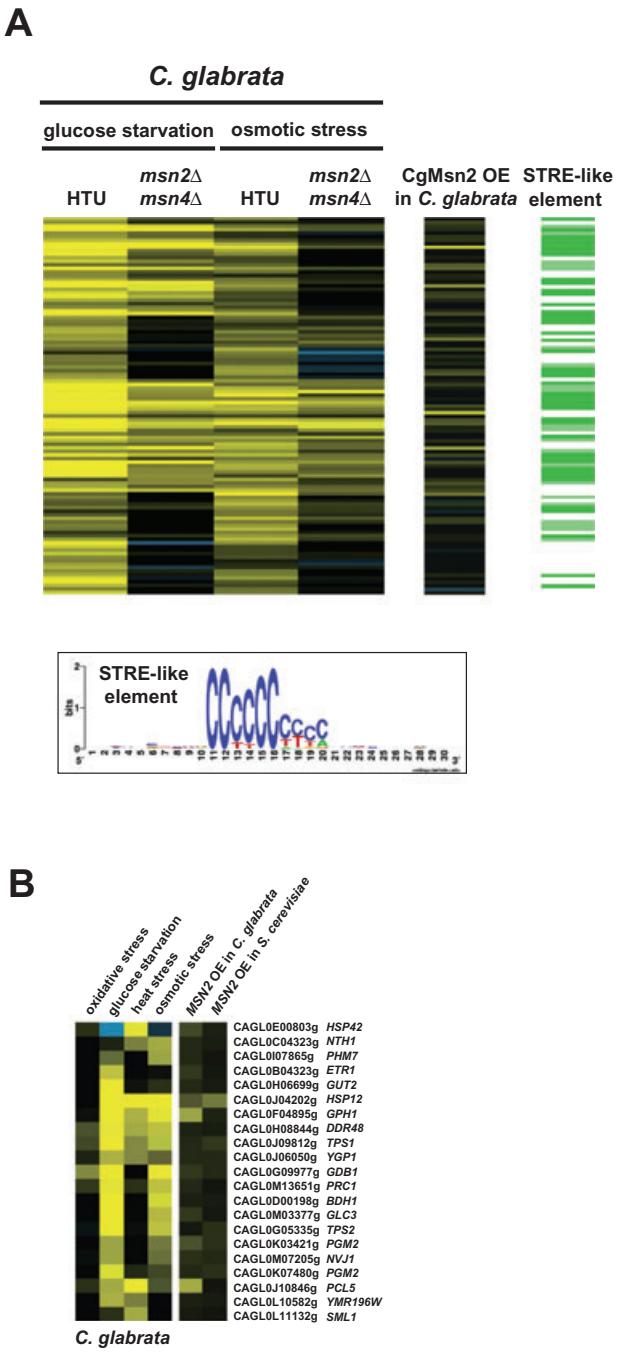

Fig. 5. Determination of genes dependent on CgMsn2/CgMsn4.
A. Wild type and *Cg msn2Δmsn4Δ* cells were exposed to osmotic stress (0.5 M NaCl) and glucose depletion and transcript profiles determined by hybridization to genome-wide *C. glabrata* microarrays. Hierarchical clustering of genes with a wild type to *Cg msn2Δmsn4Δ* ratio > 1.5 is shown. The right panel shows the transcript profile of the *CgADH1* promoter-driven overexpression (OE) of *CgMsn2–CFP* compared with *CgMSN2* native promoter-driven CgMsn2–CFP expression. Logo representation of a STRE-like sequence pattern found by AlignAce among the CgMsn2-regulated genes (indicated on the right).
B. *C. glabrata* and *S. cerevisiae* have orthologous Msn2 target genes. A core set of 21 CgESR genes is induced by overexpression of *CgMSN2* in *C. glabrata* and *ScMSN2* in *S. cerevisiae*.

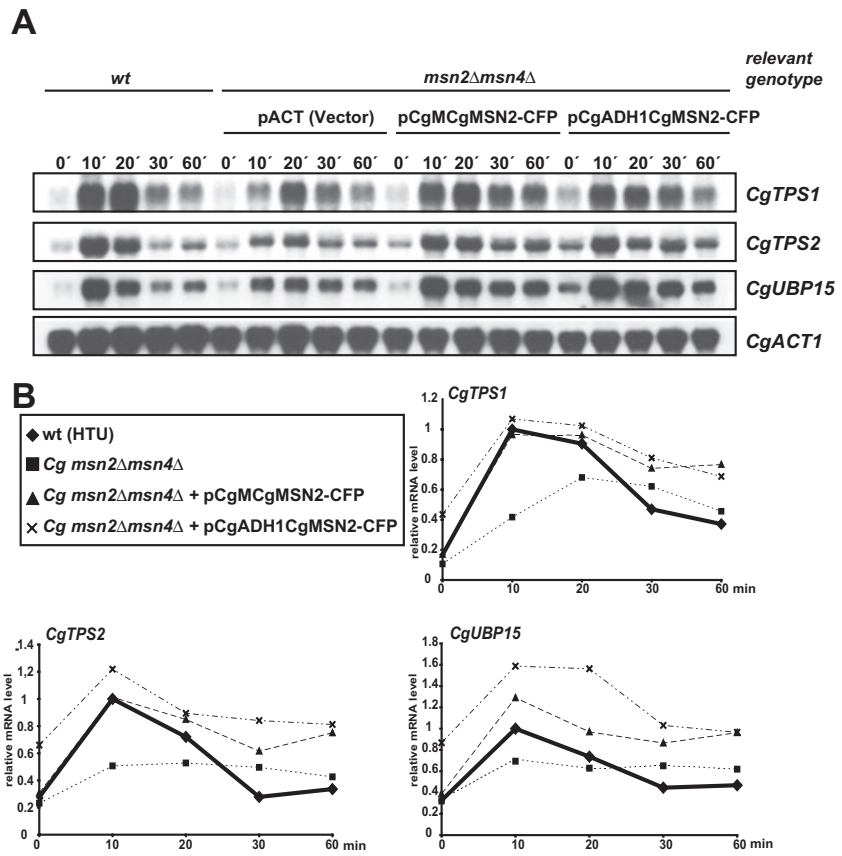

Fig. 6. CgMsn2 is required for rapid induction of transcription after osmotic stress. A. Northern blot analysis of *CgTPS1*, *CgTPS2* and *CgUBP15* transcripts during 0.5 M NaCl induced osmotic stress. *C. glabrata* wild type, *Cg msn2Δmsn4Δ* and *Cg msn2Δmsn4Δ* transformed with pCgMCgMsn2–CFP or pCgADH1CgMsn2–CFP were grown to exponential phase before 0.5 M NaCl was added. Samples for RNA extraction were taken at indicated time points. mRNA levels were visualized by hybridization of radio-labelled probes and autoradiography. *CgACT1* mRNA was used as loading control. B. Quantification of mRNA levels of *CgTPS1*, *CgTPS2* and *CgUBP15* normalized to *CgACT1* and expressed relative to the highest wild-type level.

CgTPS1, *CgTPS2* and *CgUBP15* over several time points following exposure to osmotic stress. *TPS1* and *TPS2*, encoding trehalose-6-phosphate synthase and phosphatase respectively, are both required for the synthesis and the storage of the carbohydrate trehalose. *UBP15*, coding for an ubiquitin-specific protease, is induced by heat and osmotic stress in *S. cerevisiae*. Northern blot analysis of *CgTPS1*, *CgTPS2* and *CgUBP15* showed rapid induction upon treatment with 0.5 M NaCl (30°C and 37°C gave similar results) in the *C. glabrata* wild type, and also in *C. glabrata msn2Δmsn4Δ* mutant cells supplemented with CgMsn2 on a plasmid under its own promoter (pCgMCgMSN2) (Fig. 6A). Cg*ADH1* promoter-driven expression of CgMsn2 in this strain (*C. glabrata msn2Δmsn4Δ*, pCgADH1CgMsn2–CFP) enhanced the signals of all genes in untreated and treated conditions. The CFP tag of CgMsn2 did not disrupt its activity (Fig. S4). In the absence of CgMsn2 and CgMsn4, mRNA levels were severely reduced. Stress-induced expression is not completely abolished in the double mutant cells, suggesting the parallel action of other factors reminiscent of *S. cerevisiae* (Reiser *et al.*, 1999). These data confirm a direct role for CgMsn2 during osmostress induction. The impact of CgMsn4 remains to be elucidated. We conclude that general stress response mechanisms are at least partially conserved between *C. glabrata* and *S. cerevisiae*.

CgMsn2 is not required for virulence in a Drosophila melanogaster *infection model*

Candida glabrata is a human opportunistic pathogen. To test for a possible role of CgMsn2 in virulence, we tested the *C. glabrata msn2Δmsn4Δ* mutant in a *D. melanogaster* model of infection. Wild type flies are resistant to injection of 7500 *C. glabrata* cells (ΔHTU) (Fig. 7). In contrast, *MyD88* mutant flies, in which Toll signalling, and thus the humoral arm of the antifungal response, are blocked, succumb in a few days to the same dose of cells. *C. glabrata* mutants lacking a functional Hog1 pathway have reduced virulence in this infection model, demonstrating its applicability for stress response mutants (not shown). However, we find that there is no difference in the survival of wild-type or immunosuppressed flies when injected either with wild type (ΔHTU) or *Cg msn2Δmsn4Δ* mutants. Similarly, we find no difference between the virulence of strains expressing *CgMsn2–CFP* under the control of the endogenous promoter or the strong constitutive *CgADH1* promoter, and the empty control plasmid. These findings are in line with a role of Msn2 during

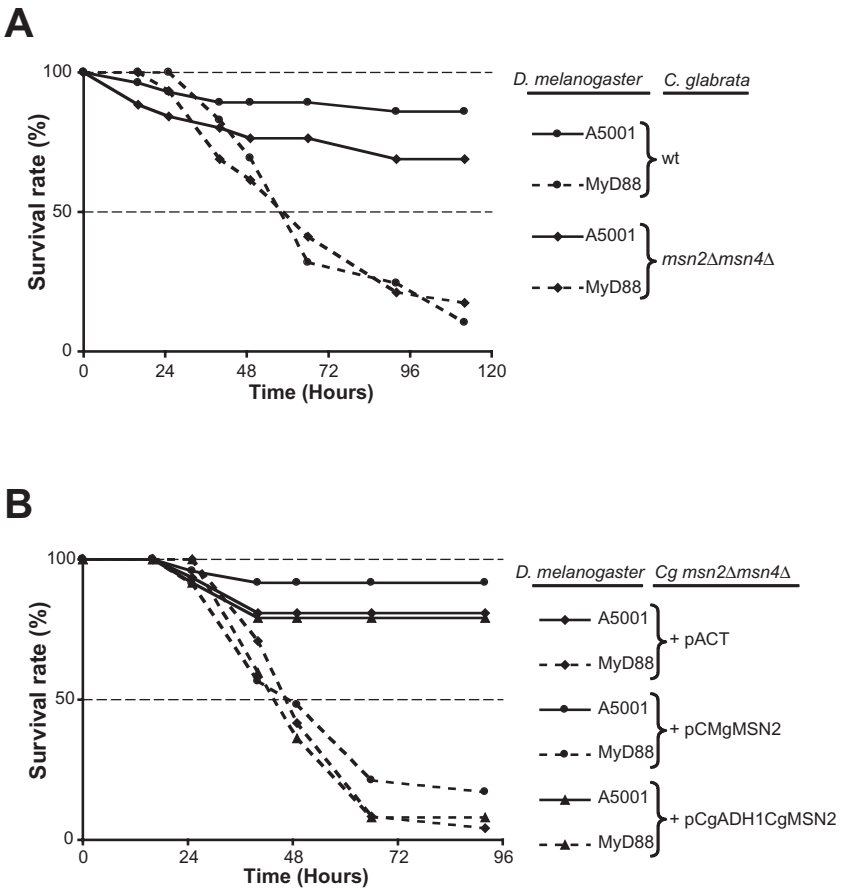

Fig. 7. Survival of *D. melanogaster* to wild type or *msn2Δmsn4Δ* mutant *C. glabrata* infection.
A. Flies were injected with 7500 *C. glabrata* cells. *MyD88* mutant flies succumbed rapidly to a challenge with either wild-type *C. glabrata* or *Cg msn2Δmsn4Δ* mutant strain. The genotypes of the infected flies are indicated (A5001: wild-type).
B. Immunosuppressed flies succumb rapidly when challenged with *Cg msn2Δmsn4Δ* transformed with either the empty pACT plasmid or plasmids expressing CgMsn2 (pCgMCgMSN2 or pCgADH1CgMSN2). Survival was monitored at 29°C. The survival rate is expressed as a percentage. These survival experiments are representative of at least three independent experiments for each panel. The slight difference observed between wild-type flies injected with wild-type or mutant yeasts is not reproducible. Similar results were observed with a lower dose of injected *C. glabrata* (5000).

extreme stress situation probably not encountered in the fly hemocoel.

Discussion

Despite their very different environmental niches and several hundred million years of phylogenetic distance, the transcriptional responses of *S. cerevisiae*, *C. albicans* and *S. pombe* to diverse environmental conditions (ESR) share significant similarities (Enjalbert *et al.*, 2006; Gasch, 2007). *C. glabrata* is phylogenetically related to *S. cerevisiae*, but it is adapted to a mammalian host environment. This is reflected by adhesin-mediated adherence to surfaces, the absence of certain biosynthetic pathways (Domergue *et al.*, 2005; Kaur *et al.*, 2005) and different physiology, for example, optimal growth at 37°C. We report an analysis of part of the CgESR. The CgESR is similar to the ScESR and we identify a conserved role for the general stress transcription factor Msn2.

In many organisms, p38 MAP kinases are central to the control of environmental responses. The *S. pombe* Sty1, *C. albicans* CaHog1 and *S. cerevisiae* Hog1 SAPK mediate the response to a variety of environmental conditions (Toone and Jones, 1998; Wysong *et al.*, 1998; Alonso-Monge *et al.*, 1999; Hwang *et al.*, 2002; Enjalbert *et al.*, 2006). *S. pombe* Sty1 is required for most SpESR regulation (Chen *et al.*, 2003). *S. cerevisiae* Hog1 is most strongly induced by osmotic stress and activated to lower levels by other stresses, including oxidative stress and weak acid stress (Bilsland *et al.*, 2004; Lawrence *et al.*, 2004; Sotelo and Rodriguez-Gabriel, 2006). However, many ScESR genes are not exclusively dependent on Hog1, but rely also on the general stress factors Msn2 and Msn4. The *C. albicans* ESR is influenced by CaHog1 and in parallel also by other pathways, but Msn2 does not play any role (Enjalbert *et al.*, 2006). This raises the question as to whether *S. cerevisiae* has developed a unique stress response mechanism involving Msn2 and Msn4.

Do functional Msn2 orthologues exist in other ascomycete fungi apart from *S. cerevisiae*? One characteristic feature of Msn2 is its DNA binding domain recognizing the corresponding recognition element STRE. Many fungal genome sequences contain ORFs with high similarity to the Msn2 DNA binding domain. However, these genes usually have very little other sequence conservation to ScMsn2. Zn-finger proteins binding to STRE-like

sequences were reported from *S. pombe* and *Trichoderma atroviridae* (Kunitomo *et al*., 2000; Seidl *et al*., 2004), although these factors are not mediating stress responses. The most significant similarity between ScMsn2 orthologues apart from the DNA binding domain (Fig. 2B) is a region designated earlier as Msn2 HD1 (Görner *et al*., 1998). This motif is not present in the Msn2 orthologue from *C. albicans* or its close relatives, including *Candida parapsilosis*, *Candida tropicalis*, *Candida lusitaniae*, *Candida guilliermondii*, *Lodderomyces elongisporus*, *Debaryomyces hansenii* and *Pichia stipitis*.

The intracellular localization of ScMsn2 rapidly changes from the cytoplasm to the nucleus in response to nutrient and stress conditions. (Görner *et al*., 1998; Beck and Hall, 1999; Görner *et al*., 2002). This switch is the result of two independent activities within ScMsn2. The NLS near the C-terminus drives nuclear import. Nuclear export of Msn2 requires the exportin Msn5 which also transports other transcription factors, such as Mig1, Crz1 and Pho4 (Kaffman *et al*., 1998; DeVit, 1999; Chi *et al*., 2001; Boustany and Cyert, 2002). Activation of Msn2 by stress and nutrient starvation requires HD1 which overlaps with the NES function (Görner *et al*., 2002; Boy-Marcotte *et al*., 2006). PKA and TOR inhibit Msn2 activity through this region. Interestingly, all close Msn2 orthologues have an embedded conserved PKA phosphorylation site (Fig. 2B). However, the function of PKA has not been explored in *C. glabrata*.

We have shown that the region including the HD1 motif of Msn2/4 from *K. lactis*, *A. gossypii*, *S. cerevisiae* and *C. glabrata* is sufficient for nuclear export. We provide direct evidence by mutation of two conserved serine residues to alanine in the CgMsn2 HD1, which leads to constitutive nuclear enrichment. Similar changes in the ScMsn2 abolish its NES function (W. Reiter, G. Ammerer and C. Schüller, unpubl. obs.). In contrast, a large part of CaMsn4 (1–517) which is devoid only of its NLS and Zn-finger region at the C-terminus does not support regulated nuclear export.

The NES of ScMsn2 is much larger than the generic exportin 1-driven signal (Wen *et al*., 1995; Kutay and Guttinger, 2005). Importantly, nuclear export of CgMsn2 expressed in *S. cerevisiae* also requires Msn5 and PKA (A. Roetzer and C. Schüller, unpubl. results). These data support our hypothesis that the HD1 is the target site for the exportin Msn5, and that the conserved PKA phosphorylation site within the HD1 site has a regulatory role. Our results suggest that the *Saccharomycotina* can be divided into two groups according to their stress response mechanisms. The HD1 motif and the stress-mediating role of Msn2 orthologues appear after the separation of *C. albicans* from the lineage leading to *S. cerevisiae* (Fig. 2B). The functional conservation of *ScMsn2* and *CgMsn2* highlights the important regulatory motifs of both proteins and will be used as a guide for further structure–function analysis.

Candida glabrata as a human commensal and occasional pathogen exists in very different environmental niches compared with *S. cerevisiae*. Our global transcript analysis of *C. glabrata* cells exposed to the generic stress types carbon starvation, heat, osmotic and oxidative stress reveals a transcription pattern related to *C. albicans*, *S. pombe* and *S. cerevisiae*. The most conserved component of the ESRs is dependent on Msn2-like factors in *C. glabrata* and *S. cerevisiae*. Several lines of evidence presented here suggest that CgMsn2 is an orthologue of ScMsn2. It can functionally substitute for ScMsn2 in *S. cerevisiae* for stress-dependent induction of an Msn2 target gene. Intracellular localization of a CgMsn2–CFP fusion protein is stress-regulated in both *S. cerevisiae* and *C. glabrata.* CgMsn2 is required for rapid and full induction of several target genes tested *CgTPS1*, *CgTPS2* and Cg*UBP15* which all contain putative STRE sequences in their promoter region. Conserved Msn2-dependent genes, such as *TPS1*, *NTH1*, *TPS2*, *HSP42*, *HSP12*, *SML1*, *DDR48 and YGP1*, are involved in stress response, glycogen and trehalose metabolism or DNA repair (*SML1*, ribonucleotide reductase) based on GO-terms analysis (P-values < 0.005). *C. glabrata* stress genes were also found in a global analysis of the CgPdr1-regulated drug response (Vermitsky *et al*., 2006).

CgMSN2 and Cg*MSN4* are not required for virulence in a *Drosophila* infection model. This may reflect an absence of extreme stressful conditions for *C. glabrata* in the fly hemocoel. Alternatively, other pathways may allow *C. glabrata* to adapt to the host environment. Finally, the fly model might not reflect all host niches *C. glabrata* is adapted to. Adhesion is essential for *C. glabrata* virulence (Cormack *et al*., 1999). We found no difference of adhesion to a plastic surface (Iraqui *et al*., 2005) in *C. glabrata* Msn2/4 deletion and Msn2 overexpression strains (data not shown). The adhesins encoded by *EPA* genes are regulated differently during environmental stress conditions. Two genes *EPA3*/CAGL0E06688g and CAGL0I00220g are highly induced by osmotic stress and glucose starvation; however, with a minor role for CgMsn2.

Our results highlight the conserved regulation of Msn2 between *S. cerevisiae* and *C. glabrata*, but we also find differences that require further investigation. Stress regulation of many Msn2 target genes is conserved up to *S. pombe*, indicating a selective advantage for such regulation regardless of the particular transcription factors. It will be of particular interest to analyse the role of Msn2 orthologues which we suspect to be stress-regulated factors in the pre-whole-genome duplication clade, such as *Kluyveromyces* species and *A. gossypii*. We suggest

Table 1. Yeast strains used in this study.

Strain	Genotype	Source
S. cerevisiae		
W303-1A	a *ura3 leu2 his3 trp1 ade2 can1*	Nasmyth K.
W303 *msn2Δmsn4Δ*	a *msn2Δ::TRP1 msn4Δ::HIS3*	Görner *et al.* (1998)
C. glabrata		
ΔHTU	*his3Δ trp1Δ ura3Δ*	Kitada *et al.* (1995)
Cg msn2Δ	*msn2Δ::CgHIS3*	This study
Cg msn2Δmsn4Δ	*msn2Δ::CgHIS3 msn4Δ::ScURA3*	This study
K. lactis	–	Nasmyth K; Oxford
C. albicans SC5314	–	Gillum *et al.* (1984)

that *C. glabrata* Msn2 functions to improve survival under severe stress conditions.

Experimental procedures

Yeast strains and plasmids

Yeast strains used in this study are listed in Table 1. Rich medium (YPD) and synthetic medium (SC) supplemented with appropriate auxotrophic components were prepared as described elsewhere (Current Protocols in Molecular Biology; Wiley). Unless otherwise indicated, all strains were grown at 30°C.

Plasmids and oligonucleotides used in this study are listed in Table 2 and Table S1 respectively. *Cg msn2Δmsn4Δ* strain was obtained by genomic integration. PCR products of *ScURA3* for *CgMSN4* and *CgHIS3* for *CgMSN4* were amplified from the plasmids pRS316 (Sikorski and Hieter, 1989) and pTW23 (Kamran *et al.*, 2004) using fusion PCR (CgMsn4, primer series MSN4; CgMsn2, primer series MSN2) (Noble and Johnson, 2005). Correct genomic integration of all fragments was verified by genomic PCR (primer series Ctrl) followed by Southern analysis using labelled probes generated by amplification with primers MSN2-5′3′/MSN2-5′5′ and MSN4-1/MSN4-3 from genomic DNA.

Cloned PCR fragments used in this study were confirmed by sequencing. Plasmid pASMG1, which was described in Görner *et al.*, (1998), is based on vector YCpLac111 (Gietz and Sugino, 1988) containing the *S. cerevisiae ADH1* promoter followed by the SV40 NLS (PKKKRKV), and a part of *MSN2* coding for amino acid position 267–568 and GFP. To create a unique SalI site after the SV40 NLS, the plasmid was modified by site-directed mutagenesis using a Quick Change Site-directed Mutagenesis Kit (Stratagene) and primers Re-SalI-5/Re-SalI-3 resulting in plasmid pASNScM2G. Sequence fragments from Msn2 orthologues were exchanged with the ScMsn2 sequences by excision with SalI/NcoI. Plasmid pASNKlM2G was created by a SalI/NcoI digest of pASNScM2G and integration of a SalI/NcoI cut fragment obtained by PCR using primers KlM2SalI and KlM2NcoI from genomic *K. lactis* DNA as a template. Plasmid pASNAgM2G was created by using an XhoI/BsmBI fragment of a PCR product generated with primers AgM2XhoI and AgM2NcoI and plasmid pAG1334 as a template. The *C. glabrata* Msn2 and Msn4 orthologues (CAGL0F05995g and CAGL0M13189g) sequences were amplified by PCR from genomic DNA from strain ΔHTU. The CgMsn2 PCR fragment obtained with primers CgM2XhoI and CgM2NcoI was cut with XhoI/NcoI, the CgMsn4 fragment (primers CgM4SalI and

Table 2. Plasmids used in this study.

Plasmids	Relevant Inserts	Source
pAMG	ScADH1-*ScMsn2–GFP* (p*AMG*)	Görner *et al.* (1998)
pSK + CTT1	*ScCTT1* PCR fragment	This study
pACgMC	ScADH1-*CgMsn2–CFP* (*SalI*/*Nco*I and *Not*I/*Not*I); *ScLEU2* marker.	This study
pCgADH1CgMsn2–CFP	CgADH1-Promoter *CgMsn2–CFP* (SphI/SacII and SacII/NsiI); *CgTRP1* marker.	This study
pCgADH1CgMSN2	CgADH1-Promoter *CgMSN2* (SphI/SacII and SacII/NsiI); *CgTRP1* marker.	This study
pCgMCgMsn2–CFP	CgMSN2-Promoter *CgMsn2–CFP* (SphI/SacII); *CgTRP1* marker.	This study
pCgMCgMSN2	CgMSN2 Promoter *CgMSN2* (SphI/SacII); *CgTRP1* marker.	This study
pCgMSCgMSN2 S230AS232A–CFP	CgMSN2 Promoter-*CgMsn2–CFP* (SphI/SacII); .S230A and S232A, *CgTRP1* marker	This study
pASMG1	ScADH-SV40NLS-ScMsn2–GFP	Görner *et al.* (1998)
pASNScM2G	ScADH1, SV40-NLS, ScMSN2 (267–568), GFP; SalI site between SV40 and MSN2 in p*ASMG1*	This study
pASNAgM2G	ScADH1, SV40-NLS, AgMSN2 (170–450), GFP	This study
pASNKlM2G	ScADH1, SV40-NLS, KlMSN2 (229–544), GFP	This study
pASNCgM2G	ScADH1, SV40-NLS, CgMSN2 (157–470), GFP	This study
pASNCgM4G	ScADH1, SV40-NLS, CgMSN4 (156–439), GFP	This study
pASNScM4G	ScADH1, SV40-NLS, ScMSN4 (213–497), GFP	This study
pASNCaM4G	ScADH1, SV40-Nls, CaMsn3 (1–517), GFP	This study
pTW23	pSK$^+$ with *CgHIS3*	Haynes K; London
pRS316	CEN6, ARSH4, *ScURA3*	Sikorski and Hieter (1989)
pAMC	ScADH1-ScMSN2-CFP, *ScLEU2*	This study
pAG1334	*MSN2* from *A. gossypii*	Philippsen P; Basel
pACT14	ARS, CEN and *TRP1* marker from *C. glabrata*	Kitada *et al.* (1996)
pGEM-ACT	ARS, CEN and *TRP1* marker from *C. glabrata*	Gregori *et al.* (2007)

CgM4NcoI) was cut with SalI/NcoI and both were inserted into the SalI/NcoI-cut pASNScM2G. pASNScM4G was created by insertion of a SalI/NcoI-digested PCR fragment obtained using primers ScM4SalI and ScM4NcoI and genomic DNA from W303-1A. The CaMsn4 fragment was amplified via PCR (primers CaMsn4-5 and CaMsn4-3) from genomic *C. albicans* DNA and cut with SalI and NcoI. pACgMC was cloned by integration of a SalI/NcoI-cut PCR fragment containing the CgMsn2 ORF into pAMC. pCgACgMsn2–CFP is a derivative of pGEM-ACT (Gregori *et al*., 2007). Nine hundred base pairs of the *CgADH1* promoter were inserted as a SphI/SacII PCR product obtained with primers CgAdhPro-SphI and CgAdhPro-SacII. The coding sequence for CgMsn2–CFP was amplified from pACgMC using primers CgMsn2Cfp-SacII and CgMsn2Cfp-NsiI, and inserted as a SacII/NsiI-cut fragment. The native promoter (860 base pairs) was inserted as a SphI/SacII PCR product obtained with primers SphI-msn2nat and SacII-msn2nat. Exchange of single amino acids in CgMsn2 was done via site-directed mutagenesis using a Quick Change Site-directed Mutagenesis Kit (Stratagene) using the primers 5-SASA and 3-SASA. Probes for Northern and Southern analysis were amplified by PCR from genomic DNA: *IPP1* from *S. cerevisiae*, *CgACT1*, *CgTPS1*, *CgTPS2* and *CgUBP15* from *C. glabrata*. For *ScCTT1*, a KpnI/SacI fragment from the plasmid pKSCTT1 was used.

Fly strains and survival experiment

Stocks were raised on standard cornmeal-agar medium at 25°C. wA5001 flies were used as wild type throughout the experiments because the MyD88 mutant was generated in this background. Batches of 25–30 wild type and mutant strains were challenged with 7500 cells of wild type or mutant *C. glabrata* using a Nanoject II apparatus (Drummond Scientific). Overnight cultures of *C. glabrata* were collected by centrifugation and washed with PBS 0.01% Tween 20. The solutions were adjusted after counting so that 7500 cells of *C. glabrata* in 13.8 nl were injected into each fly. The quantity of cells injected was checked on a culture plate. After infection, the vials were put in an incubator at 29°C and the surviving flies counted as required. Flies were usually placed into new vials every 2 days. Each infection was carried out using three independent replicates.

Northern and Southern blot analysis

RNA extraction and analysis followed essentially the protocol as described (Current Protocols In Molecular Biology; Wiley). Cells were grown over night and diluted to an OD_{600} of 0.1 in fresh medium, grown to an OD_{600} of 1 and treated as described. Cells were harvested by centrifugation and frozen immediately. For each RNA extraction, 25 ml of yeast cells was collected. Frozen pellets were re-suspended in RNA isolation buffer (50 mM Tris pH 7.5/5 mM EDTA/5% SDS/130 mM NaCl), 200 µl PCI solution (Roth) and glass beads (2/3 of total volume) were added and total RNA was extracted using FastPrep ($2 \times 12''$, speed 6, Thermo Savant). RNA samples (20 µg) were separated on a 1.1% agarose gel in FGRB (5×: 0.1 M MOPS/40 mM NaAc pH 7/5 mM EDTA) containing 2.2 M formaldehyde. After transfer to nylon membranes and UV cross-linking, the quality and amount of RNA were determined by staining with Methylene Blue. Hybridization of [^{32}P-α]-ATP-labelled probes occurred over night in hybridization buffer (0.5 M sodium phosphate buffer pH 7.2/7% SDS/1 mM EDTA) at 65°C. After washing, the membrane was exposed to an X-ray film. For DNA extraction, yeast cells were grown to an OD_{600} of 6 (10 ml), collected and washed once; cell pellets were re-suspended in Lysis buffer (2% Triton X-100/1% SDS/100 mM NaCl/10 mM Tris pH 8/1 mM EDTA). Genomic DNA was isolated by PCI extraction. Digestion of 10 µg of genomic DNA was done over night with ScaI and BglII (5 U µg^{-1} DNA). The digests were separated and blotted. After cross-linking, the radioactive labelled probes were hybridized over night at 65°C. Bands were detected by X-ray film and PhosphoImager.

Microscopy

Fluorescence microscopy was performed as described previously (Görner *et al*., 1998). GFP and CFP were visualized in live cells without fixation. Nuclei were stained by addition of 2 µg ml^{-1} 4,6-diamidino-2-phenylindol dye to the cultures 10 min prior to microscopy. All cells were viewed using a Zeiss Axioplan 2 fluorescence microscope. Images were captured with a Spot Pursuit (Sony) CCD camera using MetaVue (Molecular Devices) and Spotbasic software. Time-lapse imaging of life cell was done by adhering the cells to a coverslip with Concanavalin A (Sigma) fixed above a chamber allowing continuous flow of medium driven by a pump. Incoming medium could be switched between two sources containing rich medium without glucose and with 2% glucose. Medium flow rate was about 500 µl min^{-1}.

Candida glabrata *long-term viability*

*Cg msn2*Δ*msn4*Δ transformed with the above plasmids were grown on selective plates, replica-plated to YDP grown over night and then stored for 14 days at 4°C and on room temperature as a control. Plates were then replica-plated and incubated at 37°C over night and growth recorded. Cell patches expressing CgMSN2 S230AS232A–CFP failed to grow, suggesting loss of viability. Viability was also verified by colony-forming assay by plating showing a threefold reduced colony-forming ability (0.38 of wild type; SD = 0.12; $P = 0.05$).

Microarray analysis

Microarrays were produced (G. Butler lab) by spotting 5908 69- or 70-mer oligonucleotides synthesized at the Pasteur Institute to Corning UltraGAPS slides. Slides were pre-incubated in 0.5% $NaBH_4$ (in 75% PBS and 25% EtOH) solution, washed three times with water and dipped in isopropanol. cDNA was synthesized using 15–20 µg of RNA and Superscript III kit (Invitrogen), including either Cy3-dCTP or Cy5-dCTP (Amersham Biosciences). RNA was hydrolysed in 50 mM NaOH at 65°C for 15 min, the solution was neutralized with acetic acid and cDNA was purified using a GFX purification kit (GE Healthcare). Labelled cDNAs were con-

centrated, pooled and hybridized in 60 µl in DigEasyHyb solution (Roche Diagnostics) with 0.1 mg ml^{-1} salmon sperm DNA (Sigma) at 37°C for 14–16 h. Microarrays were disassembled in 1× SSC, washed two times in 1× SSC, 0.1% SDS at 50°C for 20 min, followed by a 1 min wash in 1× SSC at room temperature. Slides were spun dry for 5 min at 700 r.p.m. Slides were scanned immediately on an Axon4000B scanner (Axon Instruments) and analysed using GenePix Pro4.1 software (Axon Instruments). All standard protocols were provided by the Ontario Cancer Institute (Toronto; http://www.microarrays.ca/). Each experiment was repeated twice.

Analysis of microarray data

The raw data set of this study is available as supplemental material and has been deposited at array express (http://www.ebi.ac.uk/arrayexpress/ ; accession number: E-MEXP-1427). Microarrays were analysed with GenePixPro4.1. Values of not found features were excluded from further analysis. Mean ratios were calculated for features with at least four data points and their quality was approximated by their coefficient of variation (CV) values and subsequent exclusion of values with CV smaller than 1. Only genes with at least four data points and a CV > 1 were included in subsequent analysis. Genes assigned as dubious ORFs by the Genolevures consortium analysis were removed from analysis. The filtered median of ratio values were normalized. The normalized values used for further analysis are available as supplementary file *Cg_array_data.xls.* Cluster analysis (Eisen *et al.*, 1998) was performed with cluster3 and TreeView (see http://bonsai.ims.u-tokyo.ac.jp/~mdehoon/software/cluster/index.html). Association to GO terms was analysed with the T-Profiler (Boorsma *et al.*, 2005) by using the orthologous *S. cerevisiae* genes. Values of genes associated with the most significant terms were visualized by Cluster analysis using complete linkage and correlation as similarity metric. The cluster results were confirmed by K means and SOM clustering. *P*-values of overlapping gene sets were calculated by hypergeometric distribution. Of the 5063 gene features spotted in duplicate on our arrays, 4166 gave useful data under at least one tested condition. Systematic *C. glabrata* IDs were used from the Genolevures resource (5215 ORFs) and linked to systematic names of *S. cerevisiae*. The ESR was defined as the set of genes with values above a fourfold induction and below a fourfold repression after applying different stresses. To estimate the contribution of the transcription factors CgMsn2/CgMsn4, the ratio of the wild type versus double mutant and induced genes was calculated. In addition, data from an all-against-all BLASTP search of protein sequences from *S. cerevisiae*, *C. albicans* and *S. pombe* (Enjalbert *et al.*, 2006) were compared with *C. glabrata* data for osmotic and oxidative stress. Normalized values with canonical gene names are available in plain text format as supplementary data as well as Cluster3 output files corresponding to the figures. Sequence patterns were found by AlignAce (Hughes *et al.*, 2000) using the *C. glabrata* genomic DNA. The most recent annotation as of 09.Nov.2007 was used to define ORF and promoter regions. Sequence logo was generated at http://weblogo.berkeley.edu/(Crooks *et al.*, 2004).

Acknowledgements

We thank members of the Ammerer lab for discussions and advice, Elisabeth Brown for providing the Msn2–CFP plasmid, Peter Phillipsen for *A. gossypii* clones, Ken Haynes for the *C. glabrata* 'starter kit' and Steffen Rupp for a crucial advice. C.S. was supported by the Herzfelder Foundation and the FWF Grant P19966-B12, and the Vienna Hochschuljubiläumsstiftung. This work was also supported by FWF Grant F34567 and by the WWTF (HOPI-WWTF-LS133), the FP6 project EURESFUN (FP6-2004-PL518199) (to KK), and by the Wellcome Trust (072420 to G.B.) and from QUASI, a grant from the European FP6 to G.A. D.F.'s laboratory is supported by the CNRS and Fondation Recherche Médicale (Equipe FRM). Marie-Céline Lafarge's technical expertise is gratefully acknowledged. We acknowledge the support by the ERA-Net Pathogenomics programme (FWF-I125-B09 to KK and CS).

References

Alonso-Monge, R., Navarro-Garcia, F., Molero, G., Diez-Orejas, R., Gustin, M., Pla, J., *et al.* (1999) Role of the mitogen-activated protein kinase Hog1p in morphogenesis and virulence of *Candida albicans*. *J Bacteriol* **181:** 3058–3068.

Beck, T., and Hall, M.N. (1999) The TOR signalling pathway controls nuclear localization of nutrient-regulated transcription factors. *Nature* **402:** 689–692.

Bilaud, T., Koering, C.E., Binet-Brasselet, E., Ancelin, K., Pollice, A., Gasser, S.M., and Gilson, E. (1996) The telobox, a Myb-related telomeric DNA binding motif found in proteins from yeast, plants and human. *Nucleic Acids Res* **24:** 1294–1303.

Bilsland, E., Molin, C., Swaminathan, S., Ramne, A., and Sunnerhagen, P. (2004) Rck1 and Rck2 MAPKAP kinases and the HOG pathway are required for oxidative stress resistance. *Mol Microbiol* **53:** 1743–1756.

Boorsma, A., Foat, B.C., Vis, D., Klis, F., and Bussemaker, H.J. (2005) T-profiler: scoring the activity of predefined groups of genes using gene expression data. *Nucleic Acids Res* **33:** W592–W595.

Boustany, L.M., and Cyert, M.S. (2002) Calcineurin-dependent regulation of Crz1p nuclear export requires Msn5p and a conserved calcineurin docking site. *Genes Dev* **16:** 608–619.

Boy-Marcotte, E., Garmendia, C., Garreau, H., Lallet, S., Mallet, L., and Jacquet, M. (2006) The transcriptional activation region of Msn2p. *Saccharomyces cerevisiae*, is regulated by stress but is insensitive to the cAMP signalling pathway. *Mol Genet Genomics* **275:** 277–287.

Boy-Marcotte, E., Perrot, M., Bussereau, F., Boucherie, H., and Jacquet, M. (1998) Msn2p and Msn4p control a large number of genes induced at the diauxic transition which are repressed by cyclic AMP in *Saccharomyces cerevisiae*. *J Bacteriol* **180:** 1044–1052.

Bun-Ya, M., Nishimura, M., Harashima, S., and Oshima, Y. (1991) The *PHO84* gene of *Saccharomyces cerevisiae* encodes an inorganic phosphate transporter. *Mol Cell Biol* **11:** 3229–3238.

Cameroni, E., Hulo, N., Roosen, J., Winderickx, J., and De Virgilio, C. (2004) The novel yeast PAS kinase

Rim15 orchestrates g(0)-associated antioxidant defense mechanisms. *Cell Cycle* **3:** 462–468.
Causton, H.C., Ren, B., Koh, S.S., Harbison, C.T., Kanin, E., Jennings, E.G., *et al.* (2001) Remodeling of yeast genome expression in response to environmental changes. *Mol Biol Cell* **12:** 323–337.
Chen, D., Toone, W.M., Mata, J., Lyne, R., Burns, G., Kivinen, K., *et al.* (2003) Global transcriptional responses of fission yeast to environmental stress. *Mol Biol Cell* **14:** 214–229.
Chi, Y., Huddleston, M.J., Zhang, X., Young, R.A., Annan, R.S., Carr, S.A., and Deshaies, R.J. (2001) Negative regulation of Gcn4 and Msn2 transcription factors by Srb10 cyclin-dependent kinase. *Genes Dev* **15:** 1078–1092.
Choo, Y., and Klug, A. (1994) Selection of DNA binding sites for zinc fingers using rationally randomized DNA reveals coded interactions. *Proc Natl Acad Sci USA* **91:** 11168–11172.
Chua, G., Morris, Q.D., Sopko, R., Robinson, M.D., Ryan, O., Chan, E.T., *et al.* (2006) Identifying transcription factor functions and targets by phenotypic activation. *Proc Natl Acad Sci USA* **103:** 12045–12050.
Cormack, B.P., Ghori, N., and Falkow, S. (1999) An adhesin of the yeast pathogen *Candida glabrata* mediating adherence to human epithelial cells. *Science* **285:** 578–582.
Crooks, G.E., Hon, G., Chandonia, J.M., and Brenner, S.E. (2004) WebLogo: a sequence logo generator. *Genome Res* **14:** 1188–1190.
DeVit, M.J., and Johnston, M. (1999) The nuclear exportin Msn5 is required for nuclear export of the Mig1 glucose repressor of *Saccharomyces cerevisiae*. *Curr Biol* **9:** 1231–1241.
De Wever, V., Reiter, W., Ballarini, A., Ammerer, G., and Brocard, C. (2005) A dual role for PP1 in shaping the Msn2-dependent transcriptional response to glucose starvation. *EMBO J* **24:** 4115–4123.
DeRisi, J.L., Iyer, V.R., and Brown, P.O. (1997) Exploring the metabolic and genetic control of gene expression on a genomic scale. *Science* **278:** 680–686.
Domergue, R., Castano, I., De Las Penas, A., Zupancic, M., Lockatell, V., Hebel, J.R., *et al.* (2005) Nicotinic acid limitation regulates silencing of Candida adhesins during UTI. *Science* **308:** 866–870.
Durchschlag, E., Reiter, W., Ammerer, G., and Schüller, C. (2004) Nuclear localization destabilizes the stress-regulated transcription factor Msn2. *J Biol Chem* **279:** 55425–55432.
Eisen, M.B., Spellman, P.T., Brown, P.O., and Botstein, D. (1998) Cluster analysis and display of genome-wide expression patterns. *Proc Natl Acad Sci USA* **95:** 14863–14868.
Enjalbert, B., Smith, D.A., Cornell, M.J., Alam, I., Nicholls, S., Brown, A.J., and Quinn, J. (2006) Role of the Hog1 stress-activated protein kinase in the global transcriptional response to stress in the fungal pathogen *Candida albicans*. *Mol Biol Cell* **17:** 1018–1032.
Enjalbert, B., MacCallum, D.M., Odds, F.C., and Brown, A.J. (2007) Niche-specific activation of the oxidative stress response by the pathogenic fungus *Candida albicans*. *Infect Immun* **75:** 2143–2151.
Estruch, F. (2000) Stress-controlled transcription factors, stress-induced genes and stress tolerance in budding yeast. *FEMS Microbiol Rev* **24:** 469–486.
Fabrizio, P., Pozza, F., Pletcher, S.D., Gendron, C.M., and Longo, V.D. (2001) Regulation of longevity and stress resistance by Sch9 in yeast. *Science* **292:** 288–290.
Fabrizio, P., Pletcher, S.D., Minois, N., Vaupel, J.W., and Longo, V.D. (2004) Chronological aging-independent replicative life span regulation by Msn2/Msn4 and Sod2 in *Saccharomyces cerevisiae*. *FEBS Lett* **557:** 136–142.
Feldmann, H. (2000) Genolevures – a novel approach to 'evolutionary genomics'. *FEBS Lett* **487:** 1–2.
Fitzpatrick, D.A., Logue, M.E., Stajich, J.E., and Butler, G. (2006) A fungal phylogeny based on 42 complete genomes derived from supertree and combined gene analysis. *BMC Evol Biol* **6:** 99.
Garreau, H., Hasan, R.N., Renault, G., Estruch, F., Boy-Marcotte, E., and Jacquet, M. (2000) Hyperphosphorylation of Msn2p and Msn4p in response to heat shock and the diauxic shift is inhibited by cAMP in *Saccharomyces cerevisiae*. *Microbiology* **146:** 2113–2120.
Gasch, A.P. (2007) Comparative genomics of the environmental stress response in ascomycete fungi. *Yeast*.
Gasch, A.P., Spellman, P.T., Kao, C.M., Carmel-Harel, O., Eisen, M.B., Storz, G., *et al.* (2000) Genomic expression programs in the response of yeast cells to environmental changes. *Mol Biol Cell* **11:** 4241–4257.
Geber, A., Hitchcock, C.A., Swartz, J.E., Pullen, F.S., Marsden, K.E., Kwon-Chung, K.J., and Bennett, J.E. (1995) Deletion of the *Candida glabrata* ERG3 and ERG11 genes: effect on cell viability, cell growth, sterol composition, and antifungal susceptibility. *Antimicrob Agents Chemother* **39:** 2708–2717.
Gietz, R.D., and Sugino, A. (1988) New yeast-*Escherichia coli* shuttle vectors constructed with in vitro mutagenized yeast genes lacking six-base pair restriction sites. *Gene* **74:** 527–534.
Gillum, A.M., Tsay, E.Y., and Kirsch, D.R. (1984) Isolation of the *Candida albicans* gene for orotidine-5′-phosphate decarboxylase by complementation of S. cerevisiae ura3 and *E. coli* pyrF mutations. *Mol Gen Genet* **198:** 179–182.
Görner, W., Durchschlag, E., Martinez-Pastor, M.T., Estruch, F., Ammerer, G., Hamilton, B., *et al.* (1998) Nuclear localization of the C2H2 zinc finger protein Msn2p is regulated by stress and protein kinase A activity. *Genes Dev* **12:** 586–597.
Görner, W., Durchschlag, E., Wolf, J., Brown, E.L., Ammerer, G., Ruis, H., and Schüller, C. (2002) Acute glucose starvation activates the nuclear localization signal of a stress-specific yeast transcription factor. *EMBO J* **21:** 135–144.
Gregori, C., Schüller, C., Roetzer, A., Schwarzmuller, T., Ammerer, G., and Kuchler, K. (2007) The high-osmolarity glycerol response pathway in the human fungal pathogen *Candida glabrata* strain ATCC 2001 lacks a signaling branch that operates in baker's yeast. *Eukaryot Cell* **6:** 1635–1645.
Hasan, R., Leroy, C., Isnard, A.D., Labarre, J., Boy-Marcotte, E., and Toledano, M.B. (2002) The control of the yeast H_2O_2 response by the Msn2/4 transcription factors. *Mol Microbiol* **45:** 233–241.
Hirasawa, T., Ashitani, K., Yoshikawa, K., Nagahisa, K., Furusawa, C., Katakura, Y., Shimizu, H., and Shioya, S. (2006) Comparison of transcriptional responses to osmotic stresses induced by NaCl and sorbitol additions in *Saccha-*

romyces cerevisiae using DNA microarray. *J Biosci Bioeng* **102:** 568–571.
Hohmann, S. (2002) Osmotic stress signaling and osmoadaptation in yeasts. *Microbiol Mol Biol Rev* **66:** 300–372.
Hughes, J.D., Estep, P.W., Tavazoie, S., and Church, G.M. (2000) Computational identification of cis-regulatory elements associated with groups of functionally related genes in *Saccharomyces cerevisiae*. *J Mol Biol* **296:** 1205–1214.
Hwang, C.S., Rhie, G.E., Oh, J.H., Huh, W.K., Yim, H.S., and Kang, S.O. (2002) Copper- and zinc-containing superoxide dismutase (Cu/ZnSOD) is required for the protection of *Candida albicans* against oxidative stresses and the expression of its full virulence. *Microbiology* **148:** 3705–3713.
Iraqui, I., Garcia-Sanchez, S., Aubert, S., Dromer, F., Ghigo, J.M., d'Enfert, C., and Janbon, G. (2005) The Yak1p kinase controls expression of adhesins and biofilm formation in *Candida glabrata* in a Sir4p-dependent pathway. *Mol Microbiol* **55:** 1259–1271.
Jackson, D.D., and Stevens, T.H. (1997) VMA12 encodes a yeast endoplasmic reticulum protein required for vacuolar H^+-ATPase assembly. *J Biol Chem* **272:** 25928–25934.
Kaffman, A., Rank, N.M., O'Neill, E.M., Huang, L.S., and O'Shea, E.K. (1998) The receptor Msn5 exports the phosphorylated transcription factor Pho4 out of the nucleus. *Nature* **396:** 482–486.
Kamran, M., Calcagno, A.M., Findon, H., Bignell, E., Jones, M.D., Warn, P., *et al.* (2004) Inactivation of transcription factor gene *ACE2* in the fungal pathogen *Candida glabrata* results in hypervirulence. *Eukaryot Cell* **3:** 546–552.
Kaur, R., Domergue, R., Zupancic, M.L., and Cormack, B.P. (2005) A yeast by any other name: *Candida glabrata* and its interaction with the host. *Curr Opin Microbiol* **8:** 378–384.
Kitada, K., Yamaguchi, E., and Arisawa, M. (1995) Cloning of the *Candida glabrata TRP1* and *HIS3* genes, and construction of their disruptant strains by sequential integrative transformation. *Gene* **165:** 203–206.
Kitada, K., Yamaguchi, E., and Arisawa, M. (1996) Isolation of a *Candida glabrata* centromere and its use in construction of plasmid vectors. *Gene* **175:** 105–108.
Kunitomo, H., Higuchi, T., Iino, Y., and Yamamoto, M. (2000) A zinc-finger protein, Rst2p, regulates transcription of the fission yeast ste11(+) gene, which encodes a pivotal transcription factor for sexual development. *Mol Biol Cell* **11:** 3205–3217.
Kutay, U., and Guttinger, S. (2005) Leucine-rich nuclear-export signals: born to be weak. *Trends Cell Biol* **15:** 121–124.
Lawrence, C.L., Botting, C.H., Antrobus, R., and Coote, P.J. (2004) Evidence of a new role for the high-osmolarity glycerol mitogen-activated protein kinase pathway in yeast: regulating adaptation to citric acid stress. *Mol Cell Biol* **24:** 3307–3323.
Ma, B., Pan, S.J., Zupancic, M.L., and Cormack, B.P. (2007) Assimilation of NAD(+) precursors in *Candida glabrata*. *Mol Microbiol* **66:** 14–25.
Martinez-Pastor, M.T., Marchler, G., Schüller, C., Marchler-Bauer, A., Ruis, H., and Estruch, F. (1996) The *Saccharomyces cerevisiae* zinc finger proteins Msn2p and Msn4p are required for transcriptional induction through the stress response element (STRE). *EMBO J* **15:** 2227–2235.
Nicholls, S., Straffon, M., Enjalbert, B., Nantel, A., Macaskill, S., Whiteway, M., and Brown, A.J. (2004) Msn2- and Msn4-like transcription factors play no obvious roles in the stress responses of the fungal pathogen *Candida albicans*. *Eukaryot Cell* **3:** 1111–1123.
Noble, S.M., and Johnson, A.D. (2005) Strains and strategies for large-scale gene deletion studies of the diploid human fungal pathogen *Candida albicans*. *Eukaryot Cell* **4:** 298–309.
Petter, R., and Kwon-Chung, K.J. (1996) Disruption of the SNF1 gene abolishes trehalose utilization in the pathogenic yeast *Candida glabrata*. *Infect Immun* **64:** 5269–5273.
Pfaller, M.A., and Diekema, D.J. (2007) Epidemiology of invasive candidiasis: a persistent public health problem. *Clin Microbiol Rev* **20:** 133–163.
Powers, R.W., 3rd, Kaeberlein, M., Caldwell, S.D., Kennedy, B.K., and Fields, S. (2006) Extension of chronological life span in yeast by decreased TOR pathway signaling. *Genes Dev* **20:** 174–184.
Reiser, V., Ruis, H., and Ammerer, G. (1999) Kinase activity-dependent nuclear export opposes stress-induced nuclear accumulation and retention of Hog1 mitogen-activated protein kinase in the budding yeast *Saccharomyces cerevisiae*. *Mol Biol Cell* **10:** 1147–1161.
Rep, M., Krantz, M., Thevelein, J.M., and Hohmann, S. (2000) The transcriptional response of *Saccharomyces cerevisiae* to osmotic shock. Hot1p and Msn2p/Msn4p are required for the induction of subsets of high osmolarity glycerol pathway-dependent genes. *J Biol Chem* **275:** 8290–8300.
Sandven, P., Bevanger, L., Digranes, A., Haukland, H.H., Mannsaker, T., and Gaustad, P. (2006) Candidemia in Norway (1991–2003): results from a nationwide study. *J Clin Microbiol* **44:** 1977–1981.
Schüller, C., Mamnun, Y.M., Mollapour, M., Krapf, G., Schuster, M., Bauer, B.E., *et al.* (2004) Global phenotypic analysis and transcriptional profiling defines the weak acid stress response regulon in *Saccharomyces cerevisiae*. *Mol Biol Cell* **15:** 706–720.
Seidl, V., Seiboth, B., Karaffa, L., and Kubicek, C.P. (2004) The fungal STRE-element-binding protein Seb1 is involved but not essential for glycerol dehydrogenase (gld1) gene expression and glycerol accumulation in *Trichoderma atroviride* during osmotic stress. *Fungal Genet Biol* **41:** 1132–1140.
Sikorski, R.S., and Hieter, P. (1989) A system of shuttle vectors and yeast host strains designed for efficient manipulation of DNA in *Saccharomyces cerevisiae*. *Genetics* **122:** 19–27.
Smith, D.A., Nicholls, S., Morgan, B.A., Brown, A.J., and Quinn, J. (2004) A conserved stress-activated protein kinase regulates a core stress response in the human pathogen *Candida albicans*. *Mol Biol Cell* **15:** 4179–4190.
Sotelo, J., and Rodriguez-Gabriel, M.A. (2006) Mitogen-activated protein kinase Hog1 is essential for the response to arsenite in *Saccharomyces cerevisiae*. *Eukaryot Cell* **5:** 1826–1830.
Teixeira, M.C., Fernandes, A.R., Mira, N.P., Becker, J.D., and Sa-Correia, I. (2006) Early transcriptional response of *Saccharomyces cerevisiae* to stress imposed by the herbicide 2,4-dichlorophenoxyacetic acid. *FEMS Yeast Res* **6:** 230–248.

Toone, W.M., and Jones, N. (1998) Stress-activated signalling pathways in yeast. *Genes Cells* **3:** 485–498.

Vermitsky, J.P., Earhart, K.D., Smith, W.L., Homayouni, R., Edlind, T.D., and Rogers, P.D. (2006) Pdr1 regulates multidrug resistance in *Candida glabrata*: gene disruption and genome-wide expression studies. *Mol Microbiol* **61:** 704–722.

Wen, W., Meinkoth, J.L., Tsien, R.Y., and Taylor, S.S. (1995) Identification of a signal for rapid export of proteins from the nucleus. *Cell* **82:** 463–473.

Wysong, D.R., Christin, L., Sugar, A.M., Robbins, P.W., and Diamond, R.D. (1998) Cloning and sequencing of a *Candida albicans* catalase gene and effects of disruption of this gene. *Infect Immun* **66:** 1953–1961.

Supplementary material

This material is available as part of the online article from:
http://www.blackwell-synergy.com/doi/abs/10.1111/j.1365-2958.2008.06301.x
(This link will take you to the article abstract).

Please note: Blackwell Publishing is not responsible for the content or functionality of any supplementary materials supplied by the authors. Any queries (other than missing material) should be directed to the corresponding author for the article.

Figure S1

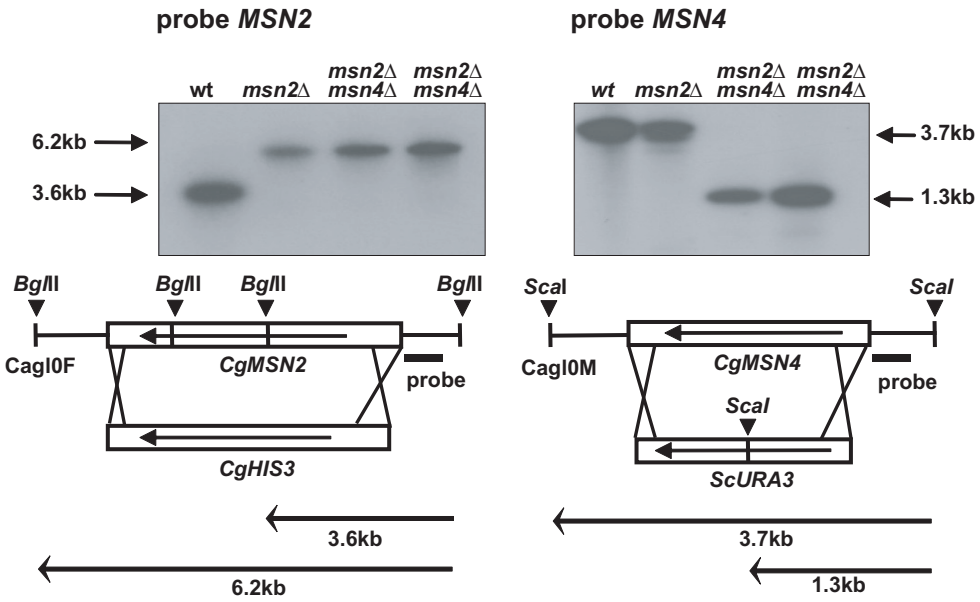
probe MSN2
probe MSN4
wt
msn2Δ
msn2Δ msn4Δ
msn2Δ msn4Δ
6.2kb
3.6kb
3.7kb
1.3kb
BglII
BglII
BglII
BglII
CagI0F
CgMSN2
probe
CgHIS3
3.6kb
6.2kb
ScaI
ScaI
CagI0M
CgMSN4
probe
ScaI
ScURA3
3.7kb
1.3kb

Figure S2

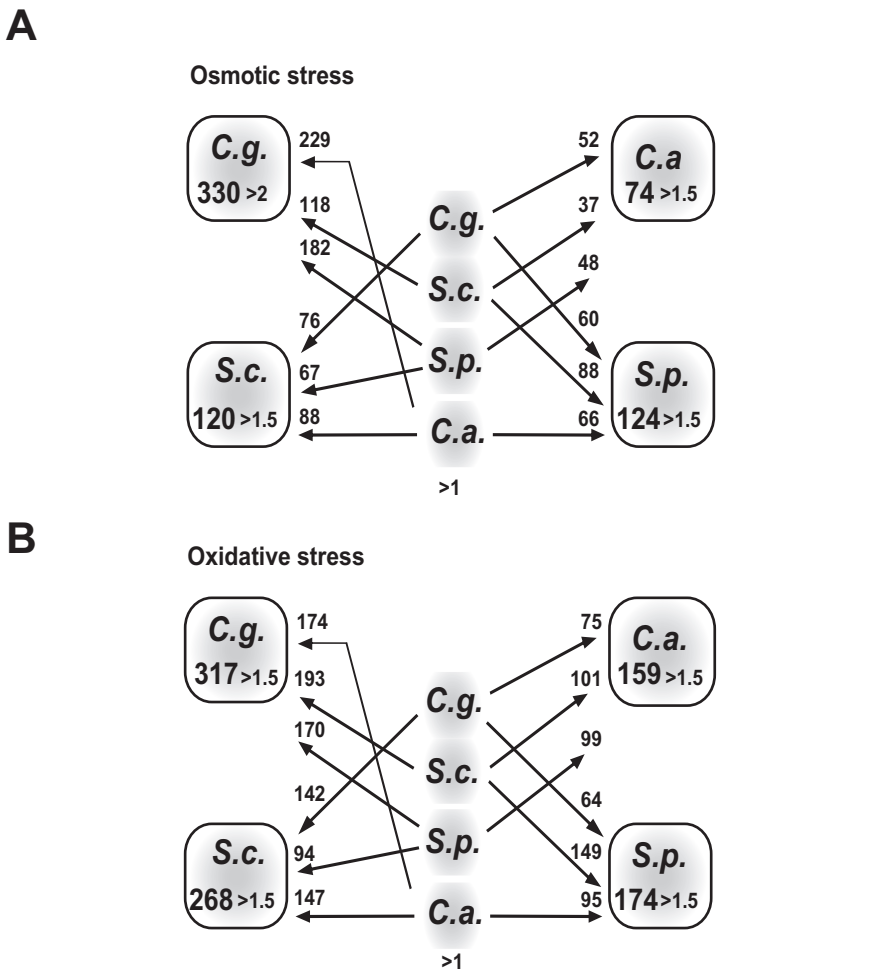
A
Osmotic stress
C.g.
330 >2
S.c.
120 >1.5
C.a
74 >1.5
S.p.
124 >1.5
229
118
182
76
67
88
52
37
48
60
88
66
C.g.
S.c.
S.p.
C.a.
>1
B
Oxidative stress
C.g.
317 >1.5
S.c.
268 >1.5
C.a.
159 >1.5
S.p.
174 >1.5
174
193
170
142
94
147
75
101
99
64
149
95
C.g.
S.c.
S.p.
C.a.
>1
C
osmotic stress
oxidative stress
C.g.
C.a.
S.c.
S.p.
Msn2 OE in C. glabrata
Msn2 OE in S. cerevisiae
YDR533c HSP31
YDR074w TPS2
YBR126c TPS1
YFL014w HSP12
YCR021c HSP30
YDL124w YDL124w
YGL037c PNC1
YPR061c JID1
YMR297w PRC1
YBR026c ETR1
YIL155c GUT2
YJR096w YJR096w
YOL084w PHM7

Figure S3

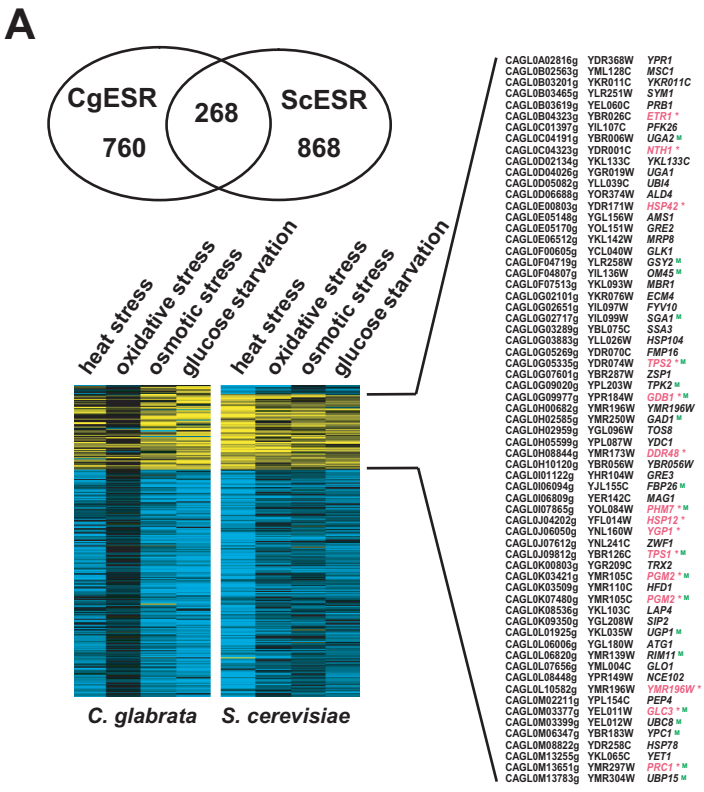
A
CgESR
760
268
ScESR
868
heat stress
oxidative stress
osmotic stress
glucose starvation
heat stress
oxidative stress
osmotic stress
glucose starvation
C. glabrata
S. cerevisiae
CAGL0A02816g YDR368W YPR1
CAGL0B02563g YML128C MSC1
CAGL0B03201g YKR011C YKR011C
CAGL0B03465g YLR251W SYM1
CAGL0B03619g YEL060C PRB1
CAGL0B04323g YBR026C ETR1 *
CAGL0C01397g YIL107C PFK26
CAGL0C04191g YBR006W UGA2 M
CAGL0C04323g YDR001C NTH1 *
CAGL0D02134g YKL133C YKL133C
CAGL0D04026g YGR019W UGA1
CAGL0D05082g YLL039C UBI4
CAGL0D06688g YOR374W ALD4
CAGL0E00803g YDR171W HSP42 *
CAGL0E05148g YGL156W AMS1
CAGL0E05170g YOL151W GRE2
CAGL0E06512g YKL142W MRP8
CAGL0F00605g YCL040W GLK1
CAGL0F04719g YLR258W GSY2 M
CAGL0F04807g YIL136W OM45 M
CAGL0F07513g YKL093W MBR1
CAGL0G02101g YKR076W ECM4
CAGL0G02651g YIL097W FYV10
CAGL0G02717g YIL099W SGA1 M
CAGL0G03289g YBL075C SSA3
CAGL0G03883g YLL026W HSP104
CAGL0G05269g YDR070C FMP16
CAGL0G05335g YDR074W TPS2 * M
CAGL0G07601g YBR287W ZSP1
CAGL0G09020g YPL203W TPK2 M
CAGL0G09977g YPR184W GDB1 * M
CAGL0H00682g YMR196W YMR196W
CAGL0H02585g YMR250W GAD1 M
CAGL0H02959g YGL096W TOS8
CAGL0H05599g YPL087W YDC1
CAGL0H08844g YMR173W DDR48 *
CAGL0H10120g YBR056W YBR056W
CAGL0I01122g YHR104W GRE3
CAGL0I06094g YJL155C FBP26 M
CAGL0I06809g YER142C MAG1
CAGL0I07865g YOL084W PHM7 * M
CAGL0J04202g YFL014W HSP12 *
CAGL0J06050g YNL160W YGP1 *
CAGL0J07612g YNL241C ZWF1
CAGL0J09812g YBR126C TPS1 * M
CAGL0K00803g YGR209C TRX2
CAGL0K03421g YMR105C PGM2 * M
CAGL0K03509g YMR110C HFD1
CAGL0K07480g YMR105C PGM2 * M
CAGL0K08536g YKL103C LAP4
CAGL0K09350g YGL208W SIP2
CAGL0L01925g YKL035W UGP1 M
CAGL0L06006g YGL180W ATG1
CAGL0L06820g YMR139W RIM11 M
CAGL0L07656g YML004C GLO1
CAGL0L08448g YPR149W NCE102
CAGL0L10582g YMR196W YMR196W *
CAGL0M02211g YPL154C PEP4
CAGL0M03377g YEL011W GLC3 * M
CAGL0M03399g YEL012W UBC8 M
CAGL0M06347g YBR183W YPC1 M
CAGL0M08822g YDR258C HSP78
CAGL0M13255g YKL065C YET1
CAGL0M13651g YMR297W PRC1 * M
CAGL0M13783g YMR304W UBP15 M

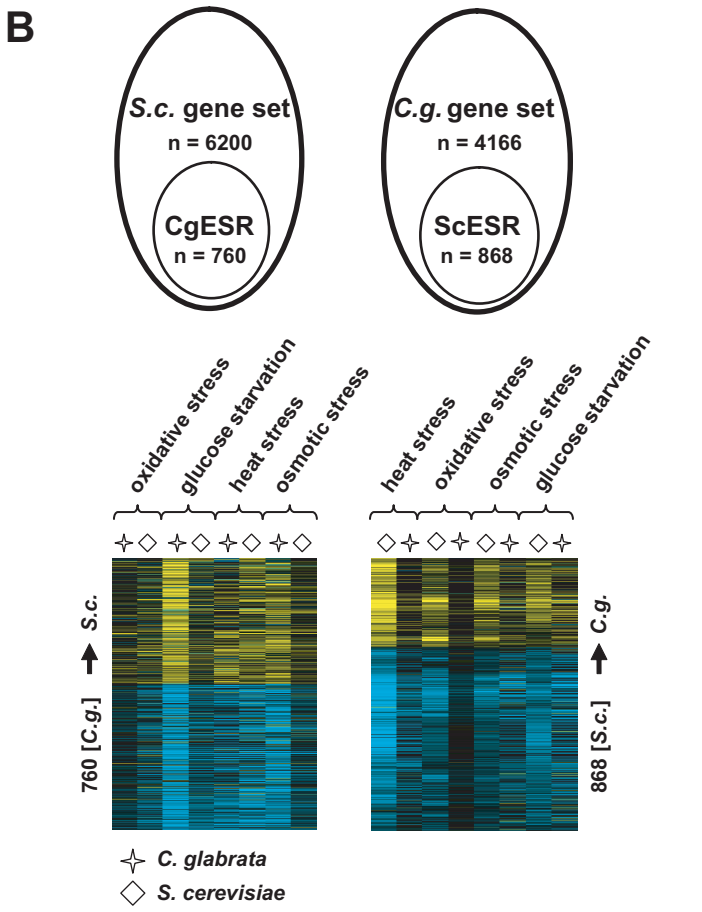
B
S.c. gene set
n = 6200
CgESR
n = 760
C.g. gene set
n = 4166
ScESR
n = 868
oxidative stress
glucose starvation
heat stress
osmotic stress
heat stress
oxidative stress
osmotic stress
glucose starvation
S.c.
760 [C.g.]
C.g.
868 [S.c.]
C. glabrata
S. cerevisiae

Figure S4

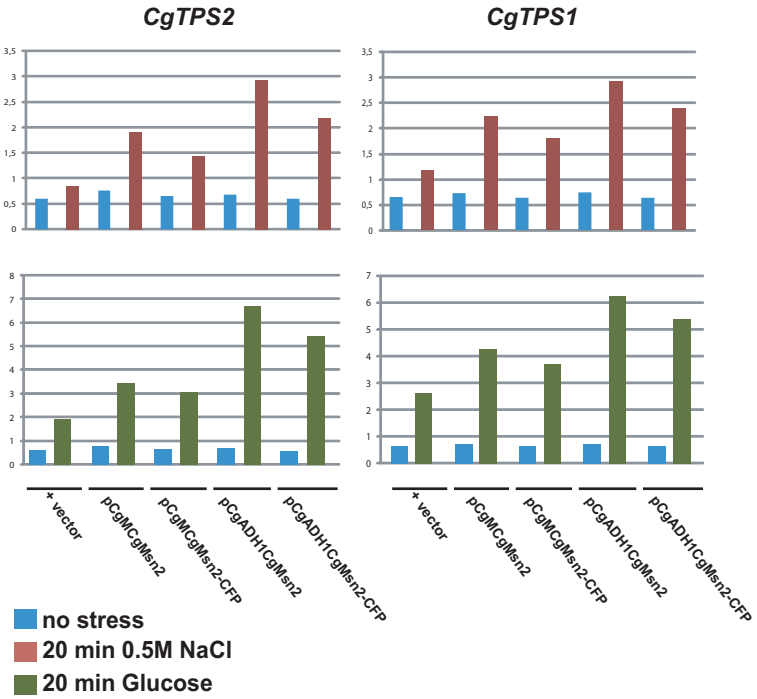
CgTPS2
CgTPS1
+ vector
pCgMCgMsn2
pCgMCgMsn2-CFP
pCgADH1CgMsn2
pCgADH1CgMsn2-CFP
no stress
20 min 0.5M NaCl
20 min Glucose

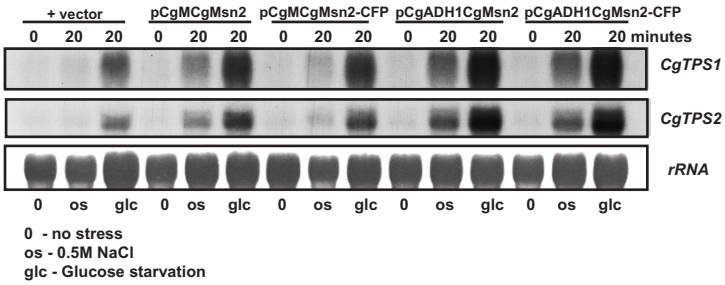
+ vector
pCgMCgMsn2
pCgMCgMsn2-CFP
pCgADH1CgMsn2
pCgADH1CgMsn2-CFP
0 20 20 0 20 20 0 20 20 0 20 20 0 20 20 minutes
CgTPS1
CgTPS2
rRNA
0 os glc 0 os glc 0 os glc 0 os glc 0 os glc
0 - no stress
os - 0.5M NaCl
glc - Glucose starvation

Figure S1. Southern analysis of *CgMSN2* and *CgMSN4* deletion strains. *CgMSN2* was replaced by *CgHIS3* and *CgMSN4* was replaced by *ScURA3.* Genomic DNA from wild type and the *msn2*Δ and *msn2*Δ*msn4*Δ deletion strains was digested with either *Bgl*II or *Sca*I. Chromosomal restriction sites are indicated. DNA fragments were detected with radio-labeled probes as indicated. Replacement of *CgMSN2* with *CgHIS3* strain abolishes two *Bgl*II cleavage sites leading to a 6.2kb fragment instead of the 3.6kb wildtype fragment (left panel). Replacement of *CgMSN4* with *ScURA3* strain introduces a *Sca*I cleavage site changing the 3.7kb wildtype fragment to a 1.3kb fragment (right panel).

Figure S2. ESR gene expression levels of four different yeasts is similar. (A, B) Pairwise overlap of stress induced orthologous genes between *C. glabrata, C. albicans, S. cerevisiae,* and *S. pombe.* Cut-off values are indicated. Expression levels of all four organisms were compared to each other during osmotic **(A)** and oxidative stress **(B).** Specific induction levels were chosen (*C. glabrata* >2-fold after osmotic stress and >1.5-fold upon oxidative stress; *S. cerevisiae* >1.5-fold upon osmotic stress and oxidative stress; *C. albicans* >1,5-fold upon osmotic stress and oxidative stress; *S. pombe* >1,5-fold upon osmotic stress and oxidative stress) and used for a selection among all expressed genes (>1) of the four yeasts during oxidative and osmotic stress, respectively (*C. glabrata*: 945, 1126; *C. albicans*: 934 , 1058; *S. cerevisiae*: 956 , 360; *S. pombe*: 916 , 1065; genes oxidative, osmotic stress). **(C)** Common Msn2 response of orthologous genes. 13 genes are induced significantly (4-fold) by at least one of the tested conditions and by overexpression of ScMsn2 and CgMsn2.

Figure S3. ESR genes are conserved between *C. glabrata* and *S. cerevisiae*. (A) Comparison of genes comprising the CgESR of *C. glabrata* versus the ScESR of *S. cerevisiae*. A set of 268 genes shared between *C. glabrata* and *S. cerevisiae* has a similar stress induction profile for the conditions tested. Color code indicates common Msn2 regulated genes. CgMsn2

regulated genes are highlighted with a green letter (M), whereas genes from core response (see Figure 5B) are in red. **(B)** CgESR from *C. glabrata* (760 genes) is compared to the expression set of *S. cerevisiae* (~ 6200 genes) (left panel), whereas in the right panel the ScESR from *S. cerevisiae* (868 genes) was aligned against the expression set of *C. glabrata* (~ 4200 genes). Data from corresponding stress treatments were chosen: 0.4mM H_2O_2 (*C.g.*) versus 0.32mM H_2O_2 (*S.c.*), 20 minutes of glucose depletion (*C.g*.) versus a corresponding time point of a starvation time course (*S.c*.), temperature shift from 30°C to 42°C (heat shock, *C.g*.) versus shift from 25°C to 37°C (*S.c*.) and 0.5M NaCl (osmotic shock, *C.g*.) versus 1M Sorbitol (*S.c*.). *S. cerevisiae* data were extracted from (Gasch *et al.*, 2000)

Figure S4. CgMsn2 and CgMsn2-CFP display similar rapid induction of transcription after applying stress. (A) mRNA levels of *CgTPS1* and *CgTPS2* were quantified and normalized to large rRNA. **(B)** Northern blot analysis of *CgTPS1* and *CgTPS2* transcripts during 0.5M NaCl induced osmotic stress and glucose starvation. *Cg msn2*Δ*msn4*Δ transformed with empty vector and *Cg msn2*Δ*msn4*Δ transformed with pCgMCgMSN2-CFP, pCgMCgMSN2, pCgADH1CgMSN2-CFP and pCgADH1CgMSN2 were grown to exponential phase. Cells were treated with 0.5M NaCl or washed twice and incubated in YP without glucose. Samples for RNA extraction were taken at indicated time points. mRNA levels were visualized by hybridization of radio-labeled probes and autoradiography. Staining of rRNA was used as a loading control.

Table S1 Oligonucleotides used.

Name	Sequence
KlM2SalI	GAG*GTCGAC*AGCTTTGAAGTTACACATTCC
KlM2NcoI	GCCA*CCATGG*AAGTTTGGCTCGTGGAAATTTGAG
AgM2XhoI	AGCTA*CTCGAG*AGTGGCGCAGGCTCGTCG
AgM2NcoI	AAACGTCTC*CCATGG*CGCCCGGAAGGCTTTTTGGATCAAGC
CgM4SalI	GTACT*GTCGAC*TCTAGTCTGGGCAATGAT
CgM4NcoI	CGT*CCATGG*AAGGTGCTAATGACCCTACGC
ScM4SalI	ATCGC*GTCGAC*AGTACAACAGGATTGAACG
ScM4NcoI	ATTT*CCATGG*AAGAGTTCATCGAGATATCATAGC
CgM2XhoI	ATC*CTCGAG*AGCGACCAAAAGGGCAGAAGGG
CgM2NcoI	GCTTT*CCATGG*ATTGGCTATTTTGCCAGGATTCC
CaMsn4-5	GGTACGTCGACATGTCTCAAGAATTCCAACC
CaMsn4-3	GGCTTCCATGGAAGTAGTGATTGGTTTGGTTG
ACT1-5	ATGTGTAAGGCCGGTTTC
ACT1-3	AGGAAGATTGAGCAGCGG
TPS1-5	ATGACACAGATTGAT
TPS1-3	ATTCTGTAGATCTCG
TPS2-5	CGCTACTAAGAAACA
TPS2-3	GTAATCGTGAATCCA
UBP15-5	ATGGGAACAAATGTTGA
UBP15-3	TTATGAAGTTATGCCAC
MSN4-1	AGTTTCTTGCGATACTATAG
MSN4-2	CCGCTGCTAGGCGCGCCGTGAGATTGTACTGAGAGTGCAC
MSN4-3	CACGGCGCGCCTAGCAGCGGAATAAACAAGACTTGCCAAT
MSN4-4	GTCAGCGGCCGCATCCCTGCTTAAAGTCTCGAGCCATTCTT
MSN4-5	GCAGGGATGCGGCCGCTGACCTGTGCGGTATTTCACACCG
MSN4-6	TGTACAAGGAGCAGCATAAA
MSN2-5´M13	ACACAGATCAACAAGAACAGCAGGAAACAGCTATGAC
MSN2-3´M13	TTGTGGAAGTACTTCCCGACCCCAGTCACGACGTTGTA
MSN2-5´3´	GTCATAGCTGTTTCCTGCTGTTCTTGTTGATCTGTGT
MSN2-3´5´	TACAACGTCGTGACTGGGGTCGGGAAGTACTTCCACA
MSN2-5´5´	GTGCGTTGAGAGTTGTCAGCC
MSN2-3´3´	CCAGGTTAGCCTTGTGATGC

5´ExMSN4-Ctrl1	TCACGCCGTGCGAACTC
URA-Ctrl2	TGCTGGCCGCATCTTCT
3´ExMSN4-Ctrl3	TCTCTTTCGGGGGCATC
URA-Ctrl4	TAGTCCTGTTGCTGCCA
5´ÉxMSN2-Ctrl1	CCCGTTTACTCAACAATGAGAC
HIS-Ctrl2	GACACGTAGACTAGCCACAATATC
3´ExMSN2-Ctrl3	TAAGTTCATTGGTCTCTCGG
HIS-Ctrl4	CACTCTACGTAGCAGGCGACCC
CgAdhPro-SphI	AGAT*GCATGC*CAACTTCACAAACACAAACA
CgAdhPro-SacII	CGCA*CCGCGG*TGTTTATGTGTTTTTTGCAG
SphI-msn2nat	AGATGCATGCTATTTTATAGAACAGTAACG
SacII-msn2nat	CGCACCGCGGCTGTTCTTGTTGATCTGTGT
5-SASA	GGCCTCTGCTAGAAATGCTATTGCACACGGTGTCGACTT
3-SASA	AAGTCGACACCGTGTGCAATAGCATTTCTAGCAGAGGCC
CgMsn2Cfp-SacII	CGCA*CCGCGG*ATGACGGTCGACCAGGAGCCT
CgMsn2Cfp-NsiI	AGAGC*ATGCAT*TTATGGGCGGCCGCTCTTGTA
CgMsn2-Cfp1SalI	TTT*GTCGAC*CAGGAGCCTAGCTCGTGG
CgMsn2-Cfp2NcoI	TTAGC*CCATGG*ATTCTTTAGTTGTGGAAGTAC
IPP1 fwd	CCCTTGTACGCTGACAAGG
IPP1 rev	GCTTCACCGGAGAAGGC
Re-SalI-5	GCGGAAGGTGGGGATC*GTCGAC*GTTTCTAGTG
Re-SalI-3	CACTAGAAAC*GTCGAC*GATCCCCACCTTCCGC

Autophagy supports *Candida glabrata* survival during phagocytosis.

Andreas Roetzer[a], Nina Gratz[b], Pavel Kovarik[b] and Christoph Schüller[a*]

From

[a] Max F. Perutz Laboratories, University of Vienna, Department of Biochemistry and Cell Biology, A-1030 Vienna, Austria

[b] Max F. Perutz Laboratories, University of Vienna, Department of Microbiology and Immunology, A-1030 Vienna, Austria

Running title: *Candida glabrata* phagocytosis response

*) To whom correspondence should be addressed:

Christoph Schüller

University of Vienna, Max F. Perutz Laboratories

Department of Biochemistry and Cell Biology

Dr. Bohr-Gasse 9/5

A-1030 Vienna, Austria

Phone: +43-1-4277-52815; Fax: +43-1-4277-9528

E-mail: Christoph.Schueller@univie.ac.at

Abstract

The opportunistic human fungal pathogen *Candida glabrata* is confronted with phagocytic cells of the host defence system. Survival of internalized cells is thought to contribute to successful dissemination. We investigated the reaction of engulfed *C. glabrata* cells using fluorescent protein fusions of the transcription factors CgYap1 and CgMig1 and catalase CgCta1. The expression level and peroxisomal localization of catalase was used to monitor the metabolic and stress status of internalized *C. glabrata* cells. These reporters revealed that the phagocytosed C. glabrata cells were exposed to transient oxidative stress and starved for carbon source. Cells trapped within macrophages increased their peroxisome numbers indicating a metabolic switch. Prolonged phagocytosis caused a pexophagy-mediated decline in peroxisome numbers. Autophagy, and in particular pexophagy, contributed to survival of *C. glabrata* during engulfment. Mutants lacking *CgATG11* or *CgATG17,* genes required for pexophagy and non-selective autophagy, respectively*,* displayed reduced survival rates. Furthermore, both CgAtg11 and CgAtg17 contribute to survival, since the double mutant was highly sensitive to engulfment. Inhibition of peroxisome formation by deletion of *CgPEX3* partially restored viability of Cg*ATG11* deletion mutants during engulfment. This suggests that peroxisome formation and maintenance might sequester resources required for optimal survival. Mobilization of intracellular resources via autophagy is an important virulence factor that supports the viability of *C. glabrata* in the phagosomal compartment of infected innate immune cells.

Keywords: Candida glabrata, catalase, peroxisomes, autophagy, pexophagy, phagocytosis

Introduction

Candida glabrata belongs to the diverse group of human fungal pathogens and is phylogenetically closely related to *Saccharomyces cerevisiae* (Kaur *et al.*, 2005, Marcet-Houben *et al.*, 2009). The high similarity of *C. glabrata* to *S. cerevisiae* suggests that also for fungi, relatively small genetic changes may be sufficient for adaptation to a pathogenic life style (Dujon *et al.*, 2004). *C. glabrata* is a common commensal, but can turn into an opportunistic pathogen with a rising frequency of isolates among immunocompromised patients and elder people (Pfaller *et al.*, 2007, Presterl *et al.*, 2007, Li *et al.*, 2007). In the host environment, *C. glabrata* has to evade or survive attacks of the cell-mediated immune system (Nicola *et al.*, 2008). Counterstrategies of fungal pathogens differ between species. *Candida albicans* destroys macrophages by hyphal outgrowth. Alternatively, *Cryptococcus neoformans* either lyses macrophages or escapes via phagosomal extrusion (Alvarez *et al.*, 2006, Ma *et al.*, 2006). *C. glabrata* engulfed by macrophages do not undergo morphological transitions such as *C. albicans* (Leberer *et al.*, 2001). An open question concerns how *C. glabrata* is coping with cells of the immune system, such as macrophages.

The phagosome is a hostile environment for fungi (reviewed in (Nicola *et al.*, 2008)). After internalization of microbial cells, the organelle maturates into the phagolysosome containing mature hydrolytic enzymes and a more acidic pH 4.5-5.5 (Geisow *et al.*, 1981, Levitz *et al.*, 1999). Additionally, the NADPH oxidase complex generates reactive oxidative species to attack internalized microorganisms (for review see (Segal, 2005, Romani, 2004)). Thus, commensal and pathogenic fungi are exposed to reactive oxygen species (ROS) produced by polymorphonuclear leucocytes, macrophages and dendritic cells (Miller *et al.*, 1997, Missall *et al.*, 2004, Gildea *et al.*, 2005). On the fungal side, antioxidant defence enzymes such as catalase, superoxide dismutase, thioredoxin- and glutathione-dependent peroxidases and reductases guard

against oxidative stress and are thus considered virulence factors (Johnson *et al.*, 2002, Cox *et al.*, 2003, Chaves *et al.*, 2007, Missall *et al.*, 2005). Oxidative stress as defence strategy is not restricted to combat fungal infections. Invading bacteria, such as *Staphylococcus aureus*, or the malaria parasites *Plasmodium sp*., face ROS stress upon engulfment (Voyich *et al.*, 2005, Becker *et al.*, 2004). ROS sensed by microbes act also as signalling molecules. The *C. albicans* catalase, an enzyme which decomposes hydrogen peroxide, has been investigated more closely. *C. albicans* induces catalase when engulfed in neutrophils or in macrophages (Rubin-Bejerano *et al.*, 2003, Lorenz *et al.*, 2004, Enjalbert *et al.*, 2007). Moreover, hydrogen peroxide promotes the morphological transition of *C. albicans* cells to hyphal growth, a form invading the host tissue (Nakagawa, 2008, Nasution *et al.*, 2008). Finally, C*. albicans* devoid of catalase was eliminated more efficiently in a mouse infection model (Nakagawa *et al.*, 2003). The filamentous fungus *Aspergillus fumigatus* lacking the catalases expressed in the mycelium exhibited delayed infection in a rat model of invasive aspergillosis (Paris *et al.*, 2003). In contrast, *C. glabrata* catalase was not a virulence determinant in an immunocompromised mouse model (Cuellar-Cruz *et al.*, 2008). In mice infected with a *C. neoformans* mutant devoid of all four catalases, mortality was unchanged (Giles *et al.*, 2006). Thus the relative importance of individual ROS scavenging enzymes varies between fungal pathogens.

Besides being exposed to oxidative stress, cells engulfed by macrophages adjust their metabolic program (Fan *et al.*, 2005, Barelle *et al.*, 2006). Engulfed *C. albicans* cells induce many genes involved in non-fermentative carbon metabolism (Prigneau *et al.*, 2003, Lorenz *et al.*, 2004). Phagocytosed *C. glabrata* induces genes encoding enzymes involved in β-oxidation, the glyoxylate cycle and gluconeogenesis (Kaur *et al.*, 2007). Moreover, the glyoxylate cycle, which is required to channel fatty acid-derived two carbon units into metabolism, was early recognized as a virulence determinant for *C. albicans* (Lorenz *et al.*, 2001). Other human fungal pathogens also induce glyoxylate cycle

components during infection conditions (Derengowski *et al.*, 2008, Rude *et al.*, 2002, Canovas *et al.*, 2006). However, *A. fumigatus* and *C. neoformans* do not require the glyoxylate cycle for virulence (Schöbel *et al.*, 2007, Idnurm *et al.*, 2007). Some of the enzymes of the glyoxylate cycle are localized in the peroxisomal matrix (for review see e.g. (Kunze *et al.*, 2006)). Peroxisomes are inducible, single membrane organelles which harbour enzymes for the oxidative catabolism of fatty acids, the glyoxylate cycle and others. Generally, peroxisome number and size vary according to metabolic needs (for review see (Yan *et al.*, 2005, Platta *et al.*, 2007)).

Autophagy continuously recycles almost all constituents of the cell (for review see (Kraft *et al.*, 2009, Mizushima *et al.*, 2007)). Different types of autophagy help organisms to overcome periods of nutrient starvation by recycling intracellular components to sustain vital cellular functions and seems to be linked to the unique niches and morphology of these pathogens (for review see (Palmer *et al.*, 2008)). For certain pathogenic fungi, autophagy has been identified as a virulence factor. *C. neoformans* requires an intact autophagy pathway during infection (Hu *et al.*, 2008). Peroxisomes and their contents are delivered to the vacuole by the pexophagy pathway, a specialized form of autophagy (Kim *et al.*, 2001, Guan *et al.*, 2001, Farre *et al.*, 2004). In *S. cerevisiae* selective pexophagy is dependent on Atg11 and partly on Atg17 which is also important for non-selective autophagy (Cheong *et al.*, 2005, Yorimitsu *et al.*, 2005).

Here we investigated responses of *C. glabrata* during its encounter with the macrophage phagosome compartment from which it cannot escape. We developed *in vivo* reporters to track fungal responses to this environment. To detect oxidative and glucose starvation stress of cells, we used fluorescent protein fusions of the *C. glabrata* orthologues of the *S. cerevisiae* transcription factors Yap1 and Mig1 (Kuge *et al.*, 1997, Carlson, 1999). We found the *C. glabrata* catalase gene *CgCTA1* and catalase activity regulated by oxidative stress and glucose starvation. Additionally, we demonstrated GFP-

CgCta1 localization to peroxisomes. *C. glabrata* peroxisomes have not been described so far and were here defined by several independent criteria. We found that *C. glabrata* cells engulfed by mouse macrophages experience a mild oxidative stress and sustained carbon starvation. Additionally, peroxisomes became transiently induced in engulfed cells. We explored the role of peroxisomes with various mutants lacking peroxisome biogenesis or autophagy pathways mediating destruction of peroxisomes. We report here that autophagy and, surprisingly, pexophagy is a likely virulence factor for *C. glabrata.* Mutants lacking CgAtg11 and/or CgAtg17 were killed more efficiently by macrophages during engulfment. Thus, for engulfed *C. glabrata* cells, nutrient deprivation represents a serious challenge and mobilization of intracellular resources via autophagy is a major contributor to sustain viability.

Results

C. glabrata catalase CgCta1 is induced by hydrogen peroxide and carbon starvation.

C. glabrata harbours one catalase gene (*CgCTA1*, CAGL0K10868g), related to the yeast peroxisomal catalase *CTA1* gene. The two catalase genes of *S. cerevisiae* are regulated differently. *CTT1,* coding for the cytoplasmic catalase, is induced by stress conditions (Marchler *et al.*, 1993). The *CTA1* gene, is expressed only during growth on non-fermentable carbon sources (Hartig *et al.*, 1986, Cohen *et al.*, 1985). To find out the regulatory pattern of the *C. glabrata* catalase, we assayed its activity in crude protein extracts from cells grown either on glucose or a non-fermentable carbon source. Cells adapting to ethanol as carbon source showed a substantial induction of catalase activity (Figure 1A). Moreover, mild oxidative stress of 0.4mM H_2O_2 induced *C. glabrata* catalase activity about ten-fold suggesting regulation by both glucose starvation and oxidative stress (Figure 1B). To verify if the *CgCTA1* gene encodes the only catalase activity in *C. glabrata*, we replaced the open reading frame with the *S. cerevisiae URA3* gene (Figure S1). Catalase activity was undetectable in extracts derived from the mutant strain (Figure 1A, B). A centromeric plasmid (p*CgCTA1*) harbouring the *CgCTA1* ORF including a 1.8kb upstream region fully restored wild type level catalase activity to the *cta1*Δ mutant (Figure 1A, B). To demonstrate that the regulation of catalase activity occurs at the level of transcription, *CgCTA1* mRNA levels were analyzed from cells shifted to medium lacking glucose or exposed to 0.4mM H_2O_2. Glucose starved cells displayed a continuous increase of *CgCTA1* mRNA immediately after shift to glucose free medium (Figure 1C). Hydrogen peroxide stress caused a rapid increase within 10 minutes. Taken together, regulation of the *C. glabrata* catalase gene *CgCTA1* by carbon source availability and oxidative stress combines elements of both *S. cerevisiae* catalases.

CgCta1 confers hydrogen peroxide stress resistance.

The similarity of the *CgCTA1* gene to the *S. cerevisiae CTA1* gene suggested its peroxisomal localization. To clarify the intracellular localization, we fused a green fluorescent protein (GFP) to the CgCta1 N-terminus (*GFP-CgCTA1*) to preserve the putative peroxisomal targeting sequence 1 (PTS1) (Figure 1C, lower panel). The preceding 1.8kb of the *CgCTA1* 5´ untranslated region conferred a wild type-like expression pattern in hydrogen peroxide stressed cells (Figure 1C). Basal catalase activity of GFP-CgCta1 was detectable in unstressed cells, whereas hydrogen peroxide stress induced activity was reduced to about 20% of the wild type level (Figure 1B).

We assessed if the reduced activity of GFP-Cta1 interferes with hydrogen peroxide stress resistance. *C. glabrata cta1*Δ mutant cells transformed with either p*GFP-CgCTA1*, p*CgCTA1* or the empty plasmid (p*ACT*) were grown in synthetic medium, the cultures were split and one part treated with 0.4mM H_2O_2. Both were subsequently exposed to higher doses of hydrogen peroxide. Growth was scored after 24 hours (Figure 1D). The *cta1*Δ mutant cells containing the empty plasmid failed to grow in medium containing 5mM H_2O_2. In contrast, the strain carrying the p*CgCTA1* plasmid was resistant to medium supplemented with up to 20mM H_2O_2, whereas pre-incubation with 0.4mM H_2O_2 pushed the growth limit to 40mM H_2O_2, similar to the wild type parent strain (ΔHTU). Cells expressing the GFP-CgCta1 derivative displayed lower basal resistance. However, naïve cells without pre-treatment tolerated 5mM H_2O_2 and failed to grow only at about 20mM H_2O_2. Pre-treatment with 0.4mM H_2O_2 shifted tolerance to about 30mM H_2O_2. Thus, the GFP tagged CgCta1 derivative, when compared to the untagged version, conferred resistance to oxidative stress to reduced but overall high level. These results suggested that H_2O_2 stress resistance of strains carrying the plasmid-encoded catalase derivatives

encompasses the oxidative stress load of 0.4mM H_2O_2 determined for the *in vivo* situation (Enjalbert *et al.*, 2007). Our data also showed that the *C. glabrata* strains tolerated a substantial higher oxidative stress load compared to *S. cerevisiae* laboratory strains, which failed to grow at concentrations higher than 3mM H_2O_2 (Davies *et al.*, 1995, Cuellar-Cruz *et al.*, 2008).

Localisation of GFP-CgCta1 is dependent on the carbon source.

Cells expressing *GFP-CgCTA1* were exposed to different stress conditions. In rich medium, GFP-CgCta1 fluorescence was hardly detectable, reflecting its low basal expression of *CgCTA1*. Oxidative stress caused induction of the GFP-CgCta1 fluorescence signal. To compare different expression levels directly, unstressed cells were marked by staining their nucleic acids with DAPI. For microscopy these marked unstressed cells were mixed to cells from the same culture treated for 1 hour with 0.4mM H_2O_2. The micrograph demonstrates induction of the fusion protein by oxidative stress and its initial localization in the cytoplasm (Figure 2A). GFP-*CgCTA1* became also induced after the glucose concentration in the growth medium dropped below 0.03% (Figure S2A). We then investigated GFP-CgCta1 distribution in cells growing on non-fermentable carbon sources. Cells expressing *GFP-CgCTA1* were grown in medium supplemented with 0.5% glucose and 1.5% ethanol. After 5 hours, glucose was exhausted, and cells were switching to the non-fermentable carbon source. (Figure 2B, left panel). Although the vast majority of GFP-CgCta1 was still located in the cytoplasm, small vesicles accumulating catalase became visible (see insert). After 20 hours, almost all GFP-CgCta1 was accumulated in vesicular structures (Figure 2B, middle panel).

CgCta1 can localize to peroxisomes.

We suspected that the vesicles accumulating GFP-CgCta1 were peroxisomes. The PTS1 of CgCta1 was a boundary case compared to *S. cerevisiae* Cta1 (Figure 2B, lower panel). To interfere with *C. glabrata* peroxisome assembly, we chose to eliminate the *CgPEX3* gene (CAGL0M01342g). The *S. cerevisiae* orthologue Pex3 has an essential function for peroxisome biogenesis (Hohfeld *et al.*, 1991). The *CgPEX3* open reading frame was replaced with the *ScURA3* gene and the correct integration was tested by Southern blot (Figure S1). In these *pex3*Δ mutant cells, GFP-CgCta1 remained distributed in the cytoplasm, even in 1.5% ethanol grown cells (Figure 2B, right panel). With oleic acid as sole carbon source, *S. cerevisiae* cells increase number and size of peroxisomes (Thieringer *et al.*, 1991). GFP-CgCta1 accumulated in vesicles in cells growing in medium containing 0.2% oleic acid, whereas in *pex3*Δ mutant cells fluorescence was dispersed in the cytoplasm (Figure 2C). The number of stained vesicles also increased substantially in cells growing on a non-fermentative carbon source (1.5% ethanol) (Figure 2D). These data suggest that *C. glabrata* accumulates GFP-CgCta1 in CgPex3-dependent structures resembling peroxisomes.

To visualize peroxisomal structures in *C. glabrata*, we fused a generic peroxisomal targeting signal peptide (KNIESKL) derived from the *S. cerevisiae* citrate synthase to the C-terminus of YFP (Lewin *et al.*, 1990, Kragler *et al.*, 1993). The *YFP-KNIESKL* fusion gene expression was driven by the strong *CgADH1* promoter. YFP fluorescence marked peroxisomes, which increased their number during growth on ethanol (Figure 3A, upper panel) and were absent in *pex3*Δ mutant cells (Figure 3A, lower panel). This result confirmed the requirement of CgPex3 for *C. glabrata* peroxisome biogenesis.

The above results indicated a partial organellar localisation of catalase, depending on the type of carbon source. To show this, we prepared cell extracts of *cta1*Δ mutant cells expressing *CgCTA1.* We separated these in an organellar pellet and a cytosolic

supernatant fraction by centrifugation and tested the fractions for catalase activity. After oxidative stress, the entire induced catalase activity was found in the cytoplasmic supernatant (Figure 3B). In extracts from cells growing with ethanol as main carbon source, catalase activity was found in the cytosolic supernatant, but about one fourth of total activity was present in the pellet fraction (Figure 3C, left panel). To confirm that the pellet fraction contained organelles, we used cytochrome C oxidase activity as marker enzyme for mitochondria. Most of the cytochrome C oxidase activity was found in the pellet fraction (Figure 3C, right panel). Separation of extracts derived from cells grown in medium containing 0.2% oleic acid showed a further shift of catalase activity towards the pellet fraction (Figure 3D). Activity of CgCta1 in the various fractions was distributed corresponding to the previously observed intracellular localisation of GFP-CgCta1. Together, these results showed a dual localization of *C. glabrata* catalase depending on the presence of peroxisomes.

Phagocytosis induces GFP-CgCta1.

Fungal pathogens are exposed to a stressful environment, when they come into contact with phagocytic cells (Nicola *et al.*, 2008). The regulation and localisation of GFP-CgCta1 made it useful to report the environmental conditions during phagocytosis. *C. glabrata cta1*Δ mutant cells expressing *GFP-CgCTA1* grown to exponential phase were used for infection of primary mouse macrophages. We used time lapse live microscopy to follow the fate of individual engulfed cells (Figure 4A). Freshly phagocytosed *C. glabrata* cells reacted to this environment with a detectable GFP-CgCta1 fluorescence signal within 40 minutes. (Figure 4A and Figure S2C). Furthermore, during prolonged phagocytosis, GFP-CgCta1 accumulated in peroxisomes. To support the idea of peroxisome proliferation during phagocytosis, we followed localisation of the YFP-KNIESKL fusion protein during

infection of macrophages. Cells were fixed and stained for microscopy immediately after infection and after 2.5, 5, 10 and 24 hours (Figure 4B). We counted cells with visible peroxisomes per macrophage at various time points (Figure 4C, left panel; Figure S3). The number of cells with peroxisomes and the number of peroxisomes within these cells transiently increased, reaching a peak after 5 hours (Figure 4C). After 24 hours, the vast majority of cells displayed a cytoplasmic/vacuolar YFP-KNIESKL fluorescence signal. Thus, engulfed cells show transient proliferation of peroxisomes.

Localization of GFP-CgYap1 and CgMig1-CFP in phagocytosed cells

The localization of CgCta1 suggested that engulfed *C. glabrata* cells might experience oxidative stress and/or carbon source starvation. To confirm this independently, we created additional fluorescent reporter constructs. In *S. cerevisiae,* the glucose-regulated transcriptional repressor Mig1 is rapidly exported from the nucleus in cells starved for glucose (De Vit *et al.*, 1997). *S. cerevisiae* Yap1 accumulates rapidly in the nucleus in cells exposed to mild oxidative stress (Kuge *et al.*, 1997). To preserve the localization signals of the orthologous transcription factors, CgYap1 was N-terminally fused to GFP whereas CgMig1 was C-terminally fused to CFP. To be detectable, both fusion genes were expressed from centromeric plasmids and driven by the *CgADH1* promoter. Nuclear localization was confirmed by simultaneous staining of nucleic acids with DAPI (Figure 5A and 5B).

GFP-CgYap1 was located in the cytoplasm in unstressed *C. glabrata* ΔHTU cells. Upon exposure to mild oxidative stress (0.4mM H_2O_2), GFP-CgYap1 rapidly accumulated in the nucleus (Figure 5A, upper panel). The fusion gene could complement the transcription defects of the corresponding deletion mutant (our unpublished observation). Within the first hour upon engulfment, cells with nuclear GFP-CgYap1 were visible (Figure

5A, middle panel). We determined the percentage of yeast cells with nuclear GFP-Yap1 per macrophage after 30 minutes, 1 hour and 5 hours (Figure 5A, lower panel) and found a peak at about 1 hour. The CgMig1-CFP fluorescence signal accumulated in the nucleus after addition of glucose (2%) to the medium of glucose starved cells, and was also nuclear in the glucose-rich environment of the macrophage culture medium (DMEM) (Figure 5B, upper panel). Immediately after phagocytosis, CgMig1-CFP accumulated in the cytoplasm and remained there constantly, indicating glucose starvation (Figure 5B, lower panel). These data showed that within the phagosome oxidative stress is transient, whereas macrophages are highly effective in depriving the carbon source.

Peroxisomes are transiently induced during phagocytosis.

Peroxisome numbers declined at later stages of engulfment (Figure 4B). In *S. cerevisiae*, key factors for pexophagy are Atg11 (Yorimitsu *et al.*, 2005) and Atg17, which is also essential for non-selective autophagy (Cheong *et al.*, 2005). We deleted the *C. glabrata CgATG11* and *CgATG17* homologues (CAGL0H08558g, CAGL0J04686g) in wild type (ΔHTU) and *pex3*Δ cells (Figure S1). We investigated engulfed *C. glabrata cta1*Δ, *pex3*Δ, *atg11*Δ, *atg17*Δ, *pex3*Δ*atg17*Δ, *pex3*Δ*atg11*Δ, and *atg11*Δ*atg17*Δ mutant cells expressing GFP-CgCta1 after 5 and 24 hours (Figure 6A, E). After 5 hours, GFP-Cta1 was located in peroxisomes in the *cta1*Δ, *atg11*Δ, and *atg17*Δ mutant cells, and, in contrast, accumulated in the cytoplasm of *pex3*Δ, *pex3*Δ*atg11*Δ, and *pex3*Δ*atg17*Δ mutant cells. However, after 5 hours, wild type, *atg11*Δ, and *atg17*Δ, had similar numbers of cells with peroxisomes, whereas after 24 hours, peroxisomes were more abundant in *atg11*Δ and *atg17*Δ mutants (Figure 6B). In *atg11*Δ mutants, peroxisome numbers remained constant between 5 and 24 hours engulfment. *C. glabrata atg17*Δ cells displayed a slight reduction of peroxisomes after 24 hours of engulfment, similar to *S.*

*cerevisiae atg17*Δ cells during prolonged starvation conditions (Cheong *et al.*, 2005), Upon internalization, the cytoplasmic localization of CgMig1-CFP demonstrated the same glucose starvation status in the *atg11*Δ, *pex3*Δ*atg11*Δ mutants and wild type (Figure S2B).

We investigated if the turnover of peroxisomes and mobilization of internal resources is relevant for survival during engulfment. Indeed, the *atg11*Δ and *atg17*Δ mutants had a significantly reduced viability after 24 hours compared to wild type, *cta1*Δ and *pex3*Δ strains. Furthermore, in *pex3*Δ*atg11*Δ and *pex3*Δ*atg17*Δ double mutants the absence of pexophagy might be compensated by absence of peroxisome biogenesis. Consistently, we found that the loss of Pex3 partially reversed the effect of *atg11*Δ with respect to survival during engulfment (Figure 6C). In contrast, the double mutant *pex3*Δ*atg17*Δ did not show this phenotype, indicating a broader function for CgAtg17-dependent non-selective autophagy during engulfment. Strikingly, the *atg11*Δ*atg17*Δ double mutant, lacking both selective and non-selective autophagy, was highly sensitive to phagocytosis.

To simulate the phagosome environment in vitro we combined nutrient starvation and acidic pH. We incubated *C. glabrata* wild type, *atg11*Δ, *pex3*Δ*atg11*Δ, *atg17*Δ, *pex3*Δ*atg17*Δ, and *atg11*Δ*atg17*Δ mutant cells in medium lacking nitrogen- and carbon-sources at pH 3.5 at 37℃ for 24 hours. The survival was determined by counting colony forming units after 24h hours relative to 2 hours treatment (Figure 6D). In comparison to the wild type, all mutants showed diminished survival. Intriguingly, the *pex3*Δ*atg11*Δ strain survived better than the *atg11*Δ strain. Furthermore, the double mutant *atg11*Δ*atg17*Δ displayed the lowest survival rate, similar to the macrophage model. In the macrophage, after 24 hours, most of the engulfed *atg11*Δ*atg17*Δ cells had lost GFP-CgCta1 fluorescence presumably due to cell death (not shown). However, after 5 hours the GFP-CgCta1 fluorescence signal indicated numerous peroxisomes (Figure 6E). These results

indicated that autophagy is beneficial for survival of *C. glabrata* during engulfment in macrophages, possibly counteracting acute nutrient starvation.

Discussion

Phagocytic cells internalize microbial cells and attack them with a range of microbicidal strategies (Chauhan *et al.*, 2006, Nicola *et al.*, 2008). Microbial pathogens have developed a number of strategies to improve their survival in the host environment (Urban *et al.*, 2006). Here we used three reporters (CgCta1, CgYap1 and CgMig1) to visualize aspects of the response of the human fungal pathogen *C. glabrata* to macrophage engulfment. We found that *C. glabrata* cells engulfed by primary mouse macrophages suffer from transient oxidative stress, show signs of carbon source starvation, and transiently induce peroxisomes. Our results revealed that the recycling of internal resources, especially peroxisomes, plays an important protective role for *C. glabrata* during engulfment in the phagosome.

The presence and/or proliferation of peroxisomes in fungal cells points to adjustment of carbon metabolism. We demonstrated accumulation of peroxisomes in *C. glabrata* during growth on non fermentable carbon sources and during engulfment in macrophages. Peroxisomes were visualized using two fluorescent reporter constructs GFP-CgCta1 and YFP-KNIESKL and further confirmed by other criteria. They were induced on medium containing ethanol and oleic acid as carbon source. Furthermore, peroxisomes were dependent on the *CgPEX3* gene, a peroxisomal integral membrane protein, whose orthologue in *S. cerevisiae* is essential for peroxisomal biogenesis (Hohfeld *et al.*, 1991). Peroxisomal catalases such as *S. cerevisiae* Cta1 (Simon *et al.*, 1991) are scavengers of hydrogen peroxide generated during peroxisomal ß-oxidation. We find that *C. glabrata* catalase expression is regulated by oxidative stress and carbon source, and its intracellular localization correlates with the presence of peroxisomes. This combines the regulation of both yeast catalases. The *CgCTA1* gene lacks synteny with the yeast *CTA1* gene and other fungal catalases (Gordon *et al.*, 2009). It is tempting to

speculate that the shuffling of the *C. glabrata* genome fostered the accumulation of regulatory elements for oxidative stress and carbon source response.

In a phagocytosis model using bone marrow-derived mouse macrophages, GFP-CgCta1 expressed under the control of the *CgCTA1* promoter was induced in the earliest stages after internalization. This could be due to oxidative stress or acute carbon starvation. Intracellular localization of two other fluorescent reporters (CgYap1 and CgMig1) supported rather low oxidative stress load and starvation for glucose of engulfed *C. glabrata* cells. High level expression was necessary for detection of GFP-transcription factor fusions and could potentially interfere with signalling. However, both factors are tightly regulated by post translational modifications and thus buffered for expression level. We found that in a population of engulfed cells a minor fraction displayed signs of acute oxidative stress. This is consistent with other reports. Only a small portion of *C. albicans* cells derived from mouse kidneys displayed an acute oxidative stress response when examined for *CaCTA1* expression (Enjalbert *et al.*, 2007).

The *C. glabrata* transcriptional response might have been selected to the specific conditions of phagocytosis. Microarray data indicated induction of a group of about 30 genes by both oxidative stress and glucose starvation (Roetzer *et al.*, 2008). Moreover, phagocytosed *C. glabrata* cells induce genes involved in gluconeogenesis, β-oxidation, glyoxylate cycle, and transporters for amino acids and acetate (Kaur *et al.*, 2007). Induction of peroxisomes after internalization by macrophages indicated adjustment of metabolism within the phagosome. Cells utilizing non fermentable carbon sources e.g. fatty acids or ethanol require peroxisomal β-oxidation and the partly peroxisomal glyoxylate cycle. The induction of non-fermentative carbon metabolism genes is beneficial for the survival of *C. albicans* (Barelle *et al.*, 2006, Lorenz *et al.*, 2004). In a mouse infection model, Fox2, the second enzyme of the β-oxidation pathway, and isocitrate lyase

(Icl1) an enzyme of the glyoxylate cycle, were required for *C. albicans* virulence (Lorenz *et al.*, 2001, Piekarska *et al.*, 2006). However, *C. albicans* mutants defective in the import receptor of PTS1 targeted peroxisomal proteins, CaPex5, displayed no attenuation of virulence (Piekarska *et al.*, 2006). The survival of *C. glabrata* devoid of peroxisomes in a *pex3*Δ mutant was not compromised in our infection model. Also, *C. neoformans pex1*Δ deletion mutants were not attenuated for virulence (Idnurm *et al.*, 2007). These data support the view that peroxisomes are not a major virulence determinant. Instead, the peroxisomal metabolic pathways, which can function to sufficient extent in the cytosol, appear to contribute to virulence.

In engulfed *C. glabrata* cells peroxisome numbers declined at later time points. Also at later time points GFP-CgCta1 accumulated partly in the cytosol. Peroxisomes are not known to export proteins, thus the cytosolic fluorescence was most probably due to de novo synthesis or peroxisome turnover. Peroxisomes are degraded by pexophagy, a selective autophagic pathway (Hutchins *et al.*, 1999, Farre *et al.*, 2004). In *S. cerevisiae,* mutants lacking Atg11 and Atg17 had a severe delay of pexophagy (Cheong *et al.*, 2005, Kim *et al.*, 2001, Cheong *et al.*, 2008). In *C. glabrata*, we found that mutants lacking *atg11*Δ or *atg17*Δ had reduced survival in macrophages and *in vitro* during starvation. Moreover, the *C. glabrata* double mutant *atg11*Δ*atg17*Δ displayed a striking additive decrease of survival. In *S. cerevisiae*, the *atg11*Δ*atg17*Δ double mutant strain did not contain any detectable autophagic bodies and had a severe autophagy defect (Cheong *et al.*, 2008). We suggest that *C. glabrata atg11*Δ*atg17*Δ is unable to induce autophagic processes in order to sustain prolonged phagocytosis. Notably, homologues of proteins of the autophagy core machinery have been found from yeast to mammals, but both Atg11 and Atg17 are not conserved and might be a target for antifungal drugs (reviewed by (Xie *et al.*, 2007)).

Autophagy is required for *C. neoformans* virulence (Hu *et al.*, 2008). Furthermore, *C. neoformans* genes involved in autophagy, peroxisome function, and lipid metabolism became also induced during infection (Fan *et al.*, 2005). *C. neoformans* could escape from macrophages through extrusions of the phagosome, without killing the phagocytic cell (Alvarez *et al.*, 2006). It has been suggested that this is a pathway for dissemination within the host. Therefore, survival in the macrophage indirectly contributes to virulence. A *C. albicans* mutant lacking Ca*ATG9* was defective for autophagy, but nevertheless was able to kill macrophages (Palmer *et al.*, 2007). In contrast to *C. albicans*, *C. glabrata* is trapped inside the phagosome. In *C. glabrata pex3*Δ*atg11*Δ cells, we found the sensitivity of *atg11*Δ partially reversed. We suggest from this genetic observation, that autophagy of peroxisomes is beneficial for engulfed *C. glabrata* cells. *C. glabrata pex3*Δ*atg17*Δ mutants did not display this effect. Selective pexophagy, which is affected in both *atg11*Δ and *atg17*Δ mutants, might help to mobilize intracellular resources during prolonged engulfment. *S. cerevisiae* uses autophagy to recycle proteins to overcome nitrogen starvation (Onodera *et al.*, 2005). Autophagic processes, such as pexophagy, are contributing to virulence of important fungal plant pathogens (Asakura *et al.*, 2009, Veneault-Fourrey *et al.*, 2006). However, an *A. fumigatus* mutant strain lacking Atg1 also remained virulent (Richie *et al.*, 2007). Thus the role of autophagy for fungal pathogens is also dependent on their morphology (Palmer *et al.*, 2008).

Beside the carbon and nitrogen starvation conditions inside the phagosome, other restrictions, such as pH, hydrolytic enzymes, and antimicrobial peptides might act in a synergistic manner. We infer from the phenotype of our autophagy mutants that macrophage engulfment is essentially a starvation situation in combination with acidic pH. Acidification of the phagosome aids the destruction of some microbes, but it might also contribute to the escape of others. For example, lysosomal acidification induced germ

tube formation of *C. albicans* and therefore contributed to its escape from the macrophage (Kaposzta *et al.*, 1999). The observed oxidative stress response of *C. glabrata* might result from a switch of metabolism rather than a macrophage-derived oxidative burst. It has been reported that in *S. cerevisiae,* a shift to oleic acid as carbon source induced a specific Yap1-dependent subset of oxidative stress response genes (Koerkamp *et al.*, 2002). However, we believe that the importance of autophagy for survival suggests a starvation situation. Furthermore, in our model system, the transient induction and degradation of peroxisomes is not supporting substantial metabolism in the phagosome.

Our results demonstrate that monitoring of the intracellular localization of proteins tagged with fluorescent reporters is a highly informative tool to reveal intracellular signalling and metabolic conditions. Here we show that the macrophage is efficiently depriving engulfed *C. glabrata* cells from nutrient sources. Autophagic processes, prolonging the survival of engulfed cells, are potentially aiding the dissemination of *C. glabrata* and the establishment of infection.

Experimental Procedures

Yeast strains and Plasmids: Yeast strains used in this study are listed in Table 1. Rich medium (YPD), synthetic medium (SC) and yeast nitrogen base medium (YNB) without amino acids and ammonium sulfate were prepared as described elsewhere (Current Protocols in Molecular Biology; Wiley). All strains were grown at 30℃ or 37° *C* as indicated. Oleate medium contained 0.2% oleic acid, 0.3% yeast extract, 0.5% peptone and 0.5% KH_2PO_4 (pH6). Oleate plates were incubated at 37℃ for 7 days. Glucose concentration between 0.5% and 0.03% (w/v) was determined using the Freestyle mini (Abbott). To assess viability of cells during starvation (Figure 6D, colony forming units were determined by spreading on rich medium, usually after 2 hours of incubation at 37℃ and after the indicated time (24h). Oligonucleotides used in this study are listed in Table S1. C. glabrata strains AR*Cg cta1*Δ, AR*Cg pex3*Δ, AR*Cg atg11*Δ, AR*Cg pex3*Δ *atg11*Δ, AR*Cg atg17*Δ, AR*Cg pex3*Δ *atg17*Δ, and ARCg *atg11*Δ *atg17*Δ were obtained by replacing the open reading frames with the S. cerevisiae URA3 gene or HIS3 gene generated by genomic integration. Knock out cassettes were synthesized using fusion PCR according to Noble (Noble *et al.*, 2005) from the plasmids pRS316 and pRS313 (Sikorski *et al.*, 1989) with the oligonucleotides CTA1-1 to 6, PEX3-1 to 6 ATG11-1 to 6 and ATG17-1 to 6. Correct genomic integration was verified by genomic PCR (primer series Ctrl) followed by Southern analysis using probes generated with primers CTA1-4/ CTA1-6, PEX3-1/PEX3-3, ATG11-4/ATG11-6 and ATG17-1/ATG17-3 or ATG17-4/ATG17-6. Probes for Southern and also for Northern analysis (CTA1-5/CTA1-3 and ACT1-5/ACT1-3) were amplified by PCR from genomic DNA.

Plasmids used in this study are listed in Table 2. To generate pGEM-ACT-CgCTA1, 1800 basepairs of the CgCTA1 promoter were inserted as a SphI/NotI PCR product obtained with primers CTAPro-up and CTAPro-down into the plasmid pGEM-ACT

(Gregori *et al.*, 2007). The coding sequence for CgCTA1 was amplified from genomic DNA using primers CTA-up-Not and CTA-down-Nsi, cut and inserted as a NotI/NsiI fragment. GFP was inserted as a NotI/NotI fragment at the N-terminus of CgCTA1. To generate pYFP-KNIESKL YFP was inserted as a NotI/NotI fragment obtained by PCR with primers YFP-Not-Start and YFP-SKL-Stop into the plasmid pGEM-ACT-CgADH1 (Roetzer *et al.*, 2008). CgYAP1 was amplified using primers CgYap5/CgYap3 containing a NotI or a NsiI site, GFP was inserted as NotI/NotI fragment into the plasmid pGEM-ACT-CgADH1 at the N-terminus of CgYAP1. CgMIG1 was amplified using primers Mig1-5sac/Mig1-3nco and inserted into NcoI and SacII cut *pGEM-ACT-CgADH1-MSN2-CFP* (Roetzer *et al.*, 2008). All cloned PCR fragments used in this study were controlled by sequencing.

Catalase and Cytochrome C oxidase assay: Crude extracts were prepared by breakage of yeast cells with glass beads. Catalase activity was assayed spectrophotometrically at 240nm as described in (Durchschlag *et al.*, 2004); protein concentrations were assayed at 280nm. For the Cytochrome C oxidase assay, 0.5g/l Sodium dithionite was added to reduce Cytochrome C (0.1mg/ml) solution. Cytochrome C has a sharp absorption band at 550nm in the reduced state. Absorption spectra of Cytochrome C were recorded between 410nm and 570nm. 5 minutes after addition of crude extracts, spectra were measured to determine the oxidized state of Cytochrome C (Lemberg, 1969).

Separation of organelles: Cells were resuspended in washing buffer (20mM HEPES pH7.4, 50mM NaCl, 0.6M sorbitol), incubated with protease inhibitor PMSF and broken using glass beads. The supernatant was centrifuged for 12 minutes at 6900 rcf to separate (post-mitochondrial) supernatant and the organellar pellet.

Northern and Southern blot analysis: RNA extraction and separation followed essentially the described protocol (Current Protocols In Molecular Biology; Wiley).

Hybridization of ^{32}P-αATP labelled probes occurred over night in hybridization buffer (0.5M Sodium phosphate buffer pH 7.2 / 7% SDS / 1mM EDTA) at 65°*C.* For DNA extraction, 10ml yeast cells (grown to an OD_{600}=6) were collected, washed once and resuspended in Lysis buffer (2% Triton X-100 / 1% SDS / 100mM NaCl / 10mM Tris pH8 / 1mM EDTA). Genomic DNA was isolated by PCI (phenol/chloroform/isoamyl alcohol) extraction. Digestion of 10µg genomic DNA was done over-night with XcmI for *CgPEX3*, EcoRV for *CgCTA1* and ClaI/NcoI for *CgATG11* (5U/µg DNA). The labelled probes were hybridized over night in hybridization buffer at 65°*C.* Signals were visualized by autoradiography.

Microscopy: *GFP*-fluorescence microscopy was performed as described previously (Görner *et al.*, 1998). GFP was visualized in live cells without fixation. All cells were monitored using a Zeiss Axioplan 2 fluorescence microscope. Images were captured with a Spot Pursuit (Sony) CCD camera using Spotbasic software. Time lapse microscopy was performed on an Olympus cell-imager system (IX81 inverted microscope) equipped for cell culture observation. Cells were incubated in a glass chamber at 37℃ connected to an active gas mixer (Ibidi, Martinsried, Germany). Pictures were taken with a Hamamatsu ORCA-ER camera and analysed using cell^{M}&cell^{R} software (Olympus). Nomarski contrasted, bright field microscopy pictures are indicated as BF. Quantification and statistical analysis of peroxisomes in *C. glabrata* cells (Figures 2D, 4C and 6B) have been added in figure S3.

Macrophage cell culture: Primary bone marrow derived macrophages (BMDMs) were obtained from the femur bone marrow of 6 – 10 weeks old C57Bl/6 mice. Cells were cultivated in DMEM supplemented with 10% FCS in the presence of L cell-derived CSF-1 as described (Baccarini *et al.*, 1985). Mice were housed under specific pathogen-free conditions. For infection assays, BMDMs were seeded at 5 x 10^5 cells per dish in 3,5-cm dishes containing medium without antibiotics. Log-phase *C. glabrata* cells were washed

with PBS supplemented with 0.1% glucose) and added to macrophages in a 4:1 ratio and incubated at 37℃. For microscopy, cells were fixed with 2% formaldehyde for 5 minutes. After washing with PBS, cells were incubated in 1% triton X-100 for 1 minute. After washing with PBS, cells were dyed with Phalloidin Texas-Red for 30 minutes. Cover slips were fixed to slides with Mowiol. For CFU assays, BMDM were seeded at 2 x 10^5 cells per dish. Exponentially growing *C. glabrata* cells were washed with PBS supplemented with 0.1% glucose and added to macrophages in a 1:2 ratio and incubated at 37℃. After 45 minutes, cells were washed three times with PBS to remove not phagocytosed yeast cells and fresh medium was added. At the indicated times deionised water was added to lyse macrophage cells. *C. glabrata* cells were spread on YPD plates, colonies were counted after incubation at 37℃ for 2 days.

Acknowledgements:

We thank Andreas Hartig, Fabian Rudolf, Claudine Kraft and especially Wolfgang Reiter for discussions, Christophe d´Énfert for critical reading and advice and Josef Gotzmann and Doris Mayer for technical support. C.S. was supported by the Herzfelder Foundation, and the Vienna Hochschuljubiläumsstiftung. This work was supported by the Austrian Research Foundation (FWF) through grants P16726-B14, I27-B03 and SFB F28 to P.K. and P19966-B12 to CS.

1 Table 1

***C.glabrata* Strain**	**Genotype**	**Source**
ΔHTU	*his3*Δ *trp1*Δ *ura3*Δ	(Kitada *et al.*, 1996)
ΔHT6	*his3*Δ *trp1*Δ	(Kitada *et al.*, 1996)
ARCg *cta1*Δ	*his3*Δ *trp1*Δ *ura3*Δ *cta1*Δ::*ScURA3*	This study
ARCg *pex3*Δ	*his3*Δ *trp1*Δ *ura3*Δ *pex3*Δ::*ScURA3*	This study
ARCg *atg11*Δ	*his3*Δ *trp1*Δ *ura3*Δ *atg11*Δ::*ScURA3*	This study
ARCg *pex3*Δ*atg11*Δ	*his3*Δ *trp1*Δ *ura3*Δ *pex3*Δ::*ScURA3* *atg11*Δ*::ScHIS3*	This study
ARCg *atg17*Δ	*his3*Δ *trp1*Δ *ura3*Δ *atg17*Δ::*ScURA3*	This study
ARCg *pex3*Δ*atg17*Δ	*his3*Δ *trp1*Δ *ura3*Δ *pex3*Δ::*ScURA3* *atg17*Δ*::ScHIS3*	This study
ARCg *atg11*Δ*atg17*Δ	*his3*Δ *trp1*Δ *ura3*Δ *atg11*Δ::*ScURA3* *atg17*Δ*::ScHIS3*	This study

2

3

4

1 Table 2

2

Plamid	Genotype	Source
p*RS316*	CEN6, ARSH4, *ScURA3*	(Sikorski *et al.*, 1989)
p*RS313*	CEN6, ARSH4, *ScHIS3*	(Sikorski *et al.*, 1989)
p*ACT14*	ARS, CEN and *TRP1* marker from *C. glabrata*	(Kitada *et al.*, 1996)
p*GEM-ACT*	ARS, CEN and *TRP1* marker from *C. glabrata*	(Gregori *et al.*, 2007)
p*CgC-GFP-CgCTA1*	CgCTA1-*GFP-CgCTA1* (*CgCTA1p*: SphI/NotI, *CgCTA1* ORF NotII/NsiI, GFP NotI/NotI) *CgTRP1*.	This study
p*CgC-CgCTA1*	CgCTA1-*CgCTA1* (SphI/NotI and NotII/NsiI); *CgTRP1* marker.	This study
p*CgCADH1-YFP-KNIESKL*	CgCADH1-*YFP-KNIESKL* (NotI/NotI fragment); *CgTRP1*.	This study
p*CgADH1-CgMSN2-CFP*	*CgADH1-CgMSN2-CFP* (*CgADH1p:* SphI/SacII and *CgMSN2:* SacII/NsiI); *CgTRP1*.	(Roetzer *et al.*, 2008)
p*CgADH1-CgMIG1-CFP*	*CgADH1-CgMIG1-CFP* (*CgMIG1:* SacII/NcoI); *CgTRP1*.	This study
p*CgADH1-GFP-CgYAP1*	*CgADH1-GFP-CgYAP1* (*CgYAP1:* NotII/NsiI); *CgTRP1*.	This study

1 Supplemental Table S1

Name	Sequence
CTAPro-up	GGATTGCATGCTCAATATTGCCTTGTTGGCA
CTAPro-down	ATGTCGACTGCGGCCCATGGTTTTTTTCAATTGTGGGAAGTTATC
CTA-up-Not	AGATGGGCGGCCGCAATCCAACTAACACTTCCGATGTTAGAGG
CTA-down-Nsi	AAGTCGACAACATCAATGCATCCAGTGAC
YFP-Not-Start	GCCTGTGCGGCCGCATGGTGAGC
YFP-SKL-Not-Stop	GTCACAGCGGCCGCATTACAGTTTACTTTCAATGTTTTTGCGCCCGCTCTTGTACAGCT
CTAPro-Seq	CAACATTATAACGCT
GFP3´-Seq	TGCTGGAGTTCGTGA
ACT1-5	ATGTGTAAGGCCGGTTTC
ACT1-3	AGGAAGATTGAGCAGCGG
CTA1-5	ATGTCCGCTAATCCAACT
CTA1-3	GCTTCATCATTGGTCAAG
CTA1-1	TACCTTGGAACTTGGGATAA
CTA1-2	CCGCTGCTAGGCGCGCCGTGAGATTGTACTGAGAGTGCAC
CTA1-3	CACGGCGCGCCTAGCAGCGGCAATTGTGGGAAGTTATCTA
CTA1-4	GTCAGCGGCCGCATCCCTGCGTGCGCTTTTGAACCACGTA
CTA1-5	GCAGGGATGCGGCCGCTGACCTGTGCGGTATTTCACACCG
CTA1-6	GCGGTACAATGGACAACATC
5´CTA1-Ctrl1	TGCATGAAGGAGAGA
URA-Ctrl2	TGCTGGCCGCATCTTCT
3´CTA1-Ctrl3	CCTGCGTTGTTAACT
URA-Ctrl4	TAGTCCTGTTGCTGCCA
PEX3-1	TGCGTCTTCAACAGCGGTAA
PEX3-3	CACGGCGCGCCTAGCAGCGGCGCTGTGCCTATCACTAGA
PEX3-4	GTCAGCGGCCGCATCCCTGCAGAATGGGGATACATAGTG
PEX3-6	AGGGTTGAGAGACGTTGTCT
PEX3-Ctrl5	TGTCCAGGAACTGCCTGGCA
PEX3-Ctrl3	GTTGCGATAAACTCGTGAAG
CgYap5	ACTAGGCGGCCGCCCAGGAATGGCTGAGGTGGATAACGG
CgYap3	GACGATGCATTTATTAAGACATGTGCTTAT
MIG1-5sac	GCTACCATGGTGCCGCCACCAGTTGGAAATTGCAAGT

MIG1-3nco	CGAGTCCGCGGATGTCTGCATCAGCGAGTCC
ATG11-1	CCGTGTCCGCGGTATGCGCT
ATG11-3	CACGGCGCGCCTAGCAGCGGTGTGTCAGCGCGATGGTATG
ATG11-4	GTCAGCGGCCGCATCCCTGCAATGAACTCTCGATACAGAA
ATG11-6	AATGATTTAATTAAAGAGA
ATG11-Ctrl5	GCTCACACAACAACACATC
ATG11-Ctrl3	GCCGATGAACAATCTATGGC
ATG17-1	GCGTAACAAGCACATATACA
ATG17-3	CACGGCGCGCCTAGCAGCGGTGTATATGTGCTTGTTACGC
ATG17-4	GTCAGCGGCCGCATCCCTGCACACTGAGGCAGATCACTAG
ATG17-6	GAAACCGTATTGATATCAGC
ATG17-Ctrl5	CAAAGTATTCAATTGGGT
ATG17-Ctrl3	GTGAGCTATCTGGAACAG

1

2

Figure legends

Figure 1. Oxidative stress and carbon source stress regulate *Cg* catalase *CgCTA1*. (A) To measure catalase activity upon glucose depletion, cells were grown to log phase in YPD and shifted to medium with 2% or 0.1% glucose and grown for 4 hours. Catalase activity was determined as described in materials and methods. (B) Cells were incubated in YPD with 0.4mM H_2O_2 for 45 minutes. Crude cell extracts were prepared and then assayed for catalase activity. (C) Northern blot analysis of *CgCTA1* mRNA levels from wild type, ARCg *cta1*Δ mutant, and complemented mutant strain was performed under stress conditions (glucose starvation, 0.4mM H_2O_2). Samples were taken at the indicated time points. *CgACT1* mRNA levels were used as loading control. mRNA levels were visualized by hybridization of radioactive probes and autoradiography. The p*CgC-GFP-CgCTA1* construct with GFP inserted at the N-terminus is illustrated. (D) *C. glabrata* ARCg *cta1*Δ mutant complemented with p*GFP-CgCTA1*, p*CgCTA1* or an empty plasmid were grown in synthetic medium to log phase, adjusted to 10^5 cells/ml and exposed to indicated doses of hydrogen peroxide. Optical density after 24 hours of incubation at 37℃ is indicated.

Figure 2. Intracellular localization of *C. glabrata* catalase. (A) Localization of GFP-CgCta1 was determined by fluorescence microscopy in ARCg *cta1*Δ cells transformed with p*CgCTA1-GFP-CgCTA1*. Cells were incubated for 1 hour after induction of oxidative stress with 0.4mM H_2O_2. Unstressed cells were stained with DAPI (2µg/ml) for 10 minutes. Aliquots of both cultures were pooled prior to microscopy. White arrows indicate unstressed cells. (B) ARCg *cta1*Δ and ARCg *pex3*Δ mutant strains transformed with p*CgC-GFP-CgCTA1* were grown in synthetic medium with 0.5% glucose and 1.5%

ethanol for 20 hours. White arrows indicate vesicular structures. Inserts show enlarged pictures of single cells. Possible peroxisomal targeting signals 1 (PTS1) detected at the C-terminus of CgCta1, ScCta1 and CaCct1 (Q6FM56, P15202, Q5AAT2; (Neuberger *et al.*, 2003)). (C) Fluorescence signals of strains as in (B) after growth in medium with 0.2% oleic acid for 20 hours. (D) Number of peroxisomes in *C. glabrata* cells during growth with ethanol (1.5%) and oleic acid (0.2%) as main carbon source.

Figure 3. CgCta1 localizes to peroxisomes upon glucose depletion. (A) *C. glabrata* ΔHTU and ARCg *pex3*Δ mutant cells expressing YFP-KNIESKL driven by the *CgADH1* promoter were grown in synthetic medium with 2% glucose or 1.5% ethanol for 20 hours. Localization of YFP was recorded by fluorescence microscopy and bright field (BF) microscopy. An overlay of YFP and BF microscopy is shown in the left panel. (B) The ARCg *cta1*Δ strain carrying pCgC-*CgCTA1* was exposed for 1 hour to oxidative stress (0.4mM H_2O_2). Pellets containing mitochondria and small organelles and post-mitochondrial supernatants were assayed for catalase activity. (C) The same strain was grown in synthetic medium with 1.5% ethanol for 20 hours. Catalase activity was measured in pellets and supernatants. Activity of Cytochrome C oxidase was measured in pellet and supernatant fractions as described in materials and methods (right panel). (D) Catalase activity in pellets and supernatant fraction collected from ARCg *cta1*Δ containing p*CgC-CgCTA1* grown in synthetic medium with 0.2% oleic acid for 20 hours.

Figure 4. *GFP-CgCTA1* is induced upon phagocytosis and is located in both cytoplasm and peroxisomes. (A) *C. glabrata* cells before and after being phagocytosed. Exponentially growing ARCg *cta1*Δ cells transformed with p*CgC-GFP-CgCTA1* were washed in PBS containing 0.1% glucose and added to macrophages in a 4:1 ratio at

37℃. Still pictures at the indicated times are shown as overlay of bright field and fluorescence signals. (B) Exponentially growing wild type cells transformed with p*CgADH1-YFP-KNIESKL1* were washed in PBS containing 0.1% glucose and added to macrophages in a 4:1 ratio at 37℃. Cells were fixed and stained with Phalloidin Texas-Red after 0, 2.5, 5, 10 and 24 hours for fluorescence microscopy. (C) Percentage of phagocytosed *C. glabrata* cells with visible peroxisomes per macrophage from the total cell number of *C. glabrata* cells per macrophage after 0, 2.5, 5, 10 and 24 hours (left panel). Number of visible peroxisomes within phagocytosed *C. glabrata* cells after 0, 2.5, 5, 10 and 24 hours (right panel).

Figure 5. Localization of GFP-CgYap1 and CgMig1-CFP during early stage of phagocytosis. (A) *C. glabrata* wild type cells transformed with p*CgADH1-GFP-CgYAP1* were grown in synthetic medium. Cells were stressed by addition of 0.4mM H_2O_2 for 10 minutes. Nuclei were stained with DAPI. An overlay of GFP and DAPI staining is shown in the right panel. GFP-CgYap1 visualized by fluorescence microscopy under phagocytosis conditions (lower panel). Cells were washed in PBS 0.1% glucose and added to macrophages in a 4:1 ratio and incubated at 37℃ for 10 minutes to follow the route of tagged transcription factors. Samples were fixed and stained with Phalloidin Texas-Red. Percentage of cells with nuclear GFP-Yap1 was calculated after 30 minutes, 1 hour and 5 hours. White arrows point to nuclear GFP-CgYap1 in yeast inside the phagosome. (B) *C. glabrata* wild type cells transformed with p*CgADH1-CgMIG1-CFP* were grown in synthetic medium until glucose depletion. Cells were incubated in fresh medium containing 2% glucose for 10 minutes or 1X DMEM. Lower panel depicts localisation of CgMig1-CFP under phagocytosis conditions. Cells were treated as described in (A).

Figure 6. Induction and pexophagy of peroxisomes upon phagocytosis. (A) Log-phase *C. glabrata* ARCg *cta1*Δ, ARCg *pex3*Δ, ARCg *atg11*Δ, ARCg *atg17*Δ, ARCg *pex3*Δ*atg17*Δ, and ARCg *atg11*Δ*atg17*Δ mutant cells transformed with p*GFP-CgCTA1* were used to infect mouse macrophages in a 4:1 ratio at 37℃. Cells were fixed for microscopy after 5 hours and 24 hours. (B) Percentage of cells with visible peroxisomes after phagocytosis in macrophages after 5 hours and 24 hours. (C) Log-phase *C. glabrata* ARCg *cta1*Δ, ARCg *pex3*Δ, ARCg *atg11*Δ, ARCg *atg17*Δ, ARCg *pex3*Δ*atg17*Δ, and ARCg *atg11*Δ*atg17*Δ mutant cells were used to infect mouse macrophages in a 1:2 ratio at 37℃. The viability of the engulfed cells was assessed by hypotonic lysis of the macrophages and quantification of colony formation (cfu) on rich medium. Assays were done in triplicate. A one-way ANOVA was performed and P values were calculated comparing the numbers of recovered colonies of the indicated strains (**, $P < 0.005$). (D) *C. glabrata* wild type, ARCg *atg11*Δ, ARCg *pex3*Δ*atg11*Δ, ARCg *atg17*Δ, ARCg *pex3*Δ*atg17*Δ and ARCg *atg11*Δ*atg17*Δ mutant cells were grown to exponential phase in rich medium; after washing with PBS supplemented with 0.1% glucose, $2x10^5$ cells were incubated in selective medium without nitrogen-sources and glucose and pH 3.5 at 37℃. After 24 hours colony formation (cfu) of mutant cells was determined. Percentage of viable cells was calculated relative to 2 hours treatment. (E) Log-phase ARCg *atg11*Δ*atg17*Δ mutant cells transformed with p*GFP-CgCTA1* were used to infect mouse macrophages in a 4:1 ratio at 37℃. Cells were fixed for microscopy after 5 hours. Overlay of GFP/Texas-Red and BF is shown.

Supplementary Figures

Figure S1. Southern blot analysis of *cta1*Δ, *pex3*Δ, *atg11*Δ and *pex3*Δ*atg11*Δ deletion strains. Both *CgCTA1* and *CgPEX3* were replaced by *ScURA3. CgATG11* was replaced by *ScURA3* in the single mutant and by *ScHIS3* in the double mutant ARCg *pex3*Δ*atg11*Δ. *CgATG17* was replaced by *ScURA3* in the single mutant and by *ScHIS3* in the double mutants ARCg *pex3*Δ*atg17*Δ and ARCg *atg11*Δ*atg17*Δ. Amplified probes and chromosomal restriction enzyme locations are indicated. Chromosomal DNA derived from ARCg *cta1Δ* digested with EcoRV and ARCg *pex3*Δ with XcmI resulted in shortened fragments relative to wild type. Digestion of chromosomal DNA from the ARCg *atg11*Δ strain with NcoI and from the ARCg *pex3*Δ*atg11*Δ double mutant strain with ClaI led to shorter fragments in both cases, since *CgATG11* contains neither a NcoI site nor a ClaI site. Picture is a composite of two exposures of the same blot, due to different amounts of DNA (lower panel). Chromosomal DNA derived from ARCg *atg17Δ* digested with AflIII and ARCg *pex3*Δ*patg17*Δ or ARCg *atg11Δatg17Δ* with NdeI resulted in shortened fragments.

Figure S2. Glucose depletion leads to induction of *GFP-CgCTA1* and cytoplasmic localization of CgMig1-CFP. (A) *GFP-CgCTA1* is induced upon glucose depletion and is located in the cytoplasm. *C. glabrata* ARCg *cta1*Δ cells transformed with p*CgC-GFP-CgCTA1* were grown in rich medium with glucose to exponential phase and washed twice and incubated in rich medium including 0.5% glucose. Every 10 minutes concentration of glucose was determined (see Material and Methods) and samples were fixed for microscopy. GFP fluorescence was visible at about 40 minutes after glucose exhaustion. (B) Localization of CgMig1-CFP in ARCg *atg11*Δ and ARCg *pex3*Δ*atg11*Δ mutants during internalization by macrophages. CgMig1-CFP was visualized by fluorescence microscopy

under phagocytosis conditions. *C. glabrata* wild type cells transformed with p*CgADH1-CgMIG1-CFP* were grown to exponential phase, washed in PBS 0.1% glucose and added to macrophages in a 4:1 ratio and incubated at 37℃ for 1 hour. Samples were fixed and stained with Phalloidin Texas-Red. (C) *GFP-CgCTA1* is induced upon phagocytosis. Still pictures from time lapse analysis are shown as overlay of bright field and fluorescence signals. Exponentially growing ARCg*cta1*Δ cells transformed with p*CgC-GFP-CgCTA1* were washed in PBS containing 0.1% glucose and added to macrophages in a 4:1 ratio at 37℃.

Figure S3. Quantification details.

References

Alvarez, M. and Casadevall, A. (2006). Phagosome extrusion and host-cell survival after *Cryptococcus neoformans* phagocytosis by macrophages. *Curr Biol* **16,** 2161-2165.

Asakura, M., Ninomiya, S., Sugimoto, M., Oku, M., Yamashita, S., Okuno, T.*, et al.* (2009). Atg26-mediated pexophagy is required for host invasion by the plant pathogenic fungus *Colletotrichum orbiculare*. *Plant Cell* **21,** 1291-1304.

Baccarini, M., Bistoni, F. and Lohmann-Matthes, M.L. (1985). In vitro natural cell-mediated cytotoxicity against *Candida albicans*: macrophage precursors as effector cells. *J Immunol* **134,** 2658-2665.

Barelle, C.J., Priest, C.L., Maccallum, D.M., Gow, N.A., Odds, F.C. and Brown, A.J. (2006). Niche-specific regulation of central metabolic pathways in a fungal pathogen. *Cell Microbiol* **8,** 961-971.

Becker, K., Tilley, L., Vennerstrom, J.L., Roberts, D., Rogerson, S. and Ginsburg, H. (2004). Oxidative stress in malaria parasite-infected erythrocytes: host-parasite interactions. *Int J Parasitol* **34,** 163-189.

Canovas, D. and Andrianopoulos, A. (2006). Developmental regulation of the glyoxylate cycle in the human pathogen *Penicillium marneffei*. *Mol Microbiol* **62,** 1725-1738.

Carlson, M. (1999). Glucose repression in yeast. *Curr Opin Microbiol* **2,** 202-207.

Chauhan, N., Latge, J.P. and Calderone, R. (2006). Signalling and oxidant adaptation in *Candida albicans* and *Aspergillus fumigatus*. *Nat Rev Microbiol* **4,** 435-444.

Chaves, G.M., Bates, S., Maccallum, D.M. and Odds, F.C. (2007). *Candida albicans GRX2*, encoding a putative glutaredoxin, is required for virulence in a murine model. *Genet Mol Res* **6,** 1051-1063.

Cheong, H., Nair, U., Geng, J. and Klionsky, D.J. (2008). The Atg1 kinase complex is involved in the regulation of protein recruitment to initiate sequestering vesicle formation for nonspecific autophagy in *Saccharomyces cerevisiae*. *Mol Biol Cell* **19,** 668-681.

Cheong, H., Yorimitsu, T., Reggiori, F., Legakis, J.E., Wang, C.W. and Klionsky, D.J. (2005). Atg17 regulates the magnitude of the autophagic response. *Mol Biol Cell* **16,** 3438-3453.

Cohen, G., Fessl, F., Traczyk, A., Rytka, J. and Ruis, H. (1985). Isolation of the catalase A gene of *Saccharomyces cerevisiae* by complementation of the *cta1* mutation. *Mol Gen Genet* **200,** 74-79.

Cox, G.M., Harrison, T.S., McDade, H.C., Taborda, C.P., Heinrich, G., Casadevall, A. and Perfect, J.R. (2003). Superoxide dismutase influences the virulence of *Cryptococcus neoformans* by affecting growth within macrophages. *Infect Immun* **71,** 173-180.

Cuellar-Cruz, M., Briones-Martin-del-Campo, M., Canas-Villamar, I., Montalvo-Arredondo, J., Riego-Ruiz, L., Castano, I. and De Las Penas, A. (2008). High resistance to oxidative stress in the fungal pathogen *Candida glabrata* is mediated by a single catalase, Cta1p, and is controlled by the transcription factors Yap1p, Skn7p, Msn2p, and Msn4p. *Eukaryot Cell* **7,** 814-825.

Davies, J.M., Lowry, C.V. and Davies, K.J. (1995). Transient adaptation to oxidative stress in yeast. *Arch Biochem Biophys* **317,** 1-6.

De Vit, M.J., Waddle, J.A. and Johnston, M. (1997). Regulated nuclear translocation of the Mig1 glucose repressor. *Mol Biol Cell* **8,** 1603-1618.

Derengowski, L.S., Tavares, A.H., Silva, S., Procopio, L.S., Felipe, M.S. and Silva-Pereira, I. (2008). Upregulation of glyoxylate cycle genes upon *Paracoccidioides brasiliensis* internalization by murine macrophages and in vitro nutritional stress condition. *Med Mycol* **46,** 125-134.

Dujon, B., Sherman, D., Fischer, G., Durrens, P., Casaregola, S., Lafontaine, I.*, et al.* (2004). Genome evolution in yeasts. *Nature* **430,** 35-44.

Durchschlag, E., Reiter, W., Ammerer, G. and Schüller, C. (2004). Nuclear localization destabilizes the stress-regulated transcription factor Msn2. *J Biol Chem* **279,** 55425-55432.

Enjalbert, B., MacCallum, D.M., Odds, F.C. and Brown, A.J. (2007). Niche-specific activation of the oxidative stress response by the pathogenic fungus *Candida albicans*. *Infect Immun* **75,** 2143-2151.

Fan, W., Kraus, P.R., Boily, M.J. and Heitman, J. (2005). *Cryptococcus neoformans* gene expression during murine macrophage infection. *Eukaryot Cell* **4,** 1420-1433.

Farre, J.C. and Subramani, S. (2004). Peroxisome turnover by micropexophagy: an autophagy-related process. *Trends Cell Biol* **14,** 515-523.

Geisow, M.J., D'Arcy Hart, P. and Young, M.R. (1981). Temporal changes of lysosome and phagosome pH during phagolysosome formation in macrophages: studies by fluorescence spectroscopy. *J Cell Biol* **89,** 645-652.

Gildea, L.A., Ciraolo, G.M., Morris, R.E. and Newman, S.L. (2005). Human dendritic cell activity against *Histoplasma capsulatum* is mediated via phagolysosomal fusion. *Infect Immun* **73,** 6803-6811.

Giles, S.S., Stajich, J.E., Nichols, C., Gerrald, Q.D., Alspaugh, J.A., Dietrich, F. and Perfect, J.R. (2006). The *Cryptococcus neoformans* catalase gene family and its role in antioxidant defense. *Eukaryot Cell* **5,** 1447-1459.

Gordon, J.L., Byrne, K.P. and Wolfe, K.H. (2009). Additions, losses, and rearrangements on the evolutionary route from a reconstructed ancestor to the modern *Saccharomyces cerevisiae* genome. *PLoS Genet* **5,** e1000485.

Görner, W., Durchschlag, E., Martinez-Pastor, M.T., Estruch, F., Ammerer, G., Hamilton, B.*, et al.* (1998). Nuclear localization of the C2H2 zinc finger protein Msn2p is regulated by stress and protein kinase A activity. *Genes Dev* **12,** 586-597.

Gregori, C., Schüller, C., Roetzer, A., Schwarzmüller, T., Ammerer, G. and Kuchler, K. (2007). The high-osmolarity glycerol response pathway in the human fungal pathogen *Candida glabrata* strain ATCC 2001 lacks a signaling branch that operates in baker's yeast. *Eukaryot Cell* **6,** 1635-1645.

Guan, J., Stromhaug, P.E., George, M.D., Habibzadegah-Tari, P., Bevan, A., Dunn, W.A., Jr. and Klionsky, D.J. (2001). Cvt18/Gsa12 is required for cytoplasm-to-vacuole transport, pexophagy, and autophagy in Saccharomyces cerevisiae and Pichia pastoris. *Mol Biol Cell* **12,** 3821-3838.

Hartig, A. and Ruis, H. (1986). Nucleotide sequence of the *Saccharomyces cerevisiae CTT1* gene and deduced amino-acid sequence of yeast catalase T. *Eur J Biochem* **160,** 487-490.

Hohfeld, J., Veenhuis, M. and Kunau, W.H. (1991). *PAS3*, a *Saccharomyces cerevisiae* gene encoding a peroxisomal integral membrane protein essential for peroxisome biogenesis. *J Cell Biol* **114,** 1167-1178.

Hu, G., Hacham, M., Waterman, S.R., Panepinto, J., Shin, S., Liu, X.*, et al.* (2008). PI3K signaling of autophagy is required for starvation tolerance and virulenceof *Cryptococcus neoformans*. *J Clin Invest* **118,** 1186-1197.

Hutchins, M.U., Veenhuis, M. and Klionsky, D.J. (1999). Peroxisome degradation in *Saccharomyces cerevisiae* is dependent on machinery of macroautophagy and the Cvt pathway. *J Cell Sci* **112 (Pt 22),** 4079-4087.

Idnurm, A., Giles, S.S., Perfect, J.R. and Heitman, J. (2007). Peroxisome function regulates growth on glucose in the basidiomycete fungus *Cryptococcus neoformans*. *Eukaryot Cell* **6,** 60-72.

Johnson, C.H., Klotz, M.G., York, J.L., Kruft, V. and McEwen, J.E. (2002). Redundancy, phylogeny and differential expression of *Histoplasma capsulatum* catalases. *Microbiology* **148,** 1129-1142.

Kaposzta, R., Marodi, L., Hollinshead, M., Gordon, S. and da Silva, R.P. (1999). Rapid recruitment of late endosomes and lysosomes in mouse macrophages ingesting *Candida albicans*. *J Cell Sci* **112 (Pt 19),** 3237-3248.

Kaur, R., Domergue, R., Zupancic, M.L. and Cormack, B.P. (2005). A yeast by any other name: *Candida glabrata* and its interaction with the host. *Curr Opin Microbiol* **8,** 378-384.

Kaur, R., Ma, B. and Cormack, B.P. (2007). A family of glycosylphosphatidylinositol-linked aspartyl proteases is required for virulence of *Candida glabrata*. *Proc Natl Acad Sci U S A* **104,** 7628-7633.

Kim, J., Kamada, Y., Stromhaug, P.E., Guan, J., Hefner-Gravink, A., Baba, M.*, et al.* (2001). Cvt9/Gsa9 functions in sequestering selective cytosolic cargo destined for the vacuole. *J Cell Biol* **153,** 381-396.

Kitada, K., Yamaguchi, E. and Arisawa, M. (1996). Isolation of a *Candida glabrata* centromere and its use in construction of plasmid vectors. *Gene* **175,** 105-108.

Koerkamp, M.G., Rep, M., Bussemaker, H.J., Hardy, G.P., Mul, A., Piekarska, K.*, et al.* (2002). Dissection of transient oxidative stress response in *Saccharomyces cerevisiae* by using DNA microarrays. *Mol Biol Cell* **13,** 2783-2794.

Kraft, C., Reggiori, F. and Peter, M. (2009). Selective types of autophagy in yeast. *Biochim Biophys Acta*.

Kragler, F., Langeder, A., Raupachova, J., Binder, M. and Hartig, A. (1993). Two independent peroxisomal targeting signals in catalase A of *Saccharomyces cerevisiae*. *J Cell Biol* **120,** 665-673.

Kuge, S., Jones, N. and Nomoto, A. (1997). Regulation of yAP-1 nuclear localization in response to oxidative stress. *EMBO J* **16,** 1710-1720.

Kunze, M., Pracharoenwattana, I., Smith, S.M. and Hartig, A. (2006). A central role for the peroxisomal membrane in glyoxylate cycle function. *Biochim Biophys Acta* **1763,** 1441-1452.

Leberer, E., Harcus, D., Dignard, D., Johnson, L., Ushinsky, S., Thomas, D.Y. and Schroppel, K. (2001). Ras links cellular morphogenesis to virulence by regulation of the MAP kinase and cAMP signalling pathways in the pathogenic fungus *Candida albicans*. *Mol Microbiol* **42,** 673-687.

Lemberg, M.R. (1969). Cytochrome oxidase. *Physiol Rev* **49,** 48-121.

Levitz, S.M., Nong, S.H., Seetoo, K.F., Harrison, T.S., Speizer, R.A. and Simons, E.R. (1999). *Cryptococcus neoformans* resides in an acidic phagolysosome of human macrophages. *Infect Immun* **67,** 885-890.

Lewin, A.S., Hines, V. and Small, G.M. (1990). Citrate synthase encoded by the *CIT2* gene of *Saccharomyces cerevisiae* is peroxisomal. *Mol Cell Biol* **10,** 1399-1405.

Li, L., Redding, S. and Dongari-Bagtzoglou, A. (2007). *Candida glabrata*: an emerging oral opportunistic pathogen. *J Dent Res* **86,** 204-215.

Lorenz, M.C., Bender, J.A. and Fink, G.R. (2004). Transcriptional response of *Candida albicans* upon internalization by macrophages. *Eukaryot Cell* **3,** 1076-1087.

Lorenz, M.C. and Fink, G.R. (2001). The glyoxylate cycle is required for fungal virulence. *Nature* **412,** 83-86.

Ma, H., Croudace, J.E., Lammas, D.A. and May, R.C. (2006). Expulsion of live pathogenic yeast by macrophages. *Curr Biol* **16,** 2156-2160.

Marcet-Houben, M. and Gabaldon, T. (2009). The tree versus the forest: the fungal tree of life and the topological diversity within the yeast phylome. *PLoS One* **4,** e4357.

Marchler, G., Schüller, C., Adam, G. and Ruis, H. (1993). A *Saccharomyces cerevisiae* UAS element controlled by protein kinase A activates transcription in response to a variety of stress conditions. *EMBO J* **12,** 1997-2003.

Miller, R.A. and Britigan, B.E. (1997). Role of oxidants in microbial pathophysiology. *Clin Microbiol Rev* **10,** 1-18.

Missall, T.A. and Lodge, J.K. (2005). Function of the thioredoxin proteins in *Cryptococcus neoformans* during stress or virulence and regulation by putative transcriptional modulators. *Mol Microbiol* **57,** 847-858.

Missall, T.A., Pusateri, M.E. and Lodge, J.K. (2004). Thiol peroxidase is critical for virulence and resistance to nitric oxide and peroxide in the fungal pathogen, *Cryptococcus neoformans*. *Mol Microbiol* **51,** 1447-1458.

Mizushima, N. and Klionsky, D.J. (2007). Protein turnover via autophagy: implications for metabolism. *Annu Rev Nutr* **27,** 19-40.

Nakagawa, Y. (2008). Catalase gene disruptant of the human pathogenic yeast *Candida albicans* is defective in hyphal growth, and a catalase-specific inhibitor can suppress hyphal growth of wild-type cells. *Microbiol Immunol* **52,** 16-24.

Nakagawa, Y., Kanbe, T. and Mizuguchi, I. (2003). Disruption of the human pathogenic yeast *Candida albicans* catalase gene decreases survival in mouse-model infection and elevates susceptibility to higher temperature and to detergents. *Microbiol Immunol* **47,** 395-403.

Nasution, O., Srinivasa, K., Kim, M., Kim, Y.J., Kim, W., Jeong, W. and Choi, W. (2008). Hydrogen peroxide induces hyphal differentiation in *Candida albicans*. *Eukaryot Cell* **7,** 2008-2011.

Neuberger, G., Maurer-Stroh, S., Eisenhaber, B., Hartig, A. and Eisenhaber, F. (2003). Prediction of peroxisomal targeting signal 1 containing proteins from amino acid sequence. *J Mol Biol* **328,** 581-592.

Nicola, A.M., Casadevall, A. and Goldman, D.L. (2008). Fungal killing by mammalian phagocytic cells. *Curr Opin Microbiol* **11,** 313-317.

Noble, S.M. and Johnson, A.D. (2005). Strains and strategies for large-scale gene deletion studies of the diploid human fungal pathogen *Candida albicans*. *Eukaryot Cell* **4,** 298-309.

Onodera, J. and Ohsumi, Y. (2005). Autophagy is required for maintenance of amino acid levels and protein synthesis under nitrogen starvation. *J Biol Chem* **280,** 31582-31586.

Palmer, G.E., Askew, D.S. and Williamson, P.R. (2008). The diverse roles of autophagy in medically important fungi. *Autophagy* **4,** 982-988.

Palmer, G.E., Kelly, M.N. and Sturtevant, J.E. (2007). Autophagy in the pathogen *Candida albicans*. *Microbiology* **153,** 51-58.

Paris, S., Wysong, D., Debeaupuis, J.P., Shibuya, K., Philippe, B., Diamond, R.D. and Latge, J.P. (2003). Catalases of *Aspergillus fumigatus*. *Infect Immun* **71,** 3551-3562.

Pfaller, M.A. and Diekema, D.J. (2007). Epidemiology of invasive candidiasis: a persistent public health problem. *Clin Microbiol Rev* **20,** 133-163.

Piekarska, K., Mol, E., van den Berg, M., Hardy, G., van den Burg, J., van Roermund, C.*, et al.* (2006). Peroxisomal fatty acid beta-oxidation is not essential for virulence of *Candida albicans*. *Eukaryot Cell* **5,** 1847-1856.

Platta, H.W. and Erdmann, R. (2007). Peroxisomal dynamics. *Trends Cell Biol* **17,** 474-484.

Presterl, E., Daxbock, F., Graninger, W. and Willinger, B. (2007). Changing pattern of candidaemia 2001-2006 and use of antifungal therapy at the University Hospital of Vienna, Austria. *Clin Microbiol Infect* **13,** 1072-1076.

Prigneau, O., Porta, A., Poudrier, J.A., Colonna-Romano, S., Noel, T. and Maresca, B. (2003). Genes involved in beta-oxidation, energy metabolism and glyoxylate cycle are induced by *Candida albicans* during macrophage infection. *Yeast* **20,** 723-730.

Richie, D.L., Fuller, K.K., Fortwendel, J., Miley, M.D., McCarthy, J.W., Feldmesser, M.*, et al.* (2007). Unexpected link between metal ion deficiency and autophagy in *Aspergillus fumigatus*. *Eukaryot Cell* **6,** 2437-2447.

Roetzer, A., Gregori, C., Jennings, A.M., Quintin, J., Ferrandon, D., Butler, G.*, et al.* (2008). *Candida glabrata* environmental stress response involves *Saccharomyces cerevisiae* Msn2/4 orthologous transcription factors. *Mol Microbiol* **69,** 603-620.

Romani, L. (2004). Immunity to fungal infections. *Nat Rev Immunol* **4,** 1-23.

Rubin-Bejerano, I., Fraser, I., Grisafi, P. and Fink, G.R. (2003). Phagocytosis by neutrophils induces an amino acid deprivation response in *Saccharomyces cerevisiae* and *Candida albicans*. *Proc Natl Acad Sci U S A* **100,** 11007-11012.

Rude, T.H., Toffaletti, D.L., Cox, G.M. and Perfect, J.R. (2002). Relationship of the glyoxylate pathway to the pathogenesis of *Cryptococcus neoformans*. *Infect Immun* **70,** 5684-5694.

Schöbel, F., Ibrahim-Granet, O., Ave, P., Latge, J.P., Brakhage, A.A. and Brock, M. (2007). *Aspergillus fumigatus* does not require fatty acid metabolism via isocitrate lyase for development of invasive aspergillosis. *Infect Immun* **75,** 1237-1244.

Segal, A.W. (2005). How neutrophils kill microbes. *Annu Rev Immunol* **23,** 197-223.

Sikorski, R.S. and Hieter, P. (1989). A system of shuttle vectors and yeast host strains designed for efficient manipulation of DNA in *Saccharomyces cerevisiae*. *Genetics* **122,** 19-27.

Simon, M., Adam, G., Rapatz, W., Spevak, W. and Ruis, H. (1991). The *Saccharomyces cerevisiae ADR1* gene is a positive regulator of transcription of genes encoding peroxisomal proteins. *Mol Cell Biol* **11,** 699-704.

Thieringer, R., Shio, H., Han, Y.S., Cohen, G. and Lazarow, P.B. (1991). Peroxisomes in *Saccharomyces cerevisiae*: immunofluorescence analysis and import of catalase A into isolated peroxisomes. *Mol Cell Biol* **11,** 510-522.

Urban, C.F., Lourido, S. and Zychlinsky, A. (2006). How do microbes evade neutrophil killing? *Cell Microbiol* **8,** 1687-1696.

Veneault-Fourrey, C., Barooah, M., Egan, M., Wakley, G. and Talbot, N.J. (2006). Autophagic fungal cell death is necessary for infection by the rice blast fungus. *Science* **312,** 580-583.

Voyich, J.M., Braughton, K.R., Sturdevant, D.E., Whitney, A.R., Said-Salim, B., Porcella, S.F.*, et al.* (2005). Insights into mechanisms used by *Staphylococcus aureus* to avoid destruction by human neutrophils. *J Immunol* **175,** 3907-3919.

Xie, Z. and Klionsky, D.J. (2007). Autophagosome formation: core machinery and adaptations. *Nat Cell Biol* **9,** 1102-1109.

Yan, M., Rayapuram, N. and Subramani, S. (2005). The control of peroxisome number and size during division and proliferation. *Curr Opin Cell Biol* **17,** 376-383.

Yorimitsu, T. and Klionsky, D.J. (2005). Atg11 links cargo to the vesicle-forming machinery in the cytoplasm to vacuole targeting pathway. *Mol Biol Cell* **16,** 1593-1605.

Figure 1

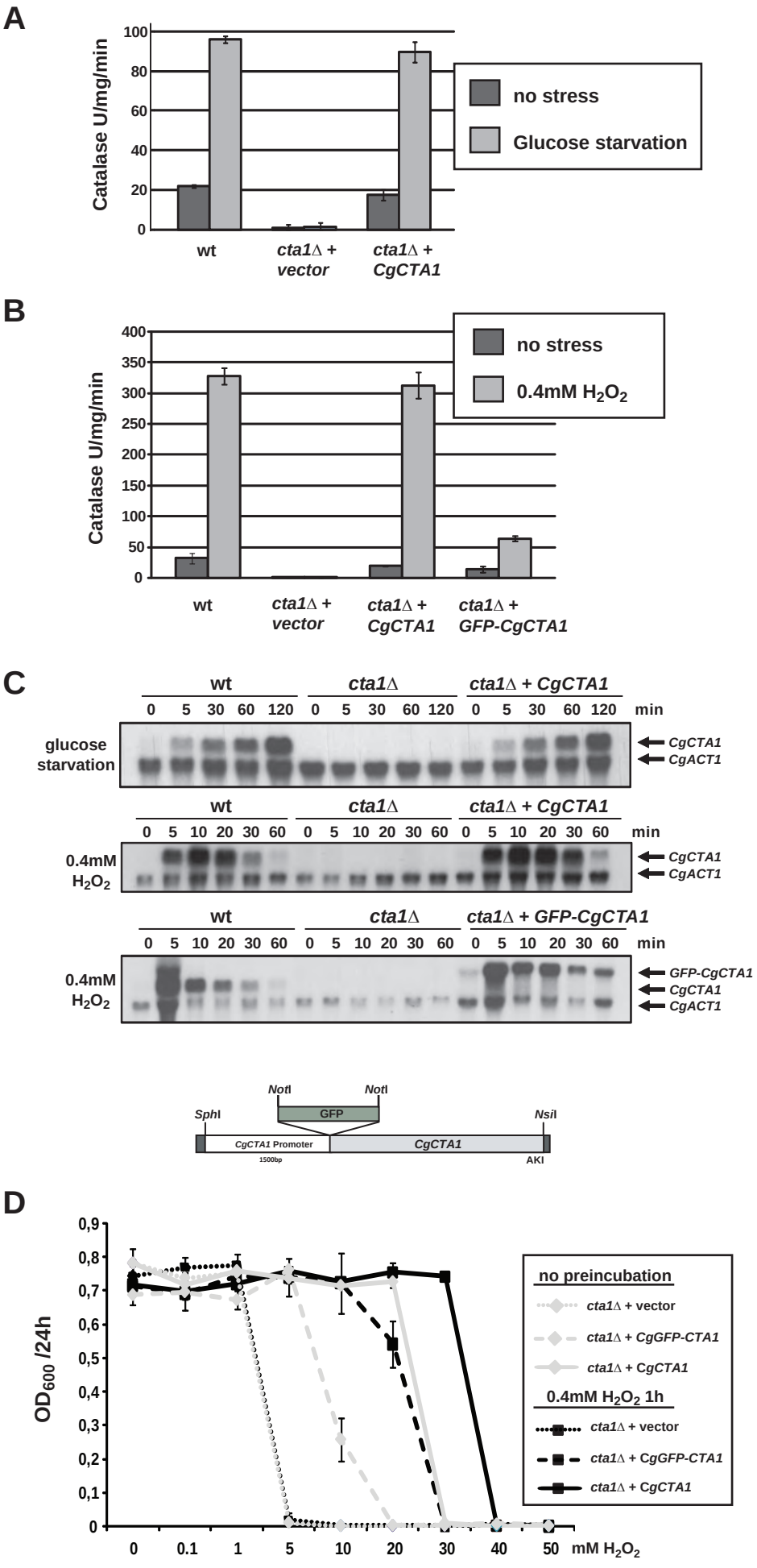
A
Catalase U/mg/min
100
80
60
40
20
0
no stress
Glucose starvation
wt
cta1Δ + vector
cta1Δ + CgCTA1
B
Catalase U/mg/min
400
350
300
250
200
150
100
50
0
no stress
0.4mM H2O2
wt
cta1Δ + vector
cta1Δ + CgCTA1
cta1Δ + GFP-CgCTA1
C
wt
cta1Δ
cta1Δ + CgCTA1
0 5 30 60 120 0 5 30 60 120 0 5 30 60 120 min
glucose starvation
CgCTA1
CgACT1
wt
cta1Δ
cta1Δ + CgCTA1
0 5 10 20 30 60 0 5 10 20 30 60 0 5 10 20 30 60 min
0.4mM H2O2
CgCTA1
CgACT1
wt
cta1Δ
cta1Δ + GFP-CgCTA1
0 5 10 20 30 60 0 5 10 20 30 60 0 5 10 20 30 60 min
0.4mM H2O2
GFP-CgCTA1
CgCTA1
CgACT1
NotI
NotI
SphI
GFP
NsiI
CgCTA1 Promoter
CgCTA1
1500bp
AKI
D
OD600 /24h
0,9
0,8
0,7
0,6
0,5
0,4
0,3
0,2
0,1
0
0 0.1 1 5 10 20 30 40 50 mM H2O2
no preincubation
cta1Δ + vector
cta1Δ + CgGFP-CTA1
cta1Δ + CgCTA1
0.4mM H2O2 1h
cta1Δ + vector
cta1Δ + CgGFP-CTA1
cta1Δ + CgCTA1

Figure 2

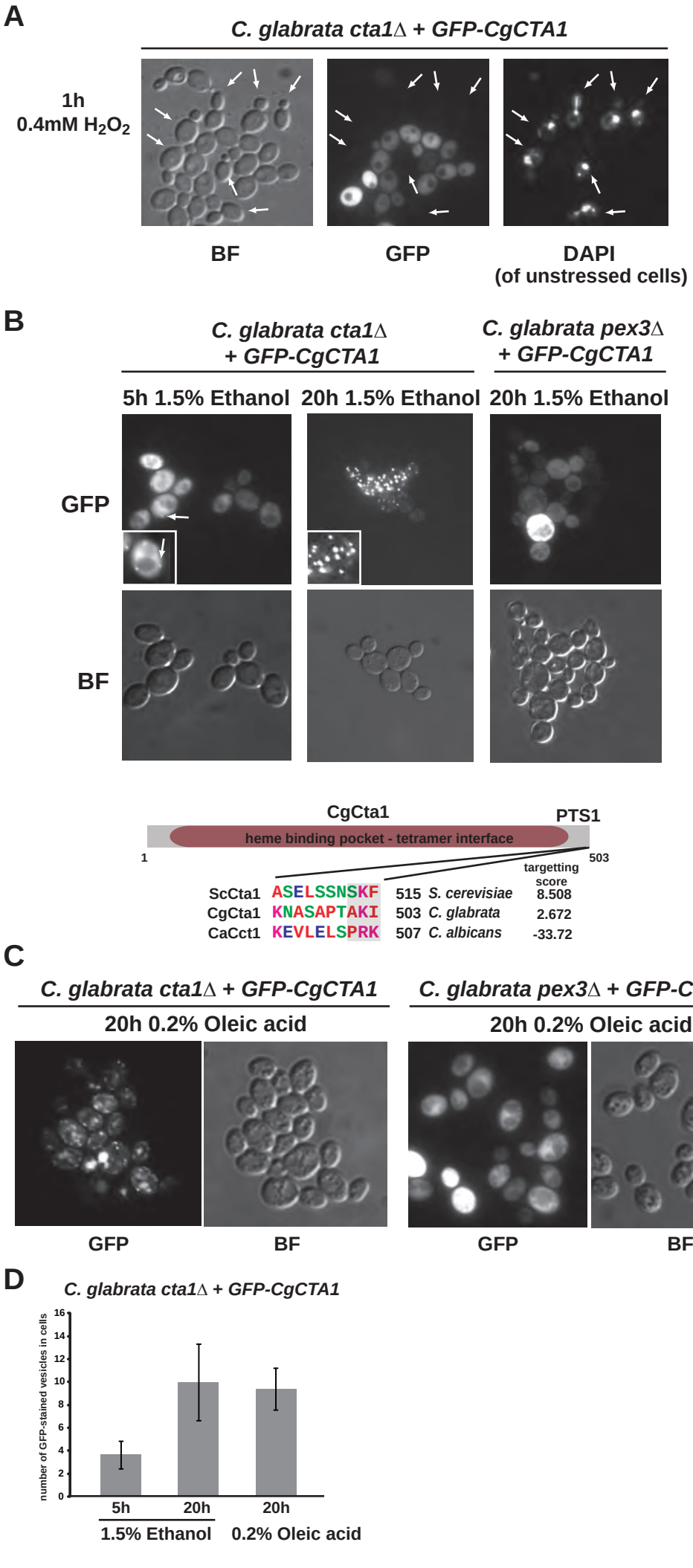
A
C. glabrata cta1Δ + GFP-CgCTA1
1h
0.4mM H2O2
BF
GFP
DAPI
(of unstressed cells)
B
C. glabrata cta1Δ
+ GFP-CgCTA1
C. glabrata pex3Δ
+ GFP-CgCTA1
5h 1.5% Ethanol
20h 1.5% Ethanol
20h 1.5% Ethanol
GFP
BF
CgCta1
PTS1
heme binding pocket - tetramer interface
1
503
targetting
score
ScCta1 ASELSSNSKF 515 S. cerevisiae 8.508
CgCta1 KNASAPTAKI 503 C. glabrata 2.672
CaCct1 KEVLELSPRK 507 C. albicans -33.72
C
C. glabrata cta1Δ + GFP-CgCTA1
C. glabrata pex3Δ + GFP-CgCTA1
20h 0.2% Oleic acid
20h 0.2% Oleic acid
GFP
BF
GFP
BF
D
C. glabrata cta1Δ + GFP-CgCTA1
number of GFP-stained vesicles in cells
0
2
4
6
8
10
12
14
16
5h
20h
20h
1.5% Ethanol
0.2% Oleic acid

Figure 3

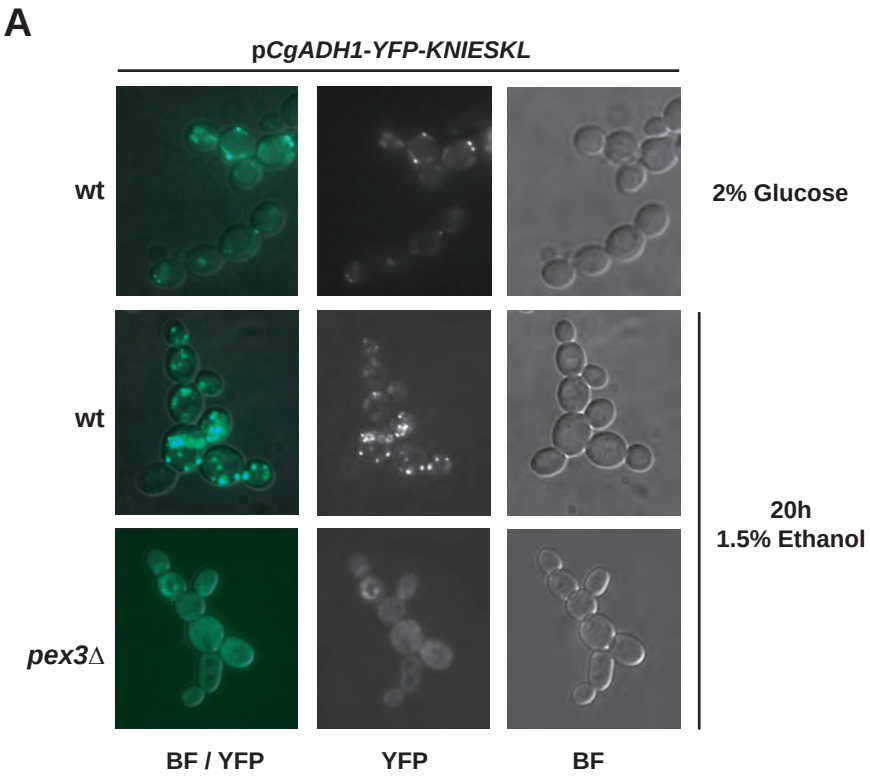
A
pCgADH1-YFP-KNIESKL
wt
wt
pex3Δ
2% Glucose
20h
1.5% Ethanol
BF / YFP
YFP
BF

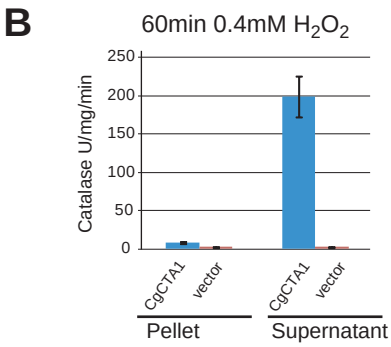
B
60min 0.4mM H2O2
Catalase U/mg/min
250
200
150
100
50
0
CgCTA1
vector
CgCTA1
vector
Pellet
Supernatant

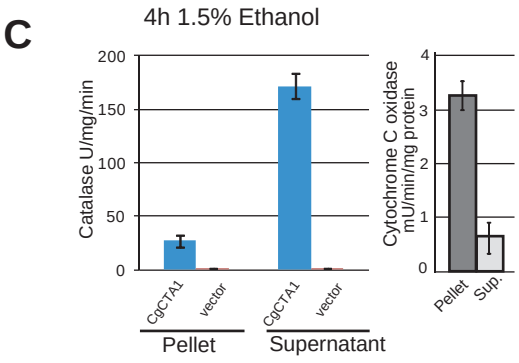
C
4h 1.5% Ethanol
Catalase U/mg/min
200
150
100
50
0
CgCTA1
vector
CgCTA1
vector
Pellet
Supernatant
Cytochrome C oxidase
mU/min/mg protein
4
3
2
1
0
Pellet
Sup.

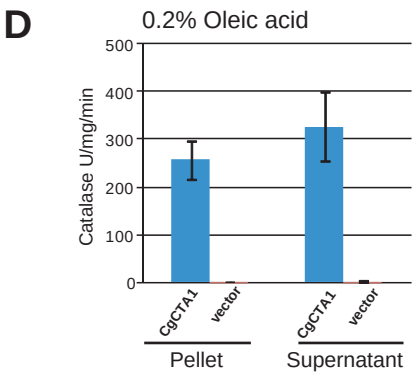
D
0.2% Oleic acid
Catalase U/mg/min
500
400
300
200
100
0
CgCTA1
vector
CgCTA1
vector
Pellet
Supernatant

Figure 4

A

C. glabrata cta1Δ + GFP-CgCTA1

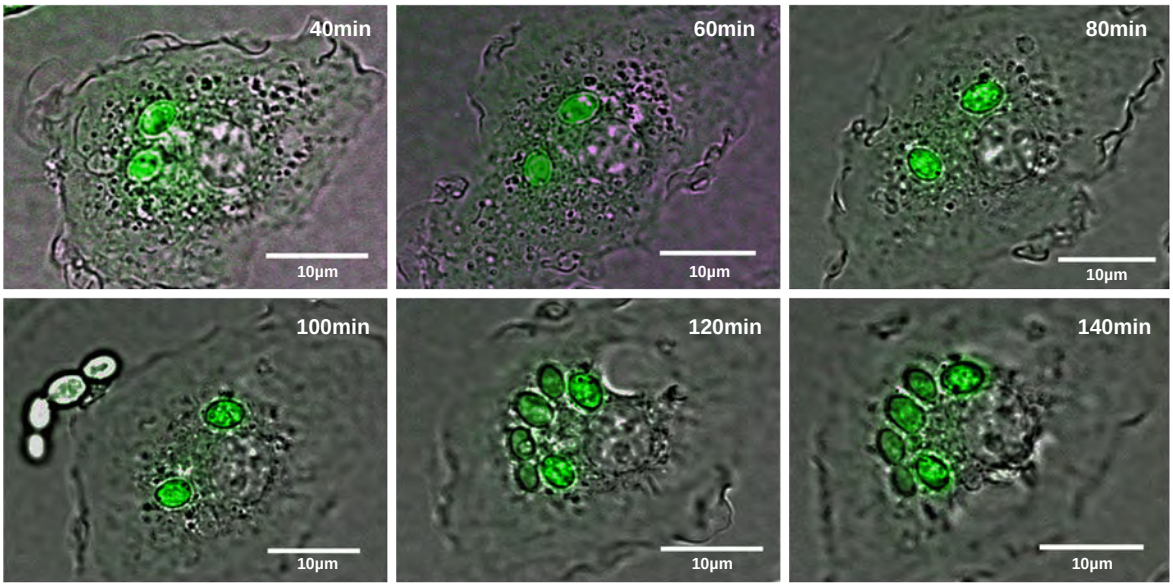

B

C. glabrata* wild type + *CgADH1-YFP-KNIESKL

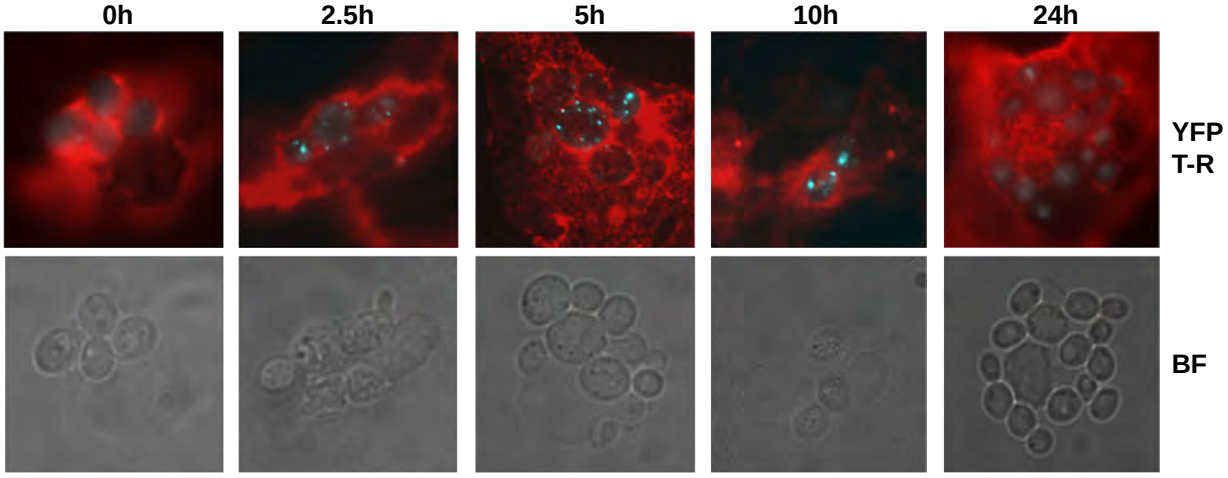

C

% *C.g.* cells in macrophages with peroxisomes

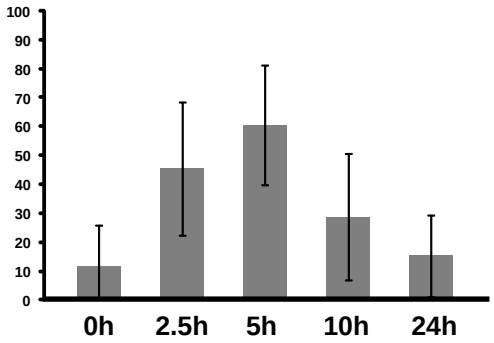

Visible peroxisomes in *C.g.* cells

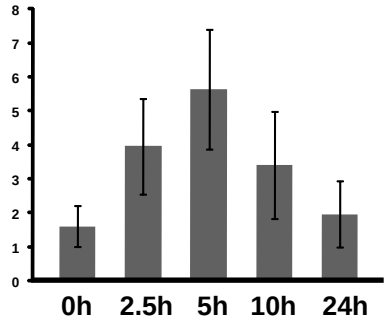

Figure 5

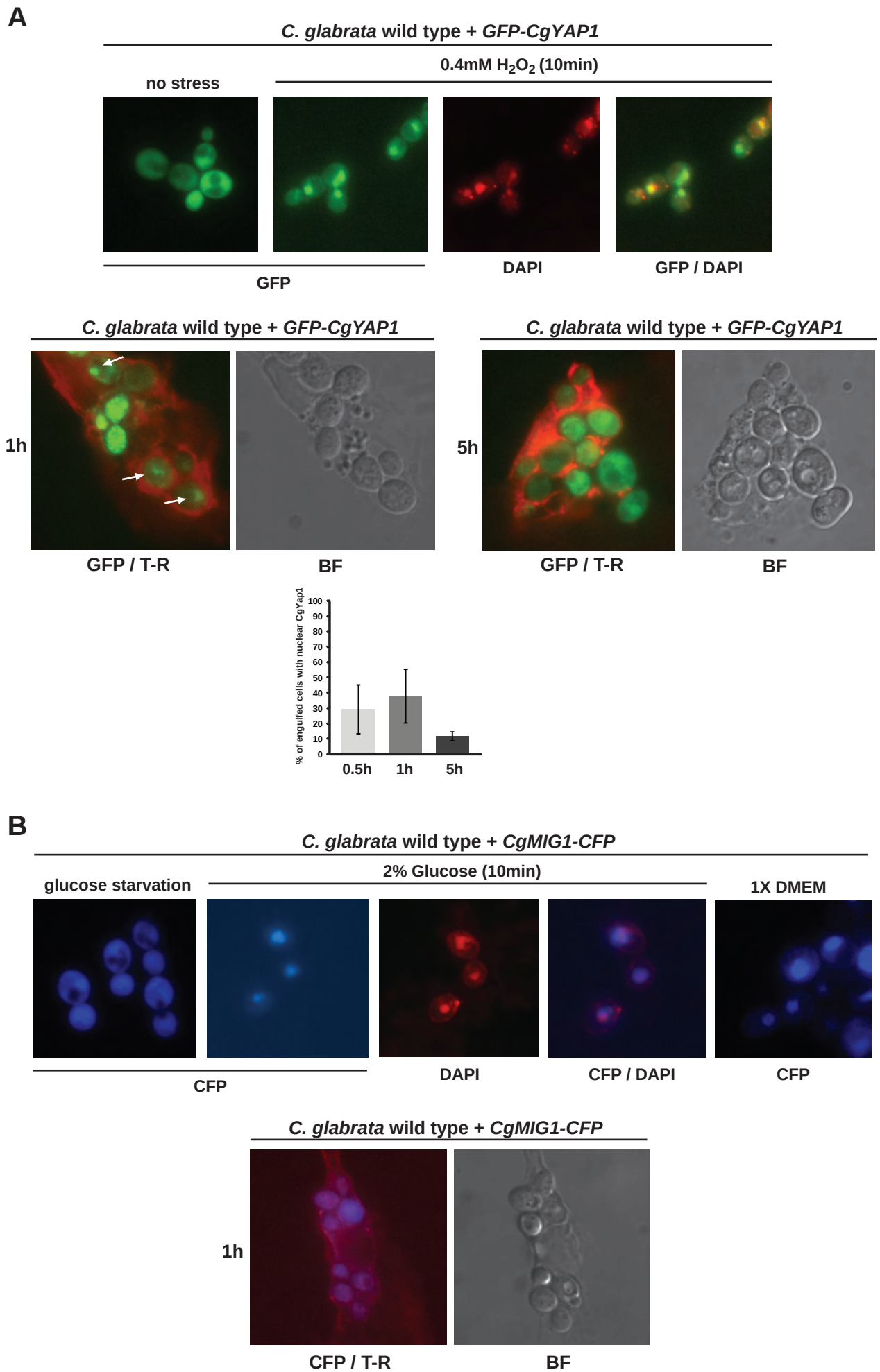
A
C. glabrata wild type + GFP-CgYAP1
no stress
0.4mM H2O2 (10min)
GFP
DAPI
GFP / DAPI
C. glabrata wild type + GFP-CgYAP1
1h
GFP / T-R
BF
C. glabrata wild type + GFP-CgYAP1
5h
GFP / T-R
BF
% of engulfed cells with nuclear CgYap1
100
90
80
70
60
50
40
30
20
10
0
0.5h
1h
5h
B
C. glabrata wild type + CgMIG1-CFP
glucose starvation
2% Glucose (10min)
1X DMEM
CFP
DAPI
CFP / DAPI
CFP
C. glabrata wild type + CgMIG1-CFP
1h
CFP / T-R
BF

Figure 6

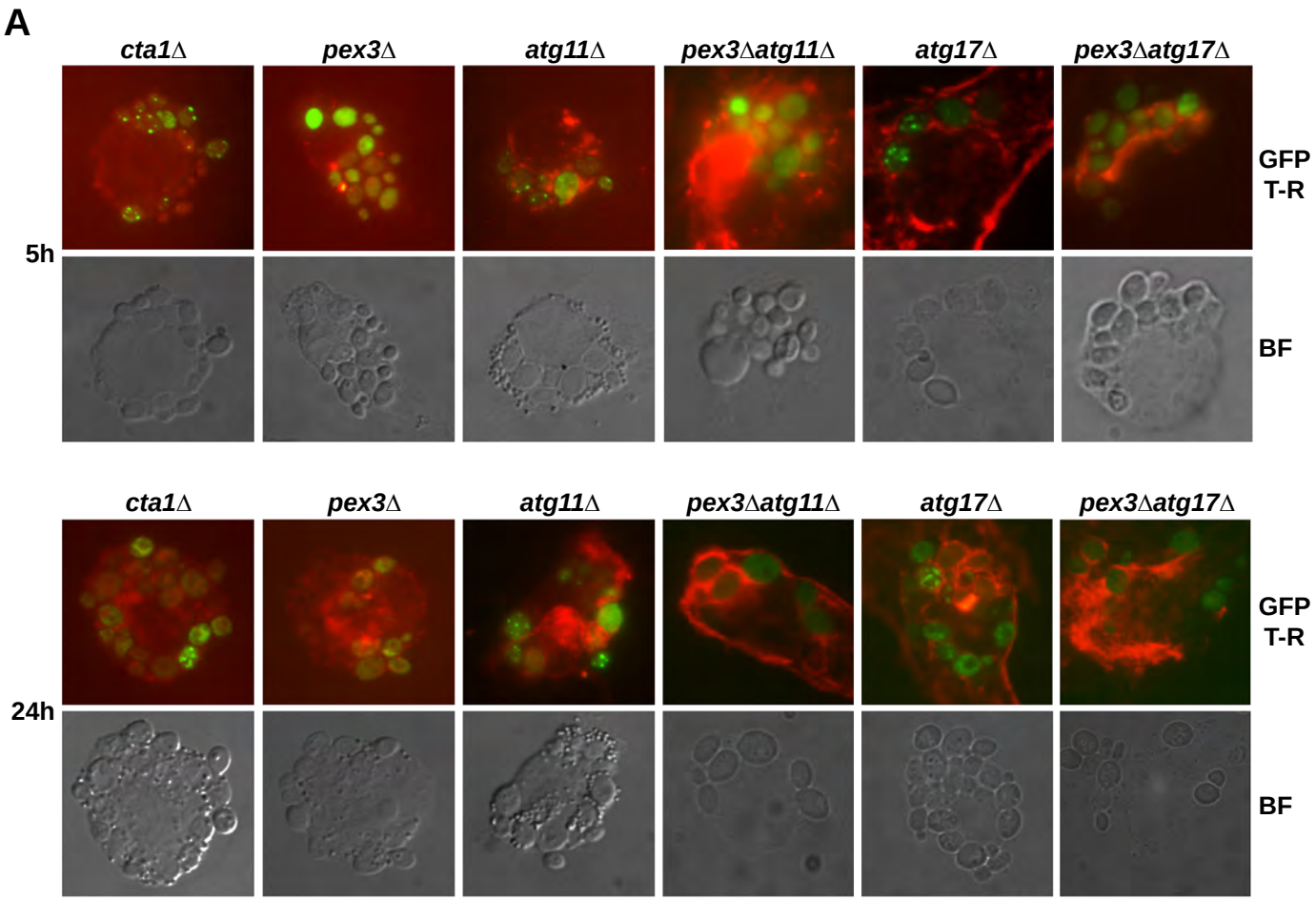
A
cta1Δ
pex3Δ
atg11Δ
pex3Δatg11Δ
atg17Δ
pex3Δatg17Δ
GFP T-R
5h
BF
24h

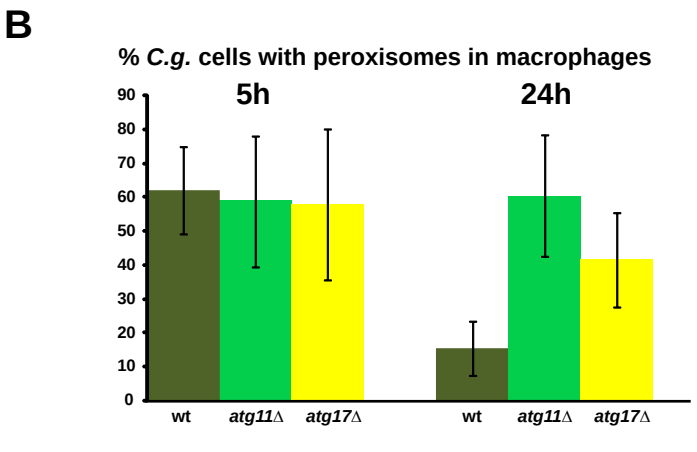
B
% C.g. cells with peroxisomes in macrophages
5h
24h
wt
atg11Δ
atg17Δ

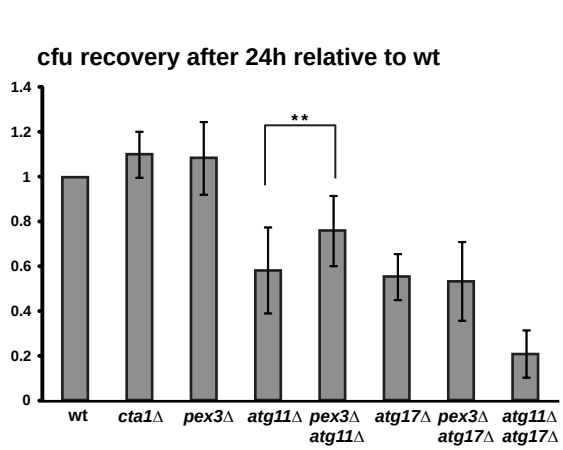
C
cfu recovery after 24h relative to wt
**
wt
cta1Δ
pex3Δ
atg11Δ
pex3Δ atg11Δ
atg17Δ
pex3Δ atg17Δ
atg11Δ atg17Δ

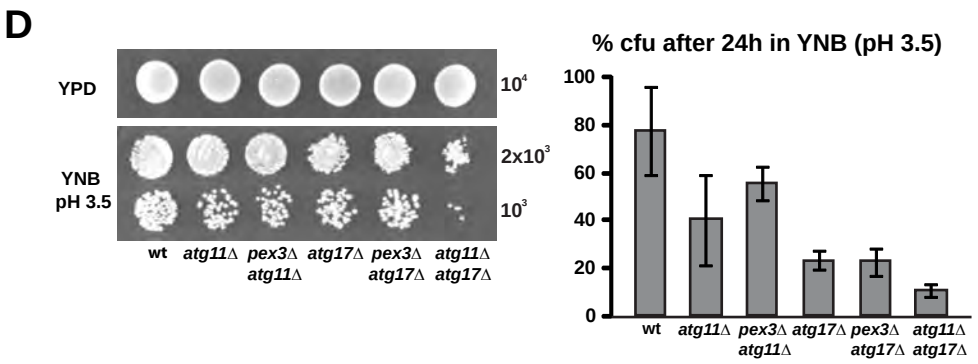
D
YPD
YNB pH 3.5
wt
atg11Δ
pex3Δ atg11Δ
atg17Δ
pex3Δ atg17Δ
atg11Δ atg17Δ
% cfu after 24h in YNB (pH 3.5)

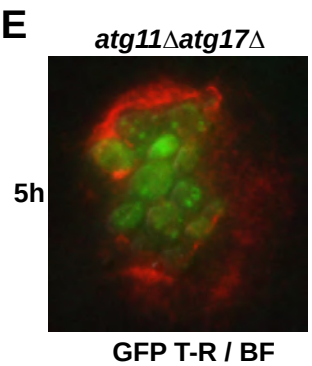
E
atg11Δatg17Δ
5h
GFP T-R / BF

Figure S1

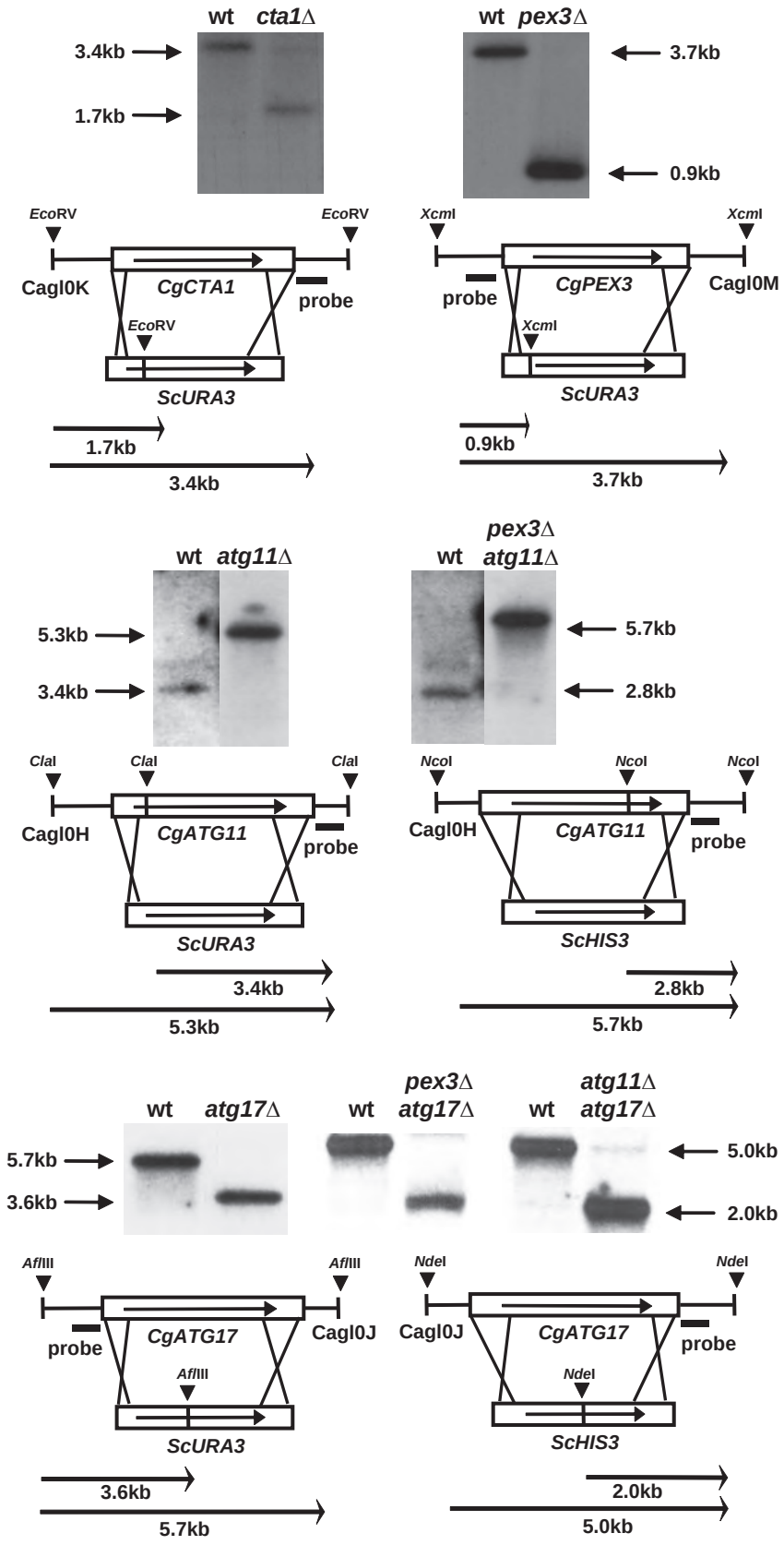
wt
cta1Δ
3.4kb
1.7kb
EcoRV
EcoRV
Cagl0K
CgCTA1
probe
EcoRV
ScURA3
1.7kb
3.4kb
wt
pex3Δ
3.7kb
0.9kb
XcmI
XcmI
probe
CgPEX3
Cagl0M
XcmI
ScURA3
0.9kb
3.7kb
wt
atg11Δ
5.3kb
3.4kb
ClaI
ClaI
ClaI
Cagl0H
CgATG11
probe
ScURA3
3.4kb
5.3kb
pex3Δ
wt
atg11Δ
5.7kb
2.8kb
NcoI
NcoI
NcoI
Cagl0H
CgATG11
probe
ScHIS3
2.8kb
5.7kb
wt
atg17Δ
5.7kb
3.6kb
wt
pex3Δ
atg17Δ
wt
atg11Δ
atg17Δ
5.0kb
2.0kb
AflIII
AflIII
probe
CgATG17
Cagl0J
AflIII
ScURA3
3.6kb
5.7kb
NdeI
NdeI
Cagl0J
CgATG17
probe
NdeI
ScHIS3
2.0kb
5.0kb

Figure S2

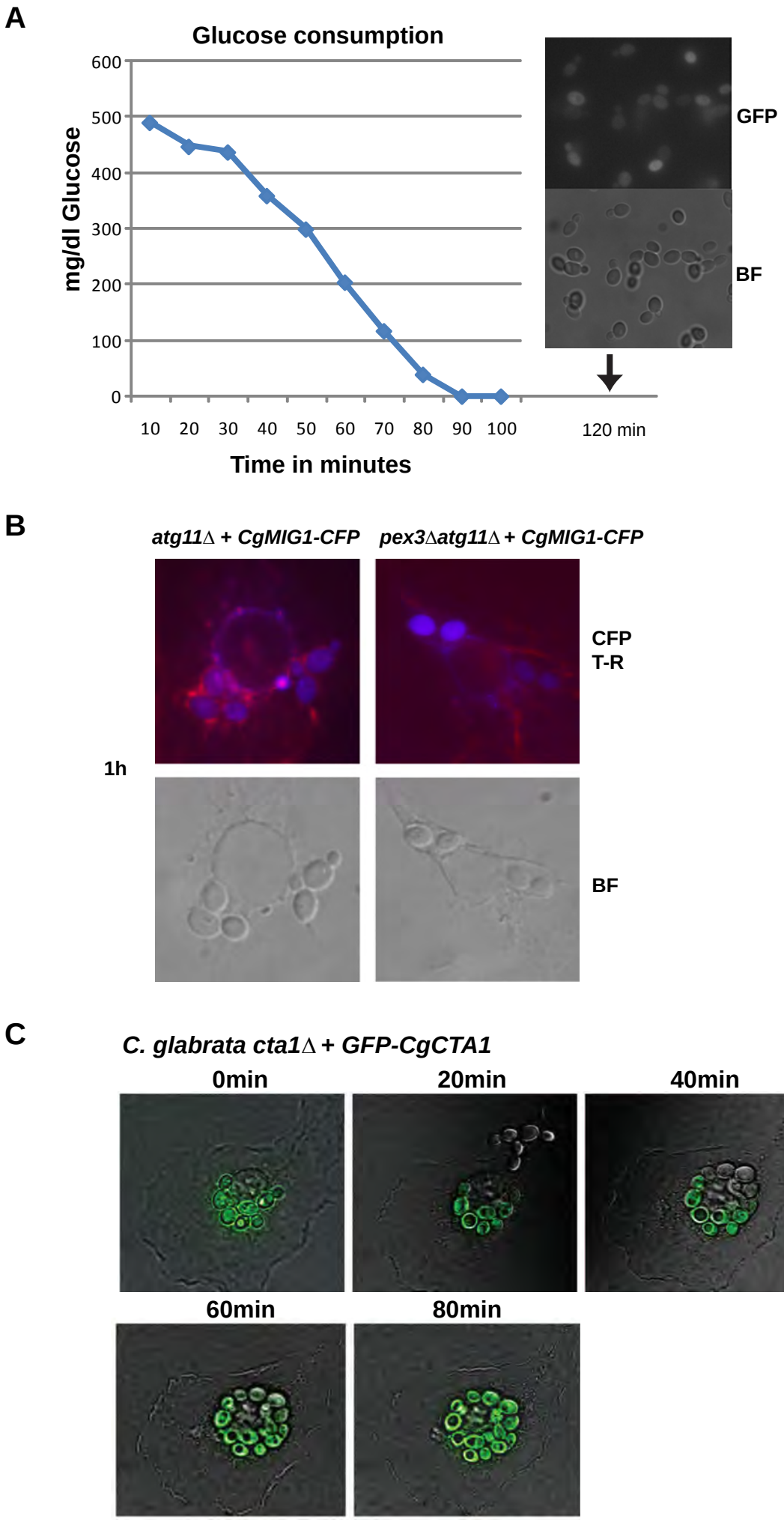
A
Glucose consumption
mg/dl Glucose
600
500
400
300
200
100
0
10 20 30 40 50 60 70 80 90 100
Time in minutes
120 min
GFP
BF
B
atg11Δ + CgMIG1-CFP
pex3Δatg11Δ + CgMIG1-CFP
1h
CFP
T-R
BF
C
C. glabrata cta1Δ + GFP-CgCTA1
0min
20min
40min
60min
80min

Figure S3

Figure 2D

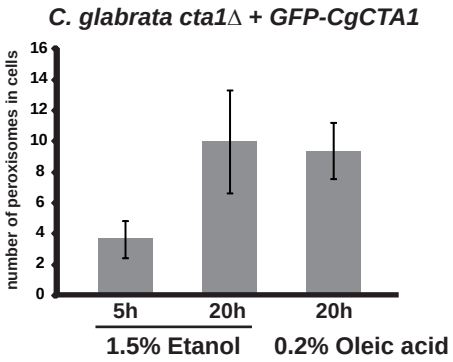

counts of peroxisomes per single cell			
time points (carbon source)	5h (etoh)	24h (etoh)	24h (oleate)
Mean	3,64705882	10	9,375
Standard Deviation	1,22173936	3,44480285	1,86063337
n(cells)	n= 17	n=16	n=24

Figure 4C

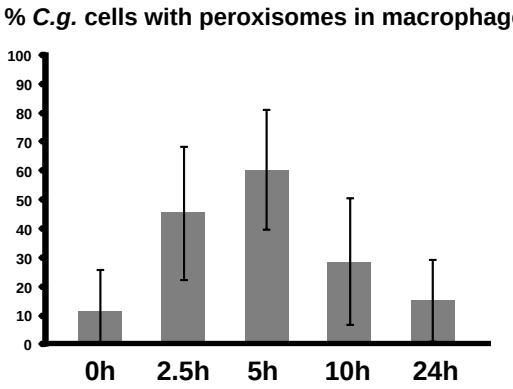

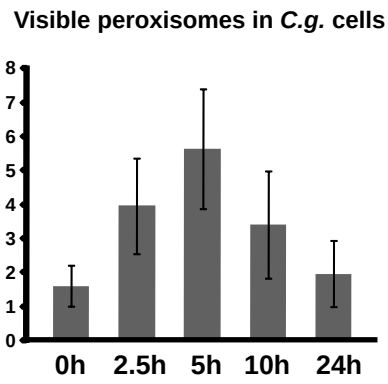

% C.g. cells with peroxisomes in macrophages					
time points	0h	2,5h	5h	10h	24h
Mean (percentages)	11,6597688	45,474793	60,4209427	28,7447479	15,2678571
Standard Deviation	14,1943982	23,1041463	21,751796	22,7299767	14,2038033
n(macrophages)	14	18	11	12	12
n(cells)	130	174	97	68	111
n(cells w peroxi)	16	82	56	21	18

Visible peroxisomes in C.g. cells					
time points	0h	2.5h	5h	12h	24h
Mean	1,6	3,96	5,62962963	3,41666667	1,97142857
Standard Deviation	0,61101009	1,39942845	1,76694229	1,57894128	0,97058787
n(cells)	30	50	27	24	35

Figure 6B

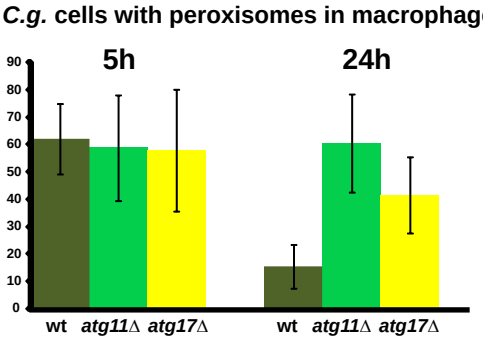

% C.g. cells with peroxisomes in macrophages						
strains	wt	wt	atg11	atg11	atg17	atg17
time points	5h	o/n	5h	o/n	5h	o/n
Mean (percentages)	62,125109	15,5166747	58,7742504	60,4093823	57,8152403	41,4793693
Standard Deviation	12,9468752	8,02710584	19,2853736	17,9638125	22,232647	13,9497083
n(macrophages)	11	9	9	8	13	16
n(cells)	136	102	73	71	102	145
n(cells w peroxi)	82	16	41	42	61	60
P-values (5h - o/n)		3,54E-08		0,8641438		0,0240757

CgSkn7 and CgYap1 mediate key responses to oxidative stress in *Candida glabrata*.

Andreas Roetzer[a], Eva Klopf[a], Nina Gratz[b], Marina Marcet-Houben[c], Toni Gabaldon[c], Pavel Kovarik[b] and Christoph Schüller[a*]

From

[a] Max F. Perutz Laboratories, University of Vienna, Department of Biochemistry A-1030 Vienna, Austria

[b] Max F. Perutz Laboratories, University of Vienna, Department of Microbiology and Immunology, A-1030 Vienna, Austria

[c] Comparative Genomics Group, Bioinformatics and Genomics Programme, Centre for Genomic Regulation, 88 08003 Barcelona, Spain

Running title: *Candida glabrata* oxidative stress response

*) To whom correspondence should be addressed:

Christoph Schüller

University of Vienna, Max F. Perutz Laboratories

Department of Biochemistry

Dr. Bohr-Gasse 9/5

A-1030 Vienna, Austria

Phone: +43-1-4277-52815; Fax: +43-1-4277-9528

E-mail: christoph.schueller@univie.ac.at

Abstract:

In this work we addressed the wiring of the transcriptional oxidative stress response regulon and its main regulators of *C. glabrata*. We showed that CgSkn7 and CgYap1 are completely interdependent for regulation of a number of genes encoding important antioxidant functions. Chromatin immunoprecipitation data revealed that this interdependence occurs at the level of promoter recognition. CgYap1 was required for protection against peroxides and peroxynitrite however not for protection against superoxide anions. Accordingly, we discovered that superoxide dismutase gene *CgSOD1* was constitutively expressed in *C. glabrata* in a CgSkn7/CgYap1 independent manner. In addition, many oxidative stress-associated genes were also upregulated during carbon source depletion, a condition met by *C. glabrata* upon engulfment by phagocytes. Furthermore, we also found CgSod1 and CgSod2 to be strongly induced by carbon source starvation. Our results support the view that *C. glabrata* has adapted the regulation of oxidative stress response genes to a host-pathogen situation. However, the *C. glabrata skn7*Δ*yap1*Δ double mutant had a similar survival rate compared to the wild type in a primary mouse macrophage model. Taken together, we conclude that the *S. cerevisiae*-like oxidative stress response is either dispensable for prolonged survival upon engulfment, or other starvation-associated factors can induce this regulon to a significant extent.

Introduction:

The human fungal pathogen *Candida glabrata* is found as a common commensal in gastrointestinal and genitourinary tracts, but can turn into an opportunistic pathogen in immunocompromised patients and elder people (52, 66, 67, 73). It is phylogenetically much closer related to baker´s yeast *Saccharomyces cerevisiae* than *Candida albicans* (38). Consistently, *C. glabrata* engulfed by phagocytic cells does not undergo characteristic morphological transitions such as *C. albicans* (47). Therefore, cells had to develop other strategies to withstand phagocytosis, which are currently under investigation.

In the mammalian host, cell-mediated immunity, which is based on efficient engulfment of pathogens by phagocytic cells, is crucial to counteract fungal infections (55). In the phagolysosome of phagocytic cells, such as macrophages and neutrophils, the NADPH oxidase complex consists of enzymes, which mediate oxidative destruction of engulfed microorganisms (7, 75). It catalyzes the production of superoxide anions ($O_2^{\cdot-}$), serving as initial source for the production of ROS, which damage the cell constituents including proteins, lipids and DNA. Other reactive oxidants produced are hydrogen peroxide (H_2O_2), which is generated by the breakdown of superoxides ($O_2^{\cdot-}$), hypochlorous acid (HOCl), which is formed by the myeloperoxidase-catalyzed oxidation of Cl^- by H_2O_2, hydroxyl radicals ($OH^{\cdot}$), produced by the reduction of H_2O_2 by Fe^{++} or Cu^+, peroxynitrite ($ONOO^-$), formed by the reaction between O_2^- and $NO^{\cdot}$, and many others (3, 81). Thus, for successful dissemination, pathogenic fungi have to counteract a broad spectrum of reactive oxidants during the oxidative burst.

Simple fungal organisms face complex oxidative stress environments inside the host, and therefore established various, often redundant, antioxidant systems (57), including a broad variety of antioxidant enzymes and cofactors (21, 48). These are catalases, superoxide dismutases, thioredoxins and glutathione-dependent peroxidases and reductases. These enzymes are known to be relevant for the survival

of several fungal pathogens (10, 14, 25, 58, 61). The loss of superoxide dismutases decreased virulence of *C. neoformans* in mice and diminished survival of *C. albicans* in macrophages (14, 25). Further it has been shown that catalase Cct1 and glutaredoxin Grx2 are necessary for full virulence of *C. albicans* in mouse infection models (10, 61). In contrast, the loss of CgCta1 did not affect survival of *C. glabrata* in mice (15). Furthermore, it has been shown recently, that *C. albicans* and *C. glabrata* can actively suppress production of ROS upon engulfment by phagocytes (88). Thus, it is essential for internalized fungal pathogens to counteract emerging reactive oxidants during phagocytosis.

Oxidative stress causes rapid changes in transcription of many gene encoding antioxidant functions. This is well described for the oxidative stress regulon of *S. cerevisiae* where this regulon is almost completely under control of the transcription factors Skn7 and Yap1 (31, 48). Yap1 contains a basic leucine zipper, and relocalizes from the cytoplasm to the nucleus upon stress induction (42). Activation of Yap1 during oxidative stress involves a C-terminal cysteine-rich domain, which contains a NES nuclear export signal (17, 18). Certain Cysteine residues in Yap1 become oxidized by the gluthatione peroxidase Gpx3 which leads in turn to the formation of inner disulfide bonds, causing a conformational change that causes Yap1 to accumulate in the nucleus and activate its target genes (18, 42). Yap1 mediates not only resistance to oxidative stress but is also involved in the response to heat, metal ions and drugs (79, 89, 90). Its role in diverse stress responses has been elucidated in several important fungi, such as *Kluyveromyces lactis*, *Ustilago maydis*, *C. albicans* and *Aspergillus fumigatus* (1, 5, 59, 68, 86). The *S. cerevisiae* transcription factor Skn7 is part of a branched two-component signaling system, involved in oxidative stress response, osmoregulation and integration of cell wall synthesis (8, 34, 53, 60, 72). The Skn7 protein localizes mainly to the nucleus, and it is thought, that Skn7 undergoes a post-translational modification by phosphorylation following exposure to reactive oxygen species (ROS), which is dependent on Yap1 (32). Furthermore, also a direct interaction

between Skn7 and Yap1 seems to be necessary for efficient induction of many oxidative stress response genes in *S. cerevisiae* (31, 32). Mutations introduced in the two component receiver domain of Skn7 were found to compromise the association of Skn7 but also Yap1 to upstream regions of oxidative stress-associated genes (31, 60). However, the precise mechanism by which these two factors interact and co-operate during oxidative stress induction of transcription is not yet clear.

Yap and Skn7 comprise a conserved regulatory unit modulating oxidative stress response in the phylum of Ascomycota. In *C. glabrata*, genes encoding putative orthologues of Yap1 and Skn7 were discovered (15). Similar to other fungi, resistance to hydrogen peroxide was found to be linked to the corresponding genes CgSkn7 and CgYap1 (12, 15). In *C. albicans*, the lack of the Skn7 orthologue led to a slight attenuation of virulence (77), whereas the impact of CaYap1 on virulence remains unclear. In contrast, in *Cryptococcus neoformans*, CnSkn7 is not required for pathogenicity (91); in addition, no obvious Yap1 orthologue was found. In *A. fumigatus*, both strains lacking AfYap1 or AfSkn7 displayed no attenuated virulence in a mouse infection model (45, 51). In the fungal plant pathogen *U. maydis,* loss of the Yap1 orthologue led to reduced virulence (59). The role of Yap1 and Skn7 is currently not fully explored in pathogenicity and may be dependent on specific host niches.

In this work we addressed the wiring of the transcriptional oxidative stress response regulon and its main regulators of *C. glabrata*. We found that CgSkn7 and CgYap1 are completely interdependent for regulation of a number of genes encoding important antioxidant functions. Chromatin immunoprecipitation data show that this interdependence occurs at the level of promoter recognition. CgYap1 was required for protection against hydrogen peroxide and peroxynitrite however not against superoxide due to menadione treatment. In addition, many oxidative stress-associated genes are also upregulated during carbon source depletion, a condition met by *C. glabrata* upon engulfment by phagocytes. Surprisingly, we observed that the superoxide dismutase

genes (CgSod1, CgSod2) are strongly induced by carbon source starvation and are not under CgYap1 and CgSkn7 control. Our results support the view that *C. glabrata* has adapted the regulation of oxidative stress response genes to a host-pathogen situation.

Materials and Methods:

Yeast strains and Plasmids: Yeast strains used in this study are listed in Table 1. Rich medium (YPD) and synthetic medium (SC) were prepared as described elsewhere (Current Protocols in Molecular Biology; Wiley). All strains were grown at 30℃ or 37° *C* as indicated. Gradient plates were prepared as described first in (80). Square plastic petri dishes (Singer) were used to establish a concentration gradient of. Plates containing menadione (Sigma), hydrogen peroxide (Merck) and hypochlorite (Neuber) were poured at room temperature; plates containing peroxynitrite (CaymanChem) - due to its instability - were poured at 4℃.

Susceptibility of *Candida glabrata* strains to CTBT was determined by zone inhibition assay, using YPD (rich medium with glucose), YPGE (rich medium with glycerol and ethanol) and YNB (minimal medium with glucose) media. The filter discs (diameter of 6 mm) soaked with 10 µg CTBT were placed on the plates which were incubated at 30℃ for 2 (rich medium) or 5 days (minimal medium) before determination of the diameter of the zone of growth inhibition.

Oligonucleotides used in this study are listed in Table S1. *C. glabrata* strains AR*Cg skn7*Δ, AR*Cg yap⊿* and AR*Cg skn7*Δ*yap1*Δ were obtained by replacing the respective open reading frames with the *S. cerevisiae* genes *URA3* or *HIS3* generated by genomic integration of knock out cassettes synthesized using fusion PCR according to Noble (64) from the plasmids pRS316 and pRS313 (76) with the oligonucleotides SKN7-1 to 6 and YAP1-1 to 6. Correct genomic integration was verified by genomic PCR (primer series Ctrl) followed by Southern analysis using probes generated with primers listed below.

Plasmids used in this study are listed in Table 2. To generate *pGEM-ACT-CgYAP1*, 1200 basepairs of the promoter were inserted as a *Sph*I/*Not*I PCR product obtained with primers ProNatYap1-5 and ProNatYap1-3 into the plasmid p*GEM-ACT* (29). The coding sequence for *CgYAP1* was amplified from genomic DNA using

primers CgYap5/CgYap3, cut and inserted as a *Not*I/*Nsi*I fragment into p*GEM-ACT-ProYAP1* and p*GEM-ACT-ProADH1*. GFP was inserted as a *Not*I/*Not*I fragment at the N-terminus of *CgYAP1*. To generate *pGEM-ACT-CgSKN7, CgSKN7* was amplified using primers SKN7-5sac/Skn7-3nco and inserted into *Nco*I and *Sac*II cut p*GEM-ACT-CgADH1-MSN2-CFP* (70). 1200 base pairs of the promoter were inserted as *Sph*I/*Sac*II PCR (using primers ProNatSkn7-5/ProNatSkn7-3) fragment into p*GEM-ACT-CgADH1-SKN7-CFP*. CFP was removed through cutting with *Nco*I and *Nsi*I, refilled and ligated. To generate *pGEM-ACT-CgYAP1CgSKN7, CgSKN7* including its promoter, was amplified using the primers Skn7-5Nsi/Skn7-3Nsi, and inserted into the plasmid *pGEM-ACT-CgYAP1*. Truncated versions of the *CgCTA1* promoter were amplified using according primers (see Table 2) and cut with *Sph*I/*Not*I for insertion into the plasmid p*CgC-CgCTA1*.

HA-tags were amplified through PCR using the primers Skn7_HA6-5/Skn7_HA6-3 and Yap1_HA6-5/Yap1_HA6-3. For *YAP1-HA*, the product was cut with *Not*I, for *SKN7-HA* the product was cut with *Nco*I. The proper insertion was tested via western blotting using an anti-HA antibody. All cloned PCR fragments used in this study were controlled by sequencing.

Probes for Northern (see supplemental Table S1) and Southern analysis (SKN7-1/ SKN7-3 and YAP1-1/YAP1-3) were amplified by PCR from genomic DNA.

Northern and Southern blot analysis: RNA extraction and separation followed essentially the described protocol (Current Protocols In Molecular Biology; Wiley). Hybridization of ^{32}P-αATP labelled probes occurred over night in hybridization buffer (0.5M Sodium phosphate buffer pH 7.2 / 7% SDS / 1mM EDTA) at 65°*C.* For DNA extraction, 10ml yeast cells (grown to an OD_{600}=6) were collected, washed once and resuspended in Lysis buffer (2% Triton X-100 / 1% SDS / 100mM NaCl / 10mM Tris pH8 / 1mM EDTA). Genomic DNA was isolated by PCI extraction. Digestion of 10µg genomic DNA was done over-night with *Mfe*I and *Msc*I for *CgSKN7* and *Bst*XI for

CgYAP1 (5U/µg DNA). The digests were separated on a 1% TAE agarose gel. After cross linking (50mJ), the radioactive labelled probes were hybridized over night in hybridization buffer at 65°*C.* Signals were visualized by autoradiography.

Catalase assay: Crude extracts were prepared by breakage of yeast cells with glass beads. Catalase activity was assayed spectrophotometrically at 240nm, protein concentrations were assayed at 280nm as described in (19).

Microscopy: *GFP*-fluorescence microscopy was performed as described previously (28). GFP/CFP was visualized in live cells without fixation. All cells were monitored using a Zeiss Axioplan 2 fluorescence microscope. Images were captured with a Spot Pursuit (Sony) CCD camera using Spotbasic software.

Macrophage cell culture: Primary bone marrow derived macrophages (BMDMs) were obtained from the femur bone marrow of 6 – 10 weeks old C57Bl/6 mice. Cells were cultivated in DMEM supplemented with 10% FCS in the presence of L cell-derived CSF-1 as described (4). Mice were housed under specific pathogen-free conditions. For infection assays, BMDMs were seeded at 5 x 10^5 cells per dish in 3,5-cm dishes containing medium without antibiotics. Log-phase *C. glabrata* cells were washed with PBS supplemented with 0.1% glucose) and added to macrophages in a 4:1 ratio and incubated at 37℃. After washing with PBS, cells were fixed with 2% formaldehyde for 5 minutes, and incubated in 1% triton for 1 minute the cover-slips were incubated with Phalloidin Texas-Red and fixed to slides with Mowiol. For CFU assays, BMDM were seeded at 2 x 10^5 cells per dish. Exponentially growing *C. glabrata* cells were washed with PBS supplemented with 0.1% glucose and added to macrophages in a 2:1 ratio and incubated at 37℃. At the indicated times deionised water was added to lyse macrophages. Cells were spread on YPD plates, incubated at 37℃ and counted.

Chromatin immunoprecipitation assay: ChIP was performed essentially as described previously (2, 43). Briefly, 50 ml of *C. glabrata* culture (OD ~ 0.4) were

treated with 0.4mM hydrogen peroxide for times indicated, followed by crosslinking with 1% Formaldehyde for 10 minutes. Cell extracts were sonicated to reach a fragment resolution of approximately 500bp. For immunoprecipitation, a commercial Anti-HA monoclonal antibody (12CA5) was used. Precipitated DNA was analyzed by quantitative Real Time PCR (Eppendorf Mastercycler) with the following primer pairs: TRR2 (-639/-511) for *CgTRR2* (CAGL0I01166g) and GPX2 (-787/-617) for *CgGPX2* (CAGL0C01705g). As a negative control a centromeric region of Chromosome B was used (fwdCGGAACTCATAACCAATAGCTCG/rev GAATTCGTTGGGAAGTATATTCC).

Results:

***C. glabrata* reacts differently to various oxidative stress causing agents.**

For the close *C. glabrata* relative *S. cerevisiae,* different responses and survival rates to specific oxidative stress causing agents such as menadione, hypochlorous acid or hydrogen peroxide have been found (23, 35, 40). We determined the role of the *C. glabrata* oxidative stress-associated transcription factors CgSkn7 and CgYap1 in the response against agents causing different oxidative stress types. Therefore, we generated strains lacking either CgSkn7 (CAGL0F09097g), CgYap1 (CAGL0H04631g) or both by homologous gene replacement with *ScURA3* and *ScHIS3* (Figure S1). We used gradient plates with concentration ranges of the ROS-generating agent menadione or with gradients of Reactive Oxygen/Nitrogen/Chloride Species (RCS = hypochlorite, RNS = peroxynitrite, ROS = hydrogen peroxide). The growth assays revealed that *C. glabrata* strains exhibit different sensitivities (Figure 1A). We observed that the loss of CgSkn7 had only minor effects on survival, whereas the lack of CgYap1 diminished growth significantly, dependent on the applied chemical agent. On plates containing menadione, we found only minimal growth differences between *C. glabrata* wild type, *skn7*Δ mutant cells and *yap1*Δ mutants. In contrast, we could not detect any varying sensitivities between these strains on plates containing hypochlorite. In addition, in the presence of peroxynitrite, which is generated in the phagosome by the reaction of nitric oxide with superoxide (16, 82), survival of *yap1*Δ and *skn7*Δ*yap1*Δ mutants was severely diminished. We observed that, with an initial inoculum of 500 colony forming units (cfu), both *yap1*Δ and *skn7*Δ*yap1*Δ mutants displayed decreased survival on gradient plates with only 0.4mM hydrogen peroxide (Figure 1A, lower left panel). The *skn7*Δ mutant showed sensitivity only at a high concentration of 10mM hydrogen peroxide. Similar to *S. cerevisiae* (35), we found that *C. glabrata* cells from over-night grown cultures which lacked glucose in the culture medium became increasingly resistant to hydrogen peroxide (Figure 1A, lower right panel). Stationary

cells displayed this phenotype on plates supplemented with 2% glucose or supplemented with 2% ethanol/1% glycerol, indicating that pre-starved cells retain their high resistance state sufficiently long even in the presence of glucose. Furthermore, the carbon source starvation induced oxidative stress resistance was also observed in the absence of CgYap1/CgSkn7 demonstrating a parallel signal contributing to oxidative stress resistance.

Further, *S. cerevisiae yap1*Δ mutants were hypersensitive to superoxide stress induced by treatment with 7-chlorotetrazolo(9)benzo(1)triazine (CTBT) (9). Therefore, we tested the susceptibility of *C. glabrata* strains lacking CgSkn7 and/or CgYap1 to CTBT using a zone inhibition assay (Figure 1B). In contrast to *S. cerevisiae*, the *C. glabrata yap1* mutant strains did not display different susceptibilities. This result was fitting to observations reported recently (49) suggesting that the roles of Yap1 and CgYap1 have partly diverged. Taken together, we conclude that the functionality of CgYap1 is crucial for *C. glabrata* cells to overcome high loads of oxidative stress causing agents.

The core oxidative stress response of *C. glabrata* is similar to *S. cerevisiae*.

To investigate the oxidative stress regulon of *C. glabrata*, the immediate transcriptional response to 0.4mM hydrogen peroxide was determined via microarray analysis (Figure 2). To avoid indirect transcriptional responses, the chosen treatment time was 20 minutes at 30℃. Transcript profiles we re determined by hybridization to genome-wide *C. glabrata* microarrays. Expression data were filtered and averaged. The entire data set was analyzed for co-regulated genes by hierarchical clustering (20). Expression levels of stressed *C. glabrata skn7*Δ and *yap1*Δ mutants were compared directly against expression levels of the stressed wild type. These patterns were aligned to the *C. glabrata* wild type oxidative stress transcriptome.

To compare the *C. glabrata* expression pattern with *S. cerevisiae* data we used a similarity based annotation of orthologous genes (22) (http://cbi.labri.fr/Genolevures/). Orthologous genes, induced by oxidative stress in *S. cerevisiae* (26), are highlighted in violet. Further, expression data from *S. cerevisiae skn7*Δ and *yap1*Δ mutants exposed to 0.2mM H_2O_2, from two-dimensional gel electrophoresis data, was extracted for comparison (48) (Figure 1 highlighted in red). Subsets of genes dependent on CgYap1/CgSkn7 or both were classified into three groups. Group1 comprised genes dependent on both CgSkn7 and CgYap1 and included many generic oxidative stress response genes (*CgTRR1/2*, *CgTRX2*, *CgTSA1/2*, *CgGPX2, CgCCP1* and *CgCTA1*) (33, 48). We designate this group of genes as ”core oxidative stress response” (COR). Further, we found a group of genes, only dependent on CgYap1 (Figure 1 Group 3), including *CgGRE2*, *CgADH6* and *CgOYE2*, which have aldo-keto reductase and oxidoreductase activity in *S. cerevisiae* (11, 46, 63).

Furthermore, we discovered a group of 18 genes upregulated in the wild type during oxidative stress however, not dependent on *Skn7* and *Yap1* (Figure 1 Group 2). Group 2 contained genes associated to mitochondrial processes (*CgACP1*, *CgOPI3*, *CgHSP10* and *CgMRP10*) (36, 56, 71, 74) similar to *S. cerevisiae* (26).Two scenarios could explain their regulation. Either, transcription of these genes is independently activated by CgSkn7 or CgYap1, or their expression is dependent on other factors. Therefore, we determined the transcription pattern upon oxidative stress of the double mutant *skn7*Δ*yap1*Δ. Indeed most genes of Group2 were highly induced in the *skn7*Δ*yap1*Δ double mutant (Figure 2). Therefore we suggest the involvement of other factors during the oxidative stress response.

Stationary *C. glabrata* cells displayed an increased resistance against oxidative stress. Thus, we compared the transcript pattern of oxidative stress and glucose starvation (70). Indeed, 26 genes of the oxidative stress regulon were found to be upregulated (Figure 2, right panel). This group also includes *CgCTA1*, *CgGPX2* and

CgTRX2, indicating an at least partially overlapping response. We suggest that *S. cerevisiae* and *C. glabrata* share a highly similar core oxidative stress response pattern, which is regulated by CgSkn7 and CgYap1.

Conserved consensus sequences for CgSkn7 and CgYap1 are present in genes involved in oxidative stress response in *C glabrata*.

The above analysis suggested that *C. glabrata* and *S. cerevisiae* share a common set of genes involved in the oxidative stress response. Further, we found a number of genes dependent on CkSkn7 and CgYap1. We performed an *in silico* analysis of the upstream regions in *C. glabrata* to identify putative *S. cerevisiae* Yap1 and Skn7 consensus sites in their promoters (Figure 3A). Consensus-like sequences shared by the CgSkn7 and CgYap1 regulated genes were found in the upstream regions (2kB) by a systematic search allowing one deviation from the known consensus sequences in *S. cerevisiae* (31, 62, 84). Exact Yap1 and Skn7 consensus sequences were counted in the upstream regions (< -1200bp) of Groups 1, 2 and 3 (Figure 3A, for a schematic view see Figure S2). We found a highly conserved Yap1 target sequence (TTASTMA) in the majority of identified CgYap1 dependent genes in *C. glabrata*. Skn7 is known to have a broader range of consensus sequences in *S. cerevisiae* (OSREs, Skn7 oxidative stress responsive elements) (30, 31); nevertheless we also identified conserved Skn7 target sequences (GNCNNGSCS or GGCTGGC). Discovered consensus sequences from Group 1 and Group 3 are depicted in the form of sequence logos (Figure 3A, lower panel). We also found both, Yap1 and Skn7 consensus sites, but to a lesser extent in Group 2. Either CgSkn7 or CgYap1 can contribute partially to expression of these genes during oxidative stress beside other transcription factors, or those sites are not corresponding with the sites where CgSkn7 and CgYap1 bind in *C. glabrata*. Consistently, we discovered slightly altered Yap1-like and Skn7-like sites allowing one deviation at any position (see Figure S2, indicated as light blue and pink

bars) in Groups 1, 2 and 3. Another explanation for the significant number of Yap1 consensus sites in Group 2 might be that other factors of the *YAP* family, which can potentially recognize the Yap1 consensus site in *S. cerevisiae* (13, 85), regulate transcription of those genes.

To correlate the putative CgYap1 and CgSkn7 binding sites with regulatory elements, we investigated the oxidative stress regulation of the Cg*CTA1* promoter. Therefore, we created a series of truncations of the catalase promoter and fused them to the catalase open reading frame. We used the catalase activity which is tightly coupled to its mRNA levels (our unpublished observations) as a convenient read out for the activity of the promoter fragments. We transformed the promoter deletion series into a *C. glabrata* c*ta1*Δ mutant strain and tested activity of catalase in extracts upon induction by oxidative stress (Figure 3B). We found that promoter activity was significantly diminished in the construct containing up to -1000bp of the promoter and was abolished when truncated version with about 900bp. Interestingly, the perfect *S. cerevisiae* Yap1 consensus sites are located at positions -732bp and -1676bp (Figure 3B, lower panel), whereas we found a Yap1-like and a Skn7-like sequence indicated as light blue and pink bars within a -1100bp to -900bp. Therefore, we suggest that binding of both, CgYap1 and CgSkn7, is not restricted to known *S. cerevisiae* consensus sequences, but favors variants of these sites. However, the composition of the putative binding sites in the upstream regions of oxidative stress genes pointed to a predominantly CgYap1 controlled oxidative stress regulon.

Expression of important key enzymes to overcome oxidative stress is dependent on CgSkn7 and CgYap1.

To confirm the microarray results and to demonstrate the function of CgSkn7 and CgYap1 for oxidative stress regulated transcription, we measured the expression levels of several exemplary genes of Groups 1, 2 and 3 over several time points

following exposure to hydrogen peroxide (Figure 4). We chose *CgCTA1*, *CgTRR2, CgGPX2* and *CgTSA1* of Group 1 comprising CgSkn7 and CgYap1 dependent genes (see Figure 4A). Northern blot analysis showed rapid induction upon treatment with 0.4mM H_2O_2 in *C. glabrata* wild type and in *C. glabrata skn7*Δ and *yap1*Δ mutant cells supplemented with *CgSKN7* or *CgYAP1* on a plasmid under their own promoters (p*CgSkn7*, p*CgYap1*). In *C. glabrata* wild type cells, expression of *CgTRR2* and *CgTSA1* decreased after 20 minutes again, whereas expression of *CgCTA1* and *CgGPX2* was still induced after 40 minutes. In the absence of CgSkn7 and CgYap1, mRNA levels were severely reduced. However, stress-induced expression of *CgTRR2* and *CgGPX2* is not completely abolished in *skn7*Δ mutant cells, suggesting either the parallel involvement of other factors or that CgYap1 can induce those genes to a certain extent alone. Further, we found that *C. glabrata* strains lacking CgYap1 did not display a significantly increased susceptibility to superoxide anions (see Figure 1). Therefore we wanted to know whether expression of the superoxide dismutase *CgSOD1* is affected in *yap1*Δ or *skn7*Δ mutant cells during hydrogen peroxide induced oxidative stress. We found that *CgSOD1* was constitutively expressed, and expression was not impaired in mutant strains. We conclude that the superoxide dismutase *CgSOD1* has a housekeeping function in *C. glabrata*, which is not part of CgSkn7/CgYap1 mediated oxidative stress regulon.

Group 2 comprises genes regulated independently of CgSkn7 and CgYap1. Therefore we used the double mutant *skn7*Δ*yap1*Δ supplemented with p*CgSKN7*, p*CgYAP1* or p*CgYAP1-CgSKN7* to perform northern blot analysis (Figure 4B). We chose *CgHSP78* and *CgZWF1* to measure expression levels. Expression of *CgHSP78*, a mitochondrial matrix chaperone (50), occurred independently of CgSkn7/CgYap1, revealing the involvement of other transcription factors in the regulation of Group 2. In addition, we investigated expression pattern of Cg*ZWF1*, encoding the glucose-6-phosphate dehydrogenase, which is also involved in adapting to oxidative stress in *S.*

cerevisiae (37). It was constitutively expressed due to its role as housekeeping gene (65). Interestingly, *CgZWF1* maximum expression was dependent on the presence of either CgSkn7 or CgYap1 in *C. glabrata*. Both factors contributed independently of each other to full expression upon oxidative stress induction, which is consistent with a 550bp gap between putative consensus sites of CgSkn7 and CgYap1 in the corresponding upstream region. Microarray data predicted a group of genes to be solely dependent on CgYap1 (Group 3). We chose *CgHSP31* to follow its expression pattern upon oxidative stress induction (78). Indeed, we observed a strict dependency on CgYap1. These data confirm a direct role for CgSkn7 and CgYap1 during induction of transcription by oxidative stress. Nevertheless, our analysis showed that other factors are involved in oxidative stress induced gene expression in *C. glabrata*.

Since nutrient starvation-associated genes are known to be also upregulated during phagocytosis (39), we investigated expression levels of oxidative stress genes during glucose depletion (Figure 4C). *CgCTA1* and *CgGPX2* displayed the same transcriptional pattern: after one hour, both occurred to be upregulated in a CgSkn7 and CgYap1 independent manner. Further, we wanted to know whether expression of the superoxide dismutases *CgSOD1* and *CgSOD2* is affected in *yap1*Δ mutant cells during glucose starvation (Figure 4C, lower panel). Indeed, elevated expression of *CgSOD2* and *CgSOD1* did not change in *C. glabrata skn7*Δ, *yap1*Δ and *skn7*Δ*yap1*Δ mutants, pointing to a different regulation pattern of the *C. glabrata* orthologues of *SOD1* and *SOD2* than in *S. cerevisiae* (6). Members of the *SOD* family were also reported to be upregulated in *C. albicans* cells upon entering stationary phase (44).

Therefore, even genes belonging to core oxidative stress regulon might be expressed *in vivo* upon engulfment of *C. glabrata* cells due to the involvement of other transcription factors.

Catalase activity increases during glucose starvation and is not dependent on the presence of CgSkn7/CgYap1.

Since carbon starvation induced a large part of the oxidative stress regulon in *C. glabrata*, we measured catalase activity upon glucose depletion (Figure 5). Over-night cultures of *C. glabrata* wild type, *skn7*Δ, *yap1*Δ and *skn7*Δ*yap1*Δ cells displayed high catalase activities; as a control we used the *C. glabrata* catalase *cta1*Δ knock out strain (Figure 5A). CgCta1 activity was not affected by the loss of CgSkn7 or CgYap1 CgSkn7. Further cells were diluted, grown to an OD_{600} of 1 and shifted to medium containing 1.5% ethanol/0.5% glucose. After several hours we collected the cells measured the catalase activity. Again we observed an increased catalase activity, unaffected by the loss of CgSkn7/CgYap1. These results were in line with the expression levels observed in Figure 4, indicating the presence of different starvation-associated factors, which can induce genes belonging to the oxidative stress regulon.

Further, we wanted to uncover the part of the upstream region of *CgCTA1* which is crucial for full induction during glucose starvation (Figure 5B). Truncated promoter versions expressing *CgCTA1* (similar to Figure 3B), were used to measure remaining catalase activity. We discovered an area between -950bp and -900bp to be essential for full induction upon glucose depletion. Taken together, we assume that during glucose starvation, *C. glabrata* cells switch their transcriptional pattern including at least part of the oxidative stress regulon, which is then under control of other factors than CgSkn7/CgYap1.

CgSkn7 and CgYap1 are dependent on each other to induce gene expression of oxidative stress genes.

Genes comprising Group 1 are dependent on both CgSkn7 and CgYap1 for full expression. This cooperative activation of transcription might be dependent on, *e.g.* the

interaction with basal transcription machinery, or these factors might be interdependent for promoter recognition. Therefore we tested whether CgSkn7 and CgYap1 are able to bind independently to oxidative stress gene promoters. CgSkn7 was tagged with HA epitopes at the C-terminus, whereas CgYap1 was tagged at the N-terminus, to ensure their proper nuclear localization and promoter binding. The expression of the respective fusion proteins was checked on Western Blots (not shown). Both constructs were expressed from centromeric plasmids under the control of the native promoter. To elucidate the binding of these factors to the promoters, we performed chromatin immunoprecipitations. Precipitated DNA was analyzed by quantitative Real Time PCR measurements (Figure 6).

As target gene promoters we chose *CgTRR2* and *CgGPX2*, since mRNA analysis showed that the stress-induced expression of both was not completely abolished in the *C. glabrata skn7*Δ mutant (Figure 4A). Therefore, we suggested that CgYap1 alone might be able to bind to these promoters to a certain extent. HA-CgYap1, expressed in the *yap1*Δ mutant, was detected at the *CgTRR2* promoter within three minutes upon stress induction (Figure 6 upper left panel). After initial recruitment, HA-CgYap1 dissociated gradually from the *CgTRR2* promoter (< 6 minutes). In the case of *CgGPX2*, binding was detected within 3 minutes upon stress induction, but the HA-CgYap1 signal declined more slowly (> 17 minutes, Figure 6 upper right panel). However, when HA-CgYap1 was expressed in absence of CgSkn7 in the *skn7*Δ*yap1*Δ double mutant, we failed to detect recruitment to the *CgTRR2* promoter (Figure 6 upper left panel), whereas we observed a slightly increased recruitment to the *CgGPX2* promoter (Figure 6 upper right panel).

In the *skn7*Δ single mutant, CgSkn7-HA bound with similar kinetics as HA-CgYap1 within 3 minutes to the *CgTRR2* promoter. Notably, CgSkn7-HA stayed slightly longer at the *CgTRR2* promoter than HA-CgYap1 (> 9 minutes, Figure 6 lower left panel). The binding kinetics of CgSkn7-HA to the *CgGRX2* promoter was the same as

for HA-CgYap1 (> 17 minutes, Figure 6 lower right panel). Finally, in the double mutant *skn7*Δy*ap1*Δ, CgSkn7-HA was not detectable in the promoter regions (Figure 6 lower panels). Taken together, upon induction through oxidative stress, binding of CgSkn7 and CgYap1, to certain promoters, is strongly interdependent.

CgSkn7 and CgYap1 are not required for survival in a primary mouse macrophage infection model.

Since the oxidative burst is known to be part of the strategy of phagocytic cells to erase engulfed cells, we analyzed the importance of the oxidative stress transcription factors CgSkn7 and CgYap1 during phagocytosis. First, we investigated their localization *in vitro* and in our *ex vivo* macrophage model. Both factors were fused to fluorescent proteins. To preserve their nuclear localization signals CgSkn7 was C-terminally fused to CFP, whereas CgYap1 was N-terminally fused to GFP. Both fusion genes were expressed from p*ACT* derived centromeric plasmids and driven by the *CgADH1* promoter.

The CgSkn7-CFP signal was detected in the nucleus in *skn7*Δ mutant cells in rich medium (Figure 7A, upper panel). This observation is consistent with the localisation data in *S. cerevisiae* (69). The nuclear localisation pattern did not change during phagocytosis by bone marrow derived primary mouse macrophages. In contrast, GFP-CgYap1 was located in the cytoplasm in unstressed cells. Upon short exposure to oxidative stress (0.4mM H_2O_2 and 2mM As_2Cl_3), GFP-CgYap1 rapidly accumulated in the nucleus (Figure 7A, lower panel). Hydrogen peroxide is produced during the oxidative burst in a comparable concentration (21). Arsenic is known to induce a fast oxidative stress response (92). In addition, within the first hour upon macrophage engulfment, cells with nuclear GFP-CgYap1 were visible. However, we found that the

nuclear accumulation occurred only transiently in the early phase of phagocytosis (Roetzer *et al.*, submitted revised). Nevertheless, *C. glabrata* cells seemed to experience oxidative stress inside the phagosome of macrophages.

To verify if CgSkn7 and CgYap1 are required for prolonged survival upon phagocytosis, we infected macrophages with *C. glabrata skn7*Δ*yap1*Δ double mutant cells carrying either the plasmid p*CgSKN7-CgYAP1* or the empty vector (Figure 7B). *C. glabrata* cells were added to macrophages in a 2:1 ratio. After 24 hours and 48 hours, engulfed *C. glabrata* cells were recovered on YPD plates. However, the double mutant *skn7*Δ*yap1*Δ complemented with p*CgSKN7-CgYAP1* displayed the same phenotype as *skn7*Δ*yap1*Δ carrying the empty vector. Therefore, we suggest that oxidative stress is efficiently alleviated during phagocytosis of *C. glabrata* and that CgYap1 and CgSkn7 function for induction of the oxidative stress defence response is complemented by independent other environmental cues.

Discussion:

Upon phagocytosis, microbes need to counteract reactive oxygen and nitrogen species produced through the oxidative burst inside the phagosome of phagocytic cells (3, 7, 75). How does the fungal pathogen *C. glabrata* change its oxidative stress-associated transcriptional pattern to sustain a massive increase of ROS and RNS upon internalization? We explored here the oxidative stress regulon of *C. glabrata*, and subsequently analysed the contribution of the two prominent transcription factors CgSkn7 and CgYap1. In this study, we defined a *C. glabrata* core set of the oxidative stress response (COR), and we showed that CgSkn7 and CgYap1 are interdependent for regulation of at least some of these genes, indicating that the interaction is conserved between *C. glabrata* and *S. cerevisiae* (31, 48). However, we found that, in a primary mouse macrophage model, the loss of CgSkn7 and CgYap1 had no impact on the survival rate compared to the wild type. This suggests that the conserved regulatory system consisting of Yap1 and Skn7 plays a dispensable role during acute phagocytosis conditions. Strikingly, a large set of oxidative stress-associated genes was also upregulated during carbon starvation, suggesting that carbon source starvation provides a parallel pathway for induction of oxidative stress response genes.

The C. glabrata oxidative stress response is similar to S. cerevisiae. In *S. cerevisiae*, at least 71 genes displayed increased expression within minutes upon exposure to hydrogen peroxide (27). Furthermore, Yap1 controlled at least 32 genes of the identified oxidative stress stimulon in *S. cerevisiae* (33, 48). 15 of these proteins required both Skn7 and Yap1 for induction. Two distinct Yap1 regulons were defined in *S. cerevisiae*, one covering the oxidative stress response, the second involved in the metabolic pathways regenerating the main cellular reducing power, GSH and NADPH (48). In *C. glabrata,* 38 genes were upregulated more than two-fold during oxidative stress. Among the oxidative stress-induced regulon we found genes to be dependent on both CgSkn7 and CgYap1 or on CgYap1 alone, respectively. In addition, a set of genes appeared to be regulated independently of CgSkn7/CgYap1. Induction of the

core response to oxidative stress (COR), which included thioredoxin peroxidases (CgTsa1, CgTsa2), thioredoxin reductases (CgTrr1, CgTrr2), the thioredoxin cofactor CgTrx2, the glutathione peroxidase CgGpx2, the mitochondrial cytochrome-c peroxidase CgCcp1 and the catalase CgCta1, was dependent on the presence of both, CgSkn7 and CgYap1. A second CgYap1-associated set of genes was encoding proteins displaying aldo-keto reductase and oxidoreductase activity (*CgADH6*, *CgGRE2*, *CgSCS7* and *CgOYE2*). Therefore, we conclude that Skn7 and Yap1 have conserved functions in the class of Saccharomycetes.

CgSkn7 and CgYap1 cooperate for promoter binding to induce the oxidative stress regulon. In *S. cerevisiae*, a direct interaction between Skn7 and Yap1 seemed to be crucial for induction of oxidative stress response genes (31, 32). The mutated receiver domain of Skn7 affected the association of Yap1 and Skn7 to upstream regions of oxidative stress genes (31, 60). However, the precise mechanism by which these two factors co-activate oxidative stress response was not clear yet. To assess the interaction of CgSkn7 and CgYap1 in *C. glabrata*, we tested whether binding of CgSkn7 and CgYap1 to oxidative stress gene promoters in *C. glabrata* is dependent on the presence of each other. Chromatin immunoprecipitation data showed that a strict interdependence occurs at the level of promoter recognition. In the presence of CgYap1, CgSkn7 was able to bind the upstream sequences of *CgTRR2* and *CgGPX2*, whereas in the absence of CgYap1, CgSkn7 could not bind to these promoters. Similarly, CgYap1 bound only in the presence of CgSkn7 to the tested upstream regions in a significant manner. This kind of interdependence was also observed in *S. cerevisiae*: an electrophoretic mobility shift assay demonstrated the presence of a Skn7-Yap1 complex at the promoter of *TSA1* (48). Here, we showed the first time, that, in *C. glabrata*, CgSkn7 needs CgYap1 and vice versa to bind to the upstream region of core oxidative stress genes. Recruitment to promoter occurred immediately upon stress induction (< 3 minutes). Both factors were detectable at the promoter for the same period of time (*CgTRR2* < 10 minutes, *CgGPX2* > 10 minutes). Although CgYap1

displayed minimal binding properties in *skn7*Δ mutant cells, we suggest, that remaining *CgGPX2* expression in *skn7*Δ mutants is carried out by other components. This is consistent to the regulation found in *S. cerevisiae*, where *GPX2* is also induced in a calcineurin/Crz1-dependent manner during oxidative stress (83).

Interestingly, we found a significant number of Yap1 consensus sites throughout the oxidative stress regulon, including the set of genes, which appeared to be upregulated even in the absence of CgYap1. To test binding properties of upstream regions we measured catalase activity of *CgCTA1* expressed by truncated promoter versions. The identified upstream region, which was crucial for full catalase activity, did not comprise *S. cerevisiae* Skn7 and Yap1 consensus sites. Present *S. cerevisiae* Skn7- and Yap1-like sequences pointed to an altered recognition pattern of CgYap1.

*C. glabrata yap1*Δ cells displayed increased susceptibility against hydrogen peroxide and peroxynitrite. However, in contrast to *S. cerevisiae* (6), the loss of CgYap1 appeared to have only minimal effects on susceptibility to superoxide anions: both menadione and CTBT induced a similar stress response pattern (our unpublished results). Consistently, we found that the superoxide dismutase gene *CgSOD1* was expressed independently of CgSkn7/CgYap1. This is in line with results found by Lelandais *et al*, that CgYap1 has a distinct recognition pattern in *C. glabrata* during benomyl response in comparison to Yap1 in *S. cerevisiae* (49). Further, we found that the superoxide dismutase CgSod1 is constitutively expressed in *C. glabrata* in a CgSkn7/CgYap1 independent manner. Therefore we conclude that the specific responses dependent on CgYap1 have further evolved in *C. glabrata* after separation from *S. cerevisiae*.

The oxidative stress response genes are under dual control. 26 genes of the oxidative stress regulon were found to be upregulated during glucose starvation (70). This group also includes *CgCTA1*, *CgGPX2* and *CgTRX2*, which were expressed independently of CgSkn7/CgYap1 upon glucose depletion. In addition, *CgSOD1/2*

appeared to be upregulated during starvation. It has been reported, that *S. cerevisiae* cells grown to stationary phase exhibit increased resistance against menadione and hydrogen peroxide (35). Contrary, we could not find a *C. glabrata*-like expression pattern in *S. cerevisiae* during the diauxic shift (26). Notably, in a *C. albicans* batch culture, stationary phase cells also exhibited induction of proteins involved in oxidative stress response (44). Adaptation to these environmental changes requires a simultaneous upregulation of a set of genes, beneficial for both, oxidative stress and glucose starvation. Interestingly, nutrient limitation can also increase resistance to acid shock and oxidative stress in bacteria, such as *Staphylococcus aureus* and *Salmonella typhimurium* (24, 87). Therefore we suggest the existence of dual control mechanisms in *C. glabrata*, which could be important inside the phagosome due to acute oxidative stress and prolonged starvation.

The impact of the oxidative stress regulon on virulence remains contradictory. Since CgSkn7 and CgYap1 regulated the core oxidative stress response, the loss of these factors might attenuate virulence. However, the *C. glabrata skn7*Δ*yap1*Δ double mutant did not display a diminished survival rate compared to the wild type situation in our primary mouse macrophage model. Accordingly, we observed that low numbers of starved *skn7*Δ*yap1*Δ cells can overcome 0.4mM H_2O_2, the concentration that *C. glabrata* cells experience inside the mammalian host (15, 21). Microarray analysis of *C. glabrata* cells engulfed by macrophages, revealed a rather inconsistent oxidative stress response: *CgCTA1*, *CgGDB1, CgHEM15* and *CgGLO1* displayed an increased expression, whereas *CgTTR1/2* and *CgTSA1/2* were downregulated during phagocytosis (39). Notably, *CgTRR1/2* and *CgTSA1/2* were also strictly downregulated during glucose depletion in our microarray experiments.

This might be explained by at least two models. One assumes a mild oxidative stress load for *C. glabrata* inside the phagosome of phagocytic cells and thus the induced expression of the respective target genes is not immediately necessary.

Wellington *et al* have shown recently, that *C. glabrata* cells can suppress ROS production upon internalization by macrophages (88). Alternatively, the crucial genes might be induced by parallel pathways (Figure 8). This latter idea is supported by the observed upregulation of oxidative stress-associated genes by environmental conditions which *C. glabrata* might encounter as well inside a phagocytic vesicle. This might be primarily starvation for nutrients and especially carbon source (39, 54). This model implies an adaptation of stress gene regulation to the prevailing situation in the host. Both scenarios suggest that *C. glabrata* can efficiently counteract the oxidative burst.

Table 1

C.glabrata Strain	Genotype	Source
ΔHTU	*his3*Δ *trp1*Δ *ura3*Δ	(41)
ARCg *skn7*Δ	*his3*Δ *trp1*Δ *ura3*Δ *skn7*Δ::*ScHIS3*	This study
ARCg *yap1*Δ	*his3*Δ *trp1*Δ *ura3*Δ *yap1*Δ::*ScURA3*	This study
ARCg*skn7*Δ*yap1*Δ	*his3*Δ *trp1*Δ *ura3*Δ *skn7*Δ::*ScHIS3* *yap*Δ::*ScURA3*	This study
ARCg *cta1*Δ	*his3*Δ *trp1*Δ *ura3*Δ *cta1*Δ::*ScURA3*	This study

Table 2

Plamid	Genotype	Source
p*RS316*	CEN6, ARSH4, *ScURA3*	(76)
p*RS313*	CEN6, ARSH4, *ScHIS3*	(76)
p*GEM-ACT*	ARS, CEN and *TRP1* marker from *C. glabrata*	(29)
p*CgADH1-CgMSN2-CFP*	*CgADH1-CgMSN2-CFP* (*Sph*I/*Sac*II and *Sac*II/*Nsi*I); *CgTRP1*.	(70)
p*CgADH1-CgSKN7-CFP*	*CgADH1-CgSKN7-CFP* (*Sac*II and *Nco*I); *CgTRP1*.	This study
p*CgSKN7*	*CgSKN7-CgSKN7* (native Promoter *Sph*I and *Sac*II); *CgTRP1*.	This study
p*GEM-ACT-CgYAP1*	Native Promoter inserted via *Sph*I/*Not*I; *CgTRP1*.	This study
p*CgYAP1CgYAP1*	*CgYAP1-CgYAP1* (*Not*I and *Nsi*I); *CgTRP1*.	This study
pCg*ADH1-GFP-CgYAP1*	Cg*ADH1-GFP-CgYAP1 (Not*II/*Nsi*I); GFP inserted via *Not*I/*Not*I; *CgTRP1*.	This study
p*CgSKN7-HA*	*CgSKN7-CgSKN7-HA* (HA tag inserted with *Nco*I); *CgTRP1*.	This study
p*HA-CgYAP1*	*CgYAP1-HA-CgYAP1* (HA tag inserted with	This study

	*Not*I); *CgTRP1*.	
p*CgYAP1-CgSKN7*	*CgSKN7-CgSKN7* inserted with *Nsi*I into p*CgYAP1CgYAP1*; *CgTRP1*marker.	This study
p*CgC-CgCTA1*	*CgCTA1-CgCTA1* (*Sph*I/*Not*I and *Not*II/*Nsi*I); *CgTRP1* marker.	This study
p*CgC1500-CgCTA1*	Insertion of 1500pb promoter of *CgCTA1* (*Sph*I/*Not*I); *CgTRP1* marker.	This study
p*CgC1200-CgCTA1*	Insertion of 1200pb promoter of *CgCTA1* (*Sph*I/*Not*I); *CgTRP1* marker.	This study
p*CgC1100-CgCTA1*	Insertion of 1100pb promoter of *CgCTA1* (*Sph*I/*Not*I); *CgTRP1* marker.	This study
p*CgC1000-CgCTA1*	Insertion of 1000pb promoter of *CgCTA1* (*Sph*I/*Not*I); *CgTRP1* marker.	This study
p*CgC950-CgCTA1*	Insertion of 950pb promoter of *CgCTA1* (*Sph*I/*Not*I); *CgTRP1* marker.	This study
p*CgC925-CgCTA1*	Insertion of 925pb promoter of *CgCTA1* (*Sph*I/*Not*I); *CgTRP1* marker.	This study
p*CgC900-CgCTA1*	Insertion of 900pb promoter of *CgCTA1* (*Sph*I/*Not*I); *CgTRP1* marker.	This study

Supplemental Table S1

Name	Sequence
Skn5	GAGTCCGCGGATGGACTACGAAGTTAATGC
Skn3	GCTACCATGGTGCCGCCCGTATGTTGCTTCTTAAATG
Yap3	GACGATGCATTTATTAAGACATGTGCTTATTTAAAGCA
Yap5	ACTAGGCGGCCGCCCAGGAATGGCTGAGGTGGATAACGG
ACT1-5	ATGTGTAAGGCCGGTTTC
ACT1-3	AGGAAGATTGAGCAGCGG
CTA1-5	ATGTCCGCTAATCCAACT
CTA1-3	GCTTCATCATTGGTCAAG
GPX2-5	CAATGGCTGCTAAGAGT
GPX2-3	CAGAATCGATGTCATTA
TSA1-5	ATGGTCGCTCAAGTTCAA
TSA1-3	CGTTCTTGAAGTACTCCT
TRR2-5	GAATCACAAGAAGGTTGT
TRR2-3	CGTTCTTGATTCTCAAGT
HSP10-5	ATGTCCACTCTACTAAAG
HSP10-3	GTTATCCTTTATCTTGGC
HSP31-5	TGGCTGCTAAGAAGGTTC
HSP31-3	AGCAGCAACAACACCGCC
HSP78-5	ATGTTAAGCAGGGTATGT
HSP78-3	TACTTCGCACCAGCGATC
ZWF5-1	ATGTCAGAACCTGTTAAG
ZWF1-3	CTCATGACTAGCAAGTTC
SOD1-5	GTTGCTGTTTTGAGAGGA
SOD1-3	TTGGTTAGGCCGATGACA
SOD2-5	ATGTTGTCTACGTCTAGG
SOD2-3	TTGGATGTTTCGTACCTC
ProNat_Skn7-5	AGATGCATGCAATATACCGTCAATTCATCC
ProNat_Skn7-3	CTCACCGCGGATTAGTTTTATAGCGTTTAT
ProNat_Yap1-5	GGACTTAGCTGCGGCCGCCTTTTACTTCCTAGTTCTTGTCTCTGTCC
ProNat_Yap1-3	TGCTGGACTAGCATGCCTGTATATTGTCTTTACCAATATATATAA
Seq_Skn7_PRO	GATAAGTATACTTTCAA
Seq_Skn7_ORF	TGCAACATCAATTGTAA
Seq_Yap1_PRO	TATGCAACAGTAACTAC
Seq_Yap1_ORF	GATGACAACGATCAAGA

Skn7-1	TGGCTATCTGTCATTCAATT
SKN7-3	CACGGCGCGCCTAGCAGCGGATTAGTTTTATAGCGTTTAT
SKN7-4	GTCAGCGGCCGCATCCCTGCTTTTGCATCTCTAACTAGTA
SKN7-6	AATGGAGGAAGTAGTAGTGA
Skn7-Ctrl5	GGCCCTCAGGTGCTT
Skn7-Ctrl3	ATGTAATTGTGATCG
HIS3-5ctrl	GTAGCAGAACAGGCC
HIS3-3ctrl	TGGCAACCGCAAGAG
URA3-5ctrl	TGCTGGCCGCATCTTCT
URA3-3ctrl	TAGTCCTGTTGCTGCCA
YAP1-1	GGCACAGAACATAGCGGAGT
YAP1-3	CACGGCGCGCCTAGCAGCGGTACTTCCTAGTTCTTGTCTC
YAP1-4	GTCAGCGGCCGCATCCCTGCTCACCTGTCTATATTATCTC
YAP1-6	GCGTGAATTATTGGGATCAG
YAP1-Ctrl5	GTGTTGGTCTTTCTCCGGTT
YAP1-Ctrl3	CAACTCATAGATCACAACAT
Skn7-3nsi	CGCTAATGCATTTATTACGTATGTTGCTTCTTAAATG
Skn7-5nsi	GAGATATGCATAATATACCGTCAATTCATCC
Skn7_HA6_5	CCTGCCATGGGTGTACCTACTAGATAC
Skn7_HA6_3	CAGGCCATGGTCATCACGACGTTGTAAA
Yap1_HA6_5	ACCTGGCGGCCGCATGTACCTACTAGATAC
Yap1_HA6_3	TCAGGGCGGCCGCCCGACGTTGTAAAACG
GPX2R5fwd	AGCACTTGCGAGATGAGACTCC
GPX2R5rev	GGAGTTAATAAAGCAGCCTCCG
TRR2R3fwd	TGTAACTTTGCACTTTGCACCC
TRR2R3rev	CGAAAGATTGAAGTTCTCTTCG
cgCEN0Bfwd	GGAACTCATAACCAATAGCTCG
cgCEN0Brev	GGAATATACTTCCCAACGAATTC
Cta1_1500	GGATTGCATGCTCTGCAGCCATAATTGGAGA
Cta1_1200	GGATTGCATGCCGGGTCATATCGGATTGCAT
Cta1_1100	GGATTGCATGCGTGATCATAAAAGTTGCATA
Cta1_1000	GGATTGCATGCTACGGGATTATATCTGGTAT
Cta1_900	GGATTGCATGCGAGATTATCACTACTAGTTA
Cta1_950	GGATTGCATGCGTTCCAGCTTCTAAGCTATT
Cta1_925	GGATTGCATGCATCTCTTTTGAGATTATCAC
CTAPro-down	ATGTCGACTGCGGCCCATGGTTTTTTTCAATTGTGGGAAGTTATC

Figure legends:

Figure 1. *C. glabrata* responds to oxidative stress in a CgYap1 and partially CgSkn7 dependent manner. (A) *C. glabrata* resistance against oxidative stress causing agents. *C. glabrata* wild type, *skn7*Δ, *yap1*Δ and *skn7*Δ*yap1*Δ mutant cells were grown to an OD_{600} of 1 in YPD. $5x10^2$ cells were dropped on gradient plates containing changing concentrations of menadione, hypochlorite, peroxynitrite and hydrogen peroxide (see Material and Methods). Plates were incubated at 37℃ over-night. Further, saturated over-night cultures were diluted and $5x10^2$ cells were dropped on gradient plates containing 0.4mM hydrogen peroxide (lower right panel). Plates were incubated at 37℃ for 48 hours. (B) Susceptibility of *Candida glabrata* strains to CTBT assessed using a zone inhibition assay (10 μg CTBT/disc) Approximately $7.5x10^6$ cells were plated onto YPD (rich medium with glucose, A), YPGE (rich medium with glycerol and ethanol, B), YNB (minimal medium with glucose, C) a YNGE (minimal medium with glycerol and ethanol, D) media.

Figure 2. Comparison of genome-wide expression levels in response to oxidative stress in *C. glabrata.* Transcript profiles were determined by hybridization to genome-wide *C. glabrata* microarrays. The sets represent average inductions of replicate profiles of *C. glabrata* wild type strain (4166 ORFs), and comparison of wild type strain versus *C. glabrata skn7*Δ and *yap1*Δ mutant strains, and the *skn7*Δ*yap1*Δ double mutant strain alone after treatment with 0.4mM H_2O_2. All treatments were done at 30℃ for 20 minutes. Genes involved in oxidative stress response were clustered after specific selection (>2-fold). Gene names correspond to *C. glabrata* systematic ORF designations and their corresponding *S. cerevisiae* orthologues. Major cluster are labeled corresponding to dependence on Skn7 and Yap1: Group 1 represents genes dependent on CgSkn7 and CgYap1, Group 2 represents genes expressed

independently of CgSkn7 or CgYap1, Group 3 represents genes dependent on CgYap1. Genes found to be upregulated in *S. cerevisiae* upon oxidative stress are highlighted in violet. Genes discovered to be dependent on Skn7 and Yap1 or Yap1 alone in *S. cerevisiae* are highlighted in red. Induction profile of corresponding genes in the *C. glabrata* wild type strain during glucose depletion is included (right lane).

Figure 3. CgSkn7 and CgYap1 dependent genes possess highly conserved consensus sequences. (A) Percentage of identified *S. cerevisiae* Skn7 and Yap1 consensus sites present within -1200bp upstream regions of *C. glabrata* genes of Groups 1, 2 and 3. For a schematic view of promoters of Group 1 and 3 see Figure S2. Verified logo representation consensus sequence patterns among the CgSkn7 and/or CgYap1 regulated genes are shown. (B) To measure catalase activity, *C. glabrata* wild type and *cta1*Δ cells bearing plasmids with *CgCTA1* including various truncated promoter versions were incubated in YPD with 0.4mM H_2O_2 for 45 minutes. Crude cell extracts were prepared and then assayed for catalase activity. Schematic representation of -2000bp upstream region of *CgCTA1* displaying all identified *S. cerevisiae* Skn7-like and Yap1-like sequences and Yap1 consensus sites (lower panel).

Figure 4. CgSkn7 and CgYap1 are required for rapid induction of transcription after oxidative stress. (A) Northern blot analysis of *CgCTA1, CgTRR2, CgGPX2*, *CgTSA1, CgSOD1* and *CgSOD2* transcripts during 0.4mM H_2O_2 induced oxidative stress. *C. glabrata* wild type, *C. glabrata skn7*Δ transformed with p*CgSKN7* and *C. glabrata yap1*Δ transformed with p*CgYAP1* were grown to exponential phase before 0.4mM H_2O_2 was added. Samples for RNA extraction were taken at indicated time points. mRNA levels were visualized by hybridization of radio-labeled probes and

autoradiography. *CgACT1* mRNA was used as loading control. (B) Northern blot analysis of *CgHSP78, CgZWF1* and *CgHSP31* transcripts during 0.4mM H_2O_2 induced oxidative stress*. C. glabrata* wild type and *C. glabrata skn7*Δ*yap1*Δ transformed with empty vector, p*CgSKN7,* p*CgYAP1* or p*CgYAP1-CgSKN7* were grown to exponential phase and treated as described in (A). (C) Northern blot analysis of *CgCTA1, CgGPX2, CgSOD1* and *CgSOD2* transcripts during glucose starvation. *C. glabrata* wild type and *C. glabrata skn7*Δ*yap1*Δ transformed with empty vector, p*CgSKN7,* p*CgYAP1* or p*CgYAP1-CgSKN7* were grown to exponential phase, washed twice and incubated in rich medium lacking glucose. Samples for RNA extraction were taken at indicated time points. mRNA levels were visualized by hybridization of radio-labeled probes and autoradiography.

Figure 5. During glucose starvation catalase CgCta1 is induced in a CgSkn7/CgYap1 independent manner. (A) To measure catalase activity, *C. glabrata* wild type, *cta1*Δ, *skn7*Δ, *yap1*Δ and *skn7*Δ*yap1*Δ cells the plasmid p*CgC-CgCTA1* were grown over-night, dilute to an OD = 0.1, grown to exponential phase (OD = 1) and shifted to medium containing 1.5% ethanol/0.5% glucose for 4 hours. Crude cell extracts were prepared and then assayed for catalase activity. (B) *C. glabrata* wild type and *cta1*Δ cells bearing plasmids with *CgCTA1* including various truncated promoter versions were incubated in YP plus 1.5% ethanol/0.5% glucose for five hours. Crude cell extracts were used for catalase activity measurements.

Figure 6. CgSkn7 and CgYap1 are interdependent for an binding to oxidative stress promoters. *C. glabrata skn7*Δ and *skn7*Δ*yap1*Δ mutant strains transformed with p*CgSKN7-HA* or p*HA-CgYAP1* were grown to early log phase (OD ~ 0.4) and treated with 0.4mM H_2O_2 for times indicated, followed by crosslinking with 1% Formaldehyde for 10 minutes. Cell extracts were sonicated to reach a fragment resolution of ~800bp.

For immunoprecipitation, an Anti-HA monoclonal antibody (12CA5) was used. Precipitated DNA was analyzed by Quantitative Real Time PCR.

Figure 7. *C. glabrata skn7*Δ*yap1*Δ double mutant display a similar survival rate compared to the wild type. (A) *C. glabrata skn7*Δ and *yap1*Δ mutant cells transformed with p*CgADH1-CgSKN7-CFP* or p*CgADH1-GFP-CgYAP1* were grown in synthetic medium (left panels). Cells were stressed by addition of 0.4mM H_2O_2 or 2mM As_2Cl_3 for 10 minutes. CgSkn7-CFP and GFP-CgYap1 visualized by fluorescence microscopy under phagocytosis conditions (right panels). Cells were washed in PBS 0.1% Glucose and added to macrophages in a 4:1 ratio and incubated at 37℃ for 1 hour. Samples were fixed and stained with in Phalloidin Texas-Red. (B) Exponentially growing *C. glabrata skn7*Δ*yap1*Δ double mutant cells complemented with either the empty vector or p*CgYAP1-CgSKN7* were washed with PBS supplemented with 0.1% glucose and added to macrophages in a 2:1 ratio and incubated at 37℃ for 24 hours and 48 hours. The viability of the engulfed cells was assessed by liberating them by hypotonic lysis of the macrophages and quantification of colony formation by plating on rich medium. Assays were done in four independent experiments, three measurements each..

Figure 8. Model for the oxidative stress response regulon mediated by CgSkn7 and CgYap1 in *C. glabrata*. Both reactive oxygen and nitrogen species induce a similar stress regulon. One group of genes gets induced independently of CgSkn7 and CgYap1.Carbon starvation also leads to upregulation of this regulon. In addition, genes belonging to the *SOD* family are increasingly expressed during carbon starvation in *C. glabrata*. *CgSOD1* appeared to be constitutively expressed in a CgSkn7/CgYap1 independent manner in *C. glabrata*.

Supplementary Figures:

Figure S1. Southern blot analysis of *C. glabrata skn7*Δ, *yap1*Δ, and *skn7*Δ*yap1*Δ deletion strains. Both *CgSKN7* and *CgYAP1* were replaced by *ScURA3. CgSKN7* was replaced by *ScHIS3* in the *C. glabrata* double mutant *skn7*Δ*yap1*Δ. Amplified and labelled probes were either binding 5´ or 3´ upstream of ORFs. Chromosomal restriction enzyme locations are indicated. Chromosomal DNA derived from *C. glabrata skn7Δ* digested with *Mfe*I and *C. glabrata yap1*Δ digested with *Bst*XI resulted in longer fragments. Digestion of chromosomal DNA from the *C. glabrata skn7*Δ*yap1*Δ double mutant strain with *Msc*I led to shorter fragments, since *CgSKN7* contains no *Msc*I site.

Figure S2. CgSkn7 and CgYap1 dependent genes share conserved *S. cerevisiae* consensus sites and *S. cerevisiae* Skn7-/Yap1-like sequences. Schematic illustration of 2kb upstream promoter regions of genes with discovered consensus-like sequences. Dark blue bars indicate CgYap1 consensus sites, red bars are CgSkn7 sites. Light blue bars indicate CgYap1-like sites, whereas pink bars mark CgSkn7-like sites, respectively.

References

1. **Alarco, A. M., and M. Raymond**. 1999. The bZip transcription factor Cap1p is involved in multidrug resistance and oxidative stress response in Candida albicans. J Bacteriol **181**:700-708.

2. **Alepuz, P. M., A. Jovanovic, V. Reiser, and G. Ammerer**. 2001. Stress-induced map kinase Hog1 is part of transcription activation complexes. Mol Cell **7**:767-777.

3. **Babior, B. M.** 2000. Phagocytes and oxidative stress. Am J Med **109**:33-44.

4. **Baccarini, M., F. Bistoni, and M. L. Lohmann-Matthes**. 1985. In vitro natural cell-mediated cytotoxicity against Candida albicans: macrophage precursors as effector cells. J Immunol **134**:2658-2665.

5. **Billard, P., H. Dumond, and M. Bolotin-Fukuhara**. 1997. Characterization of an AP-1-like transcription factor that mediates an oxidative stress response in Kluyveromyces lactis. Mol Gen Genet **257**:62-70.

6. **Brombacher, K., B. B. Fischer, K. Rufenacht, and R. I. Eggen**. 2006. The role of Yap1p and Skn7p-mediated oxidative stress response in the defence of Saccharomyces cerevisiae against singlet oxygen. Yeast **23**:741-750.

7. **Brown, A. J., K. Haynes, and J. Quinn**. 2009. Nitrosative and oxidative stress responses in fungal pathogenicity. Curr Opin Microbiol.

8. **Brown, J. L., S. North, and H. Bussey**. 1993. SKN7, a yeast multicopy suppressor of a mutation affecting cell wall beta-glucan assembly, encodes a product with domains homologous to prokaryotic two-component regulators and to heat shock transcription factors. J Bacteriol **175**:6908-6915.

9. **Cernicka, J., Z. Kozovska, M. Hnatova, M. Valachovic, I. Hapala, Z. Riedl, G. Hajos, and J. Subik**. 2007. Chemosensitisation of drug-resistant and drug-sensitive yeast cells to antifungals. Int J Antimicrob Agents **29**:170-178.

10. **Chaves, G. M., S. Bates, D. M. Maccallum, and F. C. Odds**. 2007. Candida albicans GRX2, encoding a putative glutaredoxin, is required for virulence in a murine model. Genet Mol Res **6**:1051-1063.

11. **Chen, C. N., L. Porubleva, G. Shearer, M. Svrakic, L. G. Holden, J. L. Dover, M. Johnston, P. R. Chitnis, and D. H. Kohl**. 2003. Associating protein activities with their genes: rapid identification of a gene encoding a methylglyoxal reductase in the yeast Saccharomyces cerevisiae. Yeast **20**:545-554.

12. **Chen, K. H., T. Miyazaki, H. F. Tsai, and J. E. Bennett**. 2007. The bZip transcription factor Cgap1p is involved in multidrug resistance and required for activation of multidrug transporter gene CgFLR1 in Candida glabrata. Gene **386**:63-72.

13. **Cohen, B. A., Y. Pilpel, R. D. Mitra, and G. M. Church**. 2002. Discrimination between paralogs using microarray analysis: application to the Yap1p and Yap2p transcriptional networks. Mol Biol Cell **13**:1608-1614.

14. **Cox, G. M., T. S. Harrison, H. C. McDade, C. P. Taborda, G. Heinrich, A. Casadevall, and J. R. Perfect**. 2003. Superoxide dismutase influences the virulence of Cryptococcus neoformans by affecting growth within macrophages. Infect Immun **71**:173-180.

15. **Cuellar-Cruz, M., M. Briones-Martin-del-Campo, I. Canas-Villamar, J. Montalvo-Arredondo, L. Riego-Ruiz, I. Castano, and A. De Las Penas**. 2008. High resistance to oxidative stress in the fungal pathogen Candida glabrata is mediated by a single catalase, Cta1p, and is controlled by the transcription factors Yap1p, Skn7p, Msn2p, and Msn4p. Eukaryot Cell **7**:814-825.

16. **de Jesus-Berrios, M., L. Liu, J. C. Nussbaum, G. M. Cox, J. S. Stamler, and J. Heitman**. 2003. Enzymes that counteract nitrosative stress promote fungal virulence. Curr Biol **13**:1963-1968.

17. **Delaunay, A., A. D. Isnard, and M. B. Toledano**. 2000. H2O2 sensing through oxidation of the Yap1 transcription factor. EMBO J **19**:5157-5166.

18. **Delaunay, A., D. Pflieger, M. B. Barrault, J. Vinh, and M. B. Toledano**. 2002. A thiol peroxidase is an H2O2 receptor and redox-transducer in gene activation. Cell **111**:471-481.

19. **Durchschlag, E., W. Reiter, G. Ammerer, and C. Schuller**. 2004. Nuclear localization destabilizes the stress-regulated transcription factor Msn2. J Biol Chem **279**:55425-55432.

20. **Eisen, M. B., P. T. Spellman, P. O. Brown, and D. Botstein**. 1998. Cluster analysis and display of genome-wide expression patterns. Proc Natl Acad Sci U S A **95**:14863-14868.

21. **Enjalbert, B., D. M. MacCallum, F. C. Odds, and A. J. Brown**. 2007. Niche-specific activation of the oxidative stress response by the pathogenic fungus Candida albicans. Infect Immun **75**:2143-2151.

22. **Feldmann, H.** 2000. Genolevures--a novel approach to 'evolutionary genomics'. FEBS Lett **487**:1-2.

23. **Flattery-O'Brien, J., L. P. Collinson, and I. W. Dawes**. 1993. Saccharomyces cerevisiae has an inducible response to menadione which differs from that to hydrogen peroxide. J Gen Microbiol **139**:501-507.

24. **Foster, J. W., and M. P. Spector**. 1995. How Salmonella survive against the odds. Annu Rev Microbiol **49**:145-174.

25. **Frohner, I. E., C. Bourgeois, K. Yatsyk, O. Majer, and K. Kuchler**. 2009. Candida albicans cell surface superoxide dismutases degrade host-derived reactive oxygen species to escape innate immune surveillance. Mol Microbiol **71**:240-252.

26. **Gasch, A. P., P. T. Spellman, C. M. Kao, O. Carmel-Harel, M. B. Eisen, G. Storz, D. Botstein, and P. O. Brown**. 2000. Genomic expression programs in the response of yeast cells to environmental changes. Mol Biol Cell **11**:4241-4257.

27. **Godon, C., G. Lagniel, J. Lee, J. M. Buhler, S. Kieffer, M. Perrot, H. Boucherie, M. B. Toledano, and J. Labarre**. 1998. The H2O2 stimulon in Saccharomyces cerevisiae. J Biol Chem **273**:22480-22489.

28. **Görner, W., E. Durchschlag, M. T. Martinez-Pastor, F. Estruch, G. Ammerer, B. Hamilton, H. Ruis, and C. Schüller**. 1998. Nuclear localization of the C2H2 zinc finger protein Msn2p is regulated by stress and protein kinase A activity. Genes Dev **12**:586-597.

29. **Gregori, C., C. Schuller, A. Roetzer, T. Schwarzmuller, G. Ammerer, and K. Kuchler**. 2007. The high-osmolarity glycerol response pathway in the human fungal pathogen Candida glabrata strain ATCC 2001 lacks a signaling branch that operates in baker's yeast. Eukaryot Cell **6**:1635-1645.

30. **Harbison, C. T., D. B. Gordon, T. I. Lee, N. J. Rinaldi, K. D. Macisaac, T. W. Danford, N. M. Hannett, J. B. Tagne, D. B. Reynolds, J. Yoo, E. G. Jennings, J.**

Zeitlinger, D. K. Pokholok, M. Kellis, P. A. Rolfe, K. T. Takusagawa, E. S. Lander, D. K. Gifford, E. Fraenkel, and R. A. Young. 2004. Transcriptional regulatory code of a eukaryotic genome. Nature **431**:99-104.

31. **He, X. J., and J. S. Fassler**. 2005. Identification of novel Yap1p and Skn7p binding sites involved in the oxidative stress response of Saccharomyces cerevisiae. Mol Microbiol **58**:1454-1467.

32. **He, X. J., K. E. Mulford, and J. S. Fassler**. 2009. Oxidative Stress Function of the S. Cerevisiae Skn7 Receiver Domain. Eukaryot Cell.

33. **Inoue, Y., T. Matsuda, K. Sugiyama, S. Izawa, and A. Kimura**. 1999. Genetic analysis of glutathione peroxidase in oxidative stress response of Saccharomyces cerevisiae. J Biol Chem **274**:27002-27009.

34. **Izumitsu, K., A. Yoshimi, and C. Tanaka**. 2007. Two-component response regulators Ssk1p and Skn7p additively regulate high-osmolarity adaptation and fungicide sensitivity in Cochliobolus heterostrophus. Eukaryot Cell **6**:171-181.

35. **Jamieson, D. J.** 1992. Saccharomyces cerevisiae has distinct adaptive responses to both hydrogen peroxide and menadione. J Bacteriol **174**:6678-6681.

36. **Jin, C., A. M. Myers, and A. Tzagoloff**. 1997. Cloning and characterization of MRP10, a yeast gene coding for a mitochondrial ribosomal protein. Curr Genet **31**:228-234.

37. **Juhnke, H., B. Krems, P. Kotter, and K. D. Entian**. 1996. Mutants that show increased sensitivity to hydrogen peroxide reveal an important role for the pentose phosphate pathway in protection of yeast against oxidative stress. Mol Gen Genet **252**:456-464.

38. **Kaur, R., R. Domergue, M. L. Zupancic, and B. P. Cormack**. 2005. A yeast by any other name: Candida glabrata and its interaction with the host. Curr Opin Microbiol **8**:378-384.

39. **Kaur, R., B. Ma, and B. P. Cormack**. 2007. A family of glycosylphosphatidylinositol-linked aspartyl proteases is required for virulence of Candida glabrata. Proc Natl Acad Sci U S A **104**:7628-7633.

40. **King, D. A., D. M. Hannum, J. S. Qi, and J. K. Hurst**. 2004. HOCl-mediated cell death and metabolic dysfunction in the yeast Saccharomyces cerevisiae. Arch Biochem Biophys **423**:170-181.

41. **Kitada, K., E. Yamaguchi, and M. Arisawa**. 1996. Isolation of a *Candida glabrata* centromere and its use in construction of plasmid vectors. Gene **175**:105-108.

42. **Kuge, S., N. Jones, and A. Nomoto**. 1997. Regulation of yAP-1 nuclear localization in response to oxidative stress. EMBO J **16**:1710-1720.

43. **Kuras, L., and K. Struhl**. 1999. Binding of TBP to promoters in vivo is stimulated by activators and requires Pol II holoenzyme. Nature **399**:609-613.

44. **Kusch, H., S. Engelmann, R. Bode, D. Albrecht, J. Morschhauser, and M. Hecker**. 2008. A proteomic view of Candida albicans yeast cell metabolism in exponential and stationary growth phases. Int J Med Microbiol **298**:291-318.

45. **Lamarre, C., O. Ibrahim-Granet, C. Du, R. Calderone, and J. P. Latge**. 2007. Characterization of the SKN7 ortholog of Aspergillus fumigatus. Fungal Genet Biol **44**:682-690.

46. **Larroy, C., M. R. Fernandez, E. Gonzalez, X. Pares, and J. A. Biosca**. 2002. Characterization of the Saccharomyces cerevisiae YMR318C (ADH6) gene product as

a broad specificity NADPH-dependent alcohol dehydrogenase: relevance in aldehyde reduction. Biochem J **361**:163-172.

47. **Leberer, E., D. Harcus, D. Dignard, L. Johnson, S. Ushinsky, D. Y. Thomas, and K. Schroppel**. 2001. Ras links cellular morphogenesis to virulence by regulation of the MAP kinase and cAMP signalling pathways in the pathogenic fungus Candida albicans. Mol Microbiol **42**:673-687.

48. **Lee, J., C. Godon, G. Lagniel, D. Spector, J. Garin, J. Labarre, and M. B. Toledano**. 1999. Yap1 and Skn7 control two specialized oxidative stress response regulons in yeast. J Biol Chem **274**:16040-16046.

49. **Lelandais, G., V. Tanty, C. Geneix, C. Etchebest, C. Jacq, and F. Devaux**. 2008. Genome adaptation to chemical stress: clues from comparative transcriptomics in Saccharomyces cerevisiae and Candida glabrata. Genome Biol **9**:R164.

50. **Leonhardt, S. A., K. Fearson, P. N. Danese, and T. L. Mason**. 1993. HSP78 encodes a yeast mitochondrial heat shock protein in the Clp family of ATP-dependent proteases. Mol Cell Biol **13**:6304-6313.

51. **Lessing, F., O. Kniemeyer, I. Wozniok, J. Loeffler, O. Kurzai, A. Haertl, and A. A. Brakhage**. 2007. The Aspergillus fumigatus transcriptional regulator AfYap1 represents the major regulator for defense against reactive oxygen intermediates but is dispensable for pathogenicity in an intranasal mouse infection model. Eukaryot Cell **6**:2290-2302.

52. **Li, L., S. Redding, and A. Dongari-Bagtzoglou**. 2007. *Candida glabrata*: an emerging oral opportunistic pathogen. J Dent Res **86**:204-215.

53. **Li, S., S. Dean, Z. Li, J. Horecka, R. J. Deschenes, and J. S. Fassler**. 2002. The eukaryotic two-component histidine kinase Sln1p regulates OCH1 via the transcription factor, Skn7p. Mol Biol Cell **13**:412-424.

54. **Lorenz, M. C., J. A. Bender, and G. R. Fink**. 2004. Transcriptional response of Candida albicans upon internalization by macrophages. Eukaryot Cell **3**:1076-1087.

55. **Mansour, M. K., and S. M. Levitz**. 2002. Interactions of fungi with phagocytes. Curr Opin Microbiol **5**:359-365.

56. **McGraw, P., and S. A. Henry**. 1989. Mutations in the Saccharomyces cerevisiae opi3 gene: effects on phospholipid methylation, growth and cross-pathway regulation of inositol synthesis. Genetics **122**:317-330.

57. **Miller, R. A., and B. E. Britigan**. 1997. Role of oxidants in microbial pathophysiology. Clin Microbiol Rev **10**:1-18.

58. **Missall, T. A., and J. K. Lodge**. 2005. Function of the thioredoxin proteins in Cryptococcus neoformans during stress or virulence and regulation by putative transcriptional modulators. Mol Microbiol **57**:847-858.

59. **Molina, L., and R. Kahmann**. 2007. An Ustilago maydis gene involved in H2O2 detoxification is required for virulence. Plant Cell **19**:2293-2309.

60. **Morgan, B. A., G. R. Banks, W. M. Toone, D. Raitt, S. Kuge, and L. H. Johnston**. 1997. The Skn7 response regulator controls gene expression in the oxidative stress response of the budding yeast Saccharomyces cerevisiae. EMBO J **16**:1035-1044.

61. **Nakagawa, Y., T. Kanbe, and I. Mizuguchi**. 2003. Disruption of the human pathogenic yeast Candida albicans catalase gene decreases survival in mouse-model infection and elevates susceptibility to higher temperature and to detergents. Microbiol Immunol **47**:395-403.

62. **Nguyen, D. T., A. M. Alarco, and M. Raymond**. 2001. Multiple Yap1p-binding sites mediate induction of the yeast major facilitator FLR1 gene in response to drugs, oxidants, and alkylating agents. J Biol Chem **276**:1138-1145.

63. **Niino, Y. S., S. Chakraborty, B. J. Brown, and V. Massey**. 1995. A new old yellow enzyme of Saccharomyces cerevisiae. J Biol Chem **270**:1983-1991.

64. **Noble, S. M., and A. D. Johnson**. 2005. Strains and strategies for large-scale gene deletion studies of the diploid human fungal pathogen Candida albicans. Eukaryot Cell **4**:298-309.

65. **Nogae, I., and M. Johnston**. 1990. Isolation and characterization of the ZWF1 gene of Saccharomyces cerevisiae, encoding glucose-6-phosphate dehydrogenase. Gene **96**:161-169.

66. **Pfaller, M. A., and D. J. Diekema**. 2007. Epidemiology of invasive candidiasis: a persistent public health problem. Clin Microbiol Rev **20**:133-163.

67. **Presterl, E., F. Daxbock, W. Graninger, and B. Willinger**. 2007. Changing pattern of candidaemia 2001-2006 and use of antifungal therapy at the University Hospital of Vienna, Austria. Clin Microbiol Infect **13**:1072-1076.

68. **Qiao, J., D. P. Kontoyiannis, R. Calderone, D. Li, Y. Ma, Z. Wan, R. Li, and W. Liu**. 2008. Afyap1, encoding a bZip transcriptional factor of Aspergillus fumigatus, contributes to oxidative stress response but is not essential to the virulence of this pathogen in mice immunosuppressed by cyclophosphamide and triamcinolone. Med Mycol **46**:773-782.

69. **Raitt, D. C., A. L. Johnson, A. M. Erkine, K. Makino, B. Morgan, D. S. Gross, and L. H. Johnston**. 2000. The Skn7 response regulator of Saccharomyces cerevisiae interacts with Hsf1 in vivo and is required for the induction of heat shock genes by oxidative stress. Mol Biol Cell **11**:2335-2347.

70. **Roetzer, A., C. Gregori, A. M. Jennings, J. Quintin, D. Ferrandon, G. Butler, K. Kuchler, G. Ammerer, and C. Schuller**. 2008. Candida glabrata environmental stress response involves Saccharomyces cerevisiae Msn2/4 orthologous transcription factors. Mol Microbiol **69**:603-620.

71. **Rospert, S., B. S. Glick, P. Jeno, G. Schatz, M. J. Todd, G. H. Lorimer, and P. V. Viitanen**. 1993. Identification and functional analysis of chaperonin 10, the groES homolog from yeast mitochondria. Proc Natl Acad Sci U S A **90**:10967-10971.

72. **Ruprich-Robert, G., F. Chapeland-Leclerc, S. Boisnard, M. Florent, G. Bories, and N. Papon**. 2008. Contributions of the response regulators Ssk1p and Skn7p in the pseudohyphal development, stress adaptation, and drug sensitivity of the opportunistic yeast Candida lusitaniae. Eukaryot Cell **7**:1071-1074.

73. **Sandven, P., L. Bevanger, A. Digranes, H. H. Haukland, T. Mannsaker, and P. Gaustad**. 2006. Candidemia in Norway (1991 to 2003): results from a nationwide study. J Clin Microbiol **44**:1977-1981.

74. **Schneider, R., M. Massow, T. Lisowsky, and H. Weiss**. 1995. Different respiratory-defective phenotypes of Neurospora crassa and Saccharomyces cerevisiae after inactivation of the gene encoding the mitochondrial acyl carrier protein. Curr Genet **29**:10-17.

75. **Segal, A. W.** 2005. How neutrophils kill microbes. Annu Rev Immunol **23**:197-223.

76. **Sikorski, R. S., and P. Hieter**. 1989. A system of shuttle vectors and yeast host strains designed for efficient manipulation of DNA in Saccharomyces cerevisiae. Genetics **122**:19-27.

77. **Singh, P., N. Chauhan, A. Ghosh, F. Dixon, and R. Calderone**. 2004. SKN7 of Candida albicans: mutant construction and phenotype analysis. Infect Immun **72**:2390-2394.

78. **Skoneczna, A., A. Micialkiewicz, and M. Skoneczny**. 2007. Saccharomyces cerevisiae Hsp31p, a stress response protein conferring protection against reactive oxygen species. Free Radic Biol Med **42**:1409-1420.

79. **Sugiyama, K., S. Izawa, and Y. Inoue**. 2000. The Yap1p-dependent induction of glutathione synthesis in heat shock response of Saccharomyces cerevisiae. J Biol Chem **275**:15535-15540.

80. **Szybalski, W., and V. Bryson**. 1952. Genetic studies on microbial cross resistance to toxic agents. I. Cross resistance of Escherichia coli to fifteen antibiotics. J Bacteriol **64**:489-499.

81. **Temple, M. D., G. G. Perrone, and I. W. Dawes**. 2005. Complex cellular responses to reactive oxygen species. Trends Cell Biol **15**:319-326.

82. **Trujillo, M., G. Ferrer-Sueta, and R. Radi**. 2008. Peroxynitrite detoxification and its biologic implications. Antioxid Redox Signal **10**:1607-1620.

83. **Tsuzi, D., K. Maeta, Y. Takatsume, S. Izawa, and Y. Inoue**. 2004. Distinct regulatory mechanism of yeast GPX2 encoding phospholipid hydroperoxide glutathione peroxidase by oxidative stress and a calcineurin/Crz1-mediated Ca2+ signaling pathway. FEBS Lett **569**:301-306.

84. **Tsuzi, D., K. Maeta, Y. Takatsume, S. Izawa, and Y. Inoue**. 2004. Regulation of the yeast phospholipid hydroperoxide glutathione peroxidase GPX2 by oxidative stress is mediated by Yap1 and Skn7. FEBS Lett **565**:148-154.

85. **Vilela, C., B. Linz, C. Rodrigues-Pousada, and J. E. McCarthy**. 1998. The yeast transcription factor genes YAP1 and YAP2 are subject to differential control at the levels of both translation and mRNA stability. Nucleic Acids Res **26**:1150-1159.

86. **Wang, Y., Y. Y. Cao, X. M. Jia, Y. B. Cao, P. H. Gao, X. P. Fu, K. Ying, W. S. Chen, and Y. Y. Jiang**. 2006. Cap1p is involved in multiple pathways of oxidative stress response in Candida albicans. Free Radic Biol Med **40**:1201-1209.

87. **Watson, S. P., M. O. Clements, and S. J. Foster**. 1998. Characterization of the starvation-survival response of Staphylococcus aureus. J Bacteriol **180**:1750-1758.

88. **Wellington, M., K. Dolan, and D. J. Krysan**. 2009. Live Candida albicans suppresses production of reactive oxygen species in phagocytes. Infect Immun **77**:405-413.

89. **Wemmie, J. A., M. S. Szczypka, D. J. Thiele, and W. S. Moye-Rowley**. 1994. Cadmium tolerance mediated by the yeast AP-1 protein requires the presence of an ATP-binding cassette transporter-encoding gene, YCF1. J Biol Chem **269**:32592-32597.

90. **Wendler, F., H. Bergler, K. Prutej, H. Jungwirth, G. Zisser, K. Kuchler, and G. Hogenauer**. 1997. Diazaborine resistance in the yeast Saccharomyces cerevisiae reveals a link between YAP1 and the pleiotropic drug resistance genes PDR1 and PDR3. J Biol Chem **272**:27091-27098.

91. **Wormley, F. L., Jr., G. Heinrich, J. L. Miller, J. R. Perfect, and G. M. Cox**. 2005. Identification and characterization of an SKN7 homologue in Cryptococcus neoformans. Infect Immun **73**:5022-5030.

92. **Wysocki, R., P. K. Fortier, E. Maciaszczyk, M. Thorsen, A. Leduc, A. Odhagen, G. Owsianik, S. Ulaszewski, D. Ramotar, and M. J. Tamas**. 2004.

Transcriptional activation of metalloid tolerance genes in Saccharomyces cerevisiae requires the AP-1-like proteins Yap1p and Yap8p. Mol Biol Cell **15**:2049-2060.

Figure 1

A

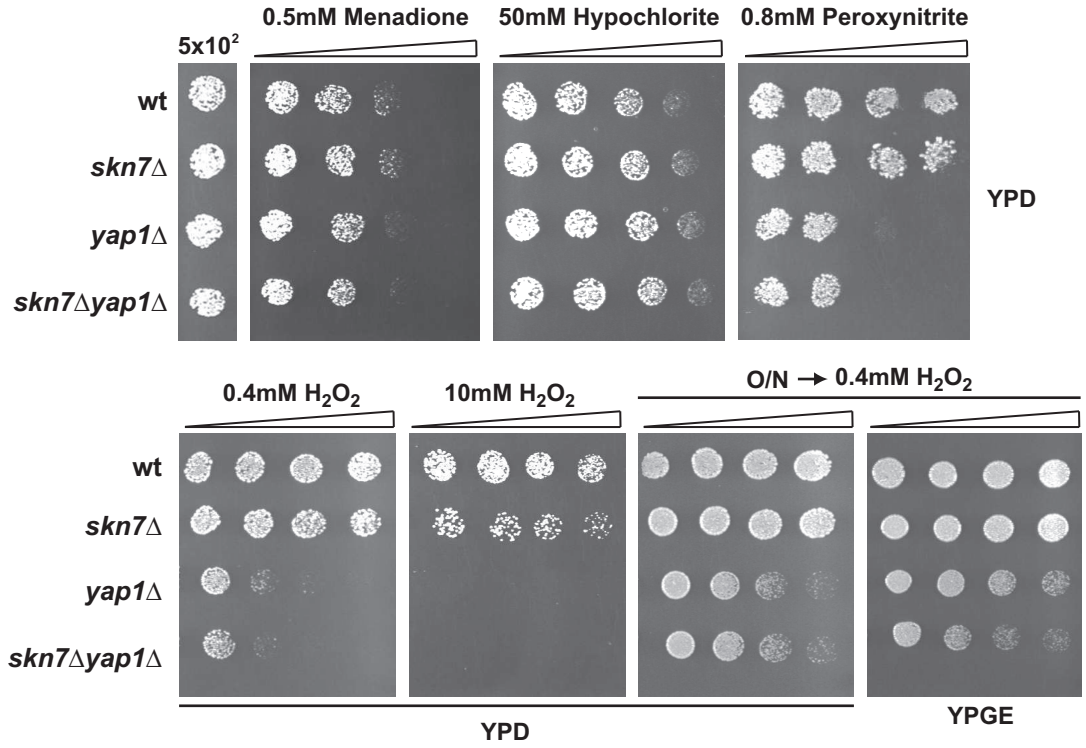
0.5mM Menadione
50mM Hypochlorite
0.8mM Peroxynitrite
5x10²
wt
skn7Δ
yap1Δ
skn7Δyap1Δ
YPD
0.4mM H2O2
10mM H2O2
O/N → 0.4mM H2O2
wt
skn7Δ
yap1Δ
skn7Δyap1Δ
YPD
YPGE

B

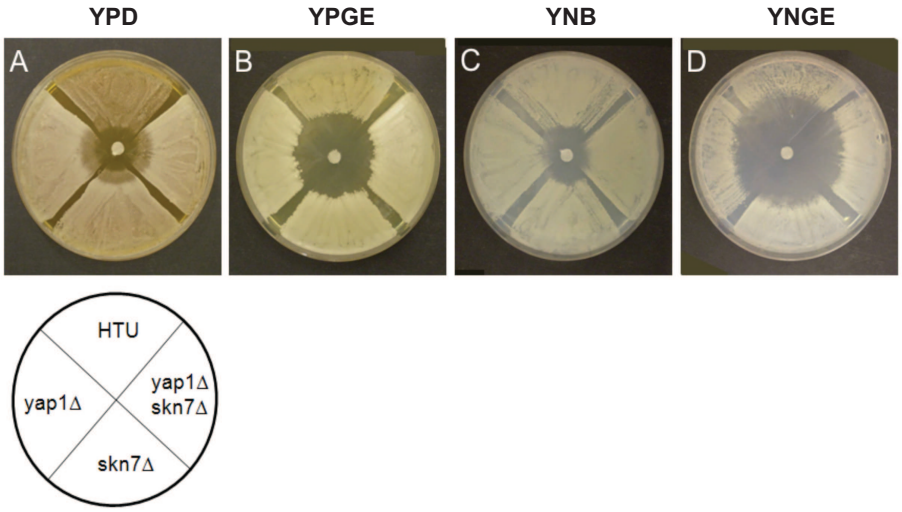
YPD
YPGE
YNB
YNGE
A
B
C
D
HTU
yap1Δ
yap1Δ skn7Δ
skn7Δ

Figure 2

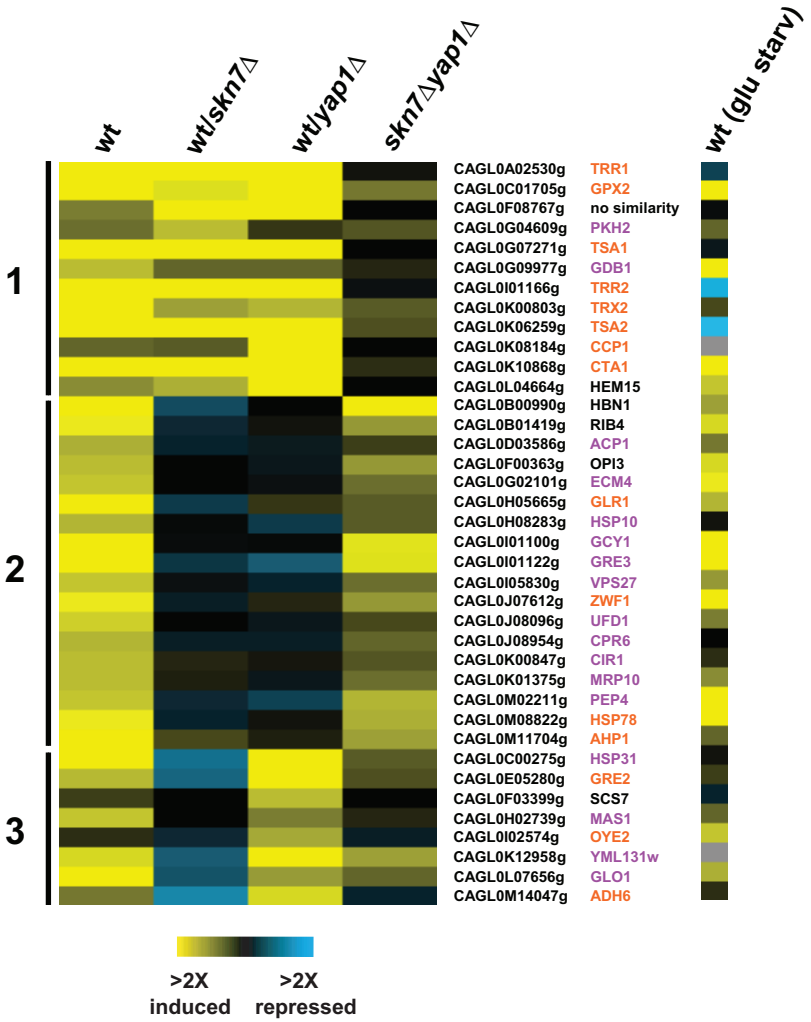
wt
wt/skn7Δ
wt/yap1Δ
skn7Δyap1Δ
wt (glu starv)
1
2
3
CAGL0A02530g TRR1
CAGL0C01705g GPX2
CAGL0F08767g no similarity
CAGL0G04609g PKH2
CAGL0G07271g TSA1
CAGL0G09977g GDB1
CAGL0I01166g TRR2
CAGL0K00803g TRX2
CAGL0K06259g TSA2
CAGL0K08184g CCP1
CAGL0K10868g CTA1
CAGL0L04664g HEM15
CAGL0B00990g HBN1
CAGL0B01419g RIB4
CAGL0D03586g ACP1
CAGL0F00363g OPI3
CAGL0G02101g ECM4
CAGL0H05665g GLR1
CAGL0H08283g HSP10
CAGL0I01100g GCY1
CAGL0I01122g GRE3
CAGL0I05830g VPS27
CAGL0J07612g ZWF1
CAGL0J08096g UFD1
CAGL0J08954g CPR6
CAGL0K00847g CIR1
CAGL0K01375g MRP10
CAGL0M02211g PEP4
CAGL0M08822g HSP78
CAGL0M11704g AHP1
CAGL0C00275g HSP31
CAGL0E05280g GRE2
CAGL0F03399g SCS7
CAGL0H02739g MAS1
CAGL0I02574g OYE2
CAGL0K12958g YML131w
CAGL0L07656g GLO1
CAGL0M14047g ADH6
>2X induced
>2X repressed

Figure 3

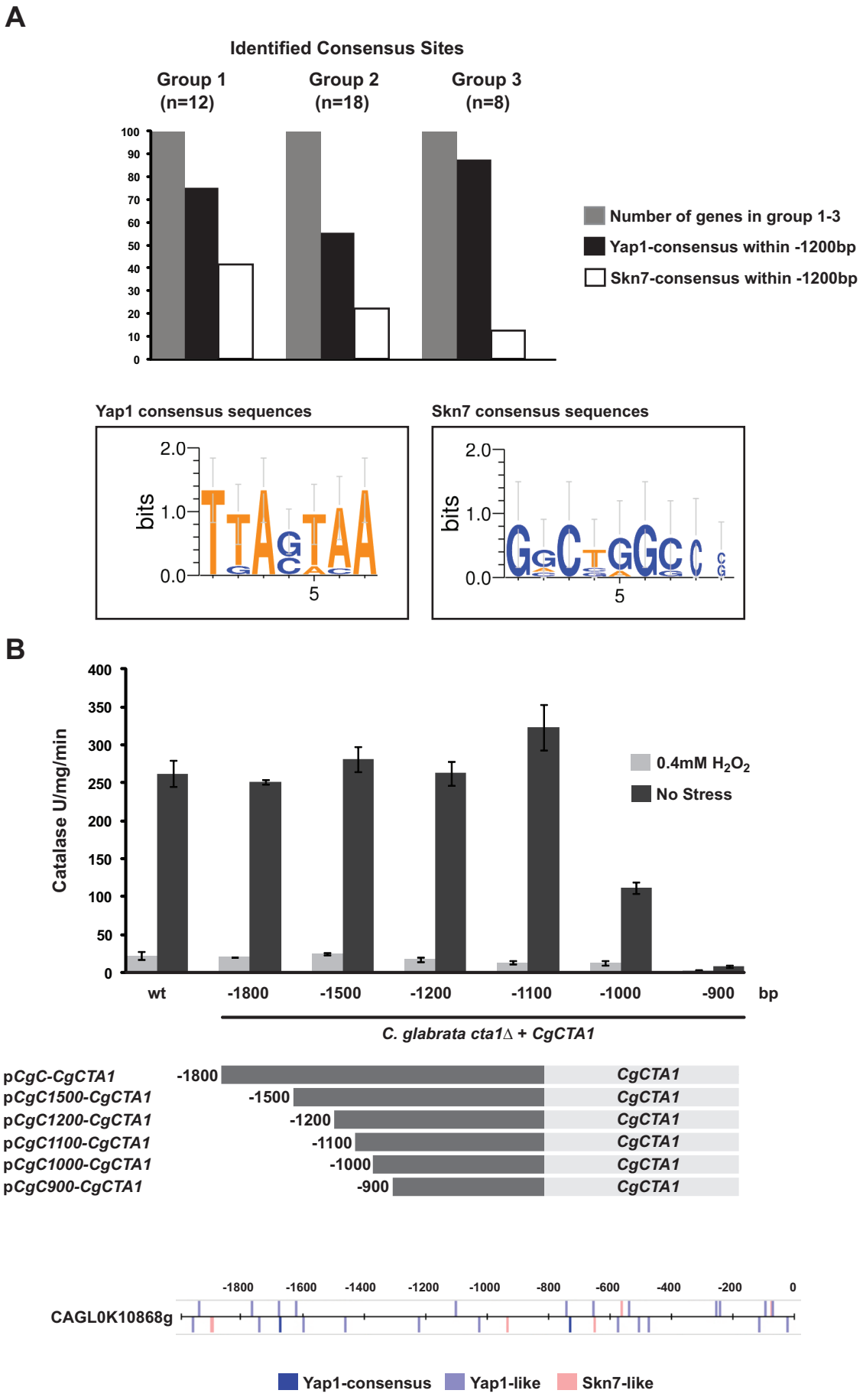
A
Identified Consensus Sites
Group 1 (n=12)
Group 2 (n=18)
Group 3 (n=8)
Number of genes in group 1-3
Yap1-consensus within -1200bp
Skn7-consensus within -1200bp
Yap1 consensus sequences
Skn7 consensus sequences
bits
B
Catalase U/mg/min
0.4mM H2O2
No Stress
wt
-1800
-1500
-1200
-1100
-1000
-900
bp
C. glabrata cta1Δ + CgCTA1
pCgC-CgCTA1
pCgC1500-CgCTA1
pCgC1200-CgCTA1
pCgC1100-CgCTA1
pCgC1000-CgCTA1
pCgC900-CgCTA1
CgCTA1
CAGL0K10868g
Yap1-consensus
Yap1-like
Skn7-like

Figure 4

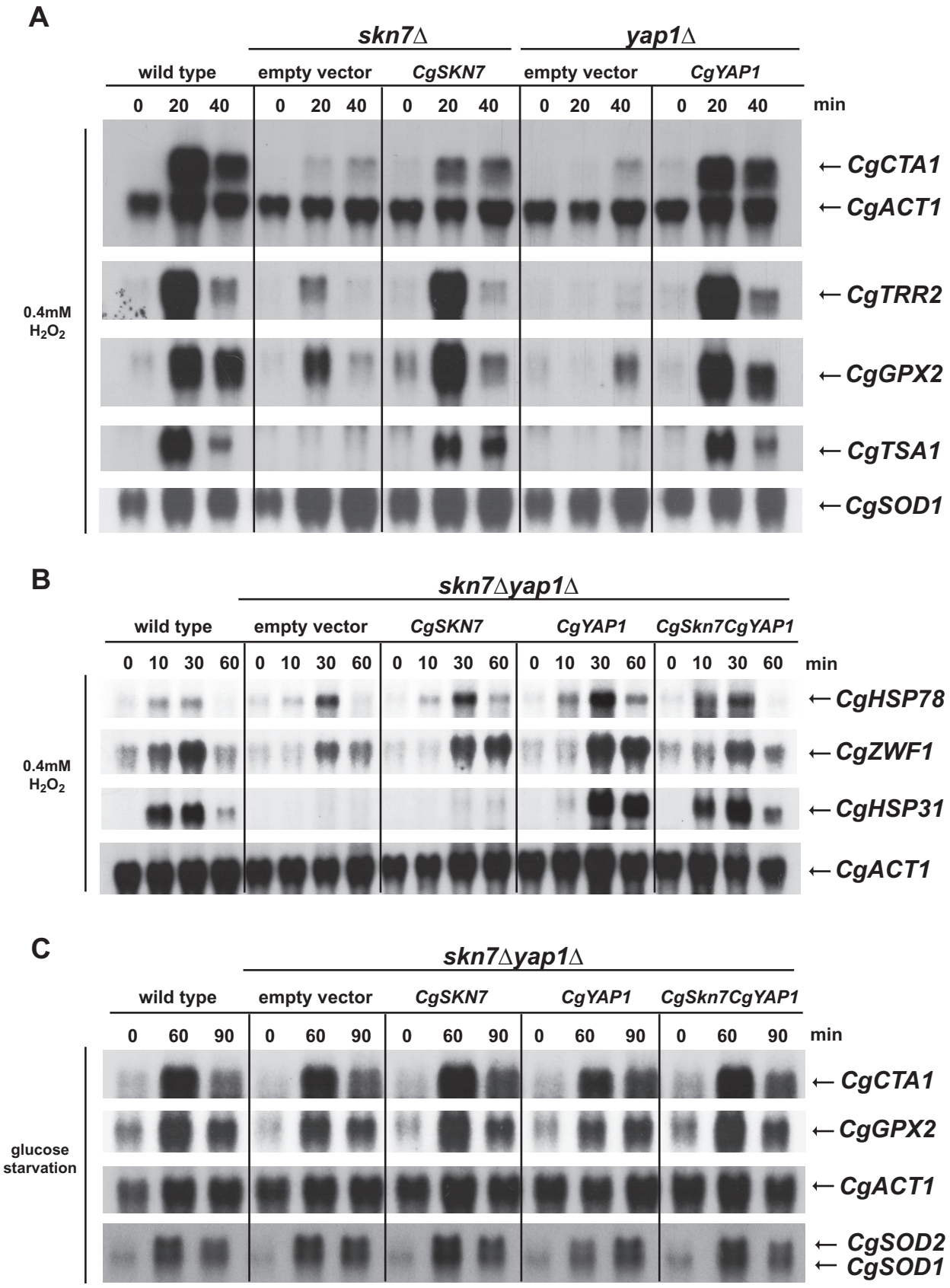
A
skn7Δ
yap1Δ
wild type
empty vector
CgSKN7
empty vector
CgYAP1
0 20 40 0 20 40 0 20 40 0 20 40
min
0.4mM H2O2
← CgCTA1
← CgACT1
← CgTRR2
← CgGPX2
← CgTSA1
← CgSOD1
B
skn7Δyap1Δ
wild type
empty vector
CgSKN7
CgYAP1
CgSkn7CgYAP1
0 10 30 60 0 10 30 60 0 10 30 60 0 10 30 60 0 10 30 60
min
0.4mM H2O2
← CgHSP78
← CgZWF1
← CgHSP31
← CgACT1
C
skn7Δyap1Δ
wild type
empty vector
CgSKN7
CgYAP1
CgSkn7CgYAP1
0 60 90 0 60 90 0 60 90 0 60 90 0 60 90
min
glucose starvation
← CgCTA1
← CgGPX2
← CgACT1
← CgSOD2
← CgSOD1

Figure 5

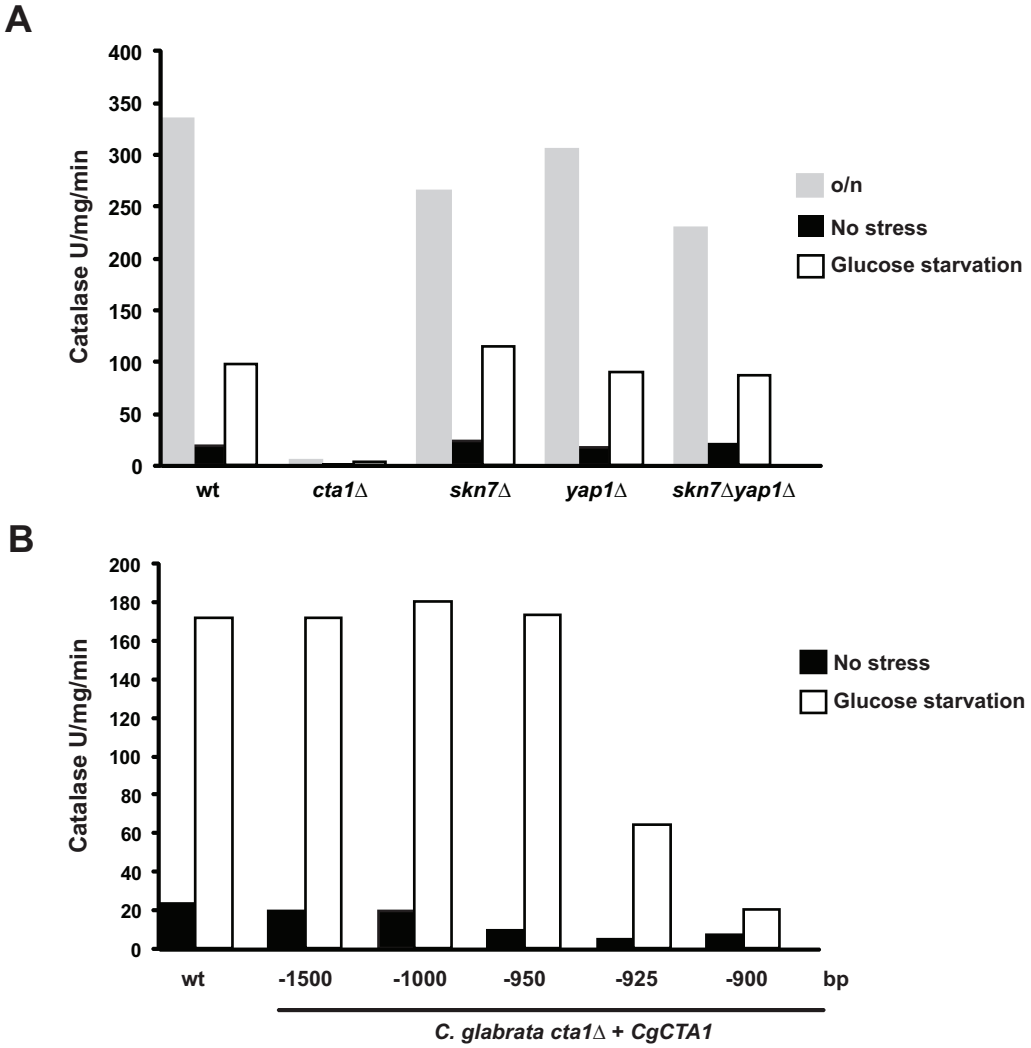
A
Catalase U/mg/min
400
350
300
250
200
150
100
50
0
o/n
No stress
Glucose starvation
wt
cta1Δ
skn7Δ
yap1Δ
skn7Δyap1Δ
B
Catalase U/mg/min
200
180
160
140
120
100
80
60
40
20
0
No stress
Glucose starvation
wt
-1500
-1000
-950
-925
-900
bp
C. glabrata cta1Δ + CgCTA1
pCgC1500-CgCTA1
-1500
CgCTA1
pCgC1200-CgCTA1
-1200
CgCTA1
pCgC1100-CgCTA1
-1100
CgCTA1
pCgC1000-CgCTA1
-1000
CgCTA1
pCgC950-CgCTA1
-950
CgCTA1
pCgC925-CgCTA1
-925
CgCTA1
pCgC900-CgCTA1
-900
CgCTA1

Figure 6

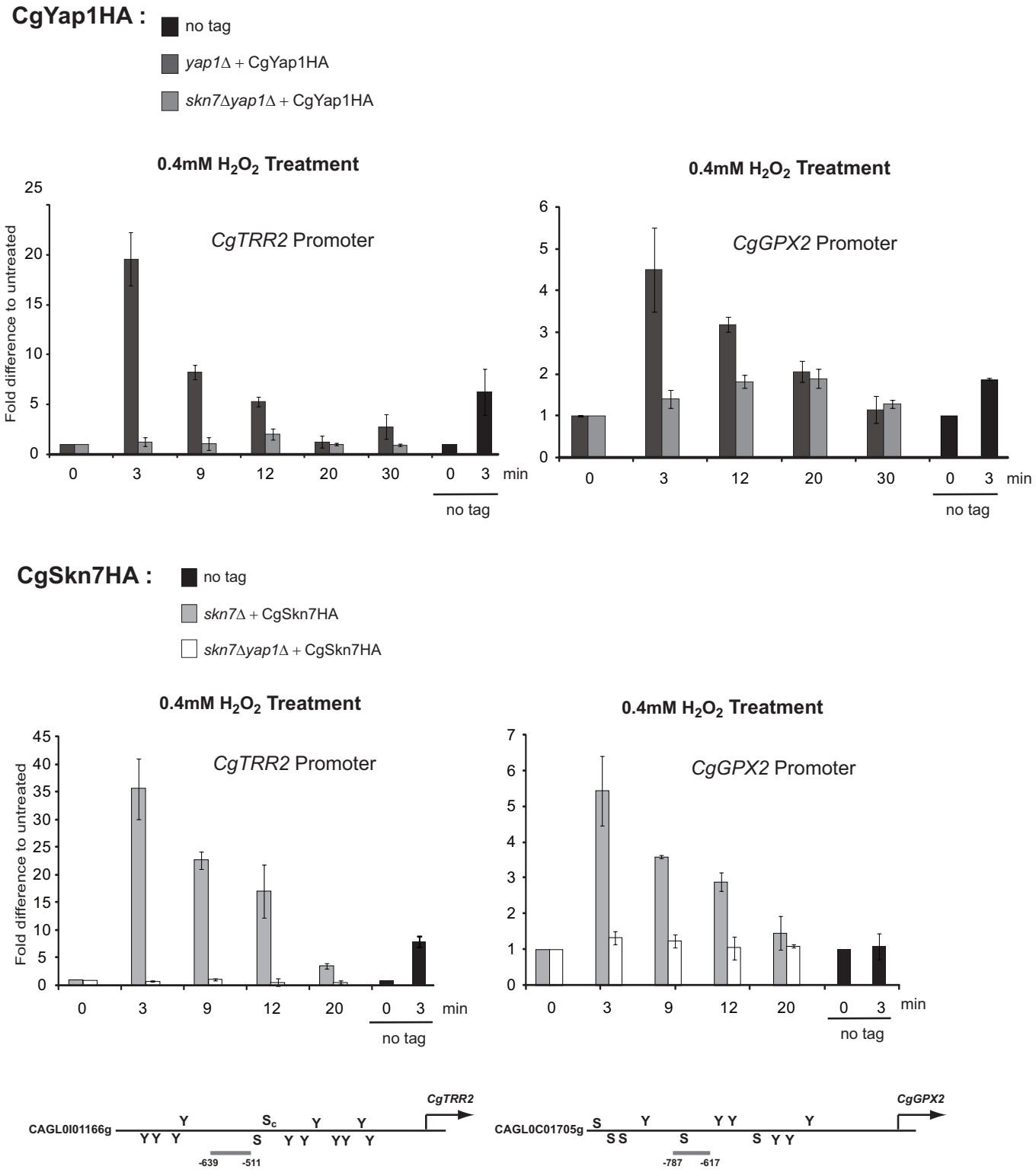
CgYap1HA :
no tag
yap1Δ + CgYap1HA
skn7Δyap1Δ + CgYap1HA
0.4mM H2O2 Treatment
CgTRR2 Promoter
Fold difference to untreated
0 3 9 12 20 30 0 3 min
no tag
0.4mM H2O2 Treatment
CgGPX2 Promoter
0 3 12 20 30 0 3 min
no tag
CgSkn7HA :
no tag
skn7Δ + CgSkn7HA
skn7Δyap1Δ + CgSkn7HA
0.4mM H2O2 Treatment
CgTRR2 Promoter
Fold difference to untreated
0 3 9 12 20 0 3 min
no tag
0.4mM H2O2 Treatment
CgGPX2 Promoter
0 3 9 12 20 0 3 min
no tag
CgTRR2
CAGL0I01166g
-639 -511
CgGPX2
CAGL0C01705g
-787 -617

Figure 7

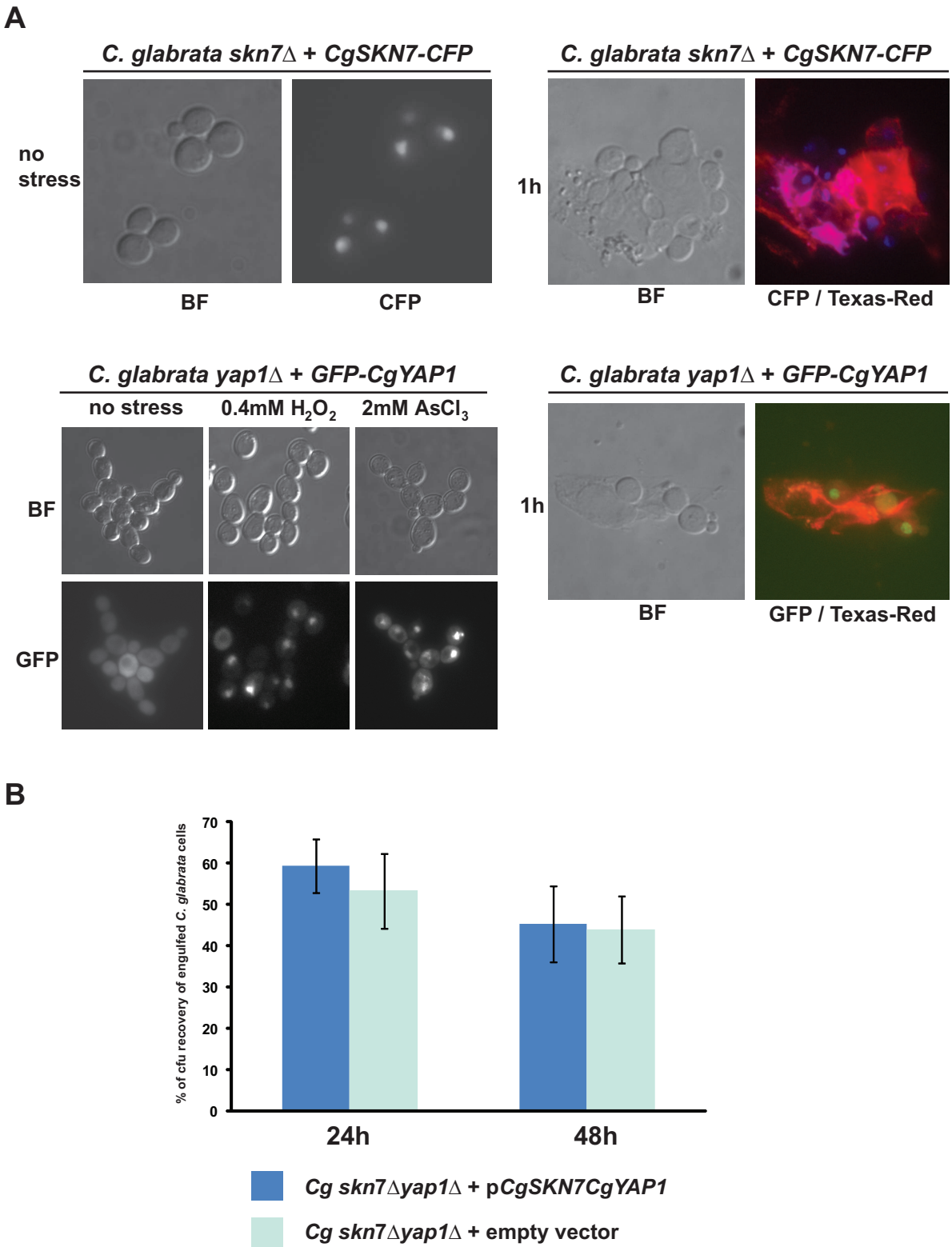
A
C. glabrata skn7Δ + CgSKN7-CFP
C. glabrata skn7Δ + CgSKN7-CFP
no stress
1h
BF
CFP
BF
CFP / Texas-Red
C. glabrata yap1Δ + GFP-CgYAP1
C. glabrata yap1Δ + GFP-CgYAP1
no stress
0.4mM H2O2
2mM AsCl3
BF
GFP
1h
BF
GFP / Texas-Red
B
% of cfu recovery of engulfed C. glabrata cells
70
60
50
40
30
20
10
0
24h
48h
Cg skn7Δyap1Δ + pCgSKN7CgYAP1
Cg skn7Δyap1Δ + empty vector

Figure 8

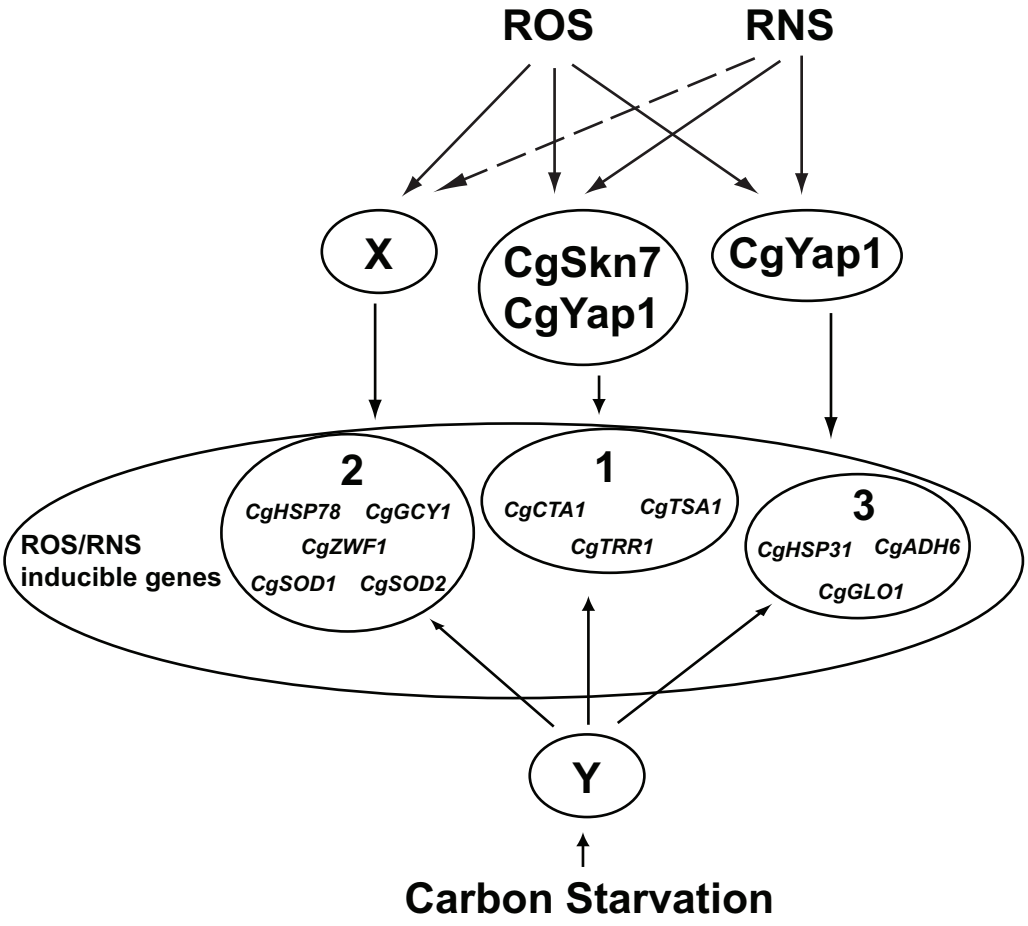
ROS
RNS
X
CgSkn7
CgYap1
CgYap1
2
CgHSP78
CgGCY1
CgZWF1
CgSOD1
CgSOD2
1
CgCTA1
CgTSA1
CgTRR1
3
CgHSP31
CgADH6
CgGLO1
ROS/RNS
inducible genes
Y
Carbon Starvation

Figure S1

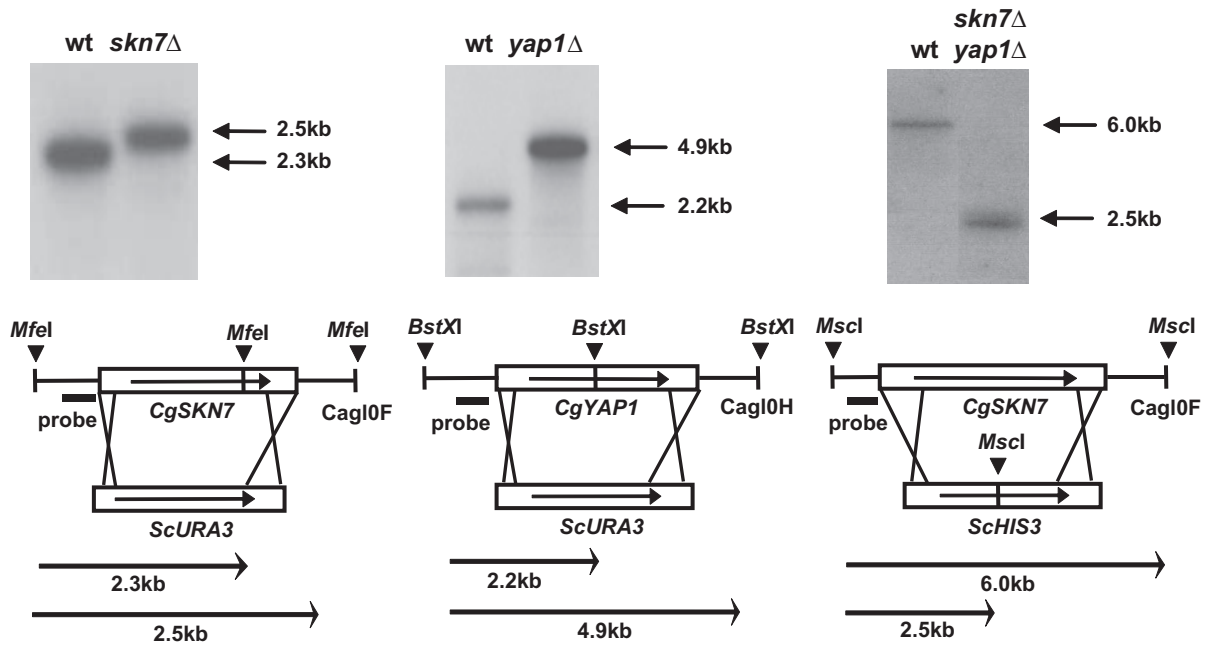
wt skn7Δ
2.5kb
2.3kb
wt yap1Δ
4.9kb
2.2kb
skn7Δ
wt yap1Δ
6.0kb
2.5kb
MfeI
MfeI
MfeI
probe
CgSKN7
CagI0F
ScURA3
2.3kb
2.5kb
BstXI
BstXI
BstXI
probe
CgYAP1
CagI0H
ScURA3
2.2kb
4.9kb
MscI
MscI
probe
CgSKN7
CagI0F
MscI
ScHIS3
6.0kb
2.5kb

Figure S2

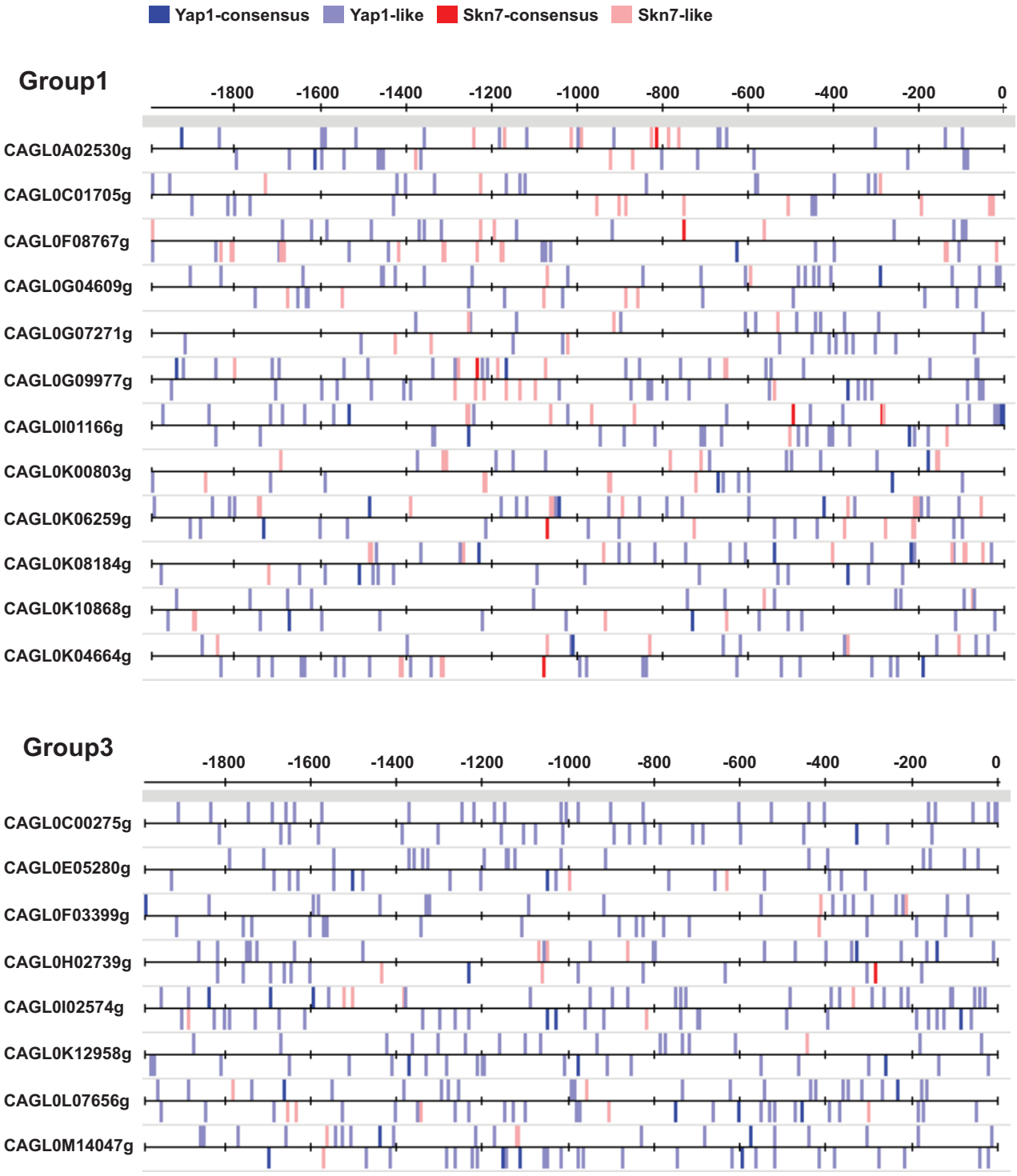
Yap1-consensus
Yap1-like
Skn7-consensus
Skn7-like
Group1
-1800
-1600
-1400
-1200
-1000
-800
-600
-400
-200
0
CAGL0A02530g
CAGL0C01705g
CAGL0F08767g
CAGL0G04609g
CAGL0G07271g
CAGL0G09977g
CAGL0I01166g
CAGL0K00803g
CAGL0K06259g
CAGL0K08184g
CAGL0K10868g
CAGL0K04664g
Group3
-1800
-1600
-1400
-1200
-1000
-800
-600
-400
-200
0
CAGL0C00275g
CAGL0E05280g
CAGL0F03399g
CAGL0H02739g
CAGL0I02574g
CAGL0K12958g
CAGL0L07656g
CAGL0M14047g

Major results obtained:

- The environmental stress response (**ESR**) pattern of *C. glabrata* is orthologous to *S. cerevisiae.*
    - **CgMsn2** and **CgMsn4** were identified as orthologous transcription factors and regulate at least part of the CgESR.
- The oxidative stress response regulon of *C. glabrata* is similar to *S. cerevisiae*, and gets partially induced during starvation conditions.
    - **CgYap1** and **CgSkn7** control the core response to oxidative stress, but are dispensable for prolonged survival in macrophages.
- Phagocytosis of *C. glabrata* cells leads to a switch to alternative carbon catabolism and induces autophagic processes.
    - **CgAtg11**, a protein essential for pexophagy, and **CgAtg17**, which is essential for non-selective autophagy, are crucial for survival of engulfed cells.

3. General Discussion:

Candida glabrata – a *S. cerevisiae*-like pathogen?

The aim of this work was to investigate the stress response of the human fungal pathogen *Candida glabrata*. *C. glabrata* is phylogenetically related to *S. cerevisiae* and displays a high degree of gene synteny but it is adapted to a mammalian host environment. This is reflected by adhesin-mediated adherence to surfaces and the absence of certain biosynthetic pathways and different physiology, for example an optimal growth temperature of 37℃ [1].

In *S. cerevisiae,* the general or environmental stress response (ESR) comprises the up- and downregulation of many genes. In this work I explored the characteristics of related responses in *C. glabrata*. The identified environmental stress response pattern in *C. glabrata* (CgESR) underlined the close relation of *C. glabrata* to *S. cerevisiae*. In addition CgMsn2, the orthologue of the yeast transcription factor Msn2, which gets activated during various stress conditions, plays also an important role in the general stress response of *C. glabrata*. The environmental stress response seems to be highly conserved among the class of *Saccharomycetes*.

Furthermore, I focused especially on the oxidative stress response of *C. glabrata*, since the oxidative burst executed by phagocytic cells is one of the main chemical weapons against engulfed foreign cells. Similar to the environmental stress response, I observed that the oxidative stress response is highly conserved between *S. cerevisiae* and *C. glabrata* including the orthologues of the crucial transcription factors Skn7 and Yap1. Interestingly, many *C. glabrata* oxidative stress-associated genes were also upregulated during glucose starvation. To assess the importance of these stress response factors as virulence determinants, I used an *ex vivo* primary mouse macrophage infection model for *C. glabrata*. To my surprise, CgSkn7 and CgYap1 did not contribute to survival during phagocytosis. Since *C. glabrata* has to counteract the oxidative burst, oxidative stress-associated genes might be upregulated by starvation conditions which *C. glabrata* cells encounter inside of phagocytes.

The third part of this thesis dealt with the situation of fungal cells inside the phagosome. Similar to *S. cerevisiae*, *C. glabrata* is unable to form true hyphae. Pseudohyphae may facilitate the invading of tissues. We could not observe such a morphologic switch to promote the escape in the engulfed situation as do hyphae for *Candida albicans*, another opportunistic human fungal pathogen [2]. Therefore, *C.*

glabrata developed other strategies to survive during engulfment. Here I demonstrated that engulfed cells are forced to break down internal resources in order to prolong their survival upon phagocytosis. One crucial process seems to be autophagy, the engulfment and degradation of large molecules and organelles. I found that factors involved in selective autophagy (CgAtg11) as well as in non-selective autophagic processes (CgAtg17) contribute to sustained survival of *C. glabrata* inside the phagosome.

In the following, I will summarize the discovered characteristics of *C. glabrata* and discuss how these findings make a contribution to our picture how a fungal opportunistic pathogen is adapted to a host environment.

Conserved features of the environmental stress response (ESR) in *C. glabrata* versus *S. cerevisiae.*

At first, I focused on the analysis of the environmental stress response of *C. glabrata*. Proliferation of cells depends on beneficial extracellular conditions. Rapid changes in the external environment always affect the internal milieu. One mechanism *S. cerevisiae* cells use to counteract effects of environmental variation is to initiate a broad gene expression program, referred to as the environmental stress response (ESR). It comprises ~900 genes, whose expression is similarly altered to diverse types of stress [3]. *C. glabrata* as a human commensal and occasional pathogen exists in a radically different environment compared to *S. cerevisiae* [4]. Mammalian mucosal areas entail nutrient shortage, osmotic changes, presence of other microorganisms and protective secretory mechanisms of the host [5-9]. Adaptation to this environment does most likely require adapted stress response patterns compared to those *S. cerevisiae* is exposed to.

Therefore, the genome wide environmental stress response (ESR) expression profile of *Candida glabrata* was determined and subsequently compared to expression profiles of baker´s yeast. In addition, known stress response patterns of the fission yeast *Schizosaccharomyces pombe* and the opportunistic fungal pathogen *Candida albicans* were included in this comparison. Strikingly, global transcript analysis of *C. glabrata* cells exposed to the generic stress types carbon starvation, heat, osmotic and oxidative stress revealed a transcription pattern highly related to *S. cerevisiae* and *S. pombe* [10, 11]. In contrast, a similar analysis of stress responses of *C. albicans* pointed to a different adaptation program [10, 12, 13]. *C. albicans* lacks a general

stress response exhibited by *S. cerevisiae*. For example, in contrast to *S. cerevisiae* and *C. glabrata*, the use of alternative carbon sources like glycogen and trehalose in response to mild stresses was not observed in *C. albicans*. However, the patterns of induced genes during specific stresses in *C. albicans* are similar to the specific stress patterns in *S. cerevisiae* [12]. Beside stress specific transcriptional responses, a niche-specific core transcriptional response to stress has been identified in *C. albicans* [13]. Despite the fact that the fungal pathogens *C. glabrata* and *C. albicans* occupy similar host niches, the overall environmental stress response of *C. glabrata* shares more similarities with the ESR of its non-pathogenic, phylogenetically close relative *S. cerevisiae*.

Since environmental stress response patterns exist, the question arises, how are the main generic stress response pathways regulated? In all organisms, various signaling pathways sense and transmit environmental alterations. Among those, the best characterized are the highly conserved MAP kinase (MAPK) pathways [14-18]. For example, in mammalian cells, two MAPK pathways exist, that respond to stress conditions and result in the activation of the SAPKs/JNKs (Stress-activated protein kinases/Jun N-terminal kinases) and the p38 kinases [18, 19]. Similar stress-activated MAPK pathways have been characterized in fungi [20-22]. In *S. cerevisiae*, one important MAP kinase is Hog1, a key regulator of the osmoregulatory signal transduction cascade, which mediates the upregulation of ~600 genes by phosphorylating several transcription factors [23-25]. The Hog1 pathway also responds to heat, oxidative and specific weak acid stress in *S. cerevisiae* [26-29]. In *S. pombe*, the MAP kinase and fission yeast homologue of Hog1, Sty1 is responsible for transducing signals from various stimuli including oxidative, osmotic and heat stress [30-32]. Further, in *C. albicans*, CaHog1 mediates the core stress response to a variety of environmental conditions [20, 33]. In *C. glabrata*, it has been found that the HOG signaling pathway is highly similar to *S. cerevisiae;* in addition, this pathway mediates the response to a broader spectrum of stress conditions including different weak acids in *C. glabrata* [34].

However, in *S. cerevisiae*, many ScESR genes are not solely dependent on Hog1 but rely on induction by the general stress factors Msn2 and Msn4 [3]. Both transcription factors (Msn2 and Msn4) are activated by a variety of stress conditions and changing nutrients, such as the depletion of the preferred carbon source glucose [35-40]. In fact, Hog1 also regulates Msn2/4 during osmotic stress in *S. cerevisiae* [41]. In contrast, the *C. albicans* Msn2-like proteins (CaMsn4 and Mln1) do not play any role in stress response [42]. We identified putative Msn2/Msn4 orthologues in *C. glabrata*.

Therefore, we wanted to know whether *S. cerevisiae* has developed a unique stress response mechanism involving Msn2 and Msn4, and whether the *C. glabrata* stress response is governed by a *S. cerevisiae* or a *C. albicans*-like mechanism.

How does CgMsn2 contribute to the general stress response (CgESR) in C. glabrata? In *C. glabrata*, transcript profiles of CgMsn2 and CgMsn4 double mutants and CgMsn2 overexpression strains confirmed the important role of CgMsn2 and CgMsn4 as major regulators of a part of the CgESR. Genes functionally connected to stress response, such as *CgHSP12*, *CgHSP42*, *CgDDR48*, *CgGPH1*, *CgGDB1* or *CgPGM2* displayed a CgMsn2/4-associated upregulation. In addition, CgMsn2 is required for full resistance against severe osmotic stress and rapid and full induction of trehalose synthesis genes (*TPS1*, *TPS2*), indicating a strikingly similar situation as in *S. cerevisiae* [43, 44]. Further, similar to baker´s yeast [45], constitutive nuclear localisation of CgMsn2 seems to be detrimental for *C. glabrata*. Resulting constitutive expression of a large set of genes leads to an unbearable waste of energy. In *C. glabrata*, CgMsn2 is beneficial under extreme stress conditions, such as high osmolarity, indicating a condition-specific role in providing future stress protection similar to Msn2 in *S. cerevisiae* [44]. Interestingly, CgMsn2 does not seem to be involved in weak acid stress response in contrast to the situation in *S. cerevisiae* [3, 39, 46], indicating the absence of a CgMsn2-associated weak acid stress pathway, since *C. glabrata* does not display higher resistance to weak acids [34]. Instead CgHog1 seems to be responsible for weak acid driven signal transduction in *C. glabrata* [34]. Taken together, the orthologues CgMsn2/CgMsn4 play a relevant role for induction of the CgESR in *C. glabrata* similar to Msn2/4 in *S. cerevisiae*. From a phylogenetic point of view, both *C. glabrata* and *S. cerevisiae* belong to the same clade among the class of *Saccharomycetes*. Therefore, I explored, whether the stress-specific role of Msn2 and Msn4 is linked to this clade.

Can the stress response-associated role of Msn2 and Msn4 be found throughout the class of Saccharomycetes? The most significant similarity between putative ScMsn2 orthologues apart from the DNA binding domain is a region designated as Msn2 homology domain 1 (HD1), which is embedded within the nuclear export sequence (NES), a domain necessary for a stress-regulated localization [47, 48]. Importantly, this motif (HD1) is not present in the Msn2-like proteins of *C. albicans* or its close relatives, including *Candida parapsilosis* and *Candida tropicalis*. Strikingly, the *C. glabrata* orthologues CgMsn2 and CgMsn4 contain the HD1 motif. Site directed mutagenesis of two conserved serines confirmed that nuclear export of CgMsn2 in *C. glabrata* requires

an intact HD1. Further, I observed that the region including the HD1 motif of Msn2/4 orthologues from *S. cerevisiae*, *C. glabrata* and two other related fungi present in this clade*, Kluyveromyces lactis* and *Ashbya gossypii*, is sufficient for nuclear export. Therefore, the HD1 motif and the stress-mediating role of Msn2 appeared after the separation of *C. albicans* from the lineage leading to *S. cerevisiae.* Accordingly, Msn2 orthologues are likely to be important stress-regulated factors in the pre-whole-genome duplication clade, including *S. cerevisiae*, *C. glabrata*, *K. lactis* and *A. gossypii*.

These results establish a *S. cerevisiae*-like general stress response in *C. glabrata*. Despite the preference for different niches, both *S. cerevisiae* and *C. glabrata* share a conserved environmental stress response. Although slight differences, such as the constant repression of *ERG* genes (involved in sterol biosynthesis), were discovered, the overall signal transducing machinery was closely related to its counterpart in *S. cerevisiae* [34].

Are CgMsn2 and CgMsn4 virulence determinants for C. glabrata? Comparison of expression levels of *C. glabrata* cells during macrophage engulfment revealed no significant overlaps to the CgMsn2-dependent part of the CgESR [49]. One exception was *CgPNC1*, encoding a nicotinamidase that converts nicotinamide to nicotinic acid as part of the NAD salvage pathway [Ghislain, 2002 #313; Lin, 2003 #315]. Accordingly, CgMsn2 seems to have no major impact on virulence. *C. glabrata msn2*Δ*msn4*Δ double mutants displayed no attenuated virulence in a *Drosophila melanogaster* infection model. Further, it has been recently shown, that CgMsn2 and CgMsn4 have only a minor impact on survival during oxidative stress [50]. Their relevance for the opportunistic lifestyle of *C. glabrata* still needs to be elucidated. In conclusion, rapid adaptation to changing environment inside the mammalian host requires rather a pathogen-specific response pattern than the general stress response mechanisms. One specific response, which might be crucial for adaptation inside the host, is the oxidative stress regulon, since phagocytic cells are able to induce an oxidative burst to attack engulfed cells.

Oxidative stress during phagocytosis: a negligible threat for engulfed *C. glabrata* cells?

Oxidative stress is caused by exposure to reactive oxygen species. It is thought that the selective release of ROS is one of the main weapons of phagocytic cells to kill engulfed pathogens, such as *C. glabrata* [51-53]. In the mature phagolysosome, the

NADPH oxidase complex mediates oxidative destruction of engulfed cells [54, 55]. It catalyzes the production of superoxide (O_2^-), serving as initial source for the production of ROS. A large number of reactive oxidants are produced, such as hypochlorous acid (HOCl), which is formed by the myeloperoxidase-catalyzed oxidation of Cl^- by H_2O_2, hydroxyl radicals (OH*), produced by the reduction of H_2O_2 by Fe^{++} or Cu^+, peroxynitrite ($ONOO^-$), formed by the reaction between O_2^- and NO*, and many others [56, 57].

To counteract emerging oxidative stress, a broad variety of enzymes and non-enzymatic substances exists, which are able to prevent the formation of ROS or can efficiently eliminate ROS in the cell. Antioxidant factors are under an elaborated control of expression [58]. In *S. cerevisiae*, the two transcription factors Skn7 and Yap1 control the oxidative stress response regulon: Yap1 controls at least 32 genes of the identified oxidative stress stimulon [Lee, 1999 #96; Inoue, 1999 #122]. 15 of these proteins require both Skn7 and Yap1 for a proper induction. Two distinct Yap1 regulons were defined in *S. cerevisiae*, one covering the oxidative stress response, the second involved in the metabolic pathways regenerating the main cellular reducing power, GSH and NADPH [59]. I tried to reveal the mechanisms of *C. glabrata* cells to overcome emerging oxidative stress in the mammalian host.

How does C. glabrata mediate the oxidative stress response? In *C. glabrata* we found 38 genes to be upregulated more than two-fold during oxidative stress. The oxidative stress response patterns of *C. glabrata skn7*Δ, *yap1*Δ and *skn7*Δ*yap1*Δ mutants were determined and aligned to discover putative dependencies on CgSkn7 and CgYap1. Similar to *S. cerevisiae*, 20 genes were dependent on CgYap1. One set of genes consisting of *CgCTA1*, *CgTRR1/2*, *CgTSA1/2*, *CgTRX2*, *CgGPX2* and *CgCCP1* was dependent on the presence of both, CgSkn7 and CgYap1, and was defined as core oxidative stress response (COR). A second CgYap1-associated group included proteins displaying aldo-keto reductase and oxidoreductase activity (*CgADH6*, *CgGRE2*, *CgSCS7* and *CgOYE2*). In the upstream regions of CgYap1 dependent genes, known *S. cerevisiae* Yap1 consensus sequences were identified [60, 61]. However, corresponding consensus sites were also found in a set of 18 genes, which did not display a decreased upregulation in *skn7*Δ and *yap1*Δ mutants during oxidative stress. In addition, catalase activity measurements of *CgCTA1* expressed by truncated promoter versions pointed to an altered recognition pattern of CgYap1, since the upstream region, which was crucial for full catalase activity, did not comprise *S. cerevisiae* Skn7 and Yap1 consensus sequences. Instead, *S. cerevisiae* Skn7- and Yap1-like sites, bearing one deviation of the known consensus sites, were found throughout the upstream regions of genes involved in oxidative stress response,

including the essential part of the *CgCTA1* promoter. Further analysis of putative *C. glabrata*-specific binding sites will be necessary to confirm my hypothesis about new consensus sites for Skn7 and Yap1 orthologues in *C. glabrata*. Nevertheless, our results suggest an oxidative stress regulon in *C. glabrata* similar to baker´s yeast.

How do CgSkn7 and CgYap1 cooperate to regulate the response to oxidative stress? In *S. cerevisiae*, a direct interaction between Skn7 and Yap1 seems to be necessary for functional induction of oxidative stress response genes [60, 62]. It is thought that Skn7 undergoes a post-translational modification by phosphorylation following exposure to ROS, which seems to be dependent on Yap1 itself [62]. Mutations introduced in the receiver domain of Skn7 were found to compromise the association of Yap1 and Skn7 to upstream regions of oxidative stress-associated genes [60, 63]. Activation of Yap1 during oxidative stress involves a C-terminal cysteine-rich domain, which contains a NES [64, 65]. Yap1 becomes oxidized by the thiol peroxidase Gpx3 which catalyzes the formation of an intramolecular disulfide bond. This causes a conformational change that drives Yap1 accumulation in the nucleus [65, 66]. Cysteine-based redox sensing is highly conserved among all living cells and *e.g.* found in the oxidative stress activation of the bacteria and mammals [67-69]. Therefore, I tried to analyze the interdependence of CgSkn7 and CgYap1 to mediate the oxidative stress response in *C. glabrata*.

To assess the interaction of CgSkn7 and CgYap1 in *C. glabrata*, I tested whether binding of CgSkn7 and CgYap1 to oxidative stress gene promoters in *C. glabrata* is dependent on the presence of the other transcription factor. For this part of my thesis, I cooperated with my colleague Eva Klopf. We chose the upstream regions of *CgTRR2* and *CgGPX2* to investigate the binding properties of CgSkn7 and CgYap1. Northern blot analysis showed that expression of both was significantly decreased in *skn7*Δ mutant cells. Further, *CgGPX2* expression was severely decreased and delayed in *yap1*Δ mutant cells, whereas *CgTRR2* expression was completely stopped. Chromatin immunoprecipitation data showed that a strict interdependence occurs at the level of promoter recognition. In the presence of CgYap1, CgSkn7 was able to bind to both upstream sequences, whereas in the absence of CgYap1, CgSkn7 could not bind to the promoters. Similarly, CgYap1 bound only in the presence of CgSkn7 to the tested upstream regions. Binding occurred immediately upon stress induction (< 3 minutes). Both factors stayed there for the same period of time (*CgTRR2* < 10 minutes, *CgGPX2* > 10 minutes). This kind of interdependence was also observed in *S. cerevisiae*: an electrophoretic mobility shift assay demonstrated *in vitro* the presence of a Skn7-Yap1 complex at promoter DNA fragments of *TSA1* [59]. However, the precise

mechanism by which these two factors co-activate oxidative stress response was not clear yet. Here, we showed the first time that, in *C. glabrata*, CgSkn7 is dependent on CgYap1 and vice versa to bind to the upstream region of certain oxidative stress genes.

Does the loss of CgSkn7 and CgYap1 affect prolonged survival upon phagocytosis? Since CgSkn7 and CgYap1 regulated the core oxidative stress response in *C. glabrata*, the loss of these factors might also attenuate virulence. We found that *C. glabrata yap1*Δ and *skn7*Δ*yap1*Δ mutant cells displayed a diminished recovery rate when exposed to hydrogen peroxide and peroxynitrite, whereas *skn7*Δ single mutant cells did not show this phenotype. In contrast, upon exposure to menadione, which induces the production of superoxide, *C. glabrata* wild type and mutant cells displayed a similar recovery rate. However, in our primary mouse macrophage model, the *C. glabrata skn7*Δ*yap1*Δ double mutant did not show a diminished survival rate compared to the wild type situation. The loss of the response coordinated by CgSkn7 and CgYap1 has no impact on survival of engulfed cells. Accordingly, it has been shown recently by Cuéllar-Cruz *et al.*, that a low but significant number of exponentially growing *skn7*Δ*yap1*Δ double mutant cells can even survive 10mM H_2O_2, which is a much higher concentration than *C. glabrata* cells experience inside the mammalian host [50, 70]. Since both factors were dispensable for survival in a macrophage infection model, I suggest either only a mild oxidative stress situation inside the phagosome of phagocytic cells or the involvement of other regulatory factors, which can induce a response protecting against oxidative stress. Microarray analysis of *C. glabrata* cells internalized by macrophages, displayed a rather diverse oxidative stress response [49]: *CgCTA1*, *CgGDB1, CgHEM15* and *CgGLO1* displayed an increased expression, whereas *CgTTR1/2* and *CgTSA1/2* were downregulated during phagocytosis. Interestingly, it has been reported recently, that *C. glabrata* cells can suppress ROS production upon internalization by macrophages [71]. Therefore, I conclude that *C. glabrata* cells have developed several lines of defence to counteract the oxidative burst.

Do other regulatory mechanisms induce oxidative stress-associated genes in C. glabrata? Microarray analysis revealed that among the highly oxidative stress induced genes, the largest group comprising 18 genes, appeared to be upregulated independently of CgSkn7 and CgYap1. *E.g.*, *CgZWF1* (encoding the glucose-6-

phosphate dehydrogenase, involved in oxidative stress adaptation [72]), and *CgHSP78*, encoding a mitochondrial chaperone [73], were expressed regardless of CgSkn7/CgYap1 presence. Notably, in *S. cerevisiae*, expression of both *ZWF1* and *HSP78* was found to be dependent on both, Skn7 and Yap1 [59], suggesting the existence of different regulatory mechanisms in *C. glabrata* adapted to the mammalian host. Furthermore, parallel upregulation of oxidative stress-associated genes via other signals might occur. Consistently, I found that among the oxidative stress regulon 26 genes were also upregulated during glucose starvation [74]. This group also includes COR genes such as *CgCTA1*, *CgGPX2* and *CgTRX2*. Interestingly I also found genes encoding for superoxide dismutases *CgSOD1* and *CgSOD2* to be upregulated during glucose starvation. Genes involved in the oxidative stress response including superoxide dismutases were also found to be upregulated during nutrient starvation in *C. albicans* [75]. Northern blot analysis of the COR genes *CgCTA1* and *CgGPX2* revealed a CgSkn7/CgYap1 independent expression behaviour upon nutrient starvation in C. *glabrata*. Therefore, I suggest the existence of a crucial set of oxidative stress-associated genes, which can get induced by parallel pathways in *C. glabrata*. This is consistent with our own unpublished results: a population of engulfed cells suffers transient oxidative stress and continuous carbon shortage inside the phagosome. Possible transcription factors, which can induce the oxidative stress regulon during other stresses, such as carbon starvation, still remain unknown. Existing *C. glabrata* knock out collections have to be screened for putative candidates. One approach to determine involved transcription factors, is based on the measurement of catalase activity, since the catalase *CgCTA1*, is also upregulated during glucose starvation. Among those stresses to overcome upon engulfment, it has been shown that nutrient shortage is a predominant issue for pathogenic yeasts [49, 76, 77]. Therefore, I tried to find out more about the nutrient situation of *C. glabrata* cells inside the phagosome.

Nutrient starvation as a major impact on survival of phagocytosed *C. glabrata* cells.

What are the specific fungicidal characteristics of the unique habitat inside of phagocytic cells? The phagolysosome is considered as oxidative, acidic and degradative milieu. As described above, the oxidative burst contributes to killing of engulfed microbes [55]. In addition, during maturation, the phagosome fuses with

lysosomes which implicates a decreased pH and activated hydrolytic enzymes [78, 79]. Furthermore, upon phagocytosis, engulfed cells are sealed from the environment and have to rely on endogenous resources or those acquired from the phagocytic cell. For example, *C. albicans* induces genes involved in non-fermentative carbon metabolism upon engulfment by macrophages [76]. During the early phase of phagocytosis, *C. albicans* cells shift from glycolysis to gluconeogenesis. Additionally, genes involved in conversion of fatty acids to glucose are induced [76, 80]. Similarly, *C. neoformans* displayed an altered transcriptional response upon phagocytosis [77]. Amongst others, genes involved in autophagy, peroxisome function, and lipid metabolism were induced. The metabolism of alternative carbon sources seems to be of significant importance for engulfed fungal pathogens.

In general, growth on non fermentable carbon sources, such as fatty acids or ethanol, requires β-oxidation and the glyoxylate cycle, which are mainly localized in peroxisomes in yeast. More precisely, the glyoxylate cycle permits the synthesis of glucose from lipids via acetate generated in fatty acid β-oxidation. The products of the glyoxylate cycle (malate and oxalacetate) can be converted to phosphoenolpyruvate, which can be used for gluconeogenesis. Interestingly, the glyoxylate cycle is a virulence determinant for *C. albicans* [80]: the first enzyme of the glyoxylate cycle, the isocitrate lyase (Icl1), which is localized in the peroxisomal matrix, is essential for pathogenicity. Fox2, the second enzyme of the β-oxidation pathway (3-hydroxyacyl-CoA dehydrogenase/enoyl-CoA hydratase) is also required for *C. albicans* virulence [81]. In contrast, mutants defective for peroxisomal import (*pex5*Δ) are not compromised for virulence [81]. Therefore, in *C. albicans*, peroxisomes per se are no major determinants for virulence but rather the contained metabolic pathways which can function apparently to a sufficient extent in the cytosol [82, 83].

What kind of stress response is prevailing in C. glabrata upon internalization? Only little is known about acute stress responses in *C. glabrata* inside the phagosome. To visualize these responses of *C. glabrata* upon macrophage engulfment at a single cell resolution, I characterized fluorescent *in vivo* reporters. Therefore I established an *ex vivo* infection model: primary macrophages were isolated from the bone marrow of mice and infected with *C. glabrata* cells. This was done in cooperation with Nina Gratz and Pavel Kovarik (Max F. Perutz Laboratories, Department of Microbiology and Immunology).

The first reporter gene was the catalase of *C. glabrata*, CgCta1. Notably, it has been shown that the loss of CgCta1 did not attenuate virulence of *C. glabrata* [50]. I demonstrated *in vitro* that expression of CgCta1 is both oxidative stress and carbon

source regulated, whereas the intracellular localization depends on the presence of peroxisomes. Consistently, *S. cerevisiae* Cta1 localized to peroxisomes during growth on non-fermentative carbon sources [84, 85]. In engulfed *C. glabrata* cells, GFP-CgCta1 is induced during the earliest stages during phagocytosis; this could be due to oxidative stress or acute carbon source starvation. Intracellular localization of two other fluorescent reporters (CgYap1 and CgMig1) suggested rather low oxidative stress load and starvation for glucose of engulfed *C. glabrata* cells. Only a minority of engulfed *C. glabrata* cells displayed nuclear localization of the oxidative stress-associated transcription factor GFP-CgYap1. The glucose-dependent repressor CgMig1-CFP was found localized in the cytoplasm of all *C. glabrata* cells immediately upon engulfment. This is consistent with previous results observed in *C. albicans*, where only a small portion of cells derived from mouse kidneys displayed an acute oxidative stress response when examined for *CaCTA1* expression [70]. Therefore, nutrient starvation may be considered a major constraint for engulfed pathogenic yeasts.

Do peroxisomes have an impact on virulence of C. glabrata? Similar to peroxisome biogenesis in *S. cerevisiae* [86, 87], *C. glabrata* peroxisomes accumulate during growth on non fermentable carbon sources. Those organelles also appeared during engulfment of *C. glabrata* cells in macrophages. GFP-tagged catalase revealed that induction of peroxisomes appeared to be transient. Induction of peroxisomes occurred a few hours after internalization, whereas no peroxisomes could be observed after 24 hours. This demonstrates efficient carbon source deprivation of *C. glabrata* within the phagosome and corresponding metabolic adjustments. Interestingly, similar to *C. albicans* cells deleted for CaPex5, which are defective for peroxisomal import [81], I found that the survival of *C. glabrata* devoid of peroxisomes in a mutant lacking CgPex3 was not compromised in our macrophage infection model. However, this does not automatically exclude carbon starvation as major problem for engulfed *C. glabrata* cells: it has been observed that the main metabolic pathways (gloxylate cycle, β-oxidation) continue to function in the cytosol in the absence of peroxisomes in *S. cerevisiae* as well as in *C. albicans* [81, 82]. Accumulation of GFP-CgCta1 to peroxisomes was reversed at later time points in *C. glabrata*. Since peroxisomes are not known to export proteins, the observed cytosolic fluorescence is most probably due to peroxisome turnover [88]. To visualize the putative peroxisomal structures, we fused a generic peroxisomal targeting signal peptide (KNIESKL) derived from the *S. cerevisiae* citrate synthase to the C-terminus of YFP [89, 90]. YFP-KNIESKL staining shifted from punctual staining of peroxisomes to diffuse vacuolar staining. This

suggests strongly that *C. glabrata* peroxisomes are degraded by pexophagy, a selective autophagy pathway during prolonged engulfment.

Do the autophagic processes contribute to virulence of C. glabrata? Since nutrient supply from within the phagosome of phagocytes seems not to be sufficient for prolonged survival [76, 77], engulfed yeast cells have to initiate degradation of their own cellular components. Importantly, cells have to maintain a balance between synthesis and recycling of intracellular resources. In general, this catabolic process is known as autophagy [91-93]. Double-membrane autophagosomes sequester macromolecules or organelles and fuse with the vacuole (or lysosomes), where the degradation takes place. At least 30 autophagy-related (Atg) proteins involved in autophagy have been identified in *S. cerevisiae* [94]. Several subtypes of autophagy have been described [95]. Selective mitophagy, pexophagy, reticulophagy and ribophagy seem to be important for a fast adaptation to regularly changing surroundings. To date, nothing is known about autophagy in *C. glabrata*. The contribution of autophagy to virulence was already investigated in other fungal pathogens: *C. neoformans* showed a markedly attenuated virulence in a mouse model of infection, upon knock down of Atg8 [96]. In contrast, *C. albicans* mutants deleted for Ca*ATG9* are defective for autophagy but killed macrophages after engulfment due to stretching [97]. The rapid filamentation response of *C. albicans* might prevent manifestation of the autophagy defect of *Caatg9*Δ mutants, since prolonged starvation inside the phagosome is prevented by the escape through hyphal outgrowth. Consistently, the filamentous fungi *A. fumigatus* lacking Atg1 also remained virulent [98]. Thus the role of autophagy for fungal pathogens is dependent on their morphology and hence their niches [92].

In contrast, *C. glabrata* is trapped inside the phagosome, and is cut off from nutrient supply. Therefore, I investigated the importance of autophagic processes upon internalization of *C. glabrata* cells. I tested the role of pexophagy in engulfed *C. glabrata* cells with mutants lacking CgAtg11. In *S. cerevisiae*, Atg11 acts as an adapter protein, directing other factors to the phagophore assembly site (PAS) [91, 99]. Pexophagy appears to involve the same machinery as nonspecific autophagy, while other pexophagy-specific components, except Atg11, have not been elucidated yet. The sequestering vesicles that form during pexophagy, the pexophagosome, enwrap only peroxisomes [88]. Indeed, in *atg11*Δ mutants, the survival rate of engulfed *C. glabrata* cells was significantly diminished. Non-selective autophagy also encompasses peroxisome degradation. In *S. cerevisiae*, one specific factor essential for functional

bulk autophagy is Atg17, which is thought to act as a scaffold for other *ATG* genes during the formation of the autophagosome [100]. The loss of Atg17 resulted in fewer and smaller autophagosomes and a severe delay of pexophagy in *S. cerevisiae* [101]. I tested whether this non-selective autophagy pathway is beneficial for the survival of *C. glabrata* upon internalization. Similar to the situation of *atg11*Δ, *atg17*Δ mutants displayed a diminished survival rate. Both, selective and non-selective autophagy, contribute to prolonged survival of engulfed *C. glabrata* cells.

Furthermore, in *C. glabrata pex3*Δ*atg11*Δ cells, I found the sensitivity of *atg11*Δ partially reversed. I suggest from this genetic observation, that autophagy of peroxisomes is beneficial for engulfed *C. glabrata* cells. In contrast, *C. glabrata pex3*Δ*atg17*Δ cells did not display this phenotype. Although the lack of peroxisome biogenesis per se had no influence on survival (*pex3*Δ) and can partially diminish the *atg11*Δ phenotype (*pex3*Δ*atg11*Δ), I argue that it did not outweigh the loss of non-selective autophagy (*pex3*Δ*atg17*Δ). Strikingly, I observed the by far severest decrease of survival in the *C. glabrata* double mutant *atg11*Δ*atg17*Δ. This is in line with results found by Cheong *et al* in *S. cerevisiae*: the *atg11*Δ*atg17*Δ strain did not contain any detectable autophagic bodies [100]. Notably, homologues of proteins of the autophagy core machinery have been found from yeast to mammals, but both Atg11 and Atg17 are not conserved and are only found in yeast [94]. Selective pexophagy, which is affected in both *atg11*Δ and *atg17*Δ mutants, might help to mobilize intracellular resources during prolonged engulfment. Other selective autophagic processes might also contribute to counteract sustained internalization, but have not been topic of this work. Of course, further important autophagy factors, such as the cytosolic protein kinase Atg1, which is essential for the vesicle formation during autophagy [102], or Atg8, which is crucial for the maturation of the autophagosome [103], are likely to attenuate virulence of engulfed *C. glabrata* cells as well. Their importance to successfully counteract phagocytosis still needs to be confirmed. Taken together, I conclude that resisting permanent nutrient starvation is of predominant importance for *C. glabrata* to survive and subsequently escape from the phagosome.

Sleeping with the enemy – what do we know about *Candida glabrata*?

As a common commensal, *C. glabrata* is likely to be isolated from the mammalian mucosa (Figure 1A) [104]. Cells are able to attach to epithelial cells (and in addition to other artificial components such as central venous catheters) due to the expression of specific adhesins [4]. In healthy individuals, *C. glabrata* is unable to spread because of the functional immune system and the bacterial flora, which counteracts fungal dissemination through nutrient restriction and secretion of toxins [105, 106]. Occasionally fungal cells form biofilms, which can exhibit resistance against antifungal agents [107, 108]. Immunocompromised patients recovering from operations or treated with antibiotics are much more susceptible to bloodstream infection of *C. glabrata* cells (Figure 1B). Inside of blood vessels, the milieu is more stable and the nutrient supply is sufficient [109]. Nevertheless, patrolling phagocytes engulf invading pathogens. Cell-mediated immunity, which is based on efficient engulfment of pathogens by phagocytic cells, is crucial to counteract fungal infections (Figure 1C). If the immune system fails to respond to *C. glabrata* infection, cells are able to enter tissues and cause severe organ failure [110]. Notably, due to its opportunistic lifestyle, quantitative and qualitative abnormalities of phagocytes benefit systemic candidiasis [111]. Amongst others, the cytokine TNF-α initiates activation of phagocytes [112, 113], and has been found to be essential to prevent systemic *C. albicans* and *C. glabrata* infections, since lack of TNF-α activity results in enhanced growth in infected tissues in mice [114, 115]. Therefore, efficient phagocytosis by monocytes, macrophages and neutrophils is essential to counteract *C. glabrata* dissemination. The question how *C. glabrata* cells can escape engulfment to cause systemic infection, still needs to be answered.

Upon internalization by phagocytes, engulfed microbes have to sustain several life-threatening restrictions (Figure 1D). Phagocytic cells initiate the so-called oxidative burst through producing reactive oxygen and nitrogen species inside the phagosome to extinct internalized cells [53, 56]. Interestingly, it was observed that engulfed *C. albicans* cells experience only low oxidative stress in macrophages, which are localized in tissues, whereas phagocytosis done by neutrophils, which are found in the bloodstream, causes a severer oxidative stress situation in engulfed cells [70]. Notably, it has been reported recently, that *Candida* species can suppress production of reactive oxygen species in murine and human phagocytes [71]. In line with these results, analysis of the transcription pattern of *C. glabrata* cells during phagocytosis did not show a significant upregulation of oxidative stress-associated genes [49]. Accordingly, I found that the loss of essential oxidative stress transcription factors did not attenuate survival of *C. glabrata* cells in a macrophage infection model. However, I observed that the oxidative stress regulon could also be induced through glucose starvation, a

situation which is prevailing inside the phagosome. Therefore, other pathways might induce the oxidative stress regulon and hence promote resistance.

Engulfed cells are sealed from environmental nutrient supply, and have to deal with carbon source depletion, which leads to a slowdown of proliferation. It has been shown for *Candida* species and *Cryptococcus neoformans*, that upon phagocytosis, alternative carbon metabolism pathways are switched on [49, 76, 77]. Consistently, the glyoxylate cycle is a virulence determinant for *C. albicans* [80]. Internalized cells have to rely on intracellular resources for prolonged survival in the phagosome. Similar to the situation of engulfed *C. neoformans* cells [96], I discovered that *C. glabrata* cells are forced to induce autophagic processes, such as pexophagy, which are crucial for prolonged survival upon phagocytosis. Notably, both microorganisms cannot form hyphae to escape from the phagosome, in contrast to *C. albicans*, which can induce hyphal growth upon engulfment [92]. Autophagy, which makes intracellular resources available, is an essential contributor for dissemination of pathogenic yeasts which are likely to be trapped in the phagosome.

There are still many important questions to answer. *E.g.*, the phagosome fuses with lysosomes in order to decrease the pH, which initiates enzymatic digestion [79, 116]. Since *C. glabrata* is unable to form hyphae, cells either have to avoid pH acidification or develop strategies to inhibit digestion by released enzymes. Further, for successful dissemination, *C. glabrata* has to escape from the phago(lyso)some. For example, *C. neoformans* can escape from macrophages through extrusion of the phagosome, without killing the phagocyte [117]. *C. glabrata* might follow a similar strategy to spread and establish systemic infection. In this respect, the duration of survival of *C. glabrata* inside phagocytic cells might directly relate to its success as a commensal and pathogen. The quantitative contribution of the various processes requires further evaluation.

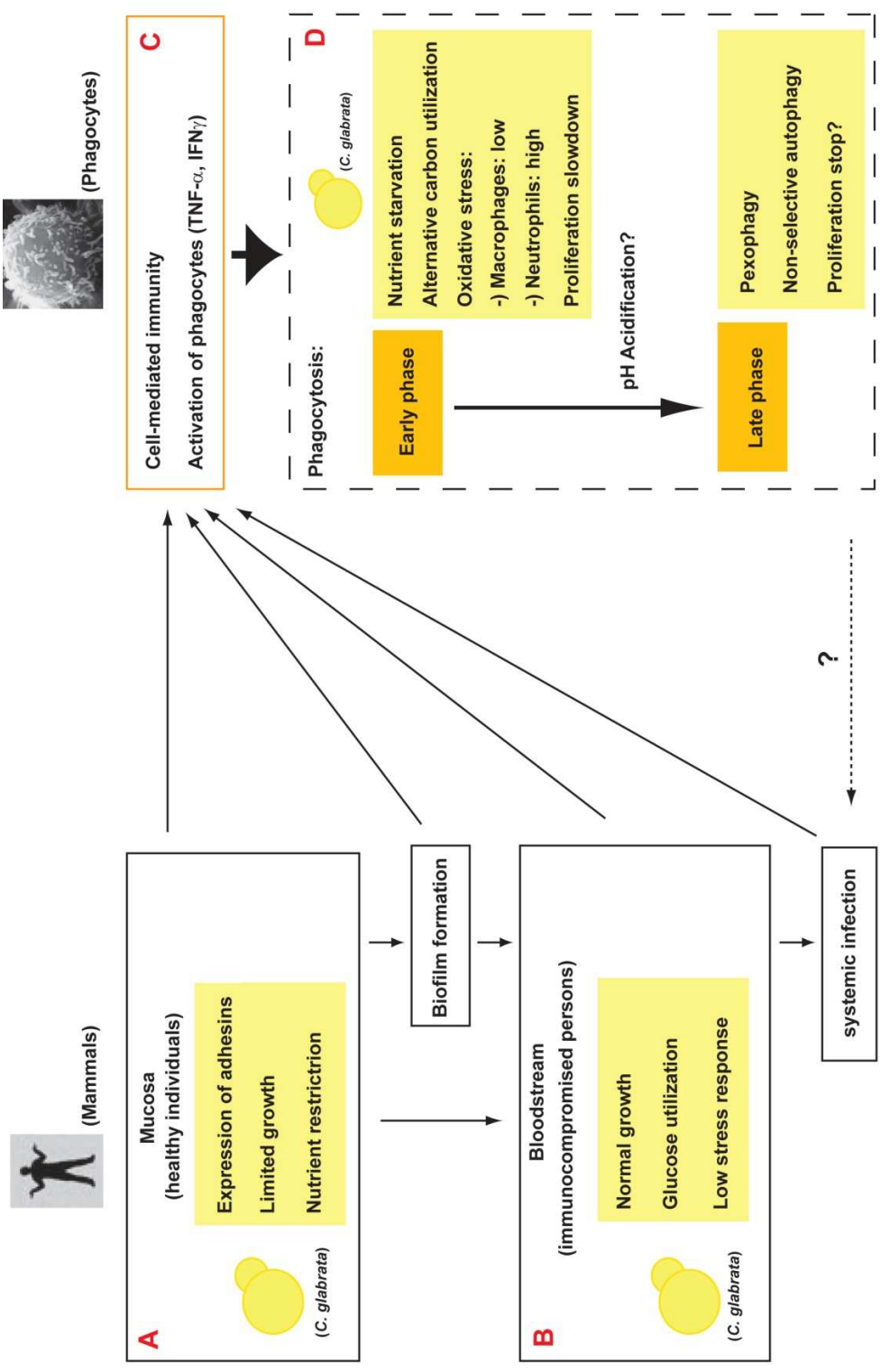

Figure 1. Schematic overview of the key points during infection of *Candida glabrata*. As a common commensal, *C. glabrata* is regularly found on mucosal areas. In immunocompromised persons, bloodstream infections and subsequent systemic infections can occur. Cell-mediated immunity, based on efficient engulfment of pathogens by phagocytic cells, is essential for containing fungal infections. During phagocytosis, *C. glabrata* has to overcome multiple stresses inside the phagosome. Nutrient limitation, oxidative stress and eventually pH acidification seem to be the major constraints upon engulfment. Interestingly, neutrophils located in the bloodstream can induce a higher oxidative stress in engulfed yeast cells, than macrophages, which are located in tissues. To sustain survival and proliferation, cells have to decompose endogenous carbon sources. Pexophagy, a subtype of autophagy, has a crucial impact on prolonged survival of *C. glabrata* inside the phagosome of macrophages. However, to date, nothing is known about the detailed strategies of *C. glabrata* to escape upon phagocytosis.

References

1. Domergue, R., *et al*., Nicotinic acid limitation regulates silencing of *Candida* adhesins during UTI. Science, 2005. **308**(5723): p. 866-70.
2. Diamond, R.D., Fungal surfaces: effects of interactions with phagocytic cells. Rev Infect Dis, 1988. **10 Suppl 2**: p. S428-31.
3. Gasch, A.P., *et al.*, Genomic expression programs in the response of yeast cells to environmental changes. Mol Biol Cell, 2000. **11**(12): p. 4241-57.
4. Kaur, R., *et al*., A yeast by any other name: *Candida glabrata* and its interaction with the host. Curr Opin Microbiol, 2005. **8**(4): p. 378-84.
5. Garside, P., O. Millington, and K.M. Smith, The anatomy of mucosal immune responses. Ann N Y Acad Sci, 2004. **1029**: p. 9-15.
6. Koh, A.Y., *et al*., Mucosal damage and neutropenia are required for *Candida albicans* dissemination. PLoS Pathog, 2008. **4**(2): p. e35.
7. Fischetti, V.A., Novel method to control pathogenic bacteria on human mucous membranes. Ann N Y Acad Sci, 2003. **987**: p. 207-14.
8. Wira, C.R., *et al.*, Innate and adaptive immunity in female genital tract: cellular responses and interactions. Immunol Rev, 2005. **206**: p. 306-35.
9. Nemeth, Z.H., *et al.*, Hyperosmotic stress induces nuclear factor-kappaB activation and interleukin-8 production in human intestinal epithelial cells. Am J Pathol, 2002. **161**(3): p. 987-96.
10. Gasch, A.P., Comparative genomics of the environmental stress response in ascomycete fungi. Yeast, 2007. **24**(11): p. 961-76.
11. Chen, D., *et al*., Global transcriptional responses of fission yeast to environmental stress. Mol Biol Cell, 2003. **14**(1): p. 214-29.
12. Enjalbert, B., A. Nantel, and M. Whiteway, Stress-induced gene expression in *Candida albicans*: absence of a general stress response. Mol Biol Cell, 2003. **14**(4): p. 1460-7.
13. Smith, D.A., *et al.*, A conserved stress-activated protein kinase regulates a core stress response in the human pathogen *Candida albicans*. Mol Biol Cell, 2004. **15**(9): p. 4179-90.
14. Toone, W.M. and N. Jones, Stress-activated signalling pathways in yeast. Genes Cells, 1998. **3**(8): p. 485-98.
15. Alonso-Monge, R., *et al*., Fungi sensing environmental stress. Clin Microbiol Infect, 2009. **15 Suppl 1**: p. 17-9.
16. Pimienta, G. and J. Pascual, Canonical and alternative MAPK signaling. Cell Cycle, 2007. **6**(21): p. 2628-32.
17. Zhang, Y. and C. Dong, Regulatory mechanisms of mitogen-activated kinase signaling. Cell Mol Life Sci, 2007. **64**(21): p. 2771-89.
18. Waskiewicz, A.J. and J.A. Cooper, Mitogen and stress response pathways: MAP kinase cascades and phosphatase regulation in mammals and yeast. Curr Opin Cell Biol, 1995. **7**(6): p. 798-805.
19. Kyriakis, J.M. and J. Avruch, Protein kinase cascades activated by stress and inflammatory cytokines. Bioessays, 1996. **18**(7): p. 567-77.
20. Alonso-Monge, R., et al., Role of the mitogen-activated protein kinase Hog1p in morphogenesis and virulence of Candida albicans. J Bacteriol, 1999. **181**(10): p. 3058-68.
21. Edmunds, J.W. and L.C. Mahadevan, MAP kinases as structural adaptors and enzymatic activators in transcription complexes. J Cell Sci, 2004. **117**(Pt 17): p. 3715-23.
22. Widmann, C., *et al*., Mitogen-activated protein kinase: conservation of a three-kinase module from yeast to human. Physiol Rev, 1999. **79**(1): p. 143-80.

23. Westfall, P.J., D.R. Ballon, and J. Thorner, When the stress of your environment makes you go HOG wild. Science, 2004. **306**(5701): p. 1511-2.
24. Hohmann, S., Osmotic stress signaling and osmoadaptation in yeasts. Microbiol Mol Biol Rev, 2002. **66**(2): p. 300-72.
25. O'Rourke, S.M. and I. Herskowitz, Unique and redundant roles for HOG MAPK pathway components as revealed by whole-genome expression analysis. Mol Biol Cell, 2004. **15**(2): p. 532-42.
26. Winkler, A., *et al.*, Heat stress activates the yeast high-osmolarity glycerol mitogen-activated protein kinase pathway, and protein tyrosine phosphatases are essential under heat stress. Eukaryot Cell, 2002. **1**(2): p. 163-73.
27. Lawrence, C.L., *et al.*, Evidence of a new role for the high-osmolarity glycerol mitogen-activated protein kinase pathway in yeast: regulating adaptation to citric acid stress. Mol Cell Biol, 2004. **24**(8): p. 3307-23.
28. Mollapour, M. and P.W. Piper, Hog1p mitogen-activated protein kinase determines acetic acid resistance in *Saccharomyces cerevisiae*. FEMS Yeast Res, 2006. **6**(8): p. 1274-80.
29. Bilsland, E., *et al*., Rck1 and Rck2 MAPKAP kinases and the *HOG* pathway are required for oxidative stress resistance. Mol Microbiol, 2004. **53**(6): p. 1743-56.
30. Shiozaki, K. and P. Russell, Cell-cycle control linked to extracellular environment by MAP kinase pathway in fission yeast. Nature, 1995. **378**(6558): p. 739-43.
31. Millar, J.B., V. Buck, and M.G. Wilkinson, Pyp1 and Pyp2 PTPases dephosphorylate an osmosensing MAP kinase controlling cell size at division in fission yeast. Genes Dev, 1995. **9**(17): p. 2117-30.
32. Kato, T., Jr., *et al.*, Stress signal, mediated by a Hog1-like MAP kinase, controls sexual development in fission yeast. FEBS Lett, 1996. **378**(3): p. 207-12.
33. Enjalbert, B., *et al.*, Role of the Hog1 stress-activated protein kinase in the global transcriptional response to stress in the fungal pathogen *Candida albicans*. Mol Biol Cell, 2006. **17**(2): p. 1018-32.
34. Gregori, C., *et al*., The high-osmolarity glycerol response pathway in the human fungal pathogen *Candida glabrata* strain ATCC 2001 lacks a signaling branch that operates in baker's yeast. Eukaryot Cell, 2007. **6**(9): p. 1635-45.
35. Martinez-Pastor, M.T., *et al.*, The *Saccharomyces cerevisiae* zinc finger proteins Msn2p and Msn4p are required for transcriptional induction through the stress response element (STRE). EMBO J, 1996. **15**(9): p. 2227-35.
36. DeRisi, J.L., V.R. Iyer, and P.O. Brown, Exploring the metabolic and genetic control of gene expression on a genomic scale. Science, 1997. **278**(5338): p. 680-6.
37. Boy-Marcotte, E., *et al*., Msn2p and Msn4p control a large number of genes induced at the diauxic transition which are repressed by cyclic AMP in *Saccharomyces cerevisiae*. J Bacteriol, 1998. **180**(5): p. 1044-52.
38. Hasan, R., *et al*., The control of the yeast H_2O_2 response by the Msn2/4 transcription factors. Mol Microbiol, 2002. **45**(1): p. 233-41.
39. Schüller, C., *et al*., Global phenotypic analysis and transcriptional profiling defines the weak acid stress response regulon in *Saccharomyces cerevisiae*. Mol Biol Cell, 2004. **15**(2): p. 706-20.
40. Teixeira, M.C., *et al.*, Early transcriptional response of *Saccharomyces cerevisiae* to stress imposed by the herbicide 2,4-dichlorophenoxyacetic acid. FEMS Yeast Res, 2006. **6**(2): p. 230-48.
41. Capaldi, A.P., *et al*., Structure and function of a transcriptional network activated by the MAPK Hog1. Nat Genet, 2008. **40**(11): p. 1300-6.
42. Nicholls, S., *et al.*, Msn2- and Msn4-like transcription factors play no obvious roles in the stress responses of the fungal pathogen *Candida albicans*. Eukaryot Cell, 2004. **3**(5): p. 1111-23.

43. Zahringer, H., J.M. Thevelein, and S. Nwaka, Induction of neutral trehalase Nth1 by heat and osmotic stress is controlled by STRE elements and Msn2/Msn4 transcription factors: variations of PKA effect during stress and growth. Mol Microbiol, 2000. **35**(2): p. 397-406.
44. Berry, D.B. and A.P. Gasch, Stress-activated genomic expression changes serve a preparative role for impending stress in yeast. Mol Biol Cell, 2008. **19**(11): p. 4580-7.
45. Durchschlag, E., *et al*., Nuclear localization destabilizes the stress-regulated transcription factor Msn2. J Biol Chem, 2004. **279**(53): p. 55425-32.
46. de Nobel, H., *et al.*, Parallel and comparative analysis of the proteome and transcriptome of sorbic acid-stressed *Saccharomyces cerevisiae*. Yeast, 2001. **18**(15): p. 1413-28.
47. Gorner, W., *et al*., Acute glucose starvation activates the nuclear localization signal of a stress-specific yeast transcription factor. EMBO J, 2002. **21**(1-2): p. 135-44.
48. Gorner, W., *et al*., Nuclear localization of the C2H2 zinc finger protein Msn2p is regulated by stress and protein kinase A activity. Genes Dev, 1998. **12**(4): p. 586-97.
49. Kaur, R., B. Ma, and B.P. Cormack, A family of glycosylphosphatidylinositol-linked aspartyl proteases is required for virulence of *Candida glabrata*. Proc Natl Acad Sci U S A, 2007. **104**(18): p. 7628-33.
50. Cuellar-Cruz, M., *et al*., High resistance to oxidative stress in the fungal pathogen *Candida glabrata* is mediated by a single catalase, Cta1p, and is controlled by the transcription factors Yap1p, Skn7p, Msn2p, and Msn4p. Eukaryot Cell, 2008. **7**(5): p. 814-25.
51. Hampton, M.B., A.J. Kettle, and C.C. Winterbourn, Inside the neutrophil phagosome: oxidants, myeloperoxidase, and bacterial killing. Blood, 1998. **92**(9): p. 3007-17.
52. Newman, S.L., Macrophages in host defense against *Histoplasma capsulatum*. Trends Microbiol, 1999. **7**(2): p. 67-71.
53. Brown, A.J., K. Haynes, and J. Quinn, Nitrosative and oxidative stress responses in fungal pathogenicity. Curr Opin Microbiol, 2009.
54. Babior, B.M., NADPH oxidase: an update. Blood, 1999. **93**(5): p. 1464-76.
55. Segal, A.W., How neutrophils kill microbes. Annu Rev Immunol, 2005. **23**: p. 197-223.
56. Babior, B.M., Phagocytes and oxidative stress. Am J Med, 2000. **109**(1): p. 33-44.
57. Temple, M.D., G.G. Perrone, and I.W. Dawes, Complex cellular responses to reactive oxygen species. Trends Cell Biol, 2005. **15**(6): p. 319-26.
58. Carmel-Harel, O. and G. Storz, Roles of the glutathione- and thioredoxin-dependent reduction systems in the *Escherichia coli* and *Saccharomyces cerevisiae* responses to oxidative stress. Annu Rev Microbiol, 2000. **54**: p. 439-61.
59. Lee, J., *et al*., Yap1 and Skn7 control two specialized oxidative stress response regulons in yeast. J Biol Chem, 1999. **274**(23): p. 16040-6.
60. He, X.J. and J.S. Fassler, Identification of novel Yap1p and Skn7p binding sites involved in the oxidative stress response of *Saccharomyces cerevisiae*. Mol Microbiol, 2005. **58**(5): p. 1454-67.
61. Nguyen, D.T., A.M. Alarco, and M. Raymond, Multiple Yap1p-binding sites mediate induction of the yeast major facilitator *FLR1* gene in response to drugs, oxidants, and alkylating agents. J Biol Chem, 2001. **276**(2): p. 1138-45.
62. He, X.J., K.E. Mulford, and J.S. Fassler, Oxidative Stress Function of the *S. cerevisiae* Skn7 Receiver Domain. Eukaryot Cell, 2009.
63. Morgan, B.A., *et al.*, The Skn7 response regulator controls gene expression in the oxidative stress response of the budding yeast *Saccharomyces cerevisiae*. EMBO J, 1997. **16**(5): p. 1035-44.
64. Delaunay, A., A.D. Isnard, and M.B. Toledano, H_2O_2 sensing through oxidation of the Yap1 transcription factor. EMBO J, 2000. **19**(19): p. 5157-66.
65. Delaunay, A., *et al*., A thiol peroxidase is an H_2O_2 receptor and redox-transducer in gene activation. Cell, 2002. **111**(4): p. 471-81.

66. Kuge, S., N. Jones, and A. Nomoto, Regulation of yAP-1 nuclear localization in response to oxidative stress. EMBO J, 1997. **16**(7): p. 1710-20.
67. Zheng, M. and G. Storz, Redox sensing by prokaryotic transcription factors. Biochem Pharmacol, 2000. **59**(1): p. 1-6.
68. Klatt, P., *et a*l., Redox regulation of c-Jun DNA binding by reversible S-glutathiolation. FASEB J, 1999. **13**(12): p. 1481-90.
69. Pineda-Molina, E., *et al.*, Glutathionylation of the p50 subunit of NF-kappaB: a mechanism for redox-induced inhibition of DNA binding. Biochemistry, 2001. **40**(47): p. 14134-42.
70. Enjalbert, B., *et al*., Niche-specific activation of the oxidative stress response by the pathogenic fungus *Candida albicans*. Infect Immun, 2007. **75**(5): p. 2143-51.
71. Wellington, M., K. Dolan, and D.J. Krysan, Live *Candida albicans* suppresses production of reactive oxygen species in phagocytes. Infect Immun, 2009. **77**(1): p. 405-13.
72. Ng, C.H., *et al.*, Adaptation to hydrogen peroxide in *Saccharomyces cerevisiae:* the role of NADPH-generating systems and the *SKN7* transcription factor. Free Radic Biol Med, 2008. **44**(6): p. 1131-45.
73. Leonhardt, S.A., et al., HSP78 encodes a yeast mitochondrial heat shock protein in the Clp family of ATP-dependent proteases. Mol Cell Biol, 1993. **13**(10): p. 6304-13.
74. Roetzer, A., *et al.*, *Candida glabrata* environmental stress response involves Saccharomyces cerevisiae Msn2/4 orthologous transcription factors. Mol Microbiol, 2008. **69**(3): p. 603-20.
75. Kusch, H., *et al*., A proteomic view of *Candida albicans* yeast cell metabolism in exponential and stationary growth phases. Int J Med Microbiol, 2008. **298**(3-4): p. 291-318.
76. Lorenz, M.C., J.A. Bender, and G.R. Fink, Transcriptional response of *Candida albicans* upon internalization by macrophages. Eukaryot Cell, 2004. **3**(5): p. 1076-87.
77. Fan, W., *et al*., *Cryptococcus neoformans* gene expression during murine macrophage infection. Eukaryot Cell, 2005. **4**(8): p. 1420-33.
78. Desjardins, M., *et al*., Biogenesis of phagolysosomes proceeds through a sequential series of interactions with the endocytic apparatus. J Cell Biol, 1994. **124**(5): p. 677-88.
79. Flannagan, R.S., G. Cosio, and S. Grinstein, Antimicrobial mechanisms of phagocytes and bacterial evasion strategies. Nat Rev Microbiol, 2009. **7**(5): p. 355-66.
80. Lorenz, M.C. and G.R. Fink, The glyoxylate cycle is required for fungal virulence. Nature, 2001. **412**(6842): p. 83-6.
81. Piekarska, K., *et al.*, Peroxisomal fatty acid beta-oxidation is not essential for virulence of Candida albicans. Eukaryot Cell, 2006. **5**(11): p. 1847-56.
82. Kunze, M., et al., Targeting of malate synthase 1 to the peroxisomes of *Saccharomyces cerevisiae* cells depends on growth on oleic acid medium. Eur J Biochem, 2002. **269**(3): p. 915-22.
83. Taylor, K.M., *et al.*, Localization and targeting of isocitrate lyases in *Saccharomyces cerevisiae*. Biochem J, 1996. **319 (Pt 1)**: p. 255-62.
84. McCammon, M.T., *et al.*, Association of glyoxylate and beta-oxidation enzymes with peroxisomes of *Saccharomyces cerevisiae*. J Bacteriol, 1990. **172**(10): p. 5816-27.
85. Thieringer, R., et al., Peroxisomes in Saccharomyces cerevisiae: immunofluorescence analysis and import of catalase A into isolated peroxisomes. Mol Cell Biol, 1991. **11**(1): p. 510-22.
86. Hartig, A., *et al.*, Differentially regulated malate synthase genes participate in carbon and nitrogen metabolism of S. cerevisiae. Nucleic Acids Res, 1992. **20**(21): p. 5677-86.
87. Purdue, P.E. and P.B. Lazarow, Peroxisome biogenesis. Annu Rev Cell Dev Biol, 2001. **17**: p. 701-52.
88. Hutchins, M.U., M. Veenhuis, and D.J. Klionsky, Peroxisome degradation in *Saccharomyces cerevisiae* is dependent on machinery of macroautophagy and the Cvt pathway. J Cell Sci, 1999. **112 (Pt 22)**: p. 4079-87.

89. Lewin, A.S., V. Hines, and G.M. Small, Citrate synthase encoded by the *CIT2* gene of *Saccharomyces cerevisiae* is peroxisomal. Mol Cell Biol, 1990. **10**(4): p. 1399-405.
90. Kragler, F., *et al*., Two independent peroxisomal targeting signals in catalase A of *Saccharomyces cerevisiae*. J Cell Biol, 1993. **120**(3): p. 665-73.
91. Yorimitsu, T. and D.J. Klionsky, Autophagy: molecular machinery for self-eating. Cell Death Differ, 2005. **12 Suppl 2**: p. 1542-52.
92. Palmer, G.E., D.S. Askew, and P.R. Williamson, The diverse roles of autophagy in medically important fungi. Autophagy, 2008. **4**(8): p. 982-8.
93. Onodera, J. and Y. Ohsumi, Autophagy is required for maintenance of amino acid levels and protein synthesis under nitrogen starvation. J Biol Chem, 2005. **280**(36): p. 31582-6.
94. Xie, Z. and D.J. Klionsky, Autophagosome formation: core machinery and adaptations. Nat Cell Biol, 2007. **9**(10): p. 1102-9.
95. Kraft, C., F. Reggiori, and M. Peter, Selective types of autophagy in yeast. Biochim Biophys Acta, 2009.
96. Hu, G., *et al.*, PI3K signaling of autophagy is required for starvation tolerance and virulenceof *Cryptococcus neoformans*. J Clin Invest, 2008. **118**(3): p. 1186-97.
97. Palmer, G.E., M.N. Kelly, and J.E. Sturtevant, Autophagy in the pathogen *Candida albicans*. Microbiology, 2007. **153**(Pt 1): p. 51-8.
98. Richie, D.L., *et al*., Unexpected link between metal ion deficiency and autophagy in *Aspergillus fumigatus*. Eukaryot Cell, 2007. **6**(12): p. 2437-47.
99. Yorimitsu, T. and D.J. Klionsky, Atg11 links cargo to the vesicle-forming machinery in the cytoplasm to vacuole targeting pathway. Mol Biol Cell, 2005. **16**(4): p. 1593-605.
100. Cheong, H., *et al*., The Atg1 kinase complex is involved in the regulation of protein recruitment to initiate sequestering vesicle formation for nonspecific autophagy in *Saccharomyces cerevisiae*. Mol Biol Cell, 2008. **19**(2): p. 668-81.
101. Cheong, H., *et al*., Atg17 regulates the magnitude of the autophagic response. Mol Biol Cell, 2005. **16**(7): p. 3438-53.
102. Matsuura, A., *et al.*, Apg1p, a novel protein kinase required for the autophagic process in *Saccharomyces cerevisiae*. Gene, 1997. **192**(2): p. 245-50.
103. Xie, Z., U. Nair, and D.J. Klionsky, Atg8 controls phagophore expansion during autophagosome formation. Mol Biol Cell, 2008. **19**(8): p. 3290-8.
104. Naglik, J.R., P.L. Fidel, Jr., and F.C. Odds, Animal models of mucosal *Candida* infection. FEMS Microbiol Lett, 2008. **283**(2): p. 129-39.
105. Corr, S.C., *et al*., Bacteriocin production as a mechanism for the antiinfective activity of *Lactobacillus salivarius* UCC118. Proc Natl Acad Sci U S A, 2007. **104**(18): p. 7617-21.
106. Pamer, E.G., Immune responses to commensal and environmental microbes. Nat Immunol, 2007. **8**(11): p. 1173-8.
107. Iraqui, I., *et al.*, The Yak1p kinase controls expression of adhesins and biofilm formation in *Candida glabrata* in a Sir4p-dependent pathway. Mol Microbiol, 2005. **55**(4): p. 1259-71.
108. Chandra, J., G. Zhou, and M.A. Ghannoum, Fungal biofilms and antimycotics. Curr Drug Targets, 2005. **6**(8): p. 887-94.
109. Barelle, C.J., *et al*., Niche-specific regulation of central metabolic pathways in a fungal pathogen. Cell Microbiol, 2006. **8**(6): p. 961-71.
110. Vardakas, K.Z., *et al.*, Candidaemia: incidence, risk factors, characteristics and outcomes in immunocompetent critically ill patients. Clin Microbiol Infect, 2009. **15**(3): p. 289-92.
111. Richardson, M. and R. Rautemaa, How the host fights against *Candida* infections. Front Biosci, 2009. **14**: p. 4363-75.
112. Riches, D.W., E.D. Chan, and B.W. Winston, TNF-alpha-induced regulation and signalling in macrophages. Immunobiology, 1996. **195**(4-5): p. 477-90.

113. Kato, T. and S. Kitagawa, Regulation of neutrophil functions by proinflammatory cytokines. Int J Hematol, 2006. **84**(3): p. 205-9.
114. Brieland, J., *et al*., Comparison of pathogenesis and host immune responses to *Candida glabrata* and *Candida albicans* in systemically infected immunocompetent mice. Infect Immun, 2001. **69**(8): p. 5046-55.
115. Louie, A., *et al.*, Tumor necrosis factor alpha has a protective role in a murine model of systemic candidiasis. Infect Immun, 1994. **62**(7): p. 2761-72.
116. Stuart, L.M. and R.A. Ezekowitz, Phagocytosis: elegant complexity. Immunity, 2005. **22**(5): p. 539-50.
117. Alvarez, M. and A. Casadevall, Phagosome extrusion and host-cell survival after *Cryptococcus neoformans* phagocytosis by macrophages. Curr Biol, 2006. **16**(21): p. 2161-5.

4. Appendix:

4.1. Summary

4.2. Zusammenfassung

4.3. Danksagung

4.4. Curriculum vitae

4.1. Summary:

The yeast *Candida glabrata* displays a two-faced fungal lifestyle. In healthy mammals it is part of the normal flora, whereas it can turn into an opportunistic human pathogen in immunocompromised persons. Strikingly, it is closely related to baker´s yeast, *Saccharomyces cerevisiae*. Therefore the question arises, which peculiarities make it a pathogen. The present work focuses on responses of *C. glabrata* to a variety of stresses and its impact on survival inside the host. To reveal similarities and discrepancies between *S. cerevisiae* and *C. glabrata*, a genome-wide transcriptional analysis upon glucose starvation, heat, oxidative and osmotic stress was performed and the involvement of according transcription factors was investigated. In *S. cerevisiae*, the transcription factor Msn2 plays an important role in the environmental stress response (ESR), a common gene expression program, which generally protects the cell during various stresses. Analysis of the stress-induced transcriptome revealed a striking similarity between *C. glabrata* and *S. cerevisiae*. Furthermore the orthologues CgMsn2 and CgMsn4 play a significant role in the general stress response of *C. glabrata*. Nevertheless, the loss of CgMsn2/CgMsn4 did not affect virulence in our ex vivo model. Therefore, other stress-associated mechanisms seem to be of predominant importance. The orthologue transcription factors CgSkn7 and CgYap1 induce – similar to *S. cerevisiae* – the majority of genes of the oxidative stress regulon. Since the so-called “oxidative burst” is a weapon of phagocytic cells to combat microbes, engulfed yeasts have to deal with oxidative stress inside the host. CgYap1 was required for protection against peroxides and peroxynitrite, but analysis of the localization of CgYap1 during phagocytosis suggested only a transient oxidative stress situation. In addition, the loss of CgSkn7 and CgYap1 had no impact on virulence in primary mouse macrophages. Finally, the nutritional status of engulfed *C. glabrata* cells was analyzed using *in vivo* reporter constructs, such as the catalase CgCta1 or the glucose-dependent repressor CgMig1, which indicated a permanent nutritional shortage inside the phagosome. Further, we observed a transient proliferation of peroxisomes, implying the urgent need of engulfed cells to metabolize alternative carbon sources. Intracellular resources seem to be last resort to overcome continuous shortage in carbon supply. One important process to recycle internal resources is autophagy. Intriguingly, degradation of peroxisomes (i.e. pexophagy) turned out to be a significant contributor to survival under these conditions. The autophagy-associated proteins CgAtg11 and CgAtg17 were found to be crucial factors to mediate this response. Taken together, in this work, general stress signaling pathways were characterized in the fungal pathogen *C. glabrata*.

4.2. Zusammenfassung:

Die Hefe *Candida glabrata* ist ein humaner opportunistischer Krankheitserreger, der vor allem für immunsupprimierte Menschen zur Gefahr werden kann. *C. glabrata* kommt ubiquitär in der mikrobiellen Flora der Säugetiere vor und ist mit der Bäckerhefe *Saccharomyces cerevisiae* nahe verwandt. Daraus ergibt sich die Frage, welche Eigenschaften *C. glabrata* zu einem pathogenen Organismus machen. Die hier präsentierten Arbeiten konzentrieren sich auf die Wahrnehmung von Umwelteinflüssen der pathogenen Hefe, und vergleichen sie mit homologen Mechanismen in *S. cerevisiae*. Um die Gemeinsamkeiten und Unterschiede zwischen *S. cerevisiae* und *C. glabrata* genauer zu erforschen, wurde das Transkriptom von *C. glabrata* bei Hitze, oxidativem und osmotischem Stress oder bei Entzug der Kohlenstoffquelle verglichen und die Rolle der zugehörigen Transkriptionsfaktoren untersucht. Msn2 ist in *S. cerevisiae* einer der Hauptakteure der sogenannten „Generellen Stressantwort“, also der Regulierung von Genen durch verschiedene Umweltstresse. Die Analyse des Stress-Transkriptoms zeigte eine überwältigende Übereinstimmung zwischen *S. cerevisiae* und *C. glabrata* und eine wichtige Rolle der Msn2 homologen Proteine CgMsn2 und CgMsn4. Die Virulenz von *C. glabrata* in einem *ex vivo* Modell wurde durch Abwesenheit von CgMsn2/4 nicht beeinträchtigt. Daraus kann auf weitere wichtige Stressresistenzmechanismen in *C. glabrata* geschlossen werden. Die Transkriptionsfaktoren CgSkn7 und CgYap1 regulieren - ähnlich wie in *S. cerevisiae* - auch viele homologe Gene in *C. glabrata* während des oxidativen Stresses. Eine Verteidigungsstrategie von phagozytierenden Zellen des Wirtes ist der sogenannte „oxidative burst“, wo eingeschlossene Mikroorganismen mittels reaktiver Sauerstoffmoleküle attackiert werden. CgYap1 wurde benötigt zum Schutz der Zellen gegen geringe Dosen von Wasserstoff Peroxid und Peroxynitrit, aber die Analyse der Lokalisation von CgYap1 während der Phagozytose deutete nur auf einen transienten oxidativen Stress. So hatte auch der Verlust von CgSkn7 und CgYap1 keinen Einfluss auf die Virulenz von *C. glabrata*. Andere Reportergene wie CgCta1 und CgMig1 deuteten auf eine andauernde Hungersituation der Zellen innerhalb des Phagosoms an. Wir beobachteten auch eine transiente Vermehrung von Peroxisomen, die auf den Versuch der Zellen alternative Kohlenstoffquellen zu benutzen hindeutete. Um den Nachschub von Kohlenstoff zu gewährleisten, muss die eingeschlossene Zelle andere intrazelluläre Quellen nützen. Eine Möglichkeit besteht in Autophagie, wobei Bestandteile der Zelle abgebaut werden. Durch die Ausschaltung von *CgATG11* und *CgATG17,* welche zwei wichtige Signalmoleküle für den autophagozytischen Prozess kodieren, wurde die Überlebensrate von phagozytierten *C. glabrata* Zellen erheblich abgeschwächt.

4.3. Danksagung:

Ich möchte mich ganz herzlich bei allen bedanken, die dazu beigetragen haben, die letzten vier Jahre so erfolgreich zu gestalten.

Mein erster Dank gilt meiner Familie für die Unterstützung und die Geduld. Weiters möchte ich mich bei all meinen Freunden und sonstigem Gesocks außerhalb der Uni bedanken, ohne euch wärs nicht gegangen. You know who you are.

Mein erster Dank innerhalb des MFPL Gebäudes gilt Christoph. Danke für die sehr nette Zeit, die Geduld und Ausdauer, und die permanenten Denkanstöße.

Weiters möchte ich die Gelegenheit nutzen und mich bei allen BiologInnen bedanken, die mich durch das ganze Studium begleitet haben, bis zum Ende dieser Zeilen. War ein unfassbarer Spaß!

Mein ganz besonderer Dank gilt Wolfi. Unnötig ein Wort darüber zu verlieren. Ein Stern….

Eines der wichtigsten Dinge in den vergangenen Jahren war die gute Atmosphäre im Labor 5. Vielen Dank an all die Personen, die dazu beigetragen haben. Mein besonderer Dank gilt natürlich unserer Gruppe (Christoph, Eva, Milka, und Rene), der Kragler Gruppe (Niko, Gregor, Dani, Koni, Shoudong, Andi und Fritz) und der Ammerer Gruppe (Wolfi, Jiri, my dude Shiam, Andriy, Veerle und Gustav). Martin, Roman, Norbert, Manfred, Sophie, Nina, Fabian und Konsorten gebührt mein Dank für regen Austausch an Enzymen und toternsten Gedanken. Silvia, Harald, Erna und Barbara gilt mein Dank für das unentwegte Beseitigen von logistischen und administrativen Hürden.

Desweiteren gilt mein Dank der Candida Community in unserem Haus: Christa, Tobi, Denes & Co. Es hat sich doch gelohnt.

Zuletzt möchte ich mich bei allen bedanken, die mich auf die eine oder andere Weise beim Schreiben unterstützt haben. Wie heißt es so schön: the memory remains.

Curriculum vitae Andreas ROETZER

Max F. Perutz Laboratories, Department of Biochemistry
University of Vienna
Dr.Bohr-Gasse 9/5, A-1030 Vienna, Austria
Fax:+43 1 4277 9528, Tel: +43 1 4277 52805
andreas.roetzer@univie.ac.at

Personal Details

Date and place of birth Vienna, 29.12.1977

Citizenship: Austria

Education:

09/84 – 07/88 Elementary School: Schulbrüder Wien-Währing

09/88 – 06/96 Grammar School: Albertus Magnus Schule (AHS)

10/97 – 12/02 Study of Biology at the University of Vienna; Branch: Microbiology

01/03 – 06/04: Diploma thesis in Lab of Prof. Timothy Skern at the Institute of Medical Biochemistry.
Protein engineering studies on enteroviral 2A proteinases

02/05 – 06/09: PhD thesis in Lab of Prof. Christoph Schüller at the Institute of Biochemistry

Stress response of the human fungal pathogen *Candida glabrata*

Internships and Research Experience:

07/99 Rhone-Polenc (Chazay, France), field tests and screening of insecticides

01/02 Analysis of *A. thaliana* gene AtMKP1 (Prof. Hirt).

03/02 Effect of temperature shift on expression of the S-layer protein SbsA of *B. stearothermophilus* (Prof. Kuen).

06/02 Experimential Immunology (Company Intercell AG, Vienna).

07/02 Biochemistry of viral proteins, HRV2 2A proteinase activity on eIF4G (Prof. Skern).

09/02 The Mg2+ influx system: Investigation of Alrp1 & Alrp2 localisation (Prof. Schweyen).

11/05 Medical Mycology Course, Austrian Society of Medical Mycology (AKH, Vienna)

Tutorials:

11/05, 10/06: practical course Microbiology II (MFPL, University of Vienna)

06/06, 06/07, 10/07: practical course Molecular Biology I (MFPL, University of Vienna)

06/08, 11/08: practical course Biochemistry I (MFPL, University of Vienna)

Attended Meetings:

05/05: Nice - 1st FEBS Lecture Course Human Fungal Pathogens

Poster: Indication of a S. cerevisiae-like general stress response in *Candida glabrata*. Functional conservation of the key transcription factor Msn2. Andreas Roetzer, Christa Gregori, Karl Kuchler, Gustav Ammerer and Christoph Schüller.

09/05: Vienna – Life Sciences (Annual joint meeting of the ÖGBM, ÖGGGT, ÖGBT and ANGT)

Poster: Indication of a S. cerevisiae-like Msn2/4 dependent general stress response in *Candida glabrata*. Andreas Roetzer, Christa Gregori, Karl Kuchler, and Christoph Schüller.

11/06: Heidelberg - 8th International EMBL PhD Student Symposium (Biology of Disease)

Poster: Living on a hostile ground: key transcription factors mediate stress response of the pathogen *Candida glabrata*. Andreas Roetzer, Christa Gregori, Karl Kuchler, and Christoph Schüller.

05/07: Nice - 2nd FEBS Lecture Course Human Fungal Pathogens

Selected short talk: Living on a hostile ground: key transcription factors mediate stress response of *Candida glabrata*. Andreas Roetzer, Christa Gregori, Karl Kuchler, and Christoph Schüller.

09/07: Göttingen - 4th International PhD Student Symposium (Horizons in Molecular Biology)

Poster: Stress response in yeast: following the route of key transcription factors in *Saccharomyces cerevisiae* and *Candida spp*. Andreas Roetzer, Christa Gregori, Anne Marie Jennings, Geraldine Butler, Karl Kuchler, Christoph Schüller.

10/08: Heidelberg - EMBO Workshop on Evolutionary and Environmental Genomics of Yeast

Poster: Stress Response in pathogenic yeasts: following the route of important transcription factors. Roetzer A, Jennings AM, Gratz N, Kovarik P, Butler G, and Schüller C. (**Poster Price**)

Publications:

Deszcz L, Seipelt J, Vassilieva E, Roetzer A, Kuechler E, Antiviral activity of caspase inibitors: effect on picornaviral 2A proteinase. FEBS Lett, 2004. 560 (1-3): p. 51-5.

Baxter NJ, Roetzer A, Liebig HD, Sedelnikova S, Hounslow AM, Skern T, Waltho JP, Structure and dynamics of coxsackievirus B4 2A proteinase, an enyzme involved in the etiology of heart disease. J Virol. 2006 Feb;80(3):1451-62.

Gregori C, Schüller C, Roetzer A, Schwarzmüller T, Ammerer G, and Kuchler K, The high osmolarity glycerol (HOG) response pathway in the human fungal pathogen *Candida glabrata* strain ATCC2001 lacks a signaling branch operating in baker's yeast. Eukaryotic Cell 2007 Sep;6(9):1635-45.

Roetzer A, Gregori C, Jennings AM, Quintin J, Ferrandon D, Butler G, Kuchler K, Ammerer G and Schüller C. *Candida glabrata* environmental stress response involves *Saccharomyces cerevisiae* Msn2/4 orthologous transcription factors. Mol Microbiol, 2008 Aug;69(3):603-20.

Roetzer A, Gratz N, Kovarik P and Schüller C. Autophagy supports survival of *Candida glabrata* during phagocytosis. Cell Microbiol, submitted revised.